Journal of Electronic Research and Application

Editor-in-Chief

Joselito A. Dolot

Lyceum of the Philippines University-Batangas, Philippines

BIO-BYWORD SCIENTIFIC PUBLISHING PTY LTD
(619 649 400)
Level 10
50 Clarence Street
SYDNEY NSW 2000
Copyright © 2024. Bio-Byword Scientific Publishing Pty Ltd.
Complimentary Copy

ISSN (ONLINE): 2208-3510
ISSN (PRINT): 2208-3502

Journal of Electronic Research and Application

Focus and Scope

Journal of Electronic Research and Application is an international, peer-reviewed and open access journal which publishes original articles, reviews, short communications, case studies and letters in the field of electronic research and application.

Topics covered but not limited to:

Automation
Circuit Analysis and Application
Electric and Electronic Measurement Systems
Electrical Engineering
Electronic Materials
Electronics and Communications Engineering
Power Systems and Power Electronics
Signal Processing
Telecommunications Engineering
Wireless and Mobile Communication

About Publisher

Bio-Byword Scientific Publishing is a fast-growing, peer-reviewed and open access journal publisher, which is located in Sydney, Australia. As a dependable and credible corporation, it promotes and serves a broad range of subject areas for the benefit of humanity. By informing and educating a global community of scholars, practitioners, researchers and students, it ndeavors to be the world's leading independent academic and professional publisher. To realize it, it keeps creative and innovative to meet the range of the authors' needs and publish the best of their work.

By cooperating with University of Sydney, University of New South Wales and other world-famous universities, Bio-Byword Scientific Publishing has established a huge publishing system based on hundreds of academic programs, and with a variety of journals in the subjects of medicine, construction, education and electronics.

Publisher Headquarter

BIO-BYWORD SCIENTIFIC PUBLISHING PTYLTD
Level 10
50 Clarence Street
Sydney NSW 2000
Website: www.bbwpublisher.com
Email: info@bbwpublisher.com

2024, Volume 8, Issue 4

Table of Contents

1 **Application of Electronic Information Engineering in Hospital Management**
Jun Xiao, Zhilan Yang

7 **Analysis of Aluminum Alloy Double-Pulse MIG Welding Arc Signal Characteristics Based on Broadband Mode Decomposition**
Yin Si, Zixiong Xia, Wei Liu, Kexin Zhang, Xiangyu Song

17 **An Underwater Robot Inspection Anomaly Localization Feedback System Based on Sonar Technology**
Siqiang Cheng, Yi Liu, Aibin Tang, Libin Yang

22 **Tactile Paving Recognition Method Based on Improved YOLOv7**
Chengyi Shi, Qun Zhao, Nan Fang, Yufeng Mao

28 **Exploration of Energy-Saving Technologies in Building Electrical System Design**
Yong Zhang

34 **Design of Intelligent Window Automatic Monitoring System Based on Microcontroller Control**
Liyan Gao, Rongfang Zong

41 **A Design of an SMTP Email Server**
Liheng Hu

48 **Research on Active and Reactive Power Decoupling Control Based on VSC-HVDC**
Hongshan Lin, Yiming Lei, Feng Ning

55 **Research on Multiple Access Algorithms for Wireless Network**
Kaifeng Yao

64 **Furnace Temperature Curve Optimization Model Based on Differential Evolution Algorithm**
Yiming Cheng

81 **Penetration Study of Key Technologies for Cybersecurity Risk Assessment**
Lin Ma

88 **Application of Bayesian Analysis Based on Neural Network and Deep Learning in Data Visualization**
Jiying Yang, Qi Long, Xiaoyun Zhu, Yuan Yang

94 Research on Integrated Communication Perception Technology Based on RIS Assistance
Hao Yang, Chuanjiang Wang, Xiaoyi Li, Qi Xiang, Taoyong He

101 Application of Power Electronics Converters in Renewable Energy
Tao Cheng

108 Research on Machine Tool Fault Diagnosis and Maintenance Optimization in Intelligent Manufacturing Environments
Feiyang Cao

115 Visual Representation and Cognitive Models in Information Visualization
Yingquan Wang, Mustaffa Halabi Azahari

121 A Cell Screening Algorithm Integrating Genetic and Numerical Differentiation
Zhen Wu, Feijing Fu, Yirga Eyasu Tenawerk, Weize Quan, Wanwen Wu

133 Integrated Experimental and Simulation Investigation of Breakdown Voltage Characteristics Across Electrode Configurations in SF_6 Circuit Breakers
Bo Guan, Qi Yu, Qingpeng Yuan, Shiwen Chen, Lailin Chen, Su Guo, Peilong Zhu

143 Crawler Vehicle Rescue Robot Based on Arduino NANO
Haiwei Wang, Juntong Chen, Tianyu Jin

148 Exploration of Construction Organization for Maintenance of Steam Turbine Equipment in Thermal Power Plants
Zhu Yang

154 Street Lamp Status Warning System Based on Internet of Things Technology
Hanli Wang, Yuanzhi Liu, Yilin Wu

161 Chip Surface Character Recognition Based on OpenCV
Lihang Yin

168 Research on the Practice of Cross-Border E-Commerce Strategies: Taking Alibaba International Station as an Example
Jiong'en Xiao, Xiaosha He, Yiyang Lu

174 Research on Electrical Automation Control Design Based on PLC Technology
He Yu

180 The Application of Intelligent Lighting in Thermal Power Plants
Xiaozhong Kang, Shuangqiang Liu, Guoqing Hu, Haibin Huang

Journal of Electronic Research and Application, 2024, Volume 8, Issue 4
http://ojs.bbwpublisher.com/index.php/JERA
ISSN Online: 2208-3510
ISSN Print: 2208-3502

Application of Electronic Information Engineering in Hospital Management

Jun Xiao[1]*, Zhilan Yang[2]*

[1]Information Department, Shiyan Hospital of Traditional Chinese Medicine, Shiyan 442000, Hubei Province, China
[2]Maintenance and Construction Department, Shiyan Hospital of Traditional Chinese Medicine, Shiyan 442000, Hubei Province, China

***Corresponding author:** Jun Xiao, 531080437@qq.com; Zhilan Yang, 82673829@qq.com

Copyright: © 2024 Author(s). This is an open-access article distributed under the terms of the Creative Commons Attribution License (CC BY 4.0), permitting distribution and reproduction in any medium, provided the original work is cited.

Abstract: To further enhance the overall service quality of China's hospitals and improve the trust of the majority of patients in hospitals, this paper takes intelligent hospital management as the object of study, analyzes the importance of electronic information engineering technology applied in hospital management, and discusses the specific application methods of electronic information engineering in hospital management. This aims the existing problems in the current hospital management, such as insufficient degree of informatization, data sharing difficulties, lack of professionals, etc. Corresponding improvement measures are proposed, including strengthening the construction of informatization, promoting data sharing, and cultivating professionals. It is hoped that this study will enable the majority of hospital managers to make better use of electronic information engineering technology to effectively solve the current problems faced by hospitals and to continuously improve the comprehensive competitiveness of China's hospitals.

Keywords: Electronic information engineering; Hospital management; Intelligence

Online publication: July 17, 2024

1. Introduction

The traditional hospital management mode has been unable to meet people's needs, especially in the face of sudden epidemics and emergencies, the drawbacks of traditional management methods are more obvious. Therefore, it is of great practical significance to strengthen the research of electronic information engineering applications in hospital management. In today's society, the rapid development of Internet technology and computer technology has brought great changes to all walks of life, and the medical industry is no exception. As an organization providing medical services, the hospital's management mode must keep pace with the times. However, due to the limited resources of hospitals, to ensure the interests of patients and the quality of medical care, hospital managers need to optimize the management of hospitals [1]. To improve management efficiency, reduce costs, and ensure that patients receive high-quality medical services, this goal can be achieved by introducing electronic information engineering technology. Electronic information engineering is a comprehensive discipline involving communication, electronics, information, and other fields, and this

technology, with digitalization, networking, and intelligence as its main features, can help hospitals achieve efficient, convenient, and safe medical services [2]. Therefore, the application of electronic information engineering technology in hospital management can not only improve the management efficiency and service quality of hospitals but also protect the privacy and safety of patients [3]. With the popularity of Internet technology, hospitals can use the Internet platform to establish online consultation, booking registration, online payment, and other services, which greatly facilitate patients' medical treatment. In addition, the electronic medical record system, remote consultation system, intelligent diagnostic system, and other technical means, can improve the diagnosis treatment level and serviceability of hospitals, and provide patients with a better medical experience.

2. The importance of electronic information engineering in hospital management

2.1. Reducing medical risks and improving medical quality

With the continuous development of China's economy, computer technology and network communication technology are more widely used in all walks of life. However, due to the large amount of information within the hospital, if the traditional way of management is used, it will lead to inefficient information transfer and is prone to problems such as misinformation. This will not only affect the diagnosis and treatment work of doctors but also affect the efficiency of the hospital. Through the introduction of electronic information engineering technology, these problems can be effectively solved to ensure that the hospital can timely access the patient's health status and treatment needs, to provide more accurate and efficient medical services. Additionally, electronic information engineering technology can also help hospitals to carry out scientific and reasonable procurement and storage of drugs and medical equipment, to achieve the optimal allocation of resources, which can not only improve the efficiency of the hospital but also reduce the medical risk and improve the quality of medical services, to meet the needs of the majority of patients.

2.2. Improve the management level of the hospital

With the continuous development of the Internet era, at present, most hospitals have established their websites and public numbers to promote their business and service content. However, due to the lack of professional operators in the hospital itself, it is difficult to present these contents effectively. Currently, the application of electronic information engineering is particularly important [4]. Electronic information engineering can integrate all kinds of information in the hospital to form a complete database so that the hospital can quickly query the required information through the database and use it as a basis for developing a more scientific and reasonable management strategy. For example, through electronic information engineering technology, hospitals can realize functions such as remote consultation and electronic medical records, thus improving the management level of hospitals.

2.3. Improve the economic efficiency of the hospital

Presently, China's hospitals generally face the problem of financial constraints, and this problem has become one of the main factors restricting the development of hospitals. Therefore, how to improve the economic efficiency of hospitals is a problem that every hospital manager must seriously think about. This problem can be solved effectively by introducing electronic information engineering technology. Firstly, electronic information engineering technology can provide hospitals with information technology infrastructure, such as hospital websites, WeChat public numbers, etc., which can effectively expand the hospital's popularity and increase the hospital's income sources. Secondly, electronic information engineering technology can also help

hospitals save manpower costs, for example, through online booking registration, mobile payment, and other ways, it can reduce the number of people queuing in the outpatient hall, thus saving a lot of manpower costs [5]. Finally, electronic information engineering technology can also help hospitals achieve intelligent management, such as intelligent medical guide systems, intelligent logistics systems, etc., which can improve the operational efficiency of hospitals, thus maximizing the economic benefits of hospitals.

3. Specific application of electronic information engineering in hospital management

3.1. Remote diagnosis

In the current hospital management, doctors will carry out various examinations on patients and feedback on the results to relevant personnel in time. With the help of electronic information engineering, remote diagnosis can be achieved through the network, which can reduce the distance between the hospital and the patient, and also improve the patient's trust. For example, when patients are sick in other cities, they can go to the local hospital directly and then be diagnosed by local doctors. Of course, if the patient wants further treatment, they can also contact the hospital's experts for consultation, to obtain the most scientific and professional treatment plan. The telemedicine system supported by electronic information engineering technology can realize services such as remote consultation and remote surgery between experts and patients, reduce medical costs, and improve medical efficiency.

3.2. Application of intelligent medical equipment

With the continuous development of China's economy, more high-tech is applied to medical services. These technologies can not only help patients to quickly complete the diagnosis of the disease, but can effectively alleviate the contradiction between doctors and patients, and reduce the probability of disputes. Therefore, in the management of hospitals, we can make full use of electronic information engineering to introduce advanced intelligent medical equipment, such as computed tomography (CT) scanning systems, magnetic resonance imaging (MRI), etc. Through these advanced equipment, doctors can more accurately determine the specific condition of the patient and formulate a more appropriate treatment plan. Concurrently, these advanced equipments can also significantly shorten the waiting time of patients, to be treated as soon as possible, and improve the overall efficiency of the hospital. The application of electronic information engineering technology also promotes the development of intelligent medical devices, such as wearable devices and mobile medical devices, which can monitor patients' physical conditions in real-time and transmit the data to the doctor's computer, which facilitates the doctor's diagnosis and treatment [6].

3.3. Information management platform

In the actual operation of the hospital, various data and information are very complicated, which is a great challenge for hospital managers. To solve this problem, a comprehensive information management platform can be constructed to facilitate the unified management and monitoring of various data and information in the hospital. Through this platform, hospital administrators can understand the work of each department in real-time and can find and solve existing problems promptly [7]. Furthermore, the platform also has good compatibility and scalability and can meet the needs of different sizes and types of hospitals, to improve the overall operational efficiency of the hospital.

3.4. Digital management

In the process of hospital management, digital management is one of the essential links. Through digital management, the daily operation of the hospital can be data processing, to achieve all-round supervision and guidance of the hospital. Moreover, digital management can also provide doctors with a clear reference basis so that they can better understand the development of the patient's condition and provide personalized services. Electronic information engineering technology can help hospitals achieve digital management, including electronic medical records (**Figure 1**), image archiving pathological tests, etc. These data can be shared among different departments to improve work efficiency, and it is also convenient for doctors to follow up and manage their patients in the long term [8]. Digital management is an indispensable part of current hospital management, which can help hospitals better adapt to the needs of the new era and improve the comprehensive competitiveness of hospitals.

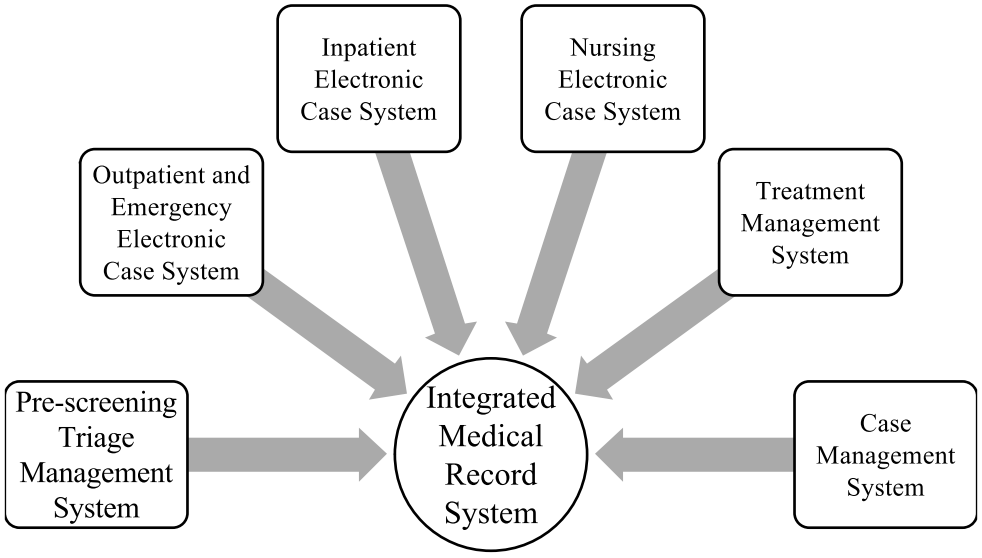


Figure 1. Integrated electronic case system

3.5. Information system construction

Electronic information engineering provides strong support for information management in hospitals. Hospitals can establish a perfect information system to achieve the integration of medical resources, patient information and diagnosis and treatment processes, and improve management efficiency and medical quality.

3.6. Data management

Electronic information engineering technology can effectively process and store a large amount of medical data to help doctors better understand the patient's condition and treatment. Simultaneously, hospitals can also predict disease development trends and preventive measures through big data analysis to improve hospital management.

4. Problems and improvement measures in current hospital management

4.1. Existing problems

Although the application of electronic information engineering in hospital management has achieved certain results, there are still some problems. Firstly, the degree of hospital informatization is insufficient. Many hospitals are still using traditional management methods and lack effective information system support. Secondly,

data sharing is difficult. Due to the imperfect information-sharing mechanism between different departments, it is difficult to integrate and utilize data, which affects the efficiency of hospital management. Thirdly, there is a lack of professional talents [9]. With the rapid development of electronic information engineering technology, hospitals need professionals with appropriate knowledge and skills to promote its application.

4.2. Improvement measures

Given the above problems, the following improvement measures can be taken:

(1) Strengthen the construction of hospital information technology. Through the establishment of a unified hospital information system, we can realize the comprehensive management of each department, division, and business process and improve management efficiency. At the same time, strengthen the construction of hospital information technology infrastructure, improve network security and data backup capacity, and guarantee information security.

(2) Promote data sharing. Formulate perfect information-sharing mechanisms and norms, clarify the responsibilities and authorities between departments, and ensure that data can be timely and accurately accessed and utilized [10]. Concurrently, doctors and medical personnel are encouraged to use the electronic medical record system to better manage and preserve patients' medical information.

(3) Cultivate professional talents. Strengthen cooperation with colleges, universities, and research institutions to cultivate a group of high-quality talents with advanced concepts and professional skills to provide strong support for the application of electronic information engineering in hospitals.

5. Advantages and future development trends of the application of electronic information engineering in hospital management

The application of electronic information engineering in hospital management has many advantages. Firstly, it can improve the management efficiency and service quality of hospitals. By establishing a perfect information system, hospitals can realize the efficient use of medical resources and improve work efficiency and service levels. Secondly, it can improve patients' medical experience. Through technical means such as telemedicine and electronic medical records, patients can obtain medical information and treatment advice more conveniently, reducing waiting time and the number of round trips. Finally, it can promote the innovative development of the medical industry. With the continuous progress of technology, hospital management will be more intelligent and personalized in the future, providing patients with more accurate and humane medical services.

Looking ahead, the application of electronic information engineering will continue to penetrate all aspects of hospital management. On the one hand, with the continuous development of artificial intelligence, big data, and other technologies, hospitals will pay more attention to data analysis and decision-making support to improve the science and accuracy of management decisions. On the other hand, with the application of emerging technologies such as the fifth generation of mobile networks (5G) and the Internet of Things (IoT), hospitals will achieve more comprehensive informatization and improve the accessibility and convenience of medical services. Furthermore, with the implementation of the Healthy China strategy, hospital management will pay more attention to public health and safety issues, and actively promote the construction of a universal health protection system.

6. Conclusion

With the continuous development of information technology, electronic information engineering has become

an important support for hospital management. By strengthening information construction and data sharing, hospital management efficiency and service quality can be improved. Simultaneously, the application of new technologies such as telemedicine and electronic medical records also provides patients with more convenient and safe medical services. In the future, electronic information engineering will continue to promote the development of hospital management, including the integration and application of artificial intelligence, the Internet of Things, and other technologies. The application of these technologies will further enhance the management level and medical service capacity of hospitals and provide patients with more high-quality and efficient medical services. However, some issues need to be noted when applying electronic information engineering technology. For example, data security, data privacy protection, and so on. Therefore, in the process of promoting the application of electronic information engineering, the formulation and improvement of relevant laws and regulations should be strengthened to ensure the security and privacy protection of medical information. Only in this way can electronic information engineering technology better support hospital management and realize the sustainable development of the medical industry.

Disclosure statement

The authors declare no conflict of interest.

References

[1] Li S, Wang Y, 2024, Analysis of the Application of Electronic Information Technology in Modern Hospital Management. Digital Communication World, 2024(04): 176–178.

[2] Song G, 2023, Analysis of the Application of Electronic Information Technology in Hospital Management. Digital Communication World, 2023(12): 126–128.

[3] Liu H, Zhang H, Jiang Y, et al., 2023, Exploration and Application of Hospital Information Technology Project Management Method. Chinese Journal of Health Information Management, 20(05): 754–760.

[4] Yu L, Liu Q, Jiang S, 2023, Practice and Thinking on the Whole Life Cycle Management of Hospital Information Technology Assets. Chinese Journal of Health Information Management, 20(05): 797–801.

[5] Yuan L, Li K, 2023, Research on the Path of Hospital Performance Improvement under the Support of Information Technology. Finance and Economics, 2023(30): 87–89.

[6] Zhang M, 2023, Thoughts on Strengthening the Management of Fixed Assets in Public Hospitals. Popular Investment Guide, 2023(20): 53–55.

[7] Huang Y, 2023, Study on the Path of Financial Management Informatization Construction in Children's Hospitals under the Background of New Medical Reform. China Management Informatization, 26(20): 70–72.

[8] Li J, Li J, Hu S, et al., 2023, Research on Hospital Informatization Framework Construction and System Standardization Management. China Modern Doctor, 61(28): 110–114.

[9] Hu R, 2023, Exploring the Role of Medical Management Information Construction in Hospital Management. China Management Informatization, 26(19): 150–153.

[10] Wang W, 2020, Application and Optimization of Electronic Information Engineering in Hospital Administration. Information and Computer (Theoretical Edition), 32(03): 3–5.

Publisher's note

Bio-Byword Scientific Publishing remains neutral with regard to jurisdictional claims in published maps and institutional affiliations.

Journal of Electronic Research and Application, 2024, Volume 8, Issue 4
http://ojs.bbwpublisher.com/index.php/JERA
ISSN Online: 2208-3510
ISSN Print: 2208-3502

Analysis of Aluminum Alloy Double-Pulse MIG Welding Arc Signal Characteristics Based on Broadband Mode Decomposition

Yin Si[1], Zixiong Xia[2], Wei Liu[1], Kexin Zhang[1], Xiangyu Song[1]*

[1]School of Information and Intelligent Engineering, Guangzhou Xinhua University, Guangzhou 510000, Guangdong Province, China
[2]School of Mechanical and Electrical Engineering, Guangdong Engineering Polytechnic, Qingyuan 511510, Guangdong Province, China

***Corresponding author:** Xiangyu Song, sxyfighting@163.com

Copyright: © 2024 Author(s). This is an open-access article distributed under the terms of the Creative Commons Attribution License (CC BY 4.0), permitting distribution and reproduction in any medium, provided the original work is cited.

Abstract: Welding voltage and current in arc signals are directly related to arc stability and welding quality. Process experiments with different parameters were organized according to the orthogonal experimental design method by constructing an aluminum alloy double-pulse metal inert gas (MIG) welding arc electric signal test platform. The data acquisition system of the aluminum alloy MIG welding process was established to obtain real-time arc signal information reflecting the welding process. The aluminum alloy's collected double-pulse arc current signals are decomposed adaptively by broadband mode decomposition (BMD). The direct current (DC) signal, pulse signal, distortion signal, ripple signal, and noise signal are separated and extracted, and the composite multiscale fuzzy entropy (CMFE) is calculated for the component set of the electrical signal. The experimental results show that the current waveform obtained by the double-pulse MIG welding current signal is consistent with the corresponding weld forming diagram. Simultaneously, the composite multiscale fuzzy entropy is calculated for the arc characteristic parameters. The rationality of matching process parameters and arc stability of aluminum alloy's double-pulse MIG welding were evaluated.

Keywords: Double-pulse MIG welding; Electric arc signal; Broadband mode decomposition; Welding stability

Online publication: August 13, 2024

1. Introduction

Aluminum alloy is used in MIG welding despite the process being prone to oxidation, cracking, and bubble formation, as well as welding deformation and other defects. Additionally, the complexity of the welding equipment, the difficulty in adjusting process parameters, and the lack of quality control measures contribute to the challenges. Any slight deviation in production conditions during the welding process makes it difficult to ensure the consistent quality of the weld [1-3]. To ensure the forming quality of aluminum alloy MIG welding, it is necessary to monitor the quality information of the process and its influencing factors [4-6]. In mechanical engineering, the adaptive time-frequency analysis method for signals has always been a hot research topic [7-9]. In recent years, adaptive time-

frequency analysis has been widely used to extract effective features from complex non-stationary signals disturbed by noise. Common methods include empirical mode decomposition (EMD), ensemble empirical mode decomposition (EEMD), variational mode decomposition (VMD), and so on. Broadband mode decomposition (BMD) is a new adaptive time-frequency analysis method [10]. The BMD method begins by establishing a joint dictionary of wideband effective signals (such as square waves and sharp waves) along with local narrowband signals. An intelligent optimization algorithm is used to search for the sparsest solution of the signal within this constructed dictionary. BMD utilizes a regularization smoothness operator as its optimization objective function, targeting the parameters such as the amplitude, frequency, and phase of the wideband effective signals, as well as the filter parameters of the local narrowband signals. Through the use of intelligent optimization algorithms, BMD achieves sparse signal decomposition during the optimization process. Compared with the previous adaptive time-frequency analysis method, the BMD method can separate the "sharp angle" wideband effective signal and local narrowband signal from the complex non-stationary signal, and realize the feature extraction of the effective mode in the wide band range.

In this paper, the direct characteristic information of arc signal during aluminum alloy double-pulse MIG welding is analyzed through the electric arc signal test experiment. The collected arc current signal is decomposed by BMD, and the distortion components of the current waveform with different frequencies are obtained. On this basis, the composite multiscale fuzzy entropy calculation (CMFE) is carried out, which provides a new experimental method and reference for the stability analysis of arc signal and welding quality evaluation of the aluminum alloy double-pulse MIG welding process.

2. Test platform

To study the characteristics of electric arc signals during welding, the experimental platform for electric arc signal testing of aluminum alloy double-pulse MIG welding in the process can not only accurately and conveniently collect electric arc signals online, but also detect and analyze arc stability and weld forming quality. This paper introduces in detail the experimental setup for aluminum alloy MIG welding and arc electric signal testing, focusing on aluminum alloy double-pulse MIG welding as the experimental subject.

2.1. The overall composition of the experimental platform

The aluminum alloy double-pulse MIG welding experiment and arc electric signal test platform setup are shown in **Figure 1**. The test platform comprises a double-pulse metal inert gas (DPMIG-500) welding machine, welding robot, wire feeding mechanism, argon tank, and arc signal data acquisition system. The experiment involves using the DPMIG-500 welding machine and welding robot for a double-pulse MIG welding surfacing experiment. The workpiece material is 6061 aluminum alloy with dimensions of 250 mm × 200 mm × 5 mm. The welding parameters include an argon flow rate of 10 L/min, dry extension of welding wire 15 mm, welding wire model ER5356, and welding wire diameter of φ1.2mm. The specific functions of each component are shown in **Table 1**.

The aluminum alloy MIG welding arc electric signal data acquisition system includes current and voltage sensors, data acquisition cards, and computers for storing and analyzing data. Through the MIG welding system, the welding current and voltage, the welding speed and the start and stop functions of the welding machine can be set respectively. The welding current and voltage signals are sent to the collection box through the hall current sensor and the electrical isolation voltage sensor is arranged in the transmission box. After processing by the acquisition system, it is transmitted to the computer by ethernet interface for oscilloscope and storage. The sampling frequency is 12 kHz, sampling 25 s per welding process, 24,000 data points were intercepted for

BMD decomposition and frequency analysis.

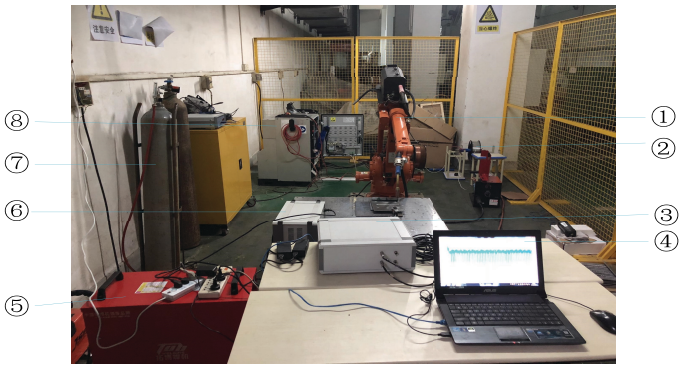


Figure 1. MIG welding experiment and test platform with (1) welding robot (2) wire feeder (3) arc signal data acquisition box (4) computer (5) welding machine (6) arc sensor box (7) argon gas storage tank 8) power supply

Table 1. Main components and functions of the experimental platform

Item	Function
DPMIG-500 aluminum welding machine	Responsible for setting welding process parameters such as welding peak voltage, welding base value voltage, welding peak current, welding base value current, duty cycle, welding frequency, and starting and stopping welding experiments.
ABB IRB1410 Industrial Robot	Control welding speed and other sizes and travel direction.
Data acquisition system	Including a sensor box, acquisition box, computer, and communication cable. For high speed and accurate storage of welding arc data.
Wire feeder	Includes wire feed tray and wire feed controller. Manual wire feeding and automatic wire feeding are available for choice.
Argon gas storage tank	Inert gas argon is provided while the wire is transported. To isolate air outside the welding area and prevent oxidation.

2.2. Double-pulse MIG welding process experiment

At different welding process parameters, the welding current signal collected synchronously during the welding process is transmitted to the industrial computer for display and storage. The collected signals are analyzed and processed with the help of MATLAB software with specific data points extracted from the DP-MIG welding current signal for detailed analysis. The welding parameters are shown in **Table 2**.

Table 2. DP-MIG process parameters

Experimental sequence number	Welding speed (mm/s)	Spike current (A)	Base current (A)	Spike voltage (V)	Base voltage (V)	Duty ratio (%)	impulse frequency (Hz)
1	1	50	40	21	17.5	50	2
2	1.5	50	40	21	17.5	50	2
3	5	50	40	21	17.5	50	2
4	5	60	40	21	17.5	50	5

Four sets of different welding process parameters were selected for double-pulse MIG welding to analyze their respective effectiveness and welding process stability. The appearance of weld formations from each experimental group is depicted in **Figure 2** respectively. **Figure 3** shows the waveform diagram of the DP-MIG welding current signal.

As shown in **Figure 2**, there is a biting phenomenon at the tail of the weld surface of experiment No. 1. The weld surface of experiment No. 3 has obvious welding defects such as lack of penetration, lack of fusion, and poor surface forming. Weld surfaces of experiments No. 2 and No. 4 formed well.

The appearance of weld No. 1 is shown in **Figure 3(a)**. Initially, the weld exhibited a uniform fish scale pattern, indicating overall good formation. However, towards the end of the weld, there was some edging observed. The weld surface appeared angular, irregular, and slightly sunken. Analysis of the intercepted 2 s welding arc current signal revealed the following: In the low-frequency pulse phase, welding commenced with automatic wire feeding, forming an arc that joined the molten pool. The arc's impact caused the coarse crystals in the molten pool to break up, achieving grain refinement. As the welding frequency in the low-frequency pulse group increased, further stirring occurred inside the molten pool, refining the weld grain. The corresponding welding arc current signal is sparse. In the high-frequency pulse group phase, the welding wire melted, and droplets formed and transitioned into the molten pool. The corresponding welding arc signal showed periodic transformation.

The appearance of weld No. 2 is presented in **Figure 3(b)**. The whole weld showed a uniform and regular fish scale pattern, but the spacing between the fish scale pattern is larger than that of weld No. 1. Analysis of the intercepted 2 s welding arc current signal revealed that in the low-frequency pulse phase, welding slowly started to arc with automatic wire feeding where the arc joins the molten pool. The impact of the arc caused the coarse crystals in the molten pool to break up to achieve the effect of grain refinement. The increase of welding frequency in the low-frequency pulse phase further stirred the inside of the weld pool, refining the weld grain and the corresponding welding arc current signal showed sparse phenomenon. In the high-frequency pulse phase, the welding wire melted and droplets slowly formed and transitioned into the molten pool. The corresponding welding arc signal presents a periodic change, but the stirring time is too long in the initial formation of the molten pool, so the distance between the figure of the fish scale pattern is large.

The appearance of weld No. 3 is shown in **Figure 3(c)**. There are obvious welding defects such as lack of penetration, lack of fusion, and poor surface forming on the surface of the whole weld. Analysis of the intercepted 2 s welding arc current signal presented that in the low-frequency pulse phase, the welding current signal is first dense and then sparse. In the high-frequency pulse phase, the current distribution is relatively uniform and dense. Thus, in a single cycle, the molten pool is formed in the low pulse group and with a large size. However, in the high pulse group, the transition density of molten drops is too large and concentrated together to form the welding hump defect. In the double-pulse MIG welding cycle of about 1.1 s and 1.5 s, the welding seam has an obvious arc-breaking phenomenon in the current waveform, hence the weld surface forms defects.

The appearance of weld No. 4 is shown in **Figure 3(d)**. The whole weld shows a uniform and regular fish scale pattern. However, the spacing between the fish scale pattern is larger than that of weld No. 1 and No. 2. Analysis of the intercepted 2 s welding arc current signal showed that in the low-frequency pulse phase, welding begins to arc slowly with automatic wire feeding where the arc joins the molten pool. The impact of the arc causes the coarse crystals in the molten pool to break up, achieving grain refinement. The welding frequency in the low-frequency pulse group increased to further stir the inside of the molten pool, refining the weld grain. The corresponding welding arc current signal is sparse. In the high-frequency pulse phase, the welding wire is melted and the molten droplets are slowly formed and transferred into the molten pool. The corresponding welding arc signal presents a periodic transformation. However, the stirring time is short at the initial stage of molten pool formation, thus the spacing between the figure of fish scales is larger.

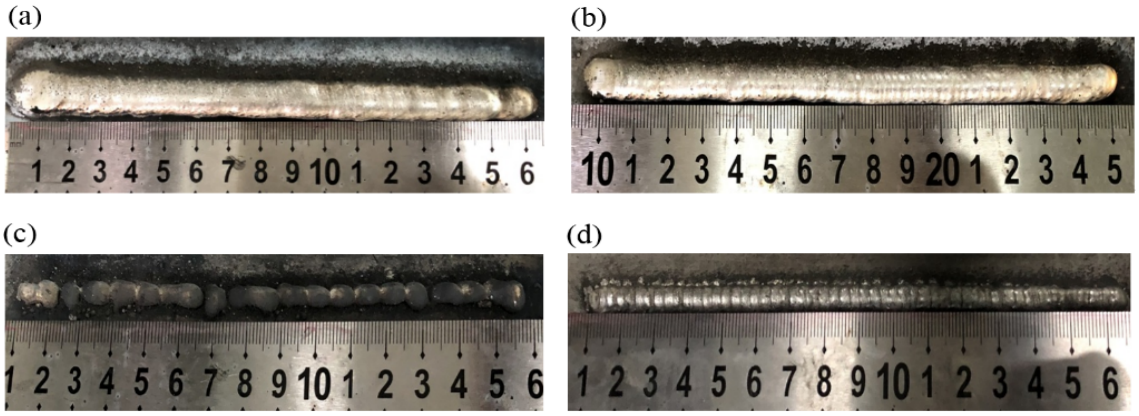


Figure 2. DP-MIG weld appearance molding

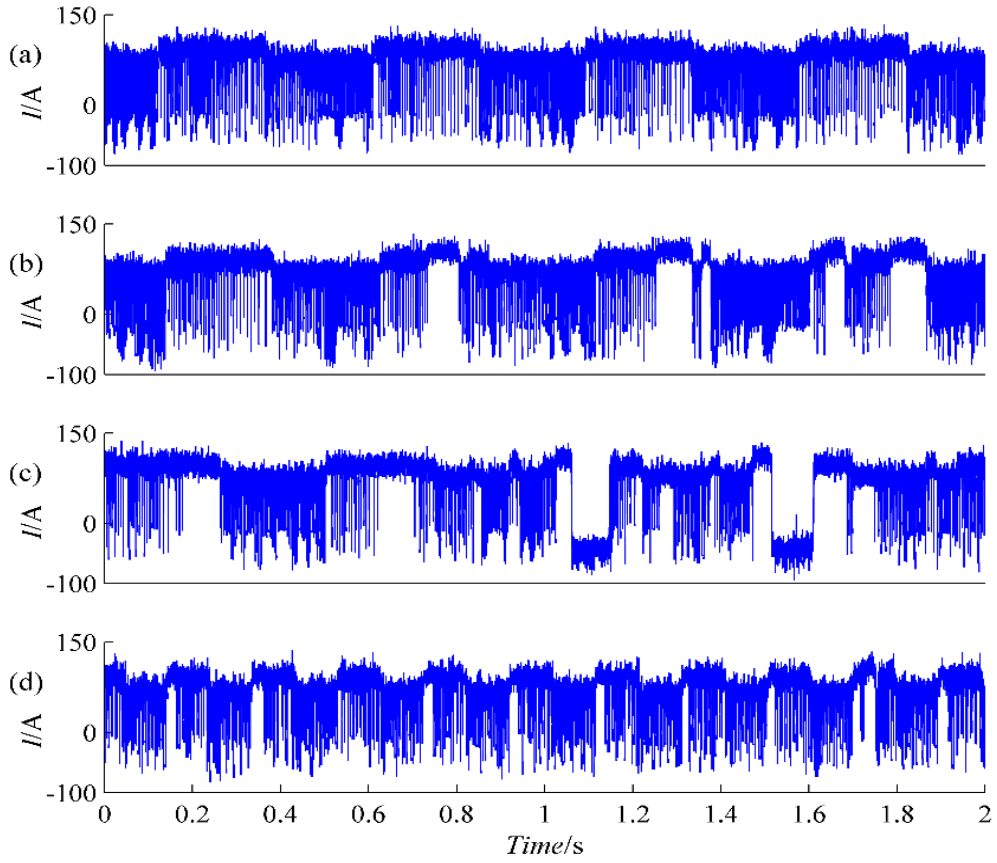


Figure 3. Waveform of DP-MIG welding current signal

3. Processing and analysis of experimental results

3.1. Welding arc signal decomposition based on BMD

BMD can effectively separate wideband signals such as square waves, sharp waves, and narrow band signals composed of sine waves from the complex non-stationary direct current signal.

For signals$x(n)$, the iterative process of the BMD method is as follows:

(1) Command $r_0(n)=x(n)$.

(2) Filter out the DC component of the signal, intrinsic mode function (IMF): $IMF_0(n)=IFFT[r_0(1)]$, where $r_0(1)$ is the first component obtained by the Fourier transform of $r_0(n)$, and command $r_1(n)=x(n)-IMF_0(n)$.

(3) Command i=1, the following constrained optimization problem P1 is established:

$$P1: Minimize \quad T_1(A_1,\omega_1,\theta_1,D_1),T_2(A_2,\omega_2,\theta_2,D_2),T_3[A_3(n),\omega_3,\theta_3(n)] \tag{1}$$

$$S.T.\ x(n)=\sum_{i=0}^{N} IMF_i(n)+res(n),\ \theta_i\in[0,\ 2\pi],\ D_i\in[0,\ 1]$$

therein:

$$T_{j(j=1,2)}=\left\|D^{(2)}\left[IMF_i^j(n)\right]\right\|_2^2+\lambda\left\|D^{(2)}\left[x(n)-IMF_i^j(n)\right]\right\|_2^2 \tag{2}$$

$$IMF_i^1(n)=A_1 square(\omega_1 n+\theta_1,D_1) \tag{3}$$

$$IMF_i^2(n)=A_2 sawtooch(\omega_2 n+\theta_2,D_2) \tag{4}$$

$$IMF_i^3(n)=A_3(n)\cos[\omega_3+\theta_3(n)] \tag{5}$$

(4) The optimization problem P1 is solved by the ACROA algorithm, to get the best $T_{j(j=1,2,3)}$, then find the smallest number with T_1, T_2 and T_3, $T_{j(best)}$, command $IMF_i(n)=IMF_i^{j(best)}(n)$ [11].

(5) Command $r_{i+1}(n)=r_i(n)-IMF_i(n)$.

(6) Determine whether the decomposition results meet the iteration termination condition $\frac{\left\|IMF_i(n)-IMF_{i-1}(n)\right\|_2^2}{\left\|IMF_{i-1}(n)\right\|_2^2}\le\varepsilon$, if yes, end the iteration process and set i=i+1, if not, return to step (3).

IMF1 and IMF2 obtained by current signal decomposition using the BMD method are shown in **Figure 4**. The BMD effectively separates the square wave components from the signal, the peak-to-peak value and pulse frequency of IMF1 obtained by decomposition are consistent with the peak-to-peak value of the square wave current signal set in **Table 2**. The decomposed IMF2 retained the nonlinear information and distortion information related to weld quality. **Figure 5** shows the instantaneous amplitude (IA) and instantaneous frequency (IF) of IMF2 obtained by the decomposition of 2 s signal intercepted in experiments No. 1–4.

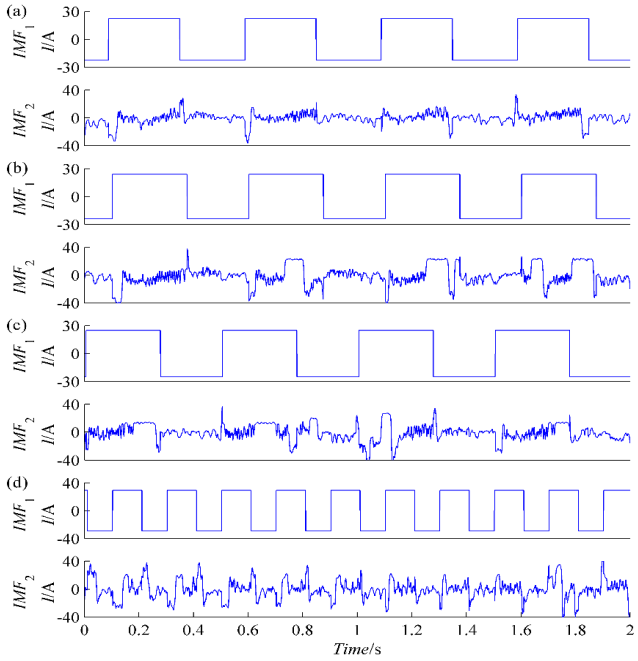


Figure 4. IMF1 and IMF2 obtained by BMD decomposition of current signals, (a)–(d) are the decomposition results of the interception 2 s of experiments No. 1–4

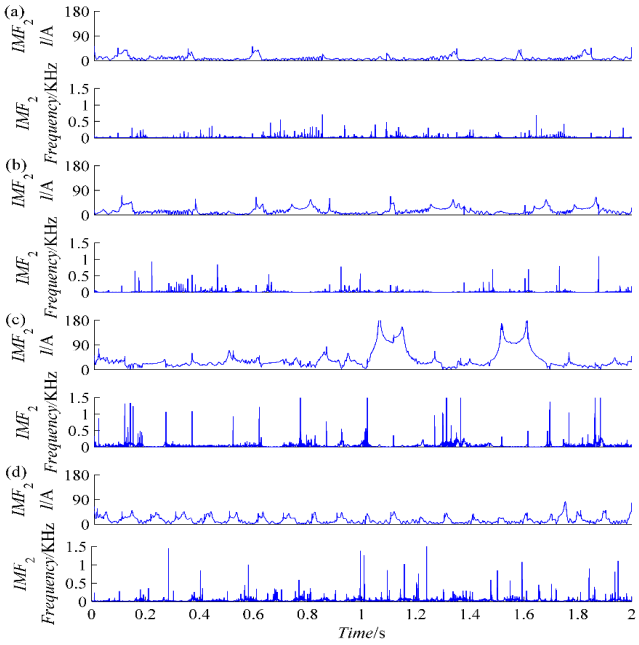


Figure 5. Time-frequency analysis of current signal BMD decomposition results (a)–(d) are the IA and IF of IMF2 components obtained by 2 s decomposition of experiments No. 1–4 current signal interception

Experiments No. 1, 2, and 3 showed consistent duty cycle and pulse frequencies in the welding current signal, each conducted at varying welding speeds. **Figure 5(c)** illustrates noticeable instantaneous amplitude changes in the time-domain waveform of the current during experiment No. 3. This is caused by the arc-breaking phenomenon due to poor welding quality. The time-frequency distributions in **Figure 5(a)–(c)** reveal that with increased welding speed, arc energy rises, leading to a significant increase in frequency component. Experiments No. 3 and 4 explored welding current signals under identical welding speed and duty cycle conditions, but with different pulse frequencies. In experiment No. 4, the time-frequency information of the IMF2 component from the intercepted signal appears more stable. This is because the arc energy in the welding process is more concentrated at higher pulse frequencies, resulting in better welding quality.

3.2. Calculation and analysis of characteristic parameters of aluminum alloy double-pulse MIG welding signal

After the signal decomposition using the BMD method, it is necessary to select a suitable eigenvalue to evaluate the effective component of the electrical signal. In this paper, the compound multiscale fuzzy entropy (CMFE) recently proposed by Jin *et al* is used to evaluate the power quality of welding inverters at different welding speeds and pulse frequencies [12].

In the CMFE algorithm, to address the impact of shorter time series on fuzzy entropy calculation in during coarse-graining, the mean fuzzy entropy value of different coarse-grained sequences with the same scale factor is used as the fuzzy entropy value for that scale factor [13].

CMFE calculation steps are as follows:

(1) For time series $\{x(i), i = 1, 2, \cdots, N\}$, define different coarse-grained sequences $y_k^{(\tau)} = \left\{ y_{k,1}^{(\tau)}\ y_{k,2}^{(\tau)} \cdots y_{k,p}^{(\tau)} \right\}$, mean:

$$y_{k,j}^{(\tau)} = \frac{1}{\tau} \sum_{i=(j-1)\tau+k}^{j\tau+k-1} x_i,\ 1 \le j \le N/\tau, 1 \le k \le \tau \tag{6}$$

(2) For each scale factor τ, the fuzzy entropy of each coarse-grain sequence $y_k^{(\tau)} (1 \le k \le \tau)$ is calculated,

then to average τ entropy, CMFE at this scale factor is obtained:

$$CMFE(X,\tau,m,n,r)=\frac{1}{\tau}\sum_{k=1}^{\tau}FuzzyEn(y_k^{(\tau)},m,n,r) \tag{7}$$

CMFE synthesizes the fuzzy entropy information of all coarse-grained sequences at the same scale. CMFE curves reflect the complexity of time series under different scale factors. For a direct current signal, the greater the calculated fuzzy entropy, the more ambiguous it is, the less stable the data, and the worse its power quality. Conversely, the lower the fuzzy entropy, the less ambiguous it is, the more stable the data, the better the power quality. The welding current signals collected in each experiment were divided into 25 groups of data at equal intervals. The duration of each set of data is 1 s, the composite multi-scale fuzzy entropy is calculated ($\tau=2$). The calculation results are shown in **Figure 6**, and the average value of composite multiscale fuzzy entropy for each group of experiments is shown in **Table 3**.

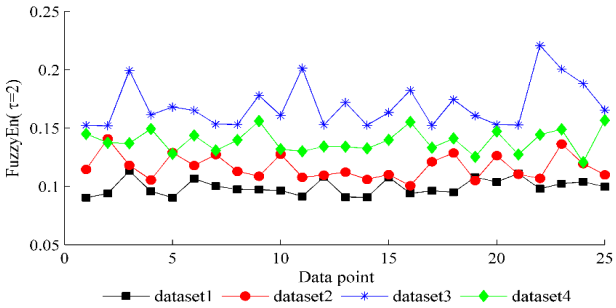


Figure 6. Composite multiscale fuzzy entropy of IMF2 component obtained from BMD decomposition of experiments No. 1–4 current signal

Table 3. The average composite multiscale fuzzy entropy of each group of experiments

Experiment number	1	2	3	4
Calculated entropy	0.0993	0.1166	0.1694	0.1388

As seen from **Table 2** and **Table 3**, the compound multi-scale fuzzy entropy increases with the increase of welding speed. This is because as the welding speed increases, the arc stability in the welding process relatively decreases, making the degree of electrical energy dispersion increase, and causing arc breakage. Thus the composite multiscale fuzzy entropy of the corresponding welding current signal increases. The weld in experiment No. 3 has an obvious arc breakage in the current waveform as it is easy to arc during the welding process, hence the entropy value is large.

At the same welding speed, duty cycle, and welding voltage, among other factors, different frequencies exhibit reduced complexity in multiscale fuzzy entropy calculation. This indicates the arc is more stable. This stability arises because, with increased frequency, the welding speed matches the frequency, leading to periodic alignment of the welding waveform. This concentrates the arc energy during the welding process, resulting in a corresponding decrease in composite multiscale fuzzy entropy of the welding current signal.

4. Conclusion

(1) In aluminum alloy double-pulse MIG welding speed, a change in frequency will result in a different distribution of arc energy in the time and frequency domains, and thus the stability of welding arc and weld forming quality are affected. Therefore, by reasonable matching of aluminum alloy MIG welding

current waveform parameters, it can effectively obtain a uniform distribution of arc energy in the time domain and frequency domain. This ensures the stability of the welding process and obtains good welding results.

(2) The BMD method is a new adaptive decomposition method suitable for the processing of non-stationary signals. Through the aluminum alloy double-pulse MIG welding arc electric signal test, real-time arc signal information reflecting the welding process was obtained. The BMD method was applied to extract the characteristic information of the electric arc signal. It can effectively separate different frequency DC components, pulsed square wave current, and current signal distortion components of double-pulse MIG welding. The composite multiscale fuzzy entropy is used to calculate the distortion component. The results showed that the BMD method combined with composite multiscale fuzzy entropy can effectively evaluate the signal quality of the welding inverter.

Funding

The 2024 University-level Higher Education Teaching Reform Project of Guangzhou Xinhua University, "Teaching Reform and Practice Based on OBE Concept: A Case Study of "University Physics Experiment" (Project No. 2024J044)

Disclosure statement

The authors declare no conflict of interest.

Author contributions

Conceptualization: Yin Si
Investigation: Yin Si, Zixiong Xia
Formal analysis: Wei Liu, Kexin Zhang, Xiangyu Song
Writing: Wei Liu, Kexin Zhang, Xiangyu Song

References

[1] Basheer UM, Noor AFM, Zuhailawati H, et al., 2013, Advances in friction welding process: A review. Science and Technology of Welding and Joining, 15(7): 534–558.

[2] Kimapong K, Watanabe T, 2005, Effect of Welding Process Parameters on Mechanical Property of FSW Lap Joint between Aluminum Alloy and Steel. Materials Transactions, 46(10): 2211–2217.

[3] Karthikeyan R, Balasubramanian V, 2012, Optimisation and sensitivity analysis of friction stir spot-welding process parameters for joining AA 6061 aluminum alloy. International Journal of Manufacturing Research, 7(3): 257–272.

[4] Li Y, Zhao Y, Zhou X, et al., 2021, Effect of Droplet Transition on the Dynamic Behavior of the Keyhole during 6061 Aluminum Alloy Laser-MIG Hybrid Welding. The International Journal of Advanced Manufacturing Technology, 119: 897–909. https://doi.org/10.1007/s00170-021-08270-1

[5] Wang JB, Nishimura H, Katayama S, et al., 2008, Study of Laser-MIG Hybrid Welding of Aluminum Alloy. Preprints of the National Meeting of JWS, 2008: 105. https://doi.org/10.14920/jwstaikai.2008s.0.5.0

[6] Wang Y, Wei B, Guo Y, et al., 2017, Microstructure and mechanical properties of the joint of 6061 aluminum alloy by plasma-MIG hybrid welding. China Welding (English Edition), 26(002): 58–64.

[7] Czerwinski RN, Jones DL, 1995, Adaptive cone-kernel time-frequency analysis. Signal Processing IEEE Transactions on Signal Processing, 43(7): 1715–1719.

[8] Hou TY, Shi Z, 2011, Adaptive Data Analysis via Sparse Time-Frequency Representation. Advances in Adaptive Data Analysis, 3(1–2): 1–28. http://dx.doi.org/10.1142/S1793536911000647

[9] Wang XK, Gao JH, He YY, 2010, Time-frequency analysis based on time-frequency-adaptive optimal-kernel. Systems Engineering and Electronics, 32(1): 22–26.

[10] Enghardt L, Moreau A, Tapken U, et al., 2013, Radial Mode Decomposition in the Outlet of a LP Turbine–Estimation of the Relative Importance of Broadband Noise. Journal of Health Communication, 19(4): 392–412.

[11] Alatas B, 2011, ACROA: Artificial Chemical Reaction Optimization Algorithm for global optimization. Expert Systems with Applications, 38(10): 13170–13180.

[12] Jin Z, Xiao Y, He D, et al., 2023, Fault diagnosis of bearing based on refined piecewise composite multivariate multiscale fuzzy entropy. Digital Signal Processing, 2023: 133.

[13] Zheng J, Pan H, Cheng J, 2017, Rolling bearing fault detection and diagnosis based on composite multiscale fuzzy entropy and ensemble support vector machines. Mechanical Systems and Signal Processing, 85: 746–759.

Publisher's note

Bio-Byword Scientific Publishing remains neutral with regard to jurisdictional claims in published maps and institutional affiliations.

Journal of Electronic Research and Application, 2024, Volume 8, Issue 4
http://ojs.bbwpublisher.com/index.php/JERA
ISSN Online: 2208-3510
ISSN Print: 2208-3502

An Underwater Robot Inspection Anomaly Localization Feedback System Based on Sonar Technology

Siqiang Cheng[1], Yi Liu[1]*, Aibin Tang[1], Libin Yang[2]

[1]Department of Information Science and Engineering, Hunan University of Humanities, Science and Technology, Loudi 417000, China
[2]Huanan Xiangdian Test and Research Institute Co., LTD., Changsha 410000, China

***Corresponding author:** Yi Liu, 511214052@qq.com

Copyright: © 2024 Author(s). This is an open-access article distributed under the terms of the Creative Commons Attribution License (CC BY 4.0), permitting distribution and reproduction in any medium, provided the original work is cited.

Abstract: This article introduces an underwater robot inspection anomaly localization feedback system comprising a real-time water surface tracking, detection, and positioning system located on the water surface, while the underwater robot inspection anomaly feedback system is housed within the underwater robot. The system facilitates the issuance of corresponding mechanical responses based on the water surface's real-time tracking, detection, and positioning, enabling recognition and feedback of anomaly information. Through sonar technology, the underwater robot inspection anomaly feedback system monitors the underwater robot in real-time, triggering responsive actions upon encountering anomalies. The real-time tracking, detection, and positioning system from the water surface identifies abnormal conditions of underwater robots based on changes in sonar images, subsequently notifying personnel for necessary intervention.

Keywords: Underwater robots; Positioning feedback system; Sonar real-time tracking

Online publication: August 12, 2024

1. Introduction

Underwater robots are mainly divided into autonomous underwater vehicles (AUV) without cables and remotely operated underwater vehicles (ROV) with cables. These two types of underwater vehicles have been widely used in many fields [1-5]. The underwater robotics and applications (URA) laboratory at the University of Tokyo has developed many AUVs with different functions, such as "Twin-Burger", "PTEROA 150", and "PTEROA 250" [6]. A small intelligent underwater autonomous navigation robot is currently being developed by Northwestern Polytechnical University in China. In recent years, underwater positioning and navigation have been a technology that provides information on the posture, speed, position, and other aspects of underwater robots [7]. It is a prerequisite for underwater robots to complete various underwater tasks. In the report of the 18th National Congress of the Communist Party of China, the goal of building a maritime power was proposed [8]. However, the existing national spatial and gravity benchmarks have not effectively covered the ocean. The ocean geodetic

benchmarks and navigation technology are lagging behind the national social, economic, and defense strategies [9]. The development of underwater terrain matching methods based on sonar image processing technology is very important for expanding the underwater application range of terrain matching and improving the error correction ability of underwater navigation systems [10]. Sonar sensors are devices based on sound signals, including matching positioning technology based on seabed terrain and landform information. The technology is based on the detection, recognition, and classification of environmental features [11]. Side scan sonar has the advantages of a long operating period, wide coverage, strong penetration ability, and large data collection [12]. Since the 1980s, scientists produced various types of sonar products, and through optimizing their performance in various aspects, preliminary research has been conducted on sonar detection equipment that can display seabed topography and landforms [13]. Due to the complex and variable underwater environment in which the robot is located, it is prone to instantaneous positioning failure [14]. Several universities and research institutions, including the Shenyang Institute of Automation, Chinese Academy of Sciences, Harbin Engineering University, and Shanghai Jiao Tong University, have increased their investment in manpower and resources and strengthened their research efforts in underwater robot technology, especially in core navigation algorithms [15].

2. Overall design plan

As shown in **Figure 1**, the underwater robot inspection anomaly localization feedback system includes a real-time water surface tracking, detection, and positioning system set on the water surface, whereas the anomaly feedback system is housed inside the underwater robot. The underwater robot system sends corresponding mechanical signals for the water surface system to recognize and provide feedback on anomalies. The underwater robot inspection anomaly feedback system uses sonar to track the underwater robot in real-time. When the underwater robot encounters an anomaly, the system responds with appropriate actions. The real-time tracking, detection, and positioning system on the water surface identifies the types of anomalies in the underwater robot through changes in sonar images and notifies the staff to handle them. The real-time tracking, detection, and positioning system is installed on the hull to continuously monitor the underwater robot.

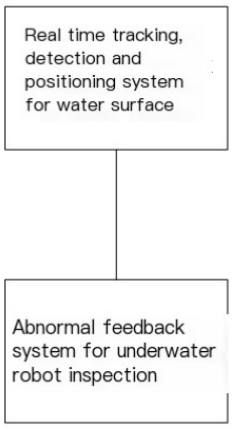


Figure 1. The overall design of the underwater robot inspection anomaly localization feedback system

3. Design scheme of underwater robot sample collection and processing subsystem

As shown in Figure 2, the underwater robot sample collection and processing subsystem includes an underwater

robot image acquisition unit, an underwater robot image processing unit, and an underwater robot contour map summary encoding unit.

The image acquisition unit is responsible for deploying the underwater sampling robot into the deep sea and determining its precise position through manual positioning. It collects sonar images from the seabed in a flat sea area using a sonar collection vessel. The vessel performs a circular motion around the underwater robot, with the radius of the motion increasing gradually. Images collected during each circular motion are saved separately, corresponding to the radius and seawater depth.

The image processing unit processes all sonar image sets, recognizing contours and edge lines to create a set of contour maps. Manual marking of the contours of the underwater sampling robot is performed, retaining the internal lines within the contours.

The contour map summary encoding unit organizes the collected contour maps into folders, encoding the specific azimuth and position information of the underwater sampling robot. Each contour map corresponds to a collection point relative to the robot's location. This unit also places each image on a two-dimensional coordinate axis, with the contour of the underwater sampling robot as the center point at the origin. Points on the contour are set as integer multiples of 64, and their polar coordinates are extracted. The polar coordinate function is obtained for all encoded contour maps, resulting in a polar coordinate function that represents the number of encoded contour maps and is a positive integer. If n is a positive integer greater than or equal to 1, all polar coordinates are used to derive the polar coordinate function. This results in a polar coordinate function for all encoded contour maps, with the number of encoded contour maps being a positive integer.

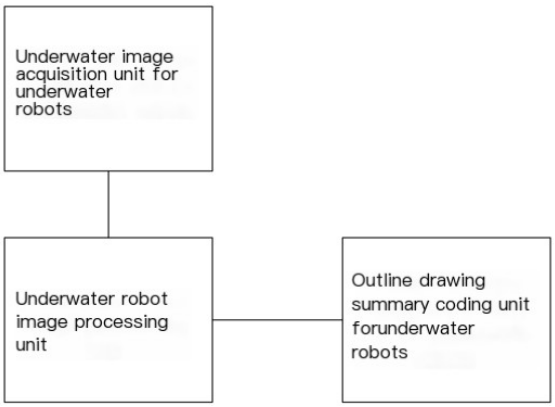


Figure 2. Sample collection and processing subsystem for underwater robots

4. Anomaly feedback system for underwater robot inspection

The underwater robot inspection anomaly localization feedback system includes an underwater robot unit, an anomaly category determination unit, and a shape change anomaly feedback unit, as shown in Figure 3. The underwater robot unit is the operating body of the underwater robot. The anomaly category determination unit is located inside the underwater robot unit, while the shape change anomaly feedback unit is situated on the outer layer.

The anomaly category determination unit continuously monitors images or videos from the underwater robot unit during inspections to identify any abnormalities. It also assesses the electrical power and overall performance of the underwater robot unit in real-time. If a fault occurs or a predefined abnormal object is detected during inspection, the anomaly category determination unit alerts the shape change anomaly feedback unit.

The shape change anomaly feedback unit responds by altering the shape of the shell or extending a marking action rod based on the type of abnormality detected. This change is then communicated to the real-time tracking and detection positioning system on the water surface.

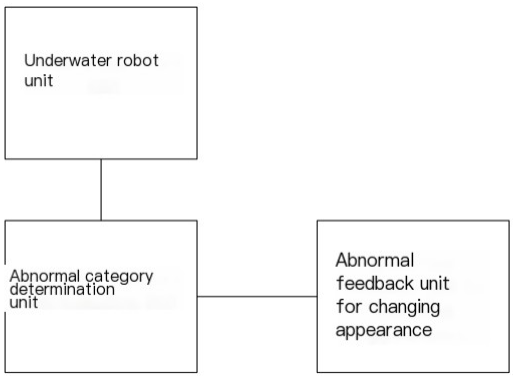


Figure 3. Abnormal feedback system for underwater robot inspection

5. Summary

This article presents the design of an underwater robot inspection anomaly localization feedback system consisting of a real-time water surface tracking, detection, and positioning system. This integrated system facilitates the acquisition of comprehensive underwater contour data for robots, offering a streamlined calculation process enabling real-time positioning and tracking capabilities.

Disclosure statement

The authors declare no conflict of interest.

References

[1] Xu Y, Li P, 2011, Development Trends of Underwater Robots. Nature Journal, 33(3): 125–132.

[2] Yuh J, 2000, Design and Control of Autonomous Underwater Robots: A Survey. Autonomous Robots, 8(1): 7–24. https://doi.org/10.1023/A:1008984701078

[3] Antonelli G, Pascal M, 2003, Underwater Robots: Motion and Force Control of Vehicle-Manipulator Systems, Springer Tracts in Advanced Robotics, Vol 2. Applied Mechanics Reviews, 6(6): B81. https://doi.org/10.1115/1.1623755

[4] Liu Q, 2021, Research and Implementation of Underwater Robot Positioning and Navigation Technology Based on Dual Inertial Navigation, thesis, Yangzhou University.

[5] Lu Y, 2006, Research on Real Time Motion Planning Method for Underwater Robots in Current Environment, thesis, Harbin Engineering University.

[6] Jia Z, 2004, Research on Simulation Model and Positioning System of Underwater Robots, thesis, Nanjing University of Technology.

[7] Fan G, Zhang Y, Zhao H, Li B, 2022, Development Status and Analysis of Underwater Robot Positioning and Navigation Technology. Journal of Weapon Equipment Engineering, 43(03): 22–29.

[8] Liu N, 2020, Research on Underwater Sound Velocity Correction Algorithm and Precision Positioning Method, thesis, Chang'an University. https://doi.org/10.26976/d.cnki.gchau.2020.000365

[9] Song Z, 2017, Research on Underwater Terrain and Landform Matching Localization Method Based on Sonar Image Processing, thesis, Harbin Engineering University.

[10] Zhang J, 2018, Research on the Application of Noise Estimation Algorithm in Side Scan Sonar Image Denoising, thesis, First Institute of Oceanography, Ministry of Natural Resources (MNR) of China.

[11] Fu N, 2019, Research on classification method of seabed sediment types based on sonar image features, thesis, Harbin Engineering University.

[12] Gao M, 2014, Design of underwater robot combined positioning based on vision and inertial navigation, thesis, Zhejiang University.

[13] Yang Y, Wang YB, Yang ZY, et al., 2024, Research on the classification of seabed sediments sonar images based on MoCo self-supervised learning. Journal of Physics: Conference Series, 2718: 012058.

[14] Shang C, Wang W, Xie G, et al., 2013, Overview of Underwater Robot Positioning Methods. Ordnance Automation, 32(12): 46–50.

[15] Ren C, 2010, Simultaneous localization and map construction algorithm and implementation of autonomous underwater robots, thesis, Ocean University of China.

Publisher's note

Bio-Byword Scientific Publishing remains neutral with regard to jurisdictional claims in published maps and institutional affiliations.

Journal of Electronic Research and Application, 2024, Volume 8, Issue 4
http://ojs.bbwpublisher.com/index.php/JERA
ISSN Online: 2208-3510
ISSN Print: 2208-3502

Tactile Paving Recognition Method Based on Improved YOLOv7

Chengyi Shi[1], Qun Zhao[1]*, Nan Fang[1], Yufeng Mao[2]

[1]School of Computer Engineering, Nanjing Institute of Technology, Nanjing 211167, China
[2]NR Electric Co., Ltd., Nanjing 211102, China

Corresponding author: Qun Zhao, qunzhaoqz@outlook.com

Copyright: © 2024 Author(s). This is an open-access article distributed under the terms of the Creative Commons Attribution License (CC BY 4.0), permitting distribution and reproduction in any medium, provided the original work is cited.

Abstract: Tactile paving is a professional road facility to ensure the safe travel of people with visual impairment. However, there are many problems with tactile paving travel in practice. For one, some tactile paving is seriously damaged, and the other is the accumulation of obstacles. How to help visually impaired people recognize and locate obstacles in tactile paving is a problem worth studying. In this paper, image recognition technology is used to recognize the tactile paving pictures with obstacles, and an attention mechanism is used to optimize samples to improve recognition accuracy.

Keywords: YOLOv7; Tactile paving recognition; Attention mechanism

Online publication: August 12, 2024

1. Technology background

In China, there are approximately 17 million people with visual impairments, accounting for 1% of the total population. With the development of modern society, most people with visual impairments mainly rely on blind canes, assistive devices, etc. to carry out their daily lives and improve their quality of life. To enable the visually impaired to walk safely outside, this paper conducts relevant research on the current tactile paving facilities and tactile paving obstacle recognition.

In the field of computer vision, object recognition is an important issue [1]. Some methods transfer objects to visually impaired individuals through one-dimensional data drawing, while others solve the problem of interaction between visually impaired individuals and the surrounding environment through the real value local dissimilarity mapping method in the measurement of inter-frame dissimilarity in images. However, in practical applications, object detection may vary in different scenarios [2]. Therefore, based on the differences in the regional distribution of different tactile paving, this paper proposes a tactile paving recognition method based on You Only Look Once (YOLOv7). At the same time, based on the attention mechanism, a top-down information screening method is used to screen out a large amount of irrelevant information, and computer resources are allocated to more meaningful work to improve the ability of neural networks to process information [3].

2. Related works

To assist visually impaired individuals in controlled environments such as hospitals and homes, Kim *et al.* proposed a new assistive device that uses data beyond one dimension to depict objects for blind individuals [4]. Additionally, the output-only program proposed by Hossein and Alireza can effectively assist blind people in extracting seismic input motion and identifying systems with severe permutation patterns [5]. To achieve an assistive device that allows blind people to adapt quickly, Alsayaydeh *et al.* built automated hardware using Raspberry Pi, aiming to enable visually impaired individuals to immediately detect objects or people in front of them and inform them of what is in front of them using audio [6]. Compared to the above-mentioned blind assistance methods, the smart home model proposed by Tayyaba *et al.* for safe and stable movement of blind people can enable them to complete daily activities without wearing heavy equipment [7]. This model uses fuzzy logic for simulation, and the output of Internet of Things (IoT) devices composed of sensors and Bluetooth serves as the input of the fuzzy controller. The output communicates through IoT devices to assist blind people or users in safe movement.

For the object detection model, this article chooses YOLOv7 as the basis. Before this, Qi and Gao proposed an improved YOLOv7 object detection model [8]. Combining the idea of feature separation and merging improves the Multi-Path Convolution (MPConv) module in the YOLOv7 network model. In addition, Wang *et al*. proposed an automatic dataset expansion method for transmission line defect detection based on the improved YOLOv7 algorithm, which can use a small number of images to establish a transmission line defect dataset [9]. Cao *et al.* also proposed an improved night pedestrian detection algorithm for YOLOv7 [10]. In the improved algorithm, the YOLOv7 tiny network is used as the baseline to meet both accuracy and high detection speed. Mao also proposed an automated road defect detection algorithm based on the YOLOv7 distillation model, which combines the advantages of high object detection accuracy and fast speed [11]. Zhang *et al.* proposed a three-dimensional detection method for autonomous driving platforms based on roadside monocular cameras [12].

3. Research methods

The YOLOv7 algorithm consists of three parts: input, backbone network, and prediction head. The backbone network adopts an efficient aggregation network structure, which allows the network to learn more features by controlling the shortest and longest gradient paths. The environment of tactile paving is complex, and some are seriously damaged or have obstacles piled up, which sometimes blocks the target tactile paving [13]. After the original image is normalized in size, the effective part of the target tactile paving will be smaller. Because the shallow features of the convolutional neural network have more local information, it is easy to cause the key information of the deep feature map to lose the tactile paving part after multiple convolution operations, thus causing false recognition. Given the above problems, this paper improves the YOLOv7 model. To improve the model's ability to extract tactile paving features in different situations, a convolutional attention module is added to the backbone network, to improve the network's attention to the target area of interest in the input image.

3.1. Multi-scale feature fusion

When facing the tactile paving and ordinary road with a small color difference, the original network structure cannot extract the local features of small occlusion well and fuse them, which results in the loss of local information of the tactile paving and the false recognition of tactile paving. YOLOv7 extracts key features from the 80 × 80, 40 × 40, and 20 × 20 feature maps in the backbone network, and performs feature fusion. To better

distinguish the tactile paving from the ordinary road and improve the accuracy of classification and recognition, a 160 × 160 feature scale is added to the original three scales. This method outputs the extracted features on the original 160 × 160 feature map of the backbone network and fuses the scale features with the original three scale features.

3.2. Convolutional Block Attention Module (CBAM) attention mechanism

The road condition of tactile paving is complex. Due to the influence of tactile paving damage, obstacle accumulation, and other factors, many interference messages appear in the picture. The attention mechanism is a dynamic selection process for important information input into an image, which is achieved through feature adaptive weights, focusing on important features of the image and suppressing unnecessary regional responses. Therefore, this article introduces the attention mechanism CBAM into YOLOv7.

The insertion position of the attention mechanism will also affect the performance of the network. In this paper, CBAM is embedded into the 11th, 24th, 37th, and 51st layers of the backbone network respectively, and the feature maps obtained from each layer of the network are used as the input feature maps. After the CBAM module, the weight of tactile paving features is added, and the feature maps are output, to further improve the ability to extract key features of the tactile paving under different feature scales, such as 160 × 160, 80 × 80, 40 × 40 and 20 × 20, which are represented by L-1 to L-4 respectively.

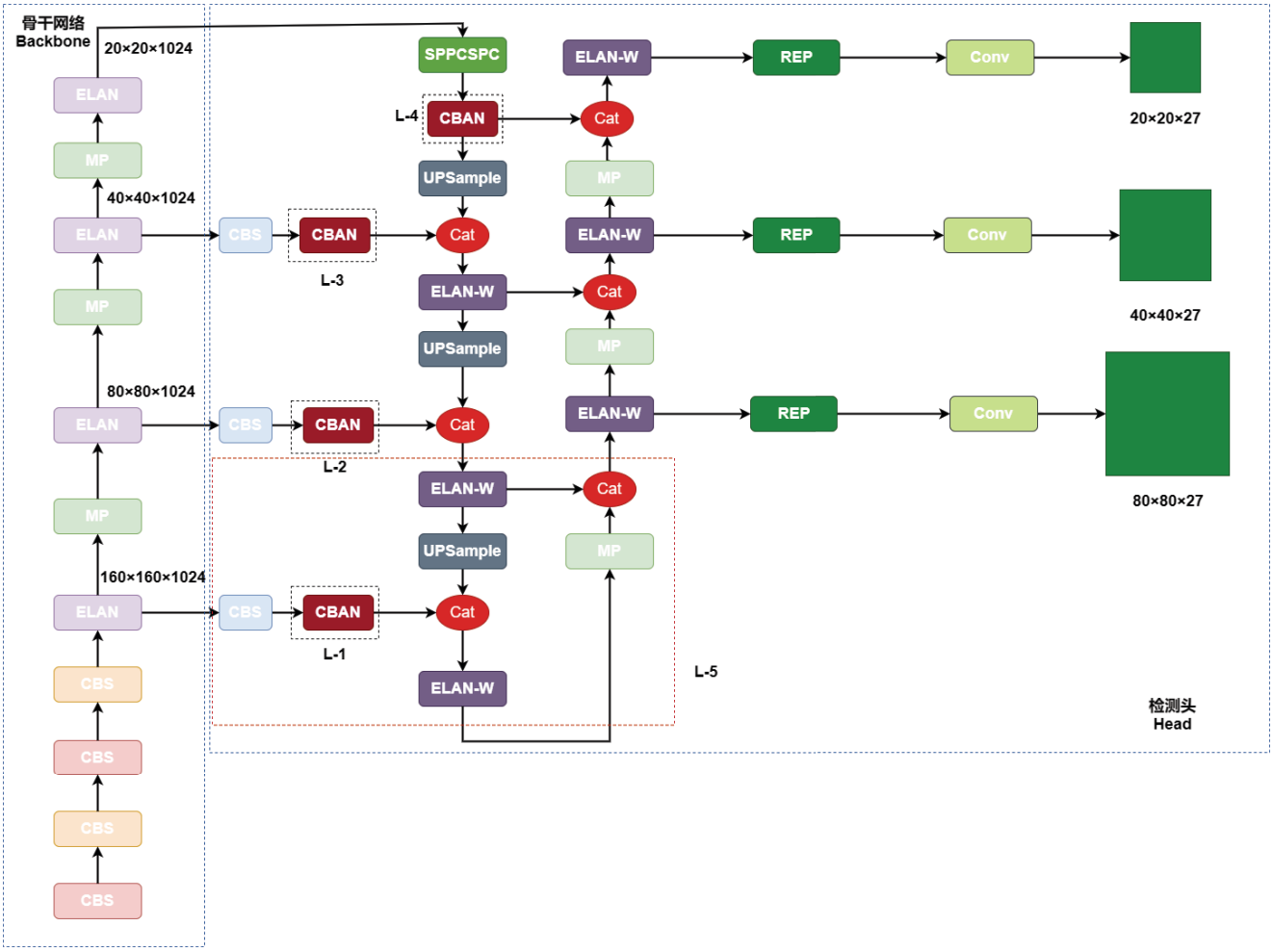


Figure 1. Improved YOLOv7 network model.

Note: L-1 to L-4 are the final addition positions of the CBAM module, and L-5 is the added 160 × 160 scale feature

4. Experiment

To evaluate the performance of the improved YOLOv7 algorithm for tactile paving recognition, this experiment conducted training and testing on the tactile paving dataset. The image data set collected in this paper comes from AI STUDIO and live scenes. The data set includes complete tactile paving, damaged tactile paving, and partially blocked tactile paving. As shown in Figure 2, use the LabelImg annotation tool to annotate. The format of the annotation information file is a text file, which contains information such as the category and bounding box of the target tactile paving. The total number of image sample data used in the experiment is 8,697. Among them, there are 6,221 training sets, 1,230 validation sets, and 1,246 test sets.



(a) Complete tactile paving (b) Damaged tactile paving (c) Covering tactile paving

Figure 2. Schematic diagram of tactile paving under different conditions

Due to limitations in experimental equipment, the input image size was scaled to 640 × 640 pixels, and the optimizer used Mini-Batch Gradient Descent (MBGD) with a learning rate of 1×10^{-2}, momentum of 0.9, and weight attenuation of 5×10^{-4}. The learning rate was adjusted using the MultiStepLR method. The batch size is 12, with a training duration of 200 epochs, alternating between 10 training epochs and 1 testing epochs.

The experiment uses the average recognition accuracy of all categories with mean average precision (mAP) at 0.5. The Intersection over Union (IoU) threshold is set to be greater than 0.5 as the evaluation indicator, and the parameters used include accuracy, recall, etc. [14].

The experiment compared the proposed algorithm with mainstream object detection methods YOLOv5, YOLOv7, and Region-based Convolutional Neural Network (RCNN). As shown in Table 1, the original YOLOv7 algorithm uses a Path Aggregation Feature Pyramid Network (PAFPN) for efficient fusion of features at different levels, but it cannot effectively handle the problem of target boundaries and angle periodicity. Therefore, compared to the original YOLOv7 model, the detection accuracy of our algorithm has been improved by 4.1 percentage points [15]. Among them, RCNN can accurately predict by adding rotation equivariant networks to extract equivariant features, but the detection accuracy is still 5.9% lower than the algorithm proposed in this paper. The sampling fusion network and loss function designed by YOLOv5 is good for small and messy target detection, but the detection effect for tactile paving is not as good as the algorithm in this paper. Experimental results show that the improved algorithm proposed in this paper has better detection performance on tactile paving data sets.

Table 1. Recognition accuracy of four methods applied to four different tactile paving

Methods	*P* (%)	*R* (%)	mAP at 0.5 (%)
YOLOv5	79.1	82.7	80.7
RCNN	81.5	77.2	79.2
YOLOv7	83.3	84.6	80.2
This article's algorithm	87.4	85.1	87.2

5. Conclusion

This paper proposes a tactile paving recognition method based on improved YOLOv7 to solve the problem of difficulty in recognizing tactile paving and obtaining information in different situations at present. By improving the multi-scale feature fusion network, this method is used to enhance the recognition sensitivity of the model to small local features, introduce the attention mechanism CBAM, improve the network's attention to the target area of interest in the input image, and improve the detection accuracy of the model to tactile paving in various situations. Compared with other typical algorithms, this method can effectively realize the recognition of tactile paving in different situations.

Funding

This work has been partially supported by the Jiangsu Province College Student Innovation Training Program (Project No. 20221127684Y) and the Talent Startup project of Nanjing Institute of Technology (Project No. YKJ202117)

Disclosure statement

The authors declare no conflict of interest.

References

[1] Yang J, Li H, Tian C, et al., 2021, Dynamic Histogram Equalization Algorithm Based on Adaptive Correction. Computer Engineering and Design, 42(5): 1264–1270.

[2] Wu X, Wu L, Wu Z, et al., 2018, A Fast Multi-Target Recognition and Synchronous Ranging Method for Visual Assistance of Blind People. Journal of Fuzhou University: Natural Science Edition, 46(4): 472–480.

[3] Wang L, Zhang L, Li S, Zhou G, 2019, Context Sensitive Question Answering Pairing Method Based on Attention Mechanism. Chinese Journal of Information Science, 33(1): 125–132.

[4] Kim JH, Park JE, Lee JM, 2020, 3-D Space Visualization System Using Ultrasonic Sensors as an Assistive Device for the Blind. IEEE Journal of Translational Engineering in Health and Medicine, 8: 2700305.

[5] Hossein J, Alireza G, 2022, Input Motion Extraction and Closely-Spaced Modes Recognition Through Partial System Identification: An Orthogonality-Aided Blind Source Separation Approach. Measurement, 2022: 200.

[6] Alsayaydeh JAJ, Irianto, Zainon M, et al., 2022, Intelligent Interfaces for Assisting Blind People Using Object Recognition Methods. International Journal of Advanced Computer Science and Applications (IJACSA), 13(5): 734–741.

[7] Tayyaba S, Ashraf MW, Alquthami T, et al., 2020, Fuzzy-Based Approach Using IoT Devices for Smart Home to Assist Blind People for Navigation. Sensors, 20(13): 3674.

[8] Qi L, Gao J, 2023, Based on the Improved Detection of Small Target YOLOv7. Computer Engineering, 49(01): 41–48. https://doi.org/10.19678/j.iSSN.1000-3428.0065942

[9] Wang Y, Shang J, Zhang Y, et al., 2023, Real-Time Transmission Line Defect Detection Method Based on Improved YOLOv7. Southern Power Grid Technology, 2023: 1–8.

[10] Cao Y, Li C, Peng Y, 2022, Night Pedestrian Detection Algorithm Based on Improved YOLOv7. Yangtze River Information and Communication, 35(10): 57–60.

[11] Mao J, 2023, Study on Algorithm of Road Defect Detection Based on YOLOV7 Distillation Model. Modern Manufacturing Technology and Equipment, 59(02): 222–224. https://doi.org/10.16107/j.cnki.mmte.2023.0084

[12] Zhang L, Wang W, Wang B, et al., 2023, A 3D Detection Method for Autonomous Driving Platforms Based on Roadside Monocular Cameras. Information and Computer, 35(2): 201–205

[13] Chen Y, 2023, Research on Small Object Detection Algorithm Based on Improved YOLOv7, thesis, Jiangsu University of Science and Technology.

[14] Xie J, Wang W, Liu T, 2021, Fabric Defect Detection Using Different Backbone Networks Based on YOLO v3 Algorithm. Measurement and Control Technology, 40(3): 61–66.

[15] Cao J, Lv J, Wu X, et al., 2021, A Fall Detection Algorithm Integrating Motion Features and Deep Learning. Computer Applications, 41(2): 583–589.

Publisher's note

Bio-Byword Scientific Publishing remains neutral with regard to jurisdictional claims in published maps and institutional affiliations.

Journal of Electronic Research and Application, 2024, Volume 8, Issue 4
http://ojs.bbwpublisher.com/index.php/JERA
ISSN Online: 2208-3510
ISSN Print: 2208-3502

Exploration of Energy-Saving Technologies in Building Electrical System Design

Yong Zhang[1]*

[1]CNNC Seventh Research and Design Institute Co., Ltd., Taiyuan 030032, Shanxi Province, China

***Corresponding author:** Yong Zhang, zhangyong@cnsi.ltd

Copyright: © 2024 Author(s). This is an open-access article distributed under the terms of the Creative Commons Attribution License (CC BY 4.0), permitting distribution and reproduction in any medium, provided the original work is cited.

Abstract: Green energy conservation is the mainstream trend in the current development of the construction industry. The application of energy-saving technology in building electrical system design can effectively reduce energy consumption, avoid unnecessary energy consumption, and truly achieve energy conservation and environmental protection. Based on this, the article elaborates on the principles of energy-saving design in building electrical systems, and actively explores the application of energy-saving technologies from different perspectives such as optimizing power supply and distribution system design, adopting high-efficiency energy-saving lighting equipment, applying renewable energy, promoting smart home technology, and improving the efficiency of building electrical equipment.

Keywords: Building electrical system design; Energy-saving technology

Online publication: August 12, 2024

1. Introduction

With the increasing global attention to environmental protection and sustainable development, green energy conservation has become a core issue in the development of the construction industry [1]. As an important component of building engineering, the application of energy-saving technology in building electrical design plays a crucial role in reducing building energy consumption, improving energy utilization efficiency, and reducing environmental pollution. This article aims to delve into the application of energy-saving technologies in building electrical design, to provide useful references for achieving green, low-carbon, and sustainable development in the construction industry [2].

2. Principles of energy-saving design for building electrical systems

The application of energy-saving technology in building electrical system design should follow the principles of economic practicality, practical demand, and environmental conservation [3].

2.1. Economic practicality

In energy-saving design of buildings, the first thing to pay attention to is the economy and practicality of electrical system design to ensure the economic benefits of the building project. Currently, with the continuous development of industrial technology, the types of electrical products on the market are not only diverse, but their functions are also becoming more complete, and their level of intelligence is also constantly improving [4,5]. However, when selecting electrical equipment, it is necessary to consider the actual needs of building design comprehensively and start from cost factors to choose electrical equipment and technology with higher cost-effectiveness [6].

2.2. Actual demand

In building electrical system design, the application of energy-saving technology also needs to meet the actual usage requirements of the building [7–9]. The purpose of electrical equipment and technology applications is to provide users with a better user experience, making people's work and life more convenient and efficient [10]. Therefore, in the energy-saving design of building electrical systems, full consideration should be given to the actual usage needs of the building, including stable circuit supply, public area lighting, etc. Based on meeting the basic application functions of the building, attention should also be paid to improving the production process, enhancing equipment performance, and reducing unnecessary energy waste.

2.3. Conservation and environmental friendliness

One of the important goals of building energy-saving electrical system design is to achieve effective energy utilization and reduce environmental pollution. Therefore, in the selection and application of energy-saving technologies, attention should be paid to environmental protection. This can be done by prioritizing the selection of renewable and clean energy sources, reducing reliance on traditional energy sources, and lowering carbon emissions. Additionally, it is necessary to optimize equipment layout and electrical system design schemes, reduce energy consumption and pollutant emissions, and achieve green and sustainable development of building electrical systems.

3. Energy-saving design measures for building electrical systems

3.1. Optimize power supply and distribution systems

The power supply and distribution system plays a crucial role in building electrical system design since its design quality directly affects the operational efficiency and energy consumption level of electrical equipment. To ensure the rationality and efficiency of the power supply and distribution system design, it is necessary to fully consider the actual needs and electrical characteristics of the building in building electrical design [11]. This can be done by selecting suitable transformers, cables, switches, and other equipment, and optimizing the distribution method to reduce energy loss in the transmission process. Firstly, understand the electricity demand and characteristics of the building. Different building uses and electrical equipment have different electricity demands, therefore, it is necessary to choose appropriate transformer capacity and distribution methods based on actual situations [12]. Simultaneously, it is necessary to choose cable types and lengths reasonably to minimize energy loss during power transmission. Secondly, optimize the distribution method. An effective distribution method can reduce power loss and energy waste. Techniques such as partitioned distribution, radial distribution, etc., can make power supply more flexible and efficient. Additionally, improving the automation level of the power supply and distribution system is crucial. Improving the level of automation can achieve intelligent

management and control of power supply and distribution systems, and improve the stability of system operation. With the development of information technology and Internet of Things technology, the automation level of power supply and distribution systems has been greatly improved [13]. The intelligent management system can monitor the status of the power supply in real-time, and provide early warning and handling of abnormal situations, thereby ensuring the stability of the power supply. Finally, pay attention to the safety of the power supply and distribution system. In the design of building electrical systems, it is necessary to fully consider the protective measures of equipment, such as setting overload protection, short circuit protection, etc., to ensure that the system can cut off power promptly in case of faults and avoid the expansion of accidents. On this basis, attention should also be paid to the grounding treatment of electrical equipment to ensure personal safety.

3.2. Adopting efficient and energy-saving lighting equipment

Lighting equipment plays an important role in electrical energy consumption. Therefore, when designing building lighting, attention should be paid to the application of efficient and energy-saving lighting equipment and technology. Specifically, the following aspects can be taken into consideration: Firstly, the use of efficient and energy-saving light sources, such as light emitting diode (LED) and other new light sources, has advantages such as high light efficiency, long lifespan, and low energy consumption, which can significantly reduce energy consumption under the same brightness conditions [14,15]. Moreover, the color temperature of LED light sources is adjustable, which can adjust the lighting effect according to different scenes and needs, thereby meeting both comfort and energy efficiency. Secondly, apply intelligent lighting control systems. The application of intelligent control systems can accurately control the brightness and color temperature of lighting equipment according to actual needs, to effectively reduce energy consumption while meeting lighting requirements. Furthermore, the application of intelligent lighting control systems can also achieve automatic switching of lighting equipment, avoiding energy waste caused by human negligence [16]. Thirdly, fully utilize natural light sources. When designing buildings, full consideration should be given to lighting performance, improving the building's lighting area and natural light intensity. This can reduce the usage of lighting equipment, reduce energy consumption, and bring more comfortable natural light into indoor spaces. Fourthly, a reasonable lighting layout. In the energy-saving design of building electrical systems, a reasonable lighting layout can avoid blind spots and excessive lighting, and reduce unnecessary energy waste. Additionally, when selecting lighting equipment, spatial functionality, and needs should also be considered to achieve personalized lighting effects and improve lighting quality. Finally, strengthen the maintenance and management of lighting equipment. Regularly inspect, repair, and replace lighting equipment to ensure its optimal operation, thereby effectively extending its service life and reducing energy consumption.

3.3. Application of renewable energy

In building electrical system design, efforts should be made to increase the application and promotion of renewable energy, such as solar energy, wind energy, etc., in order to achieve the goals of green, environmental protection, and sustainable development. The application of renewable energy in building electrical system design can not only reduce the dependence of buildings on traditional energy, reduce energy consumption and environmental pollution, but also effectively reduce the operating costs of buildings and improve economic benefits. Precisely the application of renewable energy can take the following measures: First, install solar photovoltaic panels on the roof of buildings to fully utilize solar energy resources. Solar photovoltaic panels can directly convert solar energy into electricity for internal use in buildings, effectively reducing

the building's dependence on traditional electricity resources, reducing carbon emissions, and achieving environmental protection goals. Furthermore, installing photovoltaic panels on the roof of a building can also provide insulation, reduce the temperature inside the building, and further reduce the energy consumption of air conditioning and other equipment. Secondly, actively promote wind power generation equipment in areas with abundant wind resources. Wind power generation is a clean and renewable energy source with broad application. By installing wind power generation equipment, wind energy resources can be fully utilized to provide electricity for buildings. Moreover, installing wind power generation devices in buildings can also beautify the environment and enhance the ecological quality of the surrounding areas. Thirdly, taking into account factors such as geography and climate, comprehensively utilizing multiple renewable energy sources. For example, in cold regions, geothermal energy can be used for heating whereas in the southern region, solar hot water systems can be used to provide hot water for buildings, thereby effectively reducing energy consumption and achieving energy conservation and emission reduction while meeting the actual needs of buildings. Finally, in the architectural design stage, full consideration should be given to the integration and utilization of various renewable energy sources. By optimizing architectural design, improving the insulation and thermal performance of buildings, and reducing building energy consumption. In addition, the reasonable layout of renewable energy equipment is essential to ensure the efficiency and reliability of equipment operation [17].

3.4. Promote smart home technology

With the rapid development of technology, smart home technology is gradually maturing, bringing unprecedented possibilities for building electrical energy conservation. In recent years, smart home technology has become an indispensable part of family life with its unique advantages [18]. The application of advanced technologies such as smart devices, sensors, and network communication has provided new solutions for building electrical energy conservation in China. Smart home technology can achieve intelligent management and control of household electricity consumption, significantly reducing energy consumption. For example, through smart sockets, smart switches, and other devices, users can achieve remote control of household appliances, timed switches, and other functions. Energy waste is effectively avoided when household appliances are in long-term standby and ineffective operation. In short, smart furniture technology has brought tangible energy-saving benefits to users through reasonable management and effective control of household electricity consumption. Smart home technology can also combine users' electricity habits and actual needs to provide personalized electricity solutions, thereby improving energy efficiency and providing users with a more comfortable and convenient living experience. In this process, smart home technology provides users with accurate electricity advice through the analysis and processing of a large amount of data, helping them develop good electricity habits and further reduce energy consumption.

3.5. Improve the efficiency of building electrical equipment

Improving the efficiency of building electrical equipment is an important link in building energy-saving electrical systems design. By selecting efficient and energy-saving electrical equipment and optimizing the operation of electrical equipment, energy consumption can be effectively reduced and energy utilization efficiency can be improved. Specifically, the following aspects can be taken into consideration: Firstly, selecting efficient and energy-saving electrical equipment. When selecting equipment, full consideration should be given to the energy efficiency indicators of the equipment, and electrical equipment with high efficiency and energy-saving performance. For example, in an air conditioning system, variable frequency air conditioning can be selected to achieve stable indoor temperature control and effectively reduce energy consumption by intelligently

adjusting the operating frequency of the compressor. Moreover, in the selection and procurement process of electrical equipment, the cost-effectiveness of the equipment should be fully considered, and products with high cost-effectiveness should be selected to ensure equipment performance while reducing investment costs. Secondly, optimize the operation mode of electrical equipment. By optimizing the operation mode of electrical equipment, the operational efficiency of the equipment can be improved and energy consumption can be reduced. For example, in the lighting system, an intelligent lighting control system can be used to accurately control the brightness, color temperature, etc. of lighting equipment according to actual needs, to effectively reduce energy consumption. Additionally, during the operation of electrical equipment, regular maintenance and upkeep should be carried out to ensure that the equipment operates in its optimal state, thereby effectively extending the service life of the equipment and reducing energy consumption. Thirdly, strengthen the energy efficiency management of electrical equipment. By establishing a sound energy efficiency management system and energy efficiency monitoring system, the energy consumption of electrical equipment can be monitored in real time, and abnormal energy consumption problems can be detected and solved promptly. Meanwhile, by analyzing and processing equipment operation data, data support can be provided for the energy efficiency improvement of electrical equipment, promoting the continuous improvement of equipment energy efficiency.

4. Conclusion

The exploration of energy-saving technologies in building electrical system design is of great significance for achieving green and sustainable development of buildings. In the energy-saving design of building electrical systems, measures such as optimizing the design of power supply and distribution systems, adopting efficient and energy-saving lighting equipment, applying renewable energy, improving equipment energy efficiency, and promoting smart home technology should be taken based on adhering to the principles of economic practicality, practical demand, and environmental conservation. This can effectively reduce energy consumption and environmental pollution in building electrical systems, improve energy utilization efficiency, and achieve a win-win situation for economic and social benefits. In the future, with the continuous progress of technology and the expansion of application fields, the energy-saving design of building electrical systems will pay more attention to technological innovation and system integration, promoting the green transformation and sustainable development of the building electrical industry.

Disclosure statement

The author declares no conflict of interest.

References

[1] Rui Y, 2024, Research on the Application of Green Energy Saving Technology in Electrical Design of Civil Buildings. Juye, 2024(03): 173–175.

[2] Chen P, 2024, Discussion on the application of energy-saving technology in building electrical design. Sichuan Building Materials, 50(03): 210–212.

[3] Wang H, 2024, The application of green building energy-saving technology in building electrical design. Residential and Real Estate, 2024(04): 102–104.

[4] Xu J, 2023, Energy Saving Technical Measures in Building Electrical Design. China Residential Facilities, 2023(09): 34–36.

[5] Chen L, 2023, The Research and Application of Green Building Energy-Saving Technology in Building Electrical Design. Green Building and Intelligent Building, 2023(08): 27–29.

[6] Yan P, 2023, Research on Energy-Saving Technology in Building Electrical Design. Theoretical Research on Urban Construction (Electronic Version), 2023(18): 76–78.

[7] Han W, 2023, The Application of Intelligent Technology in Building Electrical Design. Integrated Circuit Applications, 40(04): 342–343.

[8] Zhang H, 2023, The Application of Green Energy-Saving Technology in Building Electrical Design. Green Building, 15(02): 67–69.

[9] Long Q, 2022, Research on Energy-Saving Technology in Building Electrical Design. Science and Technology Innovation, 2022(34): 5–8.

[10] Wang T, 2022, Energy Saving Technical Measures in Building Electrical Design. Green Building and Intelligent Building, 2022(11): 36–39.

[11] Zhou N, 2022, Analysis of the Application of Green Energy Conservation Technology in Building Electrical Design. Popular Standardization, 2022(16): 181–183.

[12] Cheng L, 2022, Research on the Application of Green and Energy-Saving Technologies in Electrical Design of Public Buildings. Engineering and Construction, 36(04): 1156–1158.

[13] Xiao M, 2022, The Application of Energy-Saving Technology in Building Electrical Design. Fujian Construction Technology, 2022(04): 110–111 + 115.

[14] Wei Z, 2022, Research on the Application of Green Energy Saving Technology in Electrical Design of Building Engineering. Real Estate World, 2022(13): 112–114.

[15] Yan F, 2022, Energy Saving Technology and Application of Transformers in Electrical Design of Civil Intelligent Buildings. Low-Temperature Building Technology, 44(01): 45–48.

[16] Wang H, 2021, Application of Energy-Saving Technology in Building Electrical Design. China Building Decoration, 2021(10): 70–71.

[17] Yin X, 2020, Analysis of Energy-Saving Technical Measures in Building Electrical Design. Equipment Engineering of China, 2020(19): 204–206.

[18] Zhong K, 2021, Analysis on the Application Path of Green Energy-Saving Technology in the Electrical Design of Civil Buildings. Ceramic, 2021(02): 126–127. https://doi.org/10.19397/j.cnki.ceramics.2021.02.051

[19] Liu H, 2021, Application of Energy-Saving Technology in Building Electrical Design. Residential and Real Estate, 2021(15): 123–124.

Publisher's note

Bio-Byword Scientific Publishing remains neutral with regard to jurisdictional claims in published maps and institutional affiliations.

Journal of Electronic Research and Application, 2024, Volume 8, Issue 4
http://ojs.bbwpublisher.com/index.php/JERA
ISSN Online: 2208-3510
ISSN Print: 2208-3502

Design of Intelligent Window Automatic Monitoring System Based on Microcontroller Control

Liyan Gao, Rongfang Zong*

School of Electronic Engineering, JOU, Lianyungang 222005, China

***Corresponding author:** Rongfang Zong, zrf@jou.edu.cn

Copyright: © 2024 Author(s). This is an open-access article distributed under the terms of the Creative Commons Attribution License (CC BY 4.0), permitting distribution and reproduction in any medium, provided the original work is cited.

Abstract: To ensure the safety of residents' lives and property by using automatic opening and closing of ordinary windows, this article designs an intelligent window automatic monitoring system. The article proposes a software and hardware design scheme for the system, which comprises a microcontroller control module, temperature and humidity detection module, harmful gas detection module, rainfall detection module, human thermal radiation induction module, Organic Light-Emitting Diode (OLED) display module, stepper motor drive module, Wi-Fi communication module, etc. Users use this system to monitor environmental data such as temperature, humidity, rainfall, harmful gas concentrations, and human health. Users can control the opening and closing of windows through manual, microcontroller, and mobile application (app) remote methods, providing users with a more convenient, comfortable, and safe living environment.

Keywords: Smart window; Automatic monitoring; STM32 microcontroller; Mobile application

Online publication: August 12, 2024

1. Introduction

In the past, windows required residents to manually open and close them. Residents often have to close the windows themselves before going out to prevent illegal intrusion. When it rains, if the user does not close the window on time, the rain can enter and wet the room. If a room suddenly catches fire and the person involved is not paying attention while the window is closed, their life and property will be at risk. Therefore, smart furniture that can automatically assist people in handling these trivial matters has become particularly important. A smart window with an automatic monitoring system, equipped with functions such as rain, theft, and smoke prevention with the help of a Wi-Fi module, and remote control through a mobile application will provide great convenience in daily life.

2. Scheme design

The hardware of the intelligent window automatic monitoring system consists of a microcontroller control system module, a temperature and humidity acquisition module, a rainfall detection module, a harmful gas detection module, a human infrared sensing module, an alarm module, a driver module, and a Wi-Fi module [1].

The hardware components are further combined with software programming to achieve the required functions. The system diagram is shown in **Figure 1**.

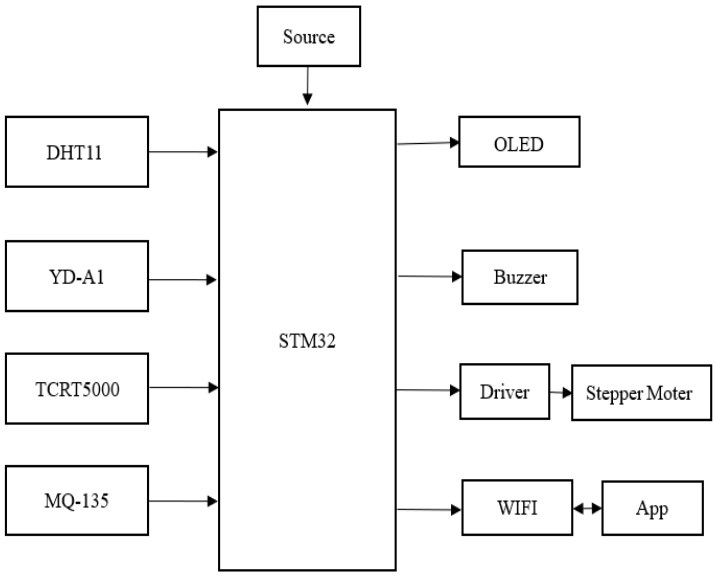


Figure 1. Composition block diagram of intelligent window automatic monitoring system

3. Hardware design

3.1. Microcontroller control module

The system adopts a microcontroller STM32F103C8T6, which has a 12-bit Analog-To-Digital Converter (ADC) and 37 General-Purpose Input/Output (GPIO) pins, providing digital processing of analog signals. This supports multiple communication interfaces, including Serial Peripheral Interface (SPI), Inter-Integrated Circuit (IIC), etc. The Receive (RX) and Transmit (TX) pins can be used to both burn programs and receive control instructions from the upper computer. The crystal oscillator circuit provides a stable clock source for the microcontroller, ensuring precise timing for its operations. The reset circuit can restore the entire system to its initial state, reload the program, and avoid system crashes.

3.2. Temperature and humidity detection module

This design uses a temperature and humidity sensor DHT11 to collect the temperature and humidity of the environment, with a temperature measurement range of 0–50 ℃ and an error of ± 2 ℃. The measurement range of humidity is 20%–90% Relative Humidity (RH), with an error of ± 5% RH [2]. Users can set a temperature and humidity threshold, and then the microcontroller compares the values detected by the sensor with the threshold, automatically controlling the opening and closing of the window. DHT11 adopts a single-bus communication protocol. After the microcontroller sends a reset signal, DHT11 switches from low-power mode to high-speed mode. After waiting for the host reset to complete, DHT11 sends a response signal and raises the bus to prepare for data transmission.

3.3. Human infrared sensing module

Using the principle of infrared reflection, when a certain part of the human body is in the infrared region, the infrared emitted by the infrared emitting tube is reflected to the infrared receiving tube due to the shielding effect of the human body. The signal is processed by the microcomputer in the integrated circuit and sent to

the microcontroller [3]. After receiving the signal, the electromagnetic valve opens the valve core according to the specified command to control the opening and closing of the window. This design uses the TCRT5000 infrared reflective sensor to detect whether there is anyone outside the window. When someone is detected in the window, the analog signal is converted into an electrical signal and input to the ADC pin to initiate Analog-To-Digital (A/D) conversion to control the window to close and activate the buzzer for vibration and alarm.

3.4. Harmful gas detection module

By detecting the concentration of harmful gases through the MQ135 air quality sensor module, it is possible to detect harmful gases such as ammonia, sulfides, and benzene, with a detection range of 10–1,000 ppm [4]. The sensor adopts a socket communication protocol, which outputs the detected data as an analog signal to the microcontroller to detect the concentration of harmful gases in the air. When the detected concentration of harmful gases exceeds the threshold, the data is transmitted to the microcontroller through the three pins of the module for processing, and then the window is automatically closed and the buzzer vibration alarm is activated.

3.5. Rainfall detection module

A raindrop sensor is used to detect whether it is raining outdoors and automatically control the window to close. This prevents rainwater from entering the home and damaging the products inside. This module uses the YD-A1 raindrop sensor. When there are no water droplets on the detection chip, the Digital Output (DO) is high and the switch indicator light is off. When drops of water are detected (exceeding the set rainfall monitoring threshold), the DO output is low and the switch indicator light is on [5]. After brushing off the water droplets (below the set rainfall monitoring threshold), it returns to the DO output high-level state.

3.6. Display module

Using a 0.96-inch OLED as the display module, the data collected by each sensor is displayed. The main advantage of this module is its self-luminous properties, which are coated with a thin layer of paint on the outside of the module. When there is current passing through, it will automatically emit light. Its communication protocol adopts IIC, Serial Clock Line (SCL), and Serial Data Line (SDA). When SCL is transmitting data at a high level, the SDA cannot be flipped. When the SDL is low, the SDA can flip [6].

3.7. Driver module

The system uses a stepper motor to simulate window opening and closing. When someone is detected or the temperature, humidity, rainfall, and gas concentration exceed the threshold, the system automatically closes the window. Before controlling the rotation of the Direct Current (DC) motor, it is essential to understand the truth value table. IN1 and IN2 control one motor, with OUT1 and OUT2 connected to both ends of the motor, and IN3 and IN4 control the other motor. When the input terminal IN1 is low and the input terminal IN2 is high, the motor is in a forward rotation state. When the input terminal IN1 is high and the input terminal IN2 is low, the motor is in a reverse state [7]. When both inputs are at high voltage, the motor is in braking mode. This setup allows precise control over the motor's direction and braking, facilitating effective window automation.

3.8. Wi-Fi module

The system achieves a Wi-Fi connection through the ESP8266 module. ESP8266 converts the received data into serial output, communicates with the microcontroller through the serial port (RX and TX), and achieves data transmission and control through transmission instructions [8]. Through the built-in ESP8266 Wi-Fi module, the smart window automatic monitoring system can connect to mobile applications and upload the collected

data through the system. The 5-pin Transmit Data (TXD) of this module is connected to the sending pin and the receiving pin of the microcontroller [9]. The instructions issued by the mobile phone are transmitted to the microcontroller through this pin. The 3-pin Receive Data (RXD) of this module is the receiving pin, and the 7-pin RESET is the reset pin, which is used to restart ESP8266. The Chip Enable Pin (EN) is the enable port, and the high-level module is effective, while the low-level module is not working [10].

4. System software design

The system software design is divided into two main parts, the automatic monitoring program and the mobile app remote control program. The automatic monitoring program compares the pre-set parameter threshold with the data collected by the sensor module, thereby automatically controlling the opening and closing of windows. The mobile app remote control program is used to remotely monitor environmental parameters, set thresholds, and control the opening and closing of windows. The overall system process is shown in **Figure 2**.

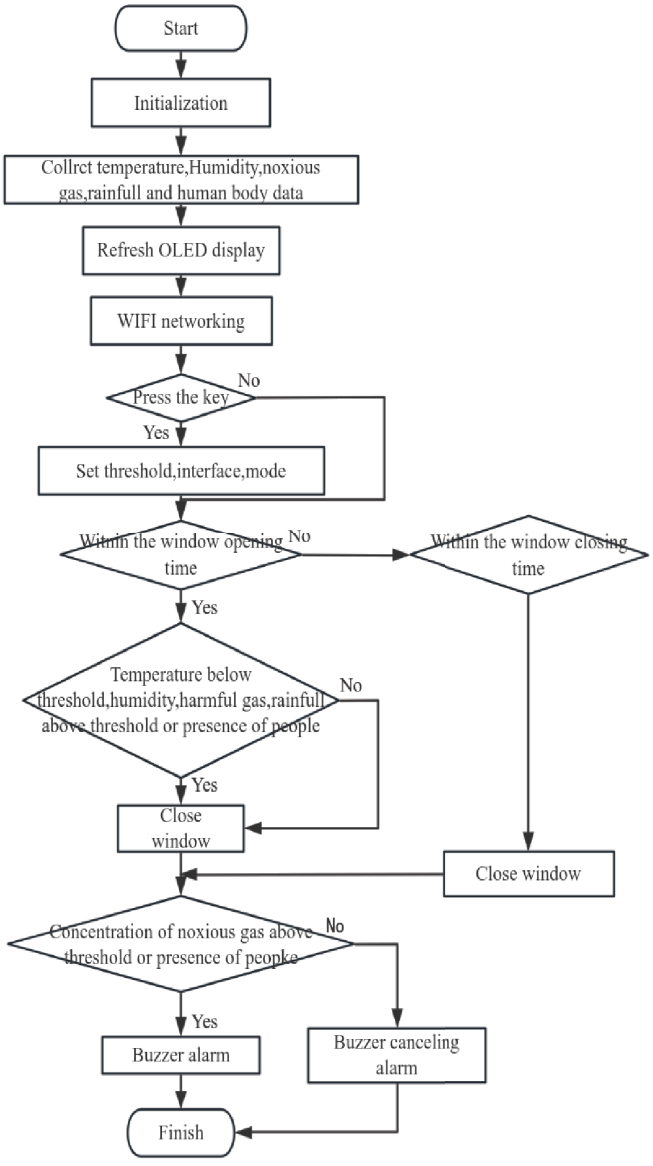


Figure 2. Overall system flow chart

4.1. Automatic monitoring program

By calling functions to drive sensors for environmental data collection, and through A/D conversion, analog signals such as temperature and humidity, harmful gas concentration, rainfall, and human infrared signals are converted into digital electrical signals, laying the foundation for later data processing. Convert the collected digital electrical signals into 01 signals compatible with the microcontroller, transmit them to the processor for data processing, and refresh the OLED display [11]. The obtained data is compared with the pre-set threshold. If the stepping motor module does not run within the window closing time, the window will remain closed. When the window is open, if the temperature is below the threshold, harmful gas concentration is detected, rainfall is greater than the threshold, and outdoor people are detected, the microcontroller will control the stepper motor drive to automatically close the windows. The system software design achieves automatic control of stepper motors through data collection, data processing, and motor drive.

4.2. Remote control program for mobile app

The programming and app connection of ESP8266 is a crucial part of the system, which is responsible for establishing communication with mobile apps and achieving remote control, data transmission, and reception. The ESP8266 module first establishes a connection with the Wi-Fi network, obtains Internet access rights, and establishes a connection through the Application Programming Interface (API) provided by the app [12]. The connection process includes login verification to ensure secure communication. STM32 sends control commands or device status data to the ESP8266 module, which encapsulates it as a Hypertext Transfer Protocol (HTTP) request and sends it to the mobile app through an interface. The mobile app receives an HTTP request from ESP8266, processes the request, and returns the corresponding response. ESP8266 will parse the response data and transmit it to the microcontroller [13]. The mobile app is installed on a client's mobile and uses the Socket communication protocol. Through the wireless ESP8266 module, it sends and receives data from the STM32 microcontroller, including collected environmental data such as temperature, humidity, and harmful gas concentrations. It can also set thresholds to remotely control the opening and closing of windows [14]. The functional block diagram of the app is shown in **Figure 3**.

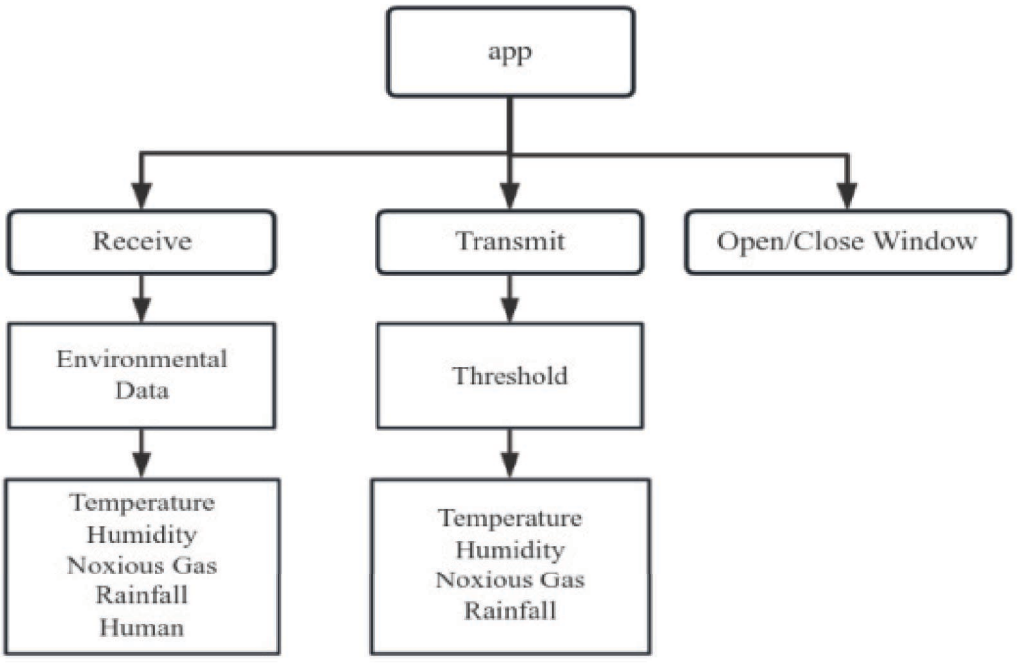


Figure 3. App function block diagram

5. System testing

Hardware debugging is an important stage in the development process of an intelligent window automatic monitoring system. Firstly, ensure that all hardware devices are properly connected. This includes connecting STM32 microcontrollers, sensors, drivers, Wi-Fi modules, OLED displays, and such. Check the wiring, pins, and connectors to ensure they are securely connected without any looseness or poor contact. After the system is powered on, a series of initializations will be carried out, and the OLED screen will begin to collect data. The content displayed in one to four lines is temperature, humidity, rainfall, and gas concentration. Press the S2 button to switch the interface. The first line displays whether the human body is present or not, and the second line displays whether the window is open or closed. Real-time transmission of data is sent to the user's mobile phone via Wi-Fi. Open the mobile hotspot, set the device name to "wlkj", and the password to "99999999". At this point, you can connect to the hardware.

6. Epilogue

This article is based on the design of an intelligent window automatic monitoring system with multiple sensors. The system uses STM32 as the main controller and utilizes various sensors to collect indoor environmental data, including temperature and humidity, harmful gas concentration, rainfall, and human body detection. The system is ultimately displayed on an OLED screen and has functions such as an abnormal alarm, automatic control of window opening and closing, and wireless communication. At the same time, to improve the level of human-computer interaction, manual threshold setting, remote monitoring, and control have been added, making the system functions more diverse and promoting intelligent measurement devices to enter daily life [15].

Disclosure statement

The authors declare no conflict of interest.

References

[1] Mao J, 2014, Intelligent Window Design Based on STC89C52 Microcontroller. Electronic Design Engineering, 2014(24): 26–28.

[2] Liu S, 2018, Improvement and Application of LEACH Algorithm, thesis, Harbin Institute of Technology.

[3] Chen Z, 2016, Research on Human Infrared Sensor Display Screen. Technology World, 2016(12): 2–3.

[4] Chen D, Tu Y, Shen Y, 2023, Remote Pet Feeding and Detection System Technology Based on STM32. Computer Science and Applications, 2023(10): 7–9.

[5] Deng T, Wang Z, 2019, Multi-functional Intelligent Clothes Hanger System. Electronic Technology and Software Engineering, 2019(16): 2–4.

[6] Liu X, 2012, Research on CMOS Image Signal Acquisition, Transmission and Imaging Based on USB, thesis, Zhejiang University of Technology.

[7] Wang Z, 2016, Design of a Dual Wheel Self-balancing Robot Based on RT Thread and STM32, thesis, North Central University.

[8] Wang L, 2019, Research on "Internet" based Electrical Control Simulation Training Equipment, thesis, Jilin University.

[9] Zhu P, Bao Y, 2023, Design and Implementation of an Intelligent Meaty Plant Breeding System Based on Microcontroller. Computer Programming Skills and Maintenance, 2023(10): 5–6.

[10] Wang B, 2021, Wireless Measurement System Based on Nanocapacitive Sensors, thesis, Guangdong University of Technology.

[11] Wang Y, 2018, Design of Intelligent Curtain System Based on Microcontroller. Communication World, 2018(12): 275–276.

[12] Xu X, Mei L, Luo D, 2018, An Intelligent Gateway Technology for Monitoring the Manufacturing Environment of Power Batteries. Information Technology and Network Security, 2018(2): 3–4.

[13] Xue F, Li J, Wang R, 2023, Design of Heating Temperature Monitoring System Based on NB IoT. Internet of Things Technology, 2023(11): 4–5.

[14] Lin Q, Duan Y, 2023, Design of Intelligent Irrigation System Based on STM32 Technology. Computer Programming Skills and Maintenance, 2023(06): 121–123.

[15] Mao J, 2014, Intelligent Window Design Based on STC89C52 Microcontroller. Electronic Design Engineering, 2014(24): 26–28.

Publisher's note

Bio-Byword Scientific Publishing remains neutral with regard to jurisdictional claims in published maps and institutional affiliations.

Journal of Electronic Research and Application, 2024, Volume 8, Issue 4
http://ojs.bbwpublisher.com/index.php/JERA
ISSN Online: 2208-3510
ISSN Print: 2208-3502

A Design of an SMTP Email Server

Liheng Hu*

School of Cybersecurity, Beijing University of Posts and Telecommunications, Beijing 100876, China

***Corresponding author:** Liheng Hu, huliheng701@gmail.com

Copyright: © 2024 Author(s). This is an open-access article distributed under the terms of the Creative Commons Attribution License (CC BY 4.0), permitting distribution and reproduction in any medium, provided the original work is cited.

Abstract: This study developed a mail server program using Socket API and Python. The program uses the Hypertext Transfer Protocol (HTTP) to receive emails from browser clients and forward them to actual email service providers via the Simple Mail Transfer Protocol (SMTP). As a web server, it handles Transmission Control Protocol (TCP) connection requests from browsers, receives HTTP commands and email data, and temporarily stores the emails in a file. Simultaneously, as an SMTP client, the program establishes a TCP connection with the actual mail server, sends SMTP commands, and transmits the previously saved emails. In addition, we also analyzed security issues and the efficiency and availability of this server, providing insights into the design of SMTP mail servers.

Keywords: Mail server; Socket API; HTTP protocol; SMTP protocol; Security analysis; Efficiency analysis

Online publication: August 13, 2024

1. Introduction

With the rapid development of information technology, email has become an indispensable part of daily communication. Both businesses and individuals rely on email for quick and effective information exchange. However, existing email service providers often restrict users to specific platforms, limiting their control and customization of email services. Additionally, privacy and security concerns have increasingly become a focal point for users. In light of this, developing an independent mail server can provide greater flexibility and customization options while enhancing user control over data privacy and security [1,2].

2. Current status of email

2.1. Evolution of email services

Email services have evolved significantly from their early days of simple text transmission to the current capability of sending formatted Hyper Text Markup Language (HTML) content, including images, links, and rich text formats. This transformation has been driven by the need to support more dynamic and visually appealing communication methods. The rise of social media and instant messaging has further pushed the evolution of email services to meet user demands for more flexible and enriched forms of interaction. Modern email services now provide a platform for a wide range of multimedia content, catering to both personal and

professional communication needs [3].

2.2. Market size and trends

According to a research report, the global email market size was approximately $6.5 billion as of 2023. It is expected to grow at a compound annual growth rate (CAGR) of about 15.5% from 2024 to 2030, reaching $30.4 billion. This growth is driven by increasing levels of digitalization and the online presence of businesses and consumers, making email a cost-effective and versatile communication tool. Additionally, the number of global email users is continuously increasing, projected to reach around 4.37 billion by 2023 [4]. The sustained growth in the email market cements its importance as a versatile and effective tool in the digital marketing arsenal.

2.3. Current state of email systems

Email systems are a crucial application for transmitting communication data over the internet. Despite the advent of new communication tools, email continues to hold a significant position in both personal and business communication. It offers a low-cost, fast, and widely accepted means of communication. Furthermore, email systems support various forms of information, including text, images, and audio. This versatility makes email an indispensable communication tool, capable of handling diverse types of content and catering to a broad audience.

2.4. Security and privacy concerns

As cyber-attacks become increasingly sophisticated, the security and privacy of email services have become major concerns for both users and service providers. To protect user data and communication content, email service providers are implementing various measures, such as encryption technologies, anti-spam, and anti-phishing strategies [5,6]. These efforts aim to safeguard the integrity and confidentiality of email communications, ensuring that sensitive information remains protected from unauthorized access and malicious activities.

3. Design outline

This program is a simple proxy server designed to receive HTTP POST requests from clients. Its design approach involves creating an HTTP-based server, listening on a specific port, and extracting the email content and data from the POST requests. Subsequently, parsed email content and data are utilized to send emails to the target mailbox using the SMTP protocol. The operational workflow (Figure 1) includes receiving client requests, parsing email data, sending emails via SMTP, and error handling during the sending process. This design aims to mimic the HTTP interface of real Webmail servers, enabling communication between clients and mail servers to facilitate the sending of electronic mail [1,7].

4. Project structure

The project is mainly divided into three parts: the startup and connection of the proxy server, extraction and parsing of email content, and email sending and forwarding. The source code is divided into several modules: HTTP request handling, email sending, logging, configuration management, etc. Through Python's modular design, the code structure is clear, with distinct module functionalities, facilitating maintenance and expansion. Through the design, a simple email forwarding proxy server is implemented, capable of receiving email content from HTTP requests and forwarding it to specified email addresses. The code structure of the entire project is clear, with well-defined functional modules, making the code easy to understand and maintain.

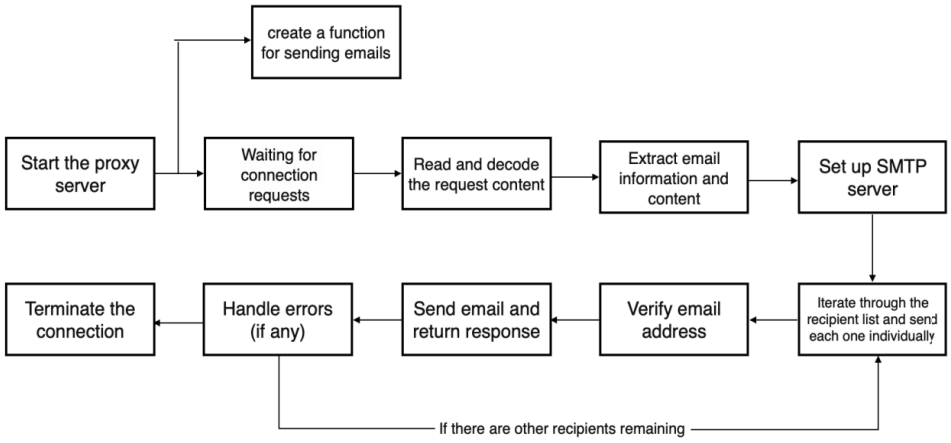


Figure 1. Email sending process

4.1. The startup and connection of the proxy server

The proxy server is created using Python's HTTPServer and BaseHTTPRequestHandler classes, listening on a specified port. When an HTTP request arrives, it parses the request content and extracts the required information, such as email content, sender, and recipient. After receiving the request, the proxy server forwards the requested content to the specified email processing module.

4.2. Extraction and parsing of email content

The server parses the email content using regular expressions or other methods, extracting recipient, sender, email subject, email content, etc. It also parses HTML-formatted email content to extract plain text content for further processing or logging.

4.3. Email sending and forwarding

Establishes a connection with the SMTP server via the SMTP protocol and logs in with authentication. Constructs the email object, including setting sender, recipient, subject, content, etc. Sends the constructed email object to the SMTP server for email forwarding. Handles possible exceptions during the email sending process, such as the recipient does not exist, the email exceeds the specified length, etc., and performs corresponding error handling.

4.4. Function test

Overall, this email server acts as a middleware between client applications generating email requests and the SMTP server responsible for delivering those emails. It handles the process of receiving, parsing, and forwarding email data, ensuring that emails are sent securely and reliably while providing error feedback to clients when necessary.

4.4.1. Email extraction and parsing

The email server functions as a proxy server, intercepting HTTP requests containing email data and forwarding them to the appropriate email processing module. Upon receiving an HTTP request, the server extracts relevant email data such as sender, recipient, subject, and email content. The server parses the email content, extracting

plain text from HTML-formatted emails and preparing it for further processing.

4.4.2. Sending and forwarding of email

The server establishes a secure connection with an SMTP server using the SMTP protocol. It then logs in to the SMTP server using the provided credentials, which include the sender's email address and password. Once authenticated, the server constructs email objects that include the sender, recipient, subject, and content information extracted from the HTTP requests. These constructed email objects are then forwarded to the SMTP server for sending to the specified recipients (Figure 2). Throughout the email sending process, the server handles potential errors (Figure 3) such as invalid recipient addresses or emails exceeding the specified length. In such cases, error messages are generated and possibly sent back to the client.

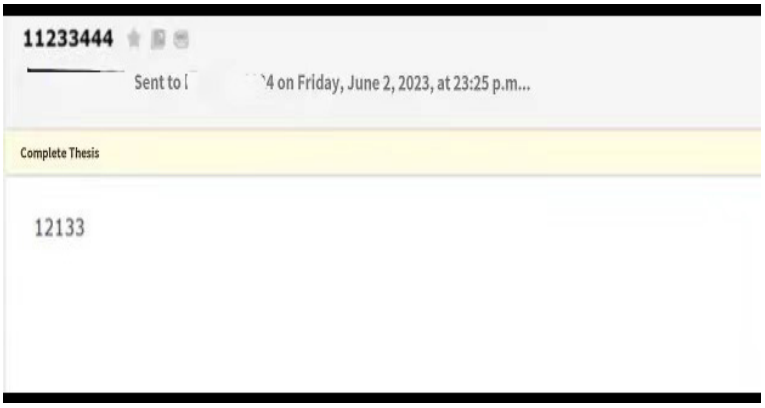


Figure 2. Email forwarded successfully



Figure 3. Incorrect email address error message

5. Analysis and improvement

5.1. Security analysis

In the design of an email server, authentication and encryption are crucial components. Ensuring that the SMTP server uses Transport Layer Security (TLS) or Secure Sockets Layer (SSL) protocols for encrypted communication effectively prevents eavesdropping and man-in-the-middle attacks, safeguarding all transmitted data, including user credentials and email contents. Similarly, employing Hypertext Transfer Protocol Secure (HTTPS) to encrypt HTTP requests further protects user data and session information. Moreover, robust

authentication mechanisms are indispensable, with strong password policies requiring users to use complex passwords and regularly change them, thereby enhancing system security. Two-Factor Authentication (2FA) adds an extra layer of security, verifying identity through codes generated by Short Message Service (SMS), email, or authentication apps, further preventing unauthorized access. For access by third-party applications, the Open Authorization (OAuth) protocol provides a secure authorization mechanism, mitigating the risk of sharing user passwords [5,6,8].

Stringent validation of all incoming data is critical to preventing injection attacks. Using regular expressions and other validation techniques to ensure incoming data conforms to expected formats effectively prevents Structured Query Language (SQL) injection and other code injection attacks. Additionally, when handling HTML content, sanitizing HTML using libraries such as Bleach or DOMPurify is essential to prevent Cross-Site Scripting (XSS) attacks. This is particularly important when parsing and displaying HTML content. Similarly, virus scanning of email attachments is essential to prevent the spread of malicious files [8].

In error handling, designing error messages that do not leak sensitive information is crucial. Avoid the disclosure of internal server details, such as stack traces or database errors. Providing generic error messages like “request processing failed” effectively prevents information leakage. Logging detailed error messages in server logs for administrator review, while ensuring the security of the logs themselves to prevent unauthorized access, is an effective security practice. Furthermore, a robust exception-handling mechanism ensures that the server remains stable and operational in the face of unforeseen errors, preventing service interruptions.

5.2. Efficiency analysis

In efficiency analysis, the modular design contributes to code maintainability and performance optimization. By separating different functionalities into independent modules, modular design not only improves code maintainability but also facilitates optimization and updates of specific functionalities. Performance analysis of various modules, especially email parsing and sending modules, identifies and optimizes performance bottlenecks. Effective system resource management is also crucial to ensuring the efficient operation of the email server. Effective memory management strategies such as object pooling and memory recycling reduce memory leaks and excessive usage. Similarly, optimizing Central Processing Unit (CPU) intensive operations, such as using more efficient algorithms and data structures, enhances overall system performance.

Implementing asynchronous processing significantly improves system concurrency. Leveraging Python’s asynchronous libraries such as asyncio increases system throughput and reduces response times. Likewise, using task queues such as Celery for background task processing effectively improves frontend response speed. In terms of scalability, ensuring system performance by adding more servers to share the load is essential. Using load balancers such as HAProxy or NGINX to distribute traffic and configuring auto-scaling policies to dynamically increase or decrease server instances based on load are effective scaling methods [9].

5.3. Maintainability and testing

When further designing the email server and officially putting it into use, maintainability and testing are also crucial factors. Adhering to coding standards and best practices, maintaining clear and readable code, and automatically checking code quality using static code analysis tools such as Pylint improves code maintainability [10]. Writing detailed documentation describing system architecture, functionality modules, and interfaces facilitates development and maintenance. Similarly, conducting regular code reviews and refactoring to identify and fix potential issues, optimize code structure, and improve readability and performance are important measures to ensure code quality. Comprehensive functional testing ensures that the server behaves as

expected in various scenarios. Implementing automated testing using tools such as Pytest for unit testing and continuous integration ensures that code changes do not introduce new issues.

5.4. Compliance

In terms of compliance, ensuring that the server complies with privacy regulations such as the General Data Protection Regulation (GDPR) is crucial. Implementing data encryption, user data access controls, and data deletion request handling effectively protects user data privacy and security. In terms of user experience, providing clear and meaningful error messages that help users understand and resolve issues while avoiding the leakage of internal details enhances user experience. Monitoring server performance and optimizing response times further improves user experience.

6. Conclusion

In terms of compliance, ensuring that the server complies with privacy regulations such as the General Data Protection Regulation (GDPR) is crucial. Implementing data encryption, user data access controls, and data deletion request handling effectively protects user data privacy and security. In terms of user experience, providing clear and meaningful error messages that help users understand and resolve issues while avoiding the leakage of internal details enhances user experience. Monitoring server performance and optimizing response times further improves user experience.

Disclosure statement

The author declares no conflict of interest.

References

[1] Sureswaran R, Al Bazar H, Abouabdalla O, et al., 2009, Active E-Mail System SMTP Protocol Monitoring Algorithm. 2009 2nd IEEE International Conference on Broadband Network & Multimedia Technology, 2009: 257–260.

[2] Dürscheid C, Frehner C, Herring SC, et al., 2013, Email communication. Handbooks of Pragmatics [HOPS], 2013(9): 35–54.

[3] Wang D, Irani D, Pu C, 2013, A Study on Evolution of Email Spam Over Fifteen Years. 9th IEEE International Conference on Collaborative Computing: Networking, Applications and Worksharing, 2013: 1–10.

[4] Email Marketing Market Research Report: Forecast (2023–2028), n.d., viewed June 24, 2024, https://www.marknteladvisors.com/research-library/email-marketing-market.html

[5] Chonka A, Xiang Y, Zhou W, et al., 2011, Cloud Security Defence to Protect Cloud Computing Against HTTP-DoS and XML-DoS Attacks. Journal of Network and Computer Applications, 34(4): 1097–1107.

[6] Foster ID, Larson J, Masich M, et al., 2015, Security by Any Other Name: On the Effectiveness of Provider Based Email Security. Proceedings of the 22nd ACM SIGSAC Conference on Computer and Communications Security, 2015: 450–464.

[7] Postel JB, 1982, Simple Mail Transfer Protocol. RFC 821.

[8] LaRoche P, Zincir-Heywood AN, Heywood M, 2011, Exploring the State Space of an Application Protocol: A Case Study of SMTP. 2011 IEEE Symposium on Computational Intelligence in Cyber Security (CICS), 2011: 152–159.

[9] Naik N, 2017, Choice of Effective Messaging Protocols for IoT Systems: MQTT, CoAP, AMQP and HTTP. 2017

IEEE International Systems Engineering Symposium (ISSE), 2017: 1–7.

[10] Boogerd C, Moonen L, 2008, Assessing the Value of Coding Standards: An Empirical Study. 2008 IEEE International Conference on Software Maintenance, 2008: 277–286.

Publisher's note

Bio-Byword Scientific Publishing remains neutral with regard to jurisdictional claims in published maps and institutional affiliations.

Journal of Electronic Research and Application, 2024, Volume 8, Issue 4
http://ojs.bbwpublisher.com/index.php/JERA
ISSN Online: 2208-3510
ISSN Print: 2208-3502

Research on Active and Reactive Power Decoupling Control Based on VSC-HVDC

Hongshan Lin, Yiming Lei, Feng Ning*

Department of Electric Power Engineering, North China Electric Power University, Baoding 071000, Hebei Province, China

***Corresponding author:** Feng Ning, ningfeng9909@163.com

Copyright: © 2024 Author(s). This is an open-access article distributed under the terms of the Creative Commons Attribution License (CC BY 4.0), permitting distribution and reproduction in any medium, provided the original work is cited.

Abstract: Voltage Source Converter-based High Voltage Direct Current (VSC-HVDC) transmission technology represents a groundbreaking approach in high voltage Direct Current (DC) transmission, offering numerous technical advantages and broad application prospects. However, in the d-q synchronous rotating coordinate system, the VSC-HVDC exhibits the coupling effect of active power and reactive power, so it needs to be decoupled. This paper introduces the basic principle and mathematical model of the VSC-HVDC transmission system. Through the combination of coordinate transformation and variable substitution, a feedforward decoupling control method is derived. Then the VSC-HVDC simulation model is designed, and the simulation analysis is carried out in the MATLAB environment. The simulation results demonstrate that the method effectively achieves decoupling control of active and reactive power, exhibiting superior dynamic performance and robustness. These findings validate the correctness and effectiveness of the control strategy.

Keywords: Voltage source converter; Decoupling control; Feedforward decoupling

Online publication: August 13, 2024

1. Introduction

VSC-HVDC has the characteristics of not being limited by transmission distance, independent control of active power and reactive power, and no risk of commutation failure [1–3]. With its unique technical advantages, it has become an important way to solve the problem of large-scale new energy delivery and a powerful means to adjust the energy structure in the future [4–6].

In a previous study, the steady-state VSC-HVDC model is analyzed, alongside proposing a PI-based nonlinear controller [7]. Yet, the interplay among the relevant physical quantities described by the model is intricate, posing challenges in determining the controller parameters. By formulating the mathematical model of the synchronous rotating coordinate system of the voltage source converter station, previous studies implemented a nonlinear decoupling controller for active and reactive power based on feedback linearization [8,9]. This approach achieves independent and rapid control over the converter station‘s active and reactive power outputs but does not discuss the power control in depth. Peng proposed to use the internal model principle to

design the controller of VSC-HVDC, though it did not specify the foundational indices for tuning the internal model controller parameters [10].

In summary, the research on the decoupling control strategy of the VSC-HVDC system is mainly aimed at the decoupling between the output active and reactive power of the converter station, and the detailed design method of the inner and outer loop controller but the basis index of the internal model controller parameters setting was not given.

This paper presents the fundamental principles and mathematical model of VSC-HVDC transmission systems. Through the combination of coordinate transformation and variable substitution, a feedforward decoupling control method that can independently control active power and reactive power and can completely decouple them is derived. The inner loop controller design method and the fundamental parameters for tuning the internal model controller are provided. With internal model control relying solely on a filter time constant, the process of tuning controller parameters is straightforward. Simulation results affirm that the designed controller exhibits high-quality dynamics, robustness, and effective resistance to system disturbances and interference.

2. VSC-HVDC principle and mathematical model

Figure 1 shows the topology of the VSC-HVDC converter [11,12]. In **Figure 1**, R and L represent the equivalent reactance and loss resistance of the system, C represents the DC capacitance, and U_{sa}, U_{sb}, and U_{sc} represent the a, b, and c phase fundamental wave components of the symmetric Alternating Current (AC) system voltage. U_{ca}, U_{cb}, and U_{cc} are the a, b, and c phase fundamental components of the VSC AC voltage measurement. I_a, I_b, and I_c are fundamental components of the a, b, and c phases of AC measurement [13].

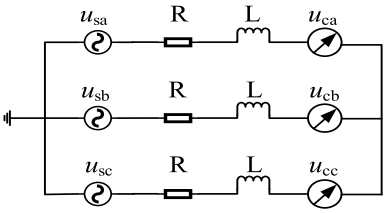


Figure 1. AC measurement equivalent circuit of the converter

According to Kirchhoff's Voltage Law (KVL), the transient mathematical model of the VSC-HVDC system on the VSC1 side in the abc three-phase stationary coordinate system is as follows:

$$\begin{cases} U_{sa} = L\dfrac{dI_a}{dt} + RI_a + U_{ca} \\ U_{sb} = L\dfrac{dI_b}{dt} + RI_b + U_{cb} \\ U_{sc} = L\dfrac{dI_c}{dt} + RI_c + U_{cc} \end{cases} \tag{1}$$

The mathematical model of the VSC-HVDC system established in the abc three-phase stationary coordinate system is a differential equation with time-varying coefficients, which is not conducive to the design of a high-performance controller. Therefore, it is necessary to analyze the d-q synchronous coordinate system: abc/d-q coordinate transformation matrix P is introduced [14]:

$$P=\frac{2}{3}\begin{bmatrix}\cos\theta & \cos(\theta-120°) & \cos(\theta+120°)\\ -\sin\theta & -\sin(\theta-120°) & -\sin(\theta+120°)\\ \frac{1}{2} & \frac{1}{2} & \frac{1}{2}\end{bmatrix} \tag{2}$$

There is no zero sequence component in the symmetric three-phase AC system, and the transient mathematical model of the commutator side in the d-q synchronous coordinate system can be obtained after the change:

$$\begin{cases} L_1\dfrac{di_{d1}}{dt}=u_{sd1}-u_{cd1}-\omega L_1 i_{q1}-R_1 i_{d1} \\ L_1\dfrac{di_{q1}}{dt}=u_{sq1}-u_{cq1}-\omega L_1 i_{d1}-R_1 i_{q1}\end{cases} \tag{3}$$

In the above formula, i_{d1} and i_{q1} represent the d-axis component and q-axis component of i_1, respectively. ω is the angular frequency of the AC system, taking ω = 2πf = 314 rad/s. u_{sd1} and u_{sq1} represent the d-axis component and q-axis component of u_{s1}, respectively. u_{cd1} and u_{cq1} represent the d-axis and q-axis components of u_{c1}, respectively.

3. Analysis of current decoupling control in inner loops

The loop controller accepts the reference value i_{dref} and i_{qref} of active and reactive current from the outer loop control and quickly tracks the reference current to realize the direct control of the current waveform and phase on the AC side of the converter. Inner loop control mainly includes inner loop current control, negative sequence voltage control, and Phae-Locked Loop (PLL) loop control. The following describes the inner loop current control strategy.

For the convenience of analysis, the VSC system function is obtained by Laplace transformation of **Equation (3)** as follows:

$$\begin{cases} (R+Ls)i_{vd}(s)=-u_{sd}(s)+u_{dref}(s)+\omega L i_{vq}(s) \\ (R+Ls)i_{vq}(s)=-u_{sq}(s)+u_{qref}(s)-\omega L i_{vd}(s)\end{cases} \tag{4}$$

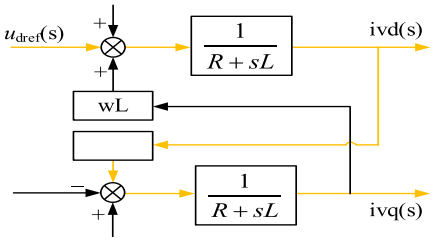


Figure 2. Program block diagram of VSC system function

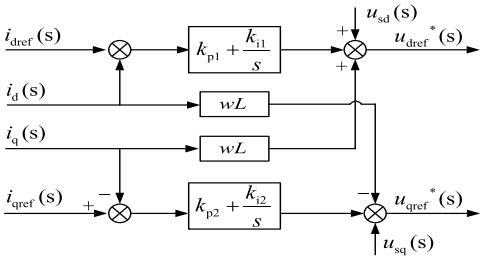


Figure 3. Current decoupling controller

It can be seen from **Figure 2** that the current of the d and q axes is affected not only by the control quantities u_{cd} and u_{cq}, but also by the current cross-coupling ωLi_{sd}, $\omega Li_{sq,}$ and the grid voltage u_{sd} and u_{sq}. To eliminate current coupling and grid voltage disturbance between the d and q axes, it is necessary to introduce

feedforward decoupling. Introduce intermediate variables $V_d(s)$ and $V_q(s)$, as follows:

$$\begin{cases} V_d(s) = \left[i_{dref}(s) - i_d(s) \right] \left(k_{p1} + \dfrac{k_{i1}}{s} \right) \\ V_q(s) = \left[i_{qref}(s) - i_q(s) \right] \left(k_{p1} + \dfrac{k_{i1}}{s} \right) \end{cases} \tag{5}$$

By substituting **Equation (4)** and **Equation (5)** into **Equation (3)**, then **Equation (6)** can be obtained, and the program block diagram is drawn as shown in **Figure 3**.

$$\begin{cases} U_{dref^*}(s) = u_{sd}(s) - \omega L i_q(s) + \left[i_{dref}(s) - i_d(s) \right] \left(k_{p1} + \dfrac{k_{i1}}{s} \right) \\ U_{qref^*}(s) = u_{sq}(s) - \omega L i_d(s) + \left[i_{qref}(s) - i_q(s) \right] \left(k_{p1} + \dfrac{k_{i1}}{s} \right) \end{cases} \tag{6}$$

Further analysis of **Figure 3** shows that after current decoupling control is adopted for the VSC converter, the d-axis and q-axis of its current controller become two independent control rings, that is, **Figure 4** can be simplified into the system structure shown in **Figure 5**.

This algorithm based on feedforward control makes the current inner loop in the mathematical model of voltage source converter realize decouple control, and the control of i_d and i_q are not affected by each other, and the dynamic performance of the system is improved by PI regulator, and the relevant current controller parameters can be easily designed to meet the requirements of the dynamic response speed of the system.

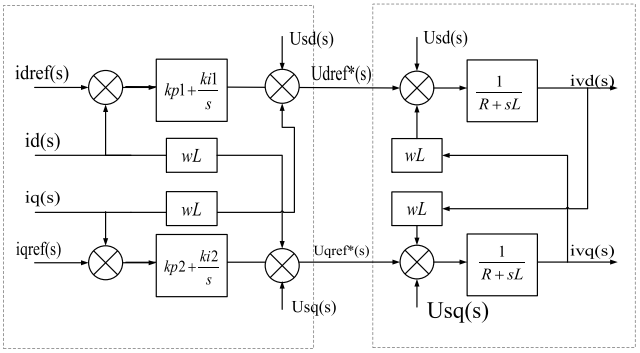


Figure 4. Internal model decoupling controller diagram of VSC system

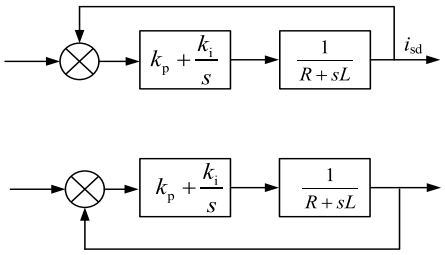


Figure 5. Simplified VSC converter station inner loop current control system structure diagram

4. Simulation analysis

Based on the MATLAB simulation platform, a three-phase, two-level, six-pulse, two-terminal VSC-HVDC system model was established. The main parameters are shown in **Table 1**.

A VSC-HVDC system model with active systems connected at both ends is established, and the parameters of the converter stations at both ends are consistent. Both the VSC1 side and the VSC2 side adopted the internal current loop. Because the reactive power is relatively small, only the VSC2 side adopts the control strategy of fixed DC voltage outer loop, and the VSC1 side directly sets the d-axis current reference value and the q-axis current reference value. Detailed control instructions are shown in **Table 2**.

Table 1. Major parameter

Parameter	Value
Frequency	50 Hz
Root Mean Square (RMS) of system 1 line voltage	220 kV
Short-circuit capacity ratio	10
Loss resistance	0.1 pu
Ac reactance	0.1 pu
Direct current capacitance	200 μF
Rated capacity of the converter station	300 MVA
Rated DC voltage	300 kV
Transformer connection mode	Yg/D1
Pulse Width Modulation (PWM) switching frequency	2600 Hz

Table 2. Major parameter

	Time (s)	1	1.5
1	I_{dref}	0.5→1	
	I_{qref}		0→0.2
2	V_{dcref}	1→1	
	I_{qref}		0→0

The simulation waveform of the sending end is the same as that of the single-ended VSC. We found that at the receiving end, at 1 s, P and i_d at the receiving end also decreased with the change of P at the sending end, because the active power at both ends was equal, and when the active power sent by the sending end was reduced, the active power at the receiving end would certainly be affected.

It can be concluded from **Figure 6** and **Figure 7** that the VSC-HVDC two-terminal model established in this paper realizes the decoupling control of the inner current loop well. The algorithm based on feedforward control makes the inner current loop realize the independent decoupling control of active and reactive power in the mathematical model of the voltage source converter so that the control of i_d and i_q do not affect each other.

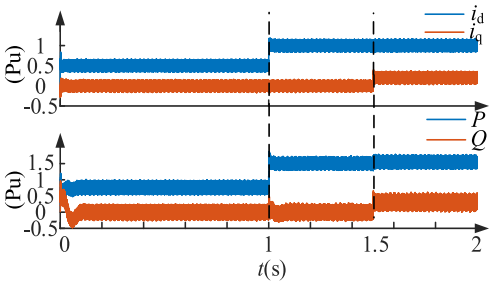


Figure 6. Send i_d, i_q and P and Q waveforms

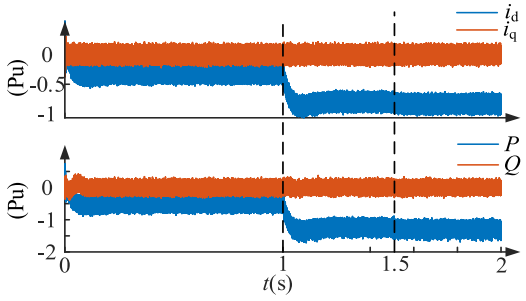


Figure 7. Receiver i_d, i_q and P and Q waveforms

5. Retrospect and prospect

This paper establishes the mathematical model of VSC-HVDC in both the abc three-phase stationary coordinate system and the d-q two-phase synchronous rotating coordinate system. Additionally, it analyzes the principles of VSC-HVDC direct current control. According to the mathematical model of VSC-HVDC in the d-q coordinate system, the feedforward decoupler is introduced by the principle of internal model control to decouple the inner current loop. Based on this theory, MATLAB is used to establish a simulation model for verification. The results indicate that the proposed scheme exhibits effective control performance. The designed controller demonstrates rapid response speed, enabling proficient active and reactive power decoupling control. Moreover, it showcases excellent tracking capabilities and robustness against external disturbances.

VSC-HVDC realizes the decoupling of active power and reactive power and has a good tracking effect and anti-interference ability. However, the switching state of the VSC-HVDC power electronic device submodule changes frequently, and the switching frequency of the VSC-HVDC power electronic device is high, which leads to its bad voltage balancing characteristic and large power loss. When the modular multilevel modulation technology is applied to the flexible DC transmission, that is, the AC voltage of the Modular Multilevel Converter (MMC) output is approximated to the modulated wave by investing and cutting out the submodules, which can meet the requirements of high voltage and high power. In this case, the harmonic problem is not serious, the stepped wave modulation can achieve good output characteristics, and its switching times are smaller than PWM, which can significantly reduce the switching loss. Later research work can also be further studied in MMC.

Disclosure statement

The authors declare no conflict of interest.

References

[1] Abedin T, Lipu MSH, Hannan MA, et al., 2021, Dynamic Modeling of HVDC for Power System Stability Assessment: A Review, Issues, and Recommendations. Energies, 14(16): 4829–4829.

[2] Garciarivas RS, Gonzalez DR, Navarro JA, et al., 2021, VSC-HVDC and its Applications for Black Start Restoration Processes. Applied Sciences, 11(12): 5648–5648.

[3] Li B, He J, Li Y, et al., 2019, A Review of the Protection for the Multi-Terminal VSC-HVDC Grid. Protection and Control of Modern Power Systems, 4(1): 1–11.

[4] Wu X, Xu Z, Zhang Z, 2021, Power Stability Analysis and Evaluation Criteria of Dual-Infeed HVDC with LCC-HVDC and VSC-HVDC. Applied Sciences, 11(13): 5847–5847.

[5] Sultan YA, Kaddah SS, Eladl AA, 2021, VSC-HVDC System-Based on Model Predictive Control Integrated with Offshore Wind Farms. IET Renewable Power Generation, 15(6): 1315–1330.

[6] Karami E, Gharehpetian BG, Mohammadpour H, et al., 2020, Generalised Representation of Multi-Terminal VSC-HVDC Systems for AC-DC Power Flow Studies. IET Energy Systems Integration, 2(1): 50–58.

[7] Xing C, Liu M, He X, et al., 2019, Research on Flexible Control Technology of HVDC. 2019 IEEE 8th International Conference on Advanced Power System Automation and Protection (APAP), Xi'an, China, 2019: 1186–1190.

[8] Gomis-Bellmunt O, Sau-Bassols J, Prieto-Araujo E, et al., 2020, Flexible Converters for Meshed HVDC Grids: From Flexible AC Transmission Systems (FACTS) to Flexible DC Grids. IEEE Transactions on Power Delivery, 35(1): 2–15.

[9] Chen Y, Moreno R, Strbac G, et al., 2018, Coordination Strategies for Securing AC/DC Flexible Transmission

Networks with Renewables. IEEE Transactions on Power Systems, 33(6): 6309–6320.

[10] Peng FZ, 2017, Flexible AC Transmission Systems (FACTS) and Resilient AC Distribution Systems (RACDS) in Smart Grid. Proceedings of the IEEE, 105(11): 2099–2115.

[11] Maza-Ortega JM, Acha E, Garcia S, et al., 2017, Overview of Power Electronics Technology and Applications in Power Generation Transmission and Distribution. Journal of Modern Power Systems and Clean Energy, 5(4): 499–514.

[12] Davari M, Mohamed YARI, 2016, Dynamics and Robust Control of a Grid-Connected VSC in Multiterminal DC Grids Considering the Instantaneous Power of DC- and AC-Side Filters and DC Grid Uncertainty. IEEE Transactions on Power Electronics, 31(3): 1942–1958.

[13] Kalari PY, Geetha RS, 2016, Performance Analysis of Paralleled VSC-HVDC Systems. 2016 International Conference on Microelectronics, Computing and Communications (MicroCom), Durgapur, India, 2016: 1–6.

[14] Rong M, Wu T, Li X, et al., 2020, Research on Grid Connection of Wind Farms Based on VSC-HVDC System. 12th IEEE PES Asia-Pacific Power and Energy Engineering Conference (APPEEC), Nanjing, China, 2020: 1–5.

Publisher's note

Bio-Byword Scientific Publishing remains neutral with regard to jurisdictional claims in published maps and institutional affiliations.

Journal of Electronic Research and Application, 2024, Volume 8, Issue 4
http://ojs.bbwpublisher.com/index.php/JERA
ISSN Online: 2208-3510
ISSN Print: 2208-3502

Research on Multiple Access Algorithms for Wireless Network

Kaifeng Yao*

Space Engineering University, Beijing 101400, China

***Corresponding author:** Kaifeng Yao, jstwg2023@163.com

Copyright: © 2024 Author(s). This is an open-access article distributed under the terms of the Creative Commons Attribution License (CC BY 4.0), permitting distribution and reproduction in any medium, provided the original work is cited.

Abstract: Nodes in the communication network mainly depend on the Media Access Control (MAC) layer protocol design. To ensure the MAC protocol achieves high throughput, low latency, and high service quality, this paper designed a "centralized-distribution" system MAC protocol combined with a slot allocation algorithm. This allows it to quickly adapt to the topology changes in the network and the overall network frame structure. For the centralized time slot allocation, since the system's frame structure changes across the entire network, the root node must gather information from other nodes. This ensures that the root node can collect the latest topology information when the network topology changes and subsequently adjust the frame structure of the whole network for the distributed time slot allocation. The simulation results show that the adaptive time-division multiple access mechanism can quickly adapt to changes in topology and the network's frame structure. It enables adaptive changes in node transmission times, ensures the rapid transmission and circulation of large-capacity data between nodes, and improves transmission efficiency.

Keywords: TDMA; Wireless network; MAC protocol; Time gap allocation

Online publication: August 13, 2024

1. Introduction

The Wireless Mesh Network (WMN) is a dynamic self-organization system composed of a group of wireless movable nodes independent of fixed network facilities [1]. Each node in the network completes the interaction and access of information through self-organization. In the hierarchical system of a wireless mesh network, the MAC layer works between the physical layer and the network layer. On the one hand, it shields the underlying technical details to realize the node access channel. On the other hand, it provides unified services to the network layer, including queuing, grouping, error control, confirmation, and other functions [2–10]. The performance of MAC layer protocol is closely related to the utilization rate of a wireless channel, thus affecting the performance of the whole network, which is an important research topic in wireless mesh network. Compared to the traditional mobile self-organized network, this network not only has the characteristics of terminal mobility, service randomness, limited wireless channel resources, and the absence of a central network, but also features high-speed terminal mobile, highly dynamic changes in network topology, high real-time

security services, and a large network load. Research on self-organized network MAC protocols focuses on how terminals access the wireless channel and effectively use channel resources. These protocols play a decisive role in important indicators such as network delay, throughput, and channel in vehicular networks. An ideal MAC protocol can effectively address issues like hidden terminals, exposed terminals, access conflicts, and merge conflicts while ensuring real-time security, network performance stability, and access fairness [11].

When the network topology structure changes dynamically, the performance of the traditional MAC protocols based on fixed time slots will decrease, lacking good scalability. Additionally, the time delay of the node access channels will fluctuate greatly due to changes in the topology structure, which is not conducive to the accurate and efficient transmission of security services [12–15]. This paper proposes a time slot allocation mechanism that can quickly adapt to changes in topology and frame structure across the whole network. This mechanism can still guarantee a high utilization rate of the channel when the network topology structure changes significantly, and it has good scalability.

2. Centralized time-slot allocation mechanism

The allocation criterion with the minimum convergence time for the node "convergence-issue" is as follows: the root node is allocated successively based on the number of node hops (relative to the root node) during the centralized allocation of control time slots and is allocated in the opposite order in the next cycle. In the frame structure design of the system, the nodes can occupy the corresponding business slot and the reverse corresponding to the scheduling slot. Therefore, to achieve the criterion minimum "convergence-distribution" convergence time allocation, the root node allocates based on the number of node hops (relative to the root node). All nodes can obtain the reverse convergence time slot, and node information converges to the root node within one convergence frame. The root node then allocates the scheduling time slot in the next cycle according to the increasing number of node hops, and the convergence time slot of the next cycle of all nodes is opposite to the scheduling time slot. Therefore, the cyclic process effectively maintains the allocation criterion of "reverse allocation of convergence time slots and forward allocation of scheduling time slots", ensuring that the convergence time of each node for "convergence-issue" is always minimized.

Suppose that node k, which has jumped from the root nodes, receives an Access Request Frame (ARF) at its network node upon startup. As part of the node's network access process, the startup node sends an ARF to request access during the allocated scheduling time slot. Upon receiving the startup node's ARF, the network node records the jump number of the startup node in the "Node Jump Information" column of the adjacent node table. Subsequently, it transmits this jump information through the Convergence Distribution Function (CDF) during its designated convergence time slot, continuously updating and forwarding the information to the root node. Because it has been assigned to the scheduling slot in the opposite slot, and the network node's scheduling slot is an incremental jump number (relative to the root node), regardless of the boot node's jump value, the jump information can be within converged to the root node within a convergence frame. Moreover, in each cycle's convergence frame, all nodes in the network should gather their jump number information to send to the root node [16–18].

During the aggregation process, each node receives CDF updates from nei_tab of other nodes in the network and generates its own CDF based on this information. This way, the jump information is constantly updated, and eventually, the nei_tab of the root node contains the jump information of all network nodes, including the startup node. The processing of nodes after receiving the CDF is shown in **Figure 1**:

(1) Check whether the node is in the network state. If yes, continue by comparing whether the root node (R_ID) of the sending node's CDF and its own root node (r_id) are identical and whether the merge status (Merge) is 0.

(2) Once the above conditions are met, the node updates all information from the CDF adjacent node table (Nei_tab) to its own neighbor node table (nei_tab). This update includes node jump information, an increased number of service time slots, and an updated number of subnet nodes. When updating node hop information, the node hop recorded in nei_tab column 0 is relative to the CDF sending node, and must be transformed to be relative to itself. The hop transformation algorithm is depicted in **Figure 2**.

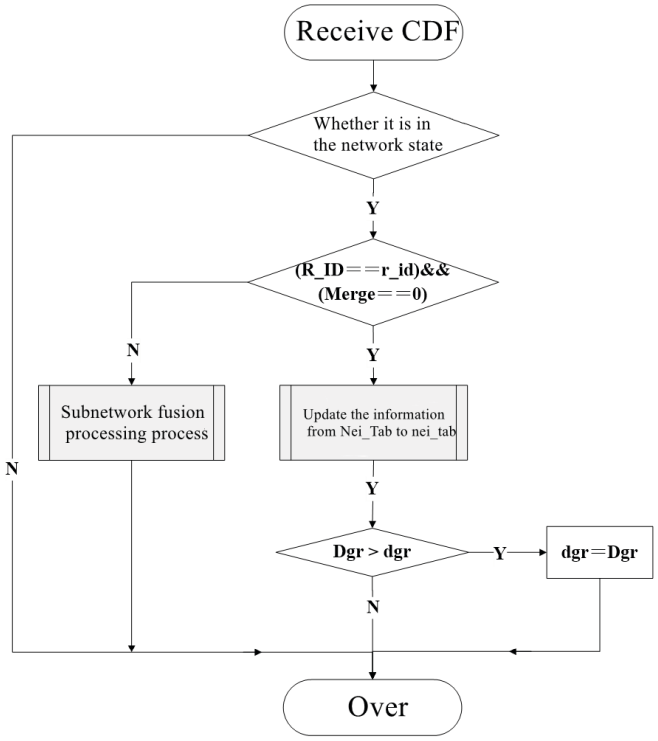


Figure 1. Processing flow when the node receives the CDF

```
1: for i from 0 to 32 do
2: if nei_tab [i] [0] = -1 then
3:    if (nei_tab[i ][0] ≠ -1) && (nei_tab[i ][0] > Nei_Tab[i ][0] + 1)  then
4: nei_tab [i] [0] = nei_tab [i] [0] + 1
5:    else if (nei_tab[i ][0] ＝ -1)
6: nei_tab [i] [0] = nei_tab [i] [0] + 1
7:      end
8:   end
9: end for
```

Figure 2. Jump transformation algorithm

In the next cycle, the root node allocates scheduling slots based on the number of nodes recorded in the next neighbor table (_tab), sorted by increasing node jumps across the entire network. When node jumps are identical, IDs are allocated in ascending order. Each node is assigned a scheduling slot sequentially starting from slot 0. The root node records the scheduling slot allocation information in the scheduling slot information column (tab column 0) and transmits it with the ARF.

When a node jumps from the root node, it updates its scheduling slot allocation information upon receiving the root node's ARF and obtaining its own scheduling slot. Concurrently, each jumping node sends ARF

during its allocated scheduling time slot. As a result of continuous updating and forwarding of scheduling time slot allocation information, all network nodes obtain their respective scheduling time slots within this cycle, including nodes that started up in the previous cycle. Distributing distribution information to the root node can also be completed within a scheduling frame, as the scheduling time slot allocation determines the direction of ARF transmission from nodes with fewer jumps to nodes with more jumps.

During the distribution process, the network node receives the ARF to update scheduling time slot distribution information. Both itself and the ARF sending node operate within the same network state. This process involves a "time slot allocation-multiplexing", as shown in **Figure 3**:

(1) The node updates the scheduling slot information (Tab column 0) and service slot increase information (Tab column 2) recorded by the ARF sending node to its own "allocation-reuse" table (tab column 0 and tab column 2), and performs the conflict detection and update process of slot reuse, and will be introduced in the later text.

(2) The node checks if there is a scheduling slot assigned to itself in the tab column 0 and if so, set the network stop identity (stop) to -1.

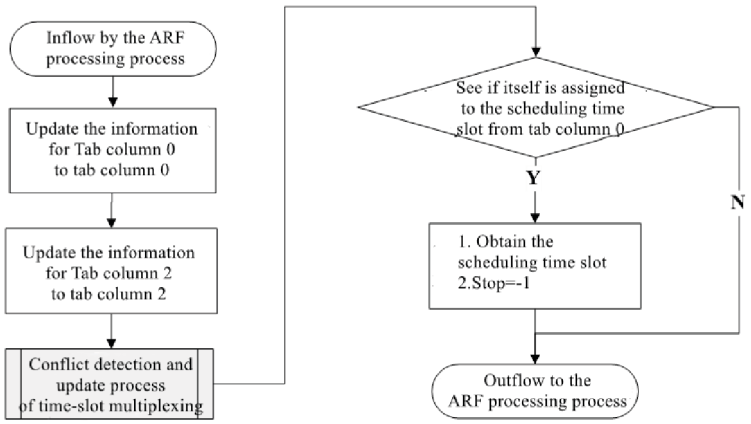


Figure 3. The "time slot allocation-reuse" processing process when the node receives the ARF

3. Distributing distribution mechanism

When the node is allocated to the scheduling time slot, it can fix and occupy the corresponding service time slot in each service frame, realizing the minimum service time slot guarantee [4]. To further improve the channel utilization of the system MAC protocol, distributed time slots can be multiplexed by interacting ARF and Feedback Frame (FF). Because each node receives information from at least two other nodes at the end of each cycle, even if there is a "convergence link interrupt" issue, a supplementary distribution mechanism can be used for scheduling slots between these nodes. Therefore, when their own scheduling slot arrives, network nodes can ensure awareness of neighboring nodes within their scope. Additionally, since each scheduling time slot corresponds to a service time slot, nodes can select unconflicting scheduling time slots for reusing service time slots after excluding the adjacent two hops. However, each node reuses time slots within the scheduling frame, the "conflict avoidance-conflict detection" method is adopted to resolve conflicts arising from time slot reuse.

For conflict avoidance, nodes collect information on service time slots reused by nodes within a two-hop range by receiving ARFs sent by other nodes before their own scheduling time slot. This allows nodes to select a service time slot outside the two-hop range to avoid conflicts when their scheduling time slot arrives. Nevertheless, since each node can only send one ARF per scheduling frame, there might be delays

in transmitting time slot multiplexing information to all nodes within the two-hop range, leading to potential multiplexing conflicts. Therefore, conflict detection between nodes is still needed.

As shown in **Figure 4**, nodes undergo the ARF or FF "slot allocation-reuse" processing, which involves time slot reuse conflict detection and update processes in two main stages. Using i for variables to find Tab or tab, and two nodes A and B for example to introduce the process. Assume node A received the ARF of node B:

(1) Node A determines whether node B multiplexes the time slot i by judging whether Tab [i] [1] is equal to 0, and proceeds to the next stage without reuse.

(2) If node B multiplexes slot i, node A checks whether slot i is multiplexed by whether the tab [i] [1] is equal to -1. If tab [i] [1] is equal to -1, node A sets tab [i] [1] to 1, indicating that slot i has been multiplexed by a hop node, and adding the ID field to ta_tab [i] indicates that the node with complex slot i is node B. And then move on to the next stage.

(3) If tab [i] [1] is not equal to -1, node A determines whether there is a hop node multiplexing time slot i but not node B by judging whether tab [i] [1] is equal to 1 and whether ta_tab [i] is equal to the ID field. If so, update the tab [i] [3] to the ID field value, indicating that node B has a reuse conflict. If otherwise, proceed to the next stage.

After entering the next stage:

(1) Node A determines whether the skip node of node B multiplexes the time slot i by judging whether Tab [i] [1] is equal to 1, if it ends otherwise.

(2) If node B multiplexes the time slot i, then determine whether it has multiplexing conflicts by judging whether the tab [i] [3] is equal to the ID. If so, tab [i] [1] is set to -1, with the multiplexing slot i abandoned, and ta_tab [i] set to 32 indicating that the slot i has been reused. If otherwise set the ta_tab [i] to 32. The process ends.

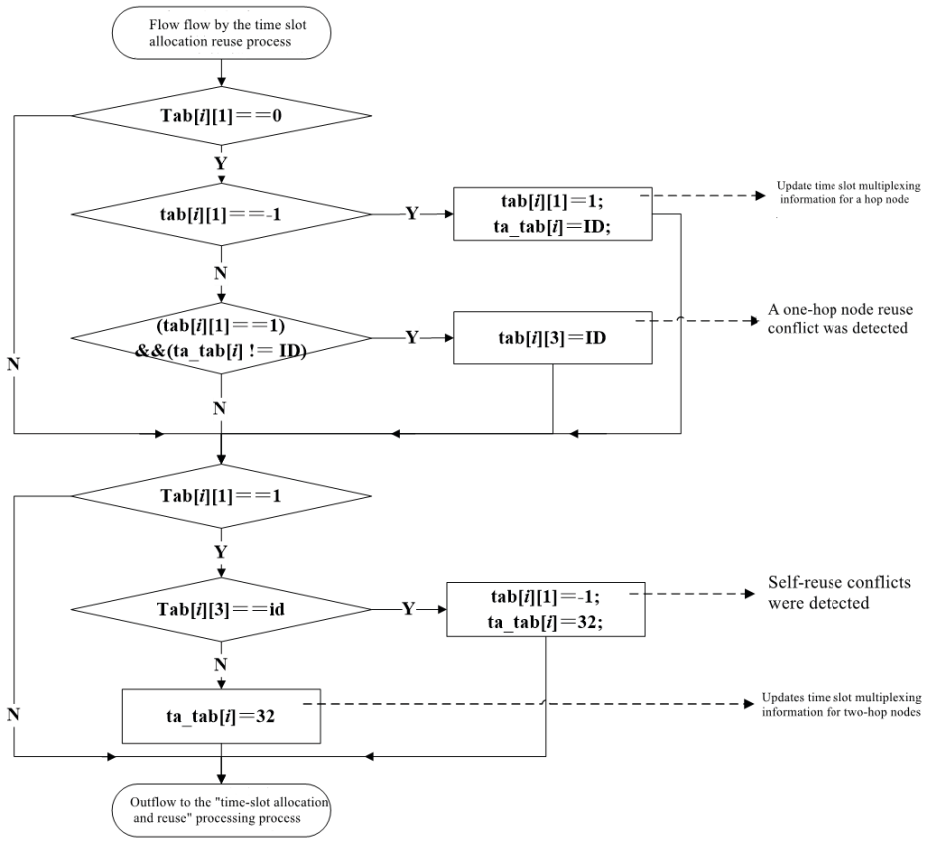


Figure 4. Multiplex conflict detection and update process

After each node sends the ARF or FF, the reuse conflict column (tab column 3) of the allocation-reuse table is initialized because the logged reuse conflict information has been sent to the hop node. However, the third column of the tab is at the end of the scheduling frame. If a conflict is reported in the next cycle, the conflict continues for one cycle. Thus, when the scheduling frame ends, the node views the tab column 3 and switches to the broadcast state if there is still reuse conflict information. In the first service frame, the node performs its own service time slot in the sequence of 10 broadcast time slots, wherein the broadcast time slot 0 sends the reuse conflict information by sending the ARF, so there is no reuse conflict in the following service frame.

4. The algorithm simulation and the results

4.1. Network model

The proposed improved algorithm was run on version 8.0 of the OPNET emulator. The network is composed of 32 mobile nodes, the wireless transmission range of each node is 150 m, and the network coverage area is 500 m. Nodes can move randomly within the scope of the network topology [5]. We performed simulations for different mobility levels using the "Random Waypoint Model". Different movement levels are achieved by adjusting the movement speed of the node and the movement pause time, which in our simulations was 0. For each scenario, the sending node and the destination node pairs are randomly selected. The sender produces a packet in an exponential distribution of one packet per second, and the effective planting load of each packet is 512 bytes. Each simulation lasted for 10 minutes. The protocol for the simulation is a comparison of the two Time Division Multiple Access (TDMA) before and after refinement with positional information. We call this basic TDMA and improved TDMA, represented by TDMA and I_TDMA, respectively. The MAC layer protocol used is IEEE802.11 with a 1 Mbit/s capacity.

4.2. Delivery success rate of the package

Figure 5 shows the packet-sending success rate for the basic TDMA and for the improved I_TDMA in three cases. It can be seen that after routing and maintaining TDMA with location information, the success rate of packet transmission is basically no different at rest, which can reach 100%. In the case of movement, we see a great improvement in the transmission success rate of TDMA after routing and maintenance using location information, with an average improvement of 40%–50%. Simulation results show that the improved algorithm not only enhances the packet-sending success rate of TDMA by 40%–50% but also reduces the end-to-end delay by an order of magnitude. Moreover, this improvement remains consistent regardless of the node's movement speed. This improvement not only greatly upgrades the performance of TDMA, but also the ability of TDMA to adapt to the dynamic topology, enhancing the applicability of TDMA in networks with highly mobile nodes.

4.3. End-to-end delay

In **Figure 6** we see that in all three cases, the improved TDMA whose end-to-end delay is much smaller than the basic TDMA, basically does not change with the node movement speed. This direct transmission of data packets through location-based routing protocol not only reduces the number of flooding but also has no process of establishing complete source routing packets, which reduces the end-to-end delay greatly.

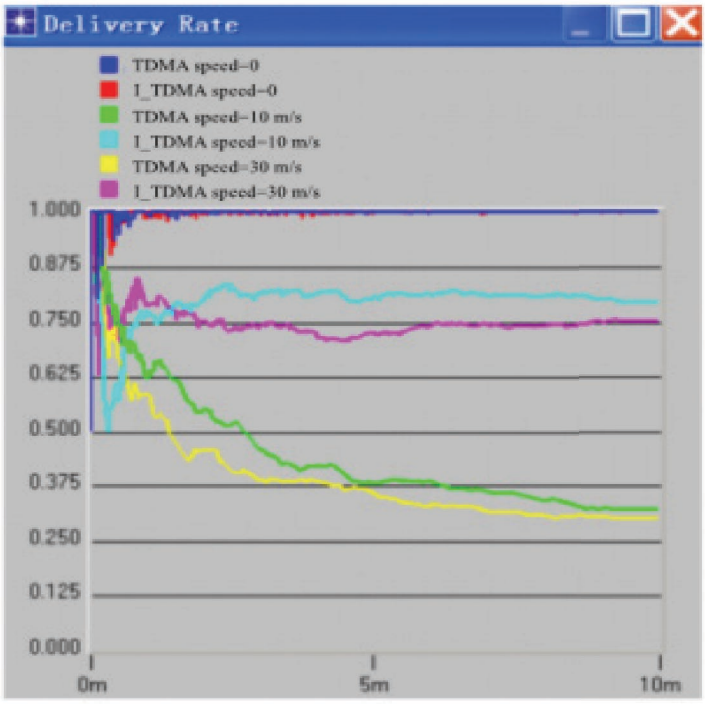


Figure 5. Comparison of delivery rates

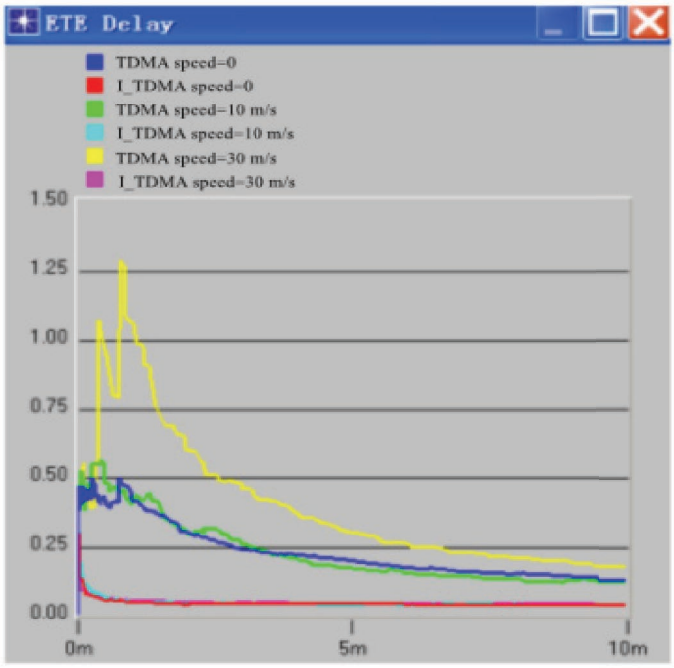


Figure 6. Comparison of ETE delays

5. Conclusion

This paper designs the "centralized-distributed" time slot allocation mechanism for the system MAC protocol. Firstly, for the centralized time slot allocation mechanism, it mainly designs the allocation process

of scheduling time slot when the frame structure changes. The whole "convergence-distributed" process only needs a scheduling frame and a convergence frame of time, to realize the rapid interaction of control information between the root nodes and other nodes. With the rapid change of frame structure in the whole network, the node also obtains the applied increased scheduling time slot or service time slot. In the next stage, for the distributed time slot allocation mechanism, it is stipulated that the nodes can multiplex the service time slot by scheduling the time slot, and the number of time slot reuses is calculated according to the maximum connectivity of the network [19,20]. In the process of reuse, the nodes schedule the slot multiplexing information, check whether the nodes are within the reuse information, and use the first service frame to broadcast the conflict information, so that the detected conflicts can be quickly eliminated.

Disclosure statement

The author declares no conflict of interest.

References

[1] Li P, Fu H, Wang K, et al., 2013, A Distributed Adaptive TDMA Time Slot Allocation Strategy in the Vehicular Ad Hoc Network. Electronic mass, 2013(01): 1–5 + 9.

[2] Zheng W, Jin H, Guo J, et al., 2018, A MAC Protocol Study of Access Threshold of Ad Hoc Network. Communication Technology, 51(07): 1602–1607.

[3] Shakhatreh H, Sawalmeh A, Al-Fuqaha A, et al., 2018, Unmanned Aerial Vehicles: A Survey on Civil Applications and Key Research Challenges. IEEE Access, 7: 48572–48634. https://doi.org/10.1109/ACCESS.2019.2909530

[4] Zheng C, 2019, Study on Distributed TDMA Resource Scheduling in UAV Cluster communication, thesis, National University of Defense Technology. https://doi.org/10.27052/d.cnki.gzjgu.2019.000677

[5] Peng G, 2006, Tactical Ad Hoc Network Media Access and Routing Algorithms Research, thesis, South China University of Technology.

[6] Jin R, Liu Z, Wang J, 2018, The TDMA Ad Hoc Time Slot Allocation Protocol Based on Full Network Frame Change. Computer Applications, 38(S1): 124–130.

[7] Song Z, Zeng G, Liang J, 2022, Dynamic Time-Slot Allocation of Space Vehicles Based on Dual-Frequency Communication. Telecommunications Technology, 62(03): 305–310.

[8] Guo Q, 2023, Wireless Network Time Slot Deployment Method Based on Distributed Time Division Multiple Access. Computer Knowledge and Technology: Academic Edition, 19(4): 80–82.

[9] Zhao Y, Li X, 2018, MAC protocol based on centralized time-division multiple access. Modern electronic technology, 41(21): 12–15 + 20. https://doi.org/10.16652/j.issn.1004-373x.2018.21.003

[10] Wang X, Li Y, Zhao S, 2017, Research Progress in Multi-Access Access Technology of Spatial Information Network. Computer Engineering and Application, 53(21): 8–16.

[11] Pei Y, 2011, LTE/LTE-Advanced uplink SC-FDMA technology study, thesis, Nanjing University of Posts and Telecommunications. https://doi.org/10.7666/d.d177369

[12] Ji H, 2016, Research on Single-Carrier Frequency Division and Multiple Access Technology in LTE-Advanced, thesis, Nanjing University of Posts and Telecommunications.

[13] Hadded M, Laouiti A, Muhlethaler P, et al., 2016, An Infrastructure-Free Slot Assignment Algorithm for Reliable Broadcast of Periodic Messages in Vehicular Ad Hoc Networks. 2016 IEEE 84th Vehicular Technology Conference (VTC-Fall), Montreal, Canada, 2016: 1–7. https://doi.org/10.1109/VTCFall.2016.7880903

[14] Borgonovo F, Capone A, Cesana M, et al., 2004, ADHOC MAC: New MAC Architecture for Ad Hoc Networks

Providing Efficient and Reliable Point-to-Point and Broadcast Services. Wireless Networks, 10(4): 359–366.

[15] Zhang R, Cheng X, Yang L, et al., 2015, A Novel Centralized TDMA-Based Scheduling Protocol for Vehicular Networks. IEEE Transactions on Intelligent Transportation Systems, 16(1): 411–416. https://doi.org/10.1109/TITS.2014.2335746

[16] Liu D, 2016, Research on Hybrid Multiple Access Protocol in Hierarchical Ad Hoc Network, thesis, Xidian University. https://doi.org/10.7666/d.D01066544

[17] Chen D, 2016, Study on Multiple Access Protocol in MIMO Link Ad Hoc Network, thesis, Xidian University.

[18] Yan P, 2014, Research on Single-Carrier Frequency Division and Multiple Access Technology in Broad-Band Wireless Communication System, thesis, University of Electronic Science and Technology of China. https://doi.org/10.7666/d.D499422

[19] Havinga PJM, Smit GJM, 2000, Energy-Efficient TDMA Medium Access Control Protocol Scheduling. 1st Asian International Mobile Computing Conference, AMOC, 2000: 1–10.

[20] Rahman SU, Ahmad M, Bazaz SA, 2012, A New Energy-Efficient TDMA-Based MAC Protocol for Periodic Sensing Applications in Wireless Sensor Networks. International Journal of Computer Science Issues (IJCSI), 9(4): 214.

Publisher's note

Bio-Byword Scientific Publishing remains neutral with regard to jurisdictional claims in published maps and institutional affiliations.

Journal of Electronic Research and Application, 2024, Volume 8, Issue 4
http://ojs.bbwpublisher.com/index.php/JERA
ISSN Online: 2208-3510
ISSN Print: 2208-3502

Furnace Temperature Curve Optimization Model Based on Differential Evolution Algorithm

Yiming Cheng*

Merchant Marine College, Shanghai Maritime University, Shanghai 201308, China

***Corresponding author:** Yiming Cheng, 13306339695@163.com

Copyright: © 2024 Author(s). This is an open-access article distributed under the terms of the Creative Commons Attribution License (CC BY 4.0), permitting distribution and reproduction in any medium, provided the original work is cited.

Abstract: When soldering electronic components onto circuit boards, the temperature curves of the reflow ovens across different zones and the conveyor belt speed significantly influence the product quality. This study focuses on optimizing the furnace temperature curve under varying settings of reflow oven zone temperatures and conveyor belt speeds. To address this, the research sequentially develops a heat transfer model for reflow soldering, an optimization model for reflow furnace conditions using the differential evolution algorithm, and an evaluation and decision model combining the differential evolution algorithm with the Technique for Order Preference by Similarity to Ideal Solution (TOPSIS) method. This approach aims to determine the optimal furnace temperature curve, zone temperatures of the reflow oven, and the conveyor belt speed.

Keywords: Furnace temperature curve; Difference equations; Differential evolution algorithms; TOPSIS methods

Online publication: August 13, 2024

1. Introduction

In the recent electronics assembly industry, the quality of soldering directly affects the reliability and performance of electronic products. As a key piece of equipment in the realization of surface mount technology, the precise control of the furnace temperature curve during the welding process is essential to ensure welding quality and production efficiency. The optimization of the furnace temperature curve can not only improve the consistency and quality of welding but also reduce energy consumption and production costs, thereby enhancing the market competitiveness of enterprises.

Traditional furnace temperature curve settings are often empirical and difficult to adapt to changing production conditions and material characteristics. With the development of computing technology, the design method of furnace temperature curves based on mathematical models and algorithm optimization has gradually become a research hotspot. Due to its simplicity, robustness, and efficiency, the differential evolution (DE) algorithm has shown great potential in solving nonlinear, multivariate, and complex system optimization problems.

In this paper, based on the heat transfer model during the welding process of the reflow furnace, an optimization model of the furnace temperature curve based on a differential evolution algorithm is constructed.

The model comprehensively considers the thermal radiation and thermal convection effect during the welding process and the thermal properties of the welding material and realizes the accurate control of the furnace temperature curve by optimizing the temperature of each temperature zone and the speed of the conveyor belt. This study not only provides a scientific method for optimizing the furnace temperature curve but also further considers the symmetry of the furnace temperature curve through the TOPSIS method, to achieve better welding results.

Through this study, we aim to provide an efficient and automated furnace temperature curve design tool for the electronics assembly industry to improve welding quality, reduce production costs, and promote the development of electronic manufacturing technology.

2. Question citation and analysis

When soldering electronic components to a circuit board, the temperature of each part of the reflow oven has a great impact on the quality of the product. In this paper, a reflow oven is taken as the research object, and there are 11 small temperature zones in the reflow furnace, the front and back areas, each small temperature zone is 30.5 cm in length, and there is a gap of 5 cm between the adjacent small temperature zones, and the length of the front and rear areas is 25 cm. In actual production, the product quality is controlled by adjusting the set temperature of each temperature zone and the furnace speed of the conveyor belt. When adjusting, the temperature in the small temperature zones 1–5 is required to be consistent, the temperature in the small temperature zones 8–9 is consistent, and the temperature in the small temperature zones 10–11 is kept at 25 ℃. The speed of the conveyor belt can be adjusted in the range of 65–100 cm/min.

The gap between the front of the furnace area, the back of the furnace area, and the small temperature zone is not subject to special temperature control, and its temperature is related to the temperature of the adjacent temperature zone. Additionally, the temperature near the boundary of each temperature zone may also be affected by the temperature of the adjacent temperature zone while the temperature of the production workshop is kept at 25 ℃. After the reflow furnace is started, the air temperature in the furnace will reach a stable level in a short time, after which the reflow furnace can be used for welding work. The temperature curve in the center of the welding area is called the furnace temperature curve, and its manufacturing boundary during production is shown in **Table 1**. The research is conducted based on this information.

Table 1. Boundary of furnace temperature curve

Boundary	Minimum value	Maximum value	Unit
Slope of temperature rise	0	3	℃/s
Slope of temperature drop	-3	0	℃/s
Time when temperature rise at 150 ℃ to 190 ℃	60	120	s
Time when the temperature is greater than 217 ℃	40	90	s
Peak temperature	240	250	℃

2.1. Mathematical model to describe temperature variation in the welding area

In this study, the temperature of each temperature zone is 173 ℃ (zones 1–5), 198 ℃ (zone 6), 230 °C (zone 7), and 257 °C (zones 8–9) respectively with a conveyor belt speed of 78 cm/min. The temperature of the center of the welding zone is listed, the temperature of the center of the welding zone at the end of the small temperature

zone 8 is plotted, and the corresponding furnace temperature curve is drawn. The temperature in the center of the soldering area every 0.5 s is stored in the result.csv spreadsheet.

To solve this problem, the analysis method in this article is as follows: Firstly, we set the target temperature of each small temperature zone of the reflow oven. After the furnace reached a steady state, we analyzed the temperature conditions in different areas of the furnace, including the middle of the small temperature zone, near the boundary, and the gap between the small temperature zones. By applying the Fourier theorem in heat transfer science, we derive the functional relationship between temperature and position in the furnace. This analysis allows us to quantify the temperature distribution in the middle of the small temperature zone, near the boundary, and in the interstitial area, and create a picture of the temperature distribution inside the reflow oven. Secondly, the process by which the printed circuit board is heated as it moves in the reflow oven. We can determine the temperature in the reflow furnace as a function of position according to the Fourier theorem in heat transfer science. The temperature in the middle of the small temperature zone, the temperature near the boundary of the small temperature zone, and the temperature of the gap in the small temperature zone were quantified, and the temperature in the reflow furnace was obtained as a function of position. For the process that the printed circuit board is heated when it moves in the reflow furnace in the second step, the relationship between the heat absorbed by the printed circuit board per unit of time and the ambient temperature of the reflow furnace and the relative motion velocity is considered, and the differential equation is listed accordingly. The differential equation is transformed into a difference equation by using the improved Euler formula algorithm. A model of the temperature change in the soldering area of the printed circuit board based on the difference equation was established in the reflow oven welding heat transfer model, and the corresponding furnace temperature curve was drawn, as shown in **Figure 1**.

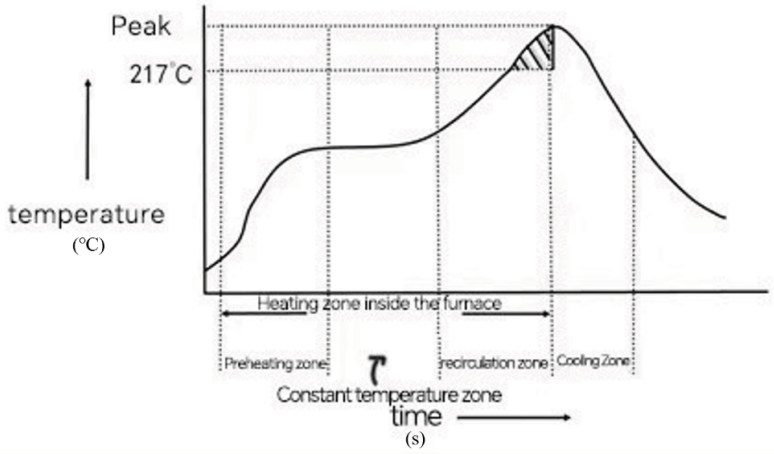


Figure 1. Furnace temperature curve

2.2. Robin Hendrick's view on blended learning

In this phase, we set the temperature of each small temperature zone of the reflow oven to 182 °C (small temperature zones 1–5), 203 °C (small temperature zone 6), 237 °C (small temperature zone 7), and 254 °C (small temperature zones 8–9), respectively. Under these conditions, our main goal was to explore the maximum speed at which the conveyor belt could safely pass through the furnace without compromising the quality of the weld.

To achieve this, we performed the following analysis: When determining the maximum furnace speed of the conveyor belt, the key limiting factor is whether the furnace temperature curve meets the established process

limits. Based on this, we adopted a meticulous approach, following the furnace temperature curve model established in the reflow oven welding heat transfer model, and simulating the furnace temperature curve at different speeds by dot drawing technology. We traverse the belt speeds in fine steps to ensure that the furnace temperature profile meets the requirements of the process at each speed.

In this process, we continuously optimize the traversal strategy by gradually increasing the speed while monitoring whether the furnace temperature curve exceeds the preset limits. As soon as we found that the furnace temperature curve was out of bounds, we adjusted the step size and performed a more detailed search to ensure that we found the maximum speed that was closest to the limit and did not cross the boundary. This method not only guarantees the safety of the welding process but also maximizes productivity.

2.3. Optimizing furnace temperature curve to minimize over-temperature areas

Temperature control in the center of the welding area is particularly critical during the welding process. The goal of this paper is to ensure that this temperature exceeds 217 °C for as short a period as possible and that the peak temperature is effectively controlled to avoid thermal damage to the material or affect the weld quality. The ideal furnace temperature curve should minimize the coverage area between 217 °C and the peak temperature while maintaining the welding results, as shown in the shaded section of **Figure 1**.

To solve this problem, this paper analyzes the minimum area of the corresponding part of the furnace temperature curve in a given temperature range and the conveyor belt passing speed range and first gives the formula for calculating the area based on the reflow oven welding heat transfer model. The area covered by the furnace temperature curve exceeding 217 °C to the peak temperature (shaded in **Figure 1**) was taken as the optimization goal, and the environmental parameters (temperature of each temperature zone, conveyor belt passing speed) were used as variables, and the differential evolution algorithm was used to continuously generate offspring through two processes, mutation and evolution, and the minimum value of the area was found.

2.4. Pursue symmetry of the furnace temperature curve and minimize the over-temperature area

During the soldering process, in addition to meeting the process limits, it is also desirable that the furnace temperature curve exceeds 217 °C on both sides of the peak temperature centerline should be as symmetrical as possible (see **Figure 1**).

To solve this problem, the analysis of this paper is as follows: skewness is often used to measure the symmetry of the probability distribution of random variables in probability statistics, and the skewness of sample X is calculated as follows:

$$Sk(X) = E\left[\left(\frac{X-\mu}{\sigma x}\right)^3\right] \quad (1)$$

where μ and X are the mean and standard deviation of sample X, respectively. *Sk(X)* can be in the range of (-1,1), and its positive and negative means that the distribution of the observed data of the sample is positively skewed and negatively skewed, and the closer *Sk(X)* is to 0, the probability is dedicated, the more symmetrical the distribution.

We were inspired by this to consider the time of the furnace temperature curve (x-axis) as the observed value of the sample, the temperature (y-axis) is normalized as the probability distribution of the observed values, and the skewness is used to quantify the peak temperature on the furnace temperature curve.

In this study, we not only pursued the minimization of the area covered by the furnace temperature curve

exceeding 217 °C to the peak temperature but also sought to achieve the symmetry of the furnace temperature curve on both sides of the peak temperature to ensure uniformity and quality of the welding process. To measure the symmetry of the furnace temperature curve, we introduce the statistic of skewness, the closer its value is to 0, the more symmetrical the furnace temperature curve is.

To comprehensively evaluate the performance of the furnace temperature curve, we used the TOPSIS method to construct an evaluation model. The model combines two key indicators, area and skewness, to generate a comprehensive evaluation index for each furnace temperature curve. This index reflects the performance of the furnace temperature curve in terms of area minimization and symmetry, providing us with comprehensive evaluation criteria.

Under the framework of the differential evolution algorithm, we use the comprehensive evaluation index as the objective function to guide the algorithm in search for the optimal solution. The algorithm starts from the initial population and continuously iterates through mutation and cross-operation to optimize the parameters of the furnace temperature curve until the optimal furnace temperature curve meets the established criteria. This process not only considers the area of the furnace temperature curve but also fully considers the symmetry of the curve to ensure the efficiency of the welding process and the consistency of product quality.

3. Model assumptions, establishment and solving

3.1. Model building

In this study, we focused on analyzing the heating dynamics of printed circuit boards inside a reflow oven. Firstly, given the relative displacement between the printed circuit board and the gas in the furnace as it moves in the furnace, our model mainly considers the influence of two heat transfer mechanisms, heat radiation and heat conduction, on the heating of the circuit board, which is based on the main heat exchange mode under relative motion [1].

Secondly, given that the printed circuit board under study is only 0.15 mm thick, its thin nature means that its surface temperature can reasonably be considered as the temperature at the center of the soldering region, an assumption that simplifies the analysis of soldering hot spots without significant loss of calculation accuracy.

Finally, the model was established without considering the influence of temperature change during the phase transformation of solder paste. This decision is based on a preliminary analysis of the thermal dynamics of each stage of the welding process, and we believe that the effect of the phase transition of the solder paste on the overall temperature distribution is of secondary importance under the specific conditions of this study. This simplification helps us to focus our research on the optimization of furnace temperature curves, thus addressing the main thermodynamic problems in the welding process more directly.

3.2. Establishment and solution of the model

3.2.1. Temperature distribution model in the reflow oven

We divided the reflow furnace into three parts: the middle of the small temperature zone, the vicinity of the boundary of the small temperature zone, and the gap between the small temperature zone. The middle of the small and medium temperature zone and the boundary of the small temperature zone are collectively called the small temperature zone, and the length of each small temperature zone is l = 30.5 cm, and the length of the temperature zone gap is d = 5 cm. In particular, we specify that near the boundary of the small temperature zone is a single strip of length of 0.05l on both sides of the small temperature zone, and the length of the middle of the small temperature zone is 0.9l. The location and dimensions of these three areas are shown in **Figure 2**.

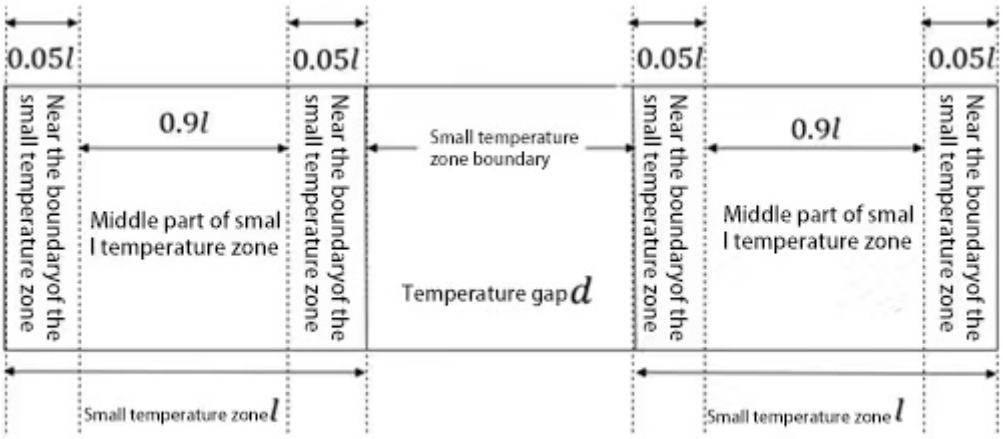


Figure 2. The location of the reflow furnace internal structure and its size

We take the two temperature zones in **Figure 2** as an example to calculate the temperature distribution inside the reflow furnace and note that the set temperature of the left small temperature zone in **Figure 2** is *T1*, and the set temperature of the right small temperature zone is *T2*. We believe that the temperature in the middle of the small temperature zone is the set temperature of the small temperature zone. Considering the system composed of the gap between the small temperature zones and the boundaries of the small temperature zones on both sides of it, after the heat transfer process is stabilized, according to the Fourier heat conduction theorem, for a microelement layer with a thickness of *dx*, the heat flux *q* passing through the layer per unit time is proportional to the temperature change rate *dT/dx*.

$$q = -\lambda \frac{dT}{dx} \tag{2}$$

Among them is the thermal conductivity. In particular, for a thin plane with a thickness of *dx*, when the heat conduction is stable, the heat coming in and out of it per unit time is equal, as shown in **Figure 3**, that is:

$$\frac{dq}{dx} = 0 \tag{3}$$

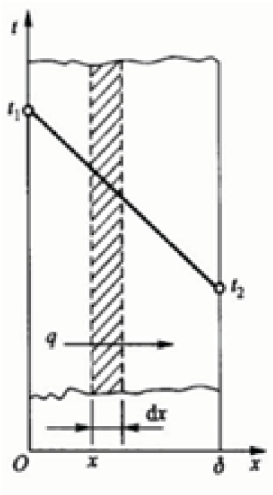


Figure 3. The heat input and output are the same

Simultaneous **Equation (2)** and **Equation (3)**, we get the second-order linear ordinary differential equation:

$$\frac{Td^2}{dx^2} = 0 \tag{4}$$

As shown in **Figure 2**, the width of the system (consisting of the small zone gap and near the boundary of the small zone on either side of it) is $d + 0.1l$. We give the following initial values of **Equation (4)**: $x = 0$, $T = T_1$, $x = d + 0.1l$, $T = T_2$. The left and right sides of **Equation (4)** are integrated twice to obtain the ambient temperature distribution of the system as:

$$T = \frac{T_2 - T_1}{d + 0.1l} x + T_1 \tag{5}$$

Let x be the position coordinates, then the final ambient temperature distribution function relationship is:

$$T_S(x) = \begin{cases} T_1(0 \le x \le 0.9l) \\ \frac{T_2 - T_1}{d + 0.1l}(x - 0.9l) + T_1(0.9l \le x \le l + d) \\ T_2(l + d \le x \le 1.9l + d) \end{cases} \tag{6}$$

The image of the temperature distribution is mapped to each part of the reflow oven to make **Figure 4**, where the thick black line represents the image of the ambient temperature in the reflow oven as a function of position.

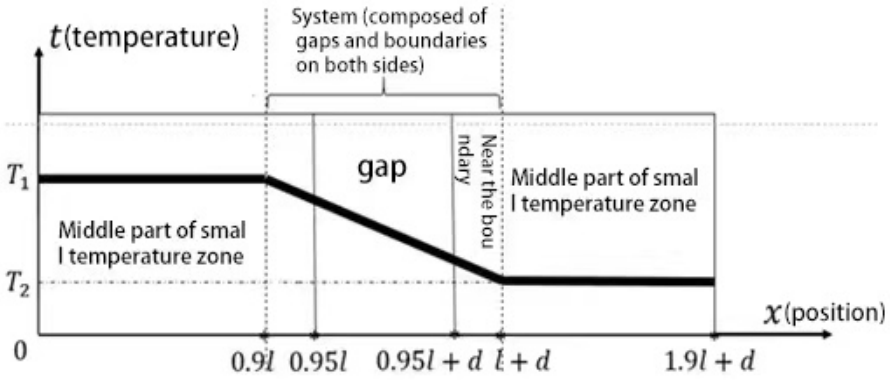


Figure 4. Image of the temperature distribution in two temperature zones

From **Figure 4**, an image of the temperature distribution between the two small temperature zones can be obtained, and as long as the set temperature of the two temperature zones is known, zone 7 can be used to calculate the temperature distribution at different locations in the reflow furnace. There are 11 temperature zones in this problem, and for temperature zones 2–10, the temperature distribution between the local temperature zone and the adjacent gaps can be obtained according to the set temperature of the other temperature zones. In particular, temperature zone 1 and temperature zone 11, are also adjacent to the area in front of the furnace and the area behind the furnace, at this time we can regard the production workshop as a stable heat source of temperature 25 ℃, that is, as the temperature zone with a set temperature of $T = 25$ ℃, and repeat the above calculation. The set values of the temperature of each temperature zone in the reflow oven welding heat transfer model are: the temperature before the furnace and the temperature after the furnace are 25 ℃, 173 ℃ (small

temperature zones 1–5), 198 ℃ (small temperature zone 6), 230 ℃ (small temperature zone 7), 257 ℃ (small temperature zones 8–9), 25 ℃ (small temperature zones 10–11). Substituting these temperatures into **Equation (5)** calculates the relationship between the ambient temperature *Ts* and position *x* in the reflow furnace is shown in **Figure 5**.

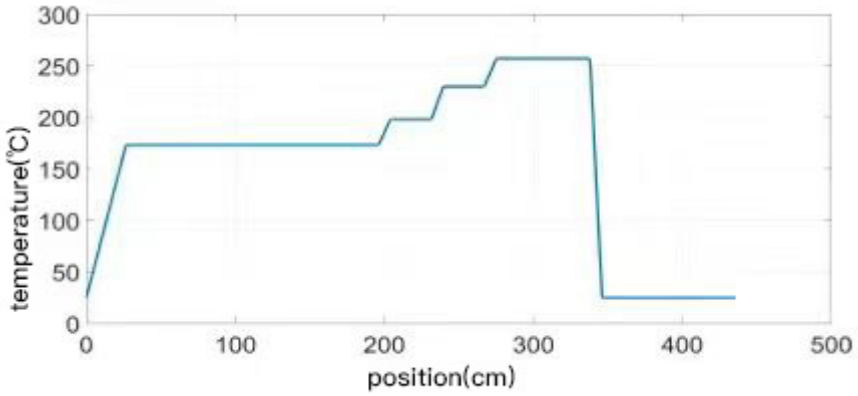


Figure 5. The relationship between the ambient temperature *Ts* of the reflow oven and the position *x*

3.2.2. Model of printed circuit board being heated inside a reflow oven

In the second step, we study the process by which the printed circuit board is heated as it moves inside the reflow oven. From the reflow oven welding heat transfer model, we only need to consider the heat transfer caused by thermal convection and thermal radiation, let the heat transferred by thermal convection of the printed circuit board be Q_1, and the heat transferred by thermal radiation be Q_2, then the total heat Q received by the printed circuit board is:

$$Q = Q_1 + Q_2 \tag{7}$$

Using the double counting method, the total heat absorbed by the printed circuit board in the reflow oven can also be written as:

$$Q = cm\Delta T \tag{8}$$

c is the specific heat capacity of the printed circuit board, m is the mass of the printed circuit board, and T is the change in the temperature of the printed circuit board, and the units are all in the International System of Units (SI units).

For the process of thermal convection, according to Newton's cooling formula, the power of the printed circuit board to absorb heat is [2]:

$$P_1 = h_c \cdot S\left(T_S - T\right) \tag{9}$$

where S is the contact area between the printed circuit board and the gas in the reflow furnace, Ts is the ambient temperature in the reflow furnace, T is the temperature in the center of the soldering area, and h_c is the convective heat transfer coefficient, which is defined as the heat that can be transferred per second in an area of 1 m^2 when the temperature difference between the solid and the flowing body is 1 ℃ [3]. According to Boltzmann's law, the heat transfer power during thermal radiation is:

$$P_2 = \varepsilon S\sigma(T_S^4 - T^4) \tag{10}$$

where ε represents the emissivity of the object, S represents the area of the printed circuit board that receives thermal radiation, and σ is the Boltzmann constant. In this problem, we take $\sigma = 5.67 \times 10^{-8}$ W/(m$^2\cdot$ K^4), Ts is the surface temperature of the object, T is the ambient temperature and the units are all in SI units. Substituting **Equation (10)** into **Equation (9)** and deriving it on both sides

$$\frac{dT}{dt} = \frac{1}{cm}\left(P_1 + P_2\right) = \frac{1}{cm}\left(h_c S\left(T_S - T\right) + \varepsilon S\sigma\left(T_S^4 - T^4\right)\right) \tag{11}$$

Let the thickness of the printed circuit board be L, then there is a basic mass relationship:

$$m = \rho SL \tag{12}$$

Substituting **Equation (12)** into **Equation (11)** calculates:

$$\frac{dT}{dt} = \frac{1}{\rho cL}\left(h_C\left(T_S - T\right) + \sigma\varepsilon\left(T_S^4 - T^4\right)\right) \tag{13}$$

The different parameters in **Equation (13)** are identified where L = 0.15 mm and the relationship between ambient temperature and position Ts has been given in **Figure 5**. For a printed circuit board, its density ρ, emissivity ε, and specific heat capacity c are all temperature-dependent. We divide the whole heating process into before reflow, during reflow, and after reflow: before reflow refers to the process of the printed circuit board passing through the preheating zone (small temperature zones 1–5) and the constant temperature zone (small temperature zones 6–7), the reflow refers to the process of the printed circuit board passing through the reflow zone (small temperature zones 8–9), and the after reflow refers to the process of the printed circuit board passing through the cooling zone (small temperature zones 10–11). For each phase, the temperature is approximately considered constant, and a given value is substituted for the value of a parameter at that stage, as shown in **Table 2** (the units of the following quantities are SI units).

Table 2. The given numerical value

	Density, ρ (kg/m^3)	**Emissivity, ε**	**Specific heat capacity, c (J/(kg·K)**
Before reflow	7310	0.82	114
During reflow	8218	0.071	238
After reflow	8218	0.071	176

For the convective heat transfer coefficient h_c, the h_c results calculated in previous research in actual industrial production are shown in **Table 3** [4].

Table 3. The h_c calculated in actual industrial production

T **(℃)**	h_c **(W/m^2·k)**
70	48.84
160	48.04
200	48.01
230	48.06
250	48.02

In the same reaction stage (before, during, and after reflow), the five values of convective heat transfer, h_c are 48.84, 48.04, 48.01, 48.06, and 48.02. The values vary slightly, suggesting that the value of h_c remains

relatively constant within each stage. The value of the convective heat transfer coefficient of the printed circuit board is set to h_{c1} when it passes through the preheating zone (small temperature zones 1–5) and the constant temperature zone (small temperature zones 6–7). The value of the convective heat transfer coefficient when the printed circuit board passes through the reflow zone (small temperature zones 8–9) is set to h_{c2}. When passing through the cooling zone (small temperature zones 10–11), the value of the convective heat transfer coefficient is set to h_{c3}.

The literature shows that the forced convection coefficient of the gas should be 20–100 W/m^2·K, and the coefficient must be non-negative, so the range is appropriately expanded, taking 0–100 W/m^2·K as a reference range for h_{c1}, h_{c2}, and h_{c3} [5]. To determine the values of h_{c1}, h_{c2}, and h_{c3}, we also need a standard furnace temperature curve as a control. In this study, 709 sets of time and temperature values were used to draw a standard furnace temperature curve. These 709 points are denoted as (t_1, T_1), and so on. For h_{c1}, h_{c2}, and h_{c3}, the first coarse adjustment is carried out, that is, the initial value is 0, the step size is 10, and the last value is 100. For each given set of h_{c1}, h_{c2}, and h_{c3}, the differential equation in **Equation (14)** is changed to a difference equation using the average form of the improved Euler formula:

$$T_P = T_n + \frac{10}{\rho cL}\left(h_C\left(T_{sn} - T_n\right) + \varepsilon\sigma\left(T_{sn}^4 - T_n^4\right)\right) \tag{14}$$

$$T_C = T_n + \frac{10}{\rho cL}\left(h_c\left(T_{S(n+1)} - T_n\right) + \varepsilon\sigma\left(T_{sn}^4 - T_n^4\right)\right) \tag{15}$$

$$Tn+1 = \frac{1}{2}\left(T_p + T_c\right) \tag{16}$$

The time for the printed circuit board to pass through the preheating zone (small temperature zones 1–5) and the constant temperature zone (small temperature zones 6–7) is t_1 = (272.5 × 60) / 78 = 209.62 s, the time for the printed circuit board to pass through the reflow zone (small temperature zones 8–9) is t_2 = (71 × 60) / 78 = 54.62 s, and the time for the printed circuit board to pass through the cooling zone (small temperature zones 10–11) is t_3 = (89 × 60) / 78 = 68.46 s. By using MATLAB to solve the system of difference **Equations (14)–(16)** with constants σ, c, and ε, we can obtain 709 sets of time and temperature data respectively, denoted as (t_1, T'_1), and so on. The newly obtained 709 points can be used to plot a furnace temperature curve. In particular, the furnace temperature curve also needs to meet the process boundaries in **Figure 1**, that is:

$$\left|\frac{T'_{i+1} - T'}{t_{i+1} - t_i}\right| < 3, i = 1, 2, 3..., 708 \tag{17}$$

$$60 \le t_k - t_i \le 90\left(t_i \le t_j \le t_{\max}\right) \tag{18}$$

$$40 \le T'_{\max} \le 250 \tag{19}$$

$$240 \le T'_{\max} \le 250 \tag{20}$$

Equation (17) depicts that the absolute value of the slope of temperature rise (fall) is small, less than 3. **Equation (18)** is to describe the time of 150 °C to 190 °C in the process of temperature rise, the temperature of T_i and T_j to meet the welding center at two moments is T'_i, T'_j, T_k, T_i meets $T'_i \ge 150$ °C and $T'_{i-1} \le 150$ °C, $T'_j \le 190$ °C and $T'_{j+1} \ge 190$ °C. **Equation (19)** is to describe the time when the temperature is greater than 217 °C: Let the time be T_k and let T_1 be the temperature at the welding center of the corresponding T_k. The conditions $T_1 = T'_k$ and T'_1 satisfies $T'_k \le 217$ °C and $T'_{k-1} \ge 217$ °C, $T_i \le 217$ °C and $T_{i+1} > 127$ °C. **Equation (20)** is the peak

temperature for T'_{max}. To sum up, the algorithm steps for obtaining h_{c1}, h_{c2}, and h_{c3} are as follows:

(1) Set the traversal conditions of h_{c1}, h_{c2}, and h_{c3}: the initial value is 0, the step size is 10, and the last value is 100.

(2) Generate a set of h_{c1}, h_{c2}, h_{c3}.

(3) For h_{c1}, h_{c2}, and h_{c3} generated in step 2, under the temperature distribution conditions of the reflow oven welding heat transfer model and the temperature distribution of question stem, respectively, check whether the calculated 709 groups (t_i, T_i) meet all the conditions of **Equations (16)–(18)**, return to step 2 if at least one condition is not satisfied, and calculate and record the sum of residuals squares of the 709 groups of data if it satisfies $\sum_{i=1}^{709}\left(T_i - T_i^{'}\right)^2$.

(4) When the traversal is completed, take the group of h_{c1}, h_{c2}, and h_{c3} corresponding to the sum of squares of the smallest residuals.

(5) After the primary traversal of steps 1–4 is completed, adjust the step size to 1, traverse at [h_{c1} -5, h_{c1} + 5], [h_{c2} – 5, h_{c2} + 5], [h_{c3} – 5, h_{c3} + 5], and repeat steps 1–4.

(6) After two iterations, the final result is: h_{c1} = 8, h_{c2} = 65, h_{c3} = 30. As mentioned above, the parameters in the difference **Equation (14)–(16)** will have different values when t is taken with different values, and the final furnace temperature curve is obtained by dotting and plotting with MATLAB, as follows:

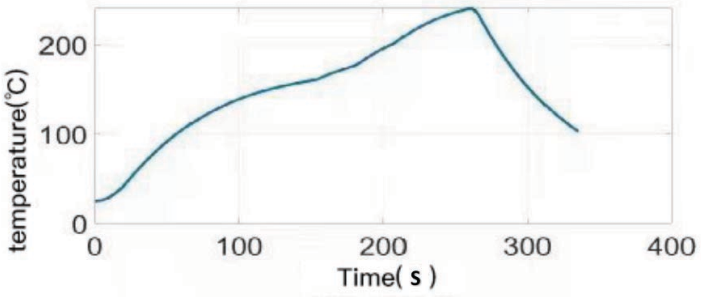


Figure 6. Furnace temperature curve

Among them, the temperatures at the midpoint of 3, 6, and 7 in the small temperature zone and the center of the welding area at the end of the small temperature zone 8 were 128.60 ℃, 169.57 ℃, 190.88 ℃ and 226.25 ℃, respectively (**Figure 6**).

3.2.3. Determine the maximum conveyor belt furnace speed to solve the model

Based on the model of the temperature distribution of the reflow oven in this study, the temperature distribution in the reflow oven can be obtained by using **Equation (5)** as long as the temperature of the small temperature zone is known. Similarly, the values of h_c, ρ, ε, and c continue to be used. Let v be the speed of the conveyor belt passing through the furnace, since the conveyor belt speed in this study is $65 \leq v \leq 100$ cm/min, to find the maximum conveyor belt pass speed, this study directly traverses with a step size of 0.01, and the specific traversal steps are as follows:

(1) Set the traversal condition of v: the initial value is 65, the step size is 0.01, and the last value is 100.

(2) According to the v generated in step 1, calculate the time t_1 before the reflow of the printed circuit board, the time t_2 when the printed circuit board is reflowed, and the time after the reflow of the printed circuit board is t_3.

(3) Obtains several groups of points (t_i, T_i) according to the temperature distribution of the reflow oven welding heat transfer that has been calculated, and the values of h_{c1}, h_{c2}, h_{c3}, t_1, t_2, t_3, ε, ρ, c in different

stages.

(4) Check whether several groups of points (t_i, T_i) meet all the conditions of **Equations (16)–(19)**, if not, return to step 1. If it is satisfied, record the velocity v at this time, return to step 1, and continue traversal.

(5) After obtaining a plurality of v, take the maximum v as the maximum conveyor belt furnace speed.

In the end, the maximum conveyor belt passing speed was v = 79.52 cm/min.

3.2.4. Optimize the furnace temperature curve to minimize the over-temperature area to solve the model

Let v be the speed of the conveyor belt, and T_1, T_2, T_3, and T_4 are the set temperatures of the small temperature zones (1–5), (6), (7), and (8–9), respectively. To facilitate the representation of unknown quantities, the vector $x = (T_1, T_2, T_3, T_4, v)$, and the value range of each component of x given in the question stem is T_{12} [165, 185], T_{22} [185, 205], T_{32} [225, 245], T_{42} [245, 265], v_2 [65, 100]. Let the furnace temperature curve exceed 217 °C and the area covered by the peak temperature is A, then A is calculated as follows: For any furnace temperature curve, considering that the furnace temperature curve is obtained by the numerical solution of the MATLAB differential equation, we take one point (t_k, T_k), which satisfies $T_k \leq 217$ °C and $T_k \geq 217$ °C. Take one more point to be the highest point of the furnace temperature curve (t_m, T_m), because there are enough points, so the area can be expressed as follows:

$$A = \sum_{i=k}^{m-1} T_i \left(x_{i+1} - x_i \right) \tag{21}$$

Let's first agree that a vector $\vec{x}$ is an individual, $\vec{x}_i(j)$ represents the $\vec{j}$ component of the $\vec{i}$ vector and the specific steps of the differential evolution algorithm are as follows:

(1) Establish a population with 6 individuals, which are denoted as $\vec{x}_1$, $\vec{x}_2$, $\vec{x}_3$, $\vec{x}_4$, $\vec{x}_5$, $\vec{x}_6$, where each component of $\vec{x}_i$ should be in the given range, let n be used as the quantity to record the algebra of the population so that n = 0.

(2) For the 6 individuals in the population in the first step, firstly, the ambient temperature Ts in the reflow furnace under the corresponding situation is calculated by **Equation (6)**, and then combined with the different parameters given in **Equations (15)–(17)** and temperature distribution model in the reflow oven, several sets of welding center temperature and time data (t_i, T_i) are obtained and these data are recorded.

(3) For a plurality of groups of data (t_i, T_i) obtained in step 2, substitute in **Equations (15)–(19)** to check whether the process limit is satisfied. If satisfied, enter step 4, and return to step 1 if not satisfied.

(4) Using the data in step 2, find the area A corresponding to 6 individuals (6 vectors) according to **Equation (19)**, take the maximum value of area A_b, so that $A_0 = A_b$. Save the vector $\vec{x}_i$ at this time, so that $\vec{x}_0 = \vec{x}_i$.

(5) Any 3 individuals are taken from the population, according to the (t_i, T_i) of each individual recorded in step 2, the area A_i is calculated according to **Equation (20)**, and the area is sorted from small to large A_w, A_m, A_b, and the corresponding vectors are $\vec{x}_b$, $\vec{x}_m$, and $\vec{x}_w$.

(6) Among the three vectors given in step 5, define the fit f_i of a vector $\vec{x}_i$ as:

$$f_i = 1 - \frac{A_i - A_w}{A_m - A_w} \tag{22}$$

Then, according to **Equation (20)**, f_b, f_m, and f_w are obtained, and the fitness of six vectors $f_1, f_2, ..., f_6$ is calculated and recorded along with their average $\bar{f}$, maximum f_m, minimum f_w.

(7) Continues from the definition of the variable in step 5, and for $_1$, define $\vec{H}_1 = \vec{x}_b + F_1 (\vec{x}_m - \vec{x}_w)$. where F_1 is the scaling factor, and its expression is as follows:

$$F_1 = 0.1 + 0.8 \cdot \frac{f_m - f_b}{f_m - f_w} \tag{23}$$

and $F_1 \in [0, 2]$. Check whether the components of $\vec{H}_1$ meet the value range given at the beginning of the model in this section, if so, record $\vec{H}_1$ and enter step 8, if not, return to step 5.

(8) Repeat steps 5–7 five more times to ensure that all 6 individuals in the population have corresponding $\vec{H}_i$ and $\vec{F}_i$.

(9) For each set of vectors $\vec{x}_i$, $\vec{H}_i$, define the crossover probability cr_i as:

$$cr_i = \begin{cases} 0.1 + 0.5 \cdot \dfrac{f_i - f_w}{f_m - f_w}, f_i > \overline{f} \\ 0.1, f_i \le \overline{f} \end{cases} \tag{24}$$

The cr_i of the six vectors is calculated and recorded according to the definition of **Equation (24)**.

(10) For each set of vectors $\vec{x}_i$ and $\vec{H}_i$, take any 1 × 5 row vector $\vec{T}_i$ and leave $\vec{T}_i$ blank as a zero vector, and then reset $\vec{T}_i$ according to the following algorithm:

$$T_i(j) = \begin{cases} x_i(j), rand(0,1) \le cr_i \\ H_i(j), rand(0,1) > cr_i \end{cases} \tag{25}$$

where rand(0,1) represents the random number generated in (0,1) and each component of $\vec{T}_i$ is reset to generate a random number at (0,1), $\vec{T}_i = \vec{x}_i$.

(11) According to the test method in steps 2 to 3, check the corresponding 6 groups of vectors in step 10. Whether the furnace temperature curve in the corresponding case of $\vec{T}_i$ meets the process limit. If satisfied, $\vec{T}_i$ is left unaltered. If not, let $\vec{T}_i = \vec{x}_i$.

(12) Let $\vec{T}_i$ be a new generation of $\vec{x}_i$ so that a new generation of 6 initial individuals will be obtained. For the new generation of individuals, repeat the operation in step 4 to find the maximum value of the area A'_0 in the new generation of individuals and compare it with A_0, and record the vector $\vec{T}_0$ at this time.

(13) If $A'_0 > A_0$, then let $A_0 = A'_0$ and $\vec{x}_0 = \vec{T}_0$, if $A'_0 \le A_0$ leave the value of A_0 unchanged.

(14) Let $n = n + 1$, if $n > 1000$, then terminate the operation, with A_0 and $\vec{x}_0$ as the final result. If $n < 1000$, go back to step 1.

Steps 5 to 7 can also be called mutation, and steps 9 to 11 can also be called crossover, which are the two most core parts of the differential evolution algorithm. After repeating the whole process of the differential evolution algorithm many times, we get the following results: the set temperature T_1 = 177.02 ℃ in the small temperature zone (1–5), the set temperature T_2 = 196.04 ℃ in the small temperature zone (6), the set temperature T_3 = 225.08 ℃ in the small temperature zone (7), the set temperature T_4 = 264.53 c in the small temperature zones (8–9), the set temperature T_5 in the small temperature zones (10–11) is 25 ℃, the conveyor belt passing speed v = 89.27 cm/min, and the minimum area A_0 = 366.43 cm^2, the optimal furnace temperature curve is shown in **Figure 7**.

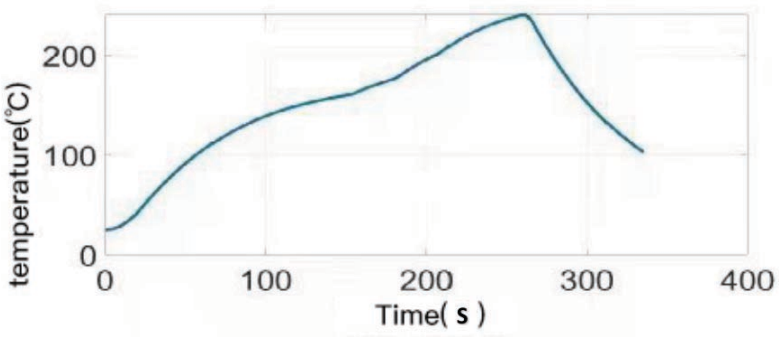


Figure 7. Furnace temperature curve

3.2.5. Pursue the symmetry of the furnace temperature curve and minimize the over-temperature region model

The "optimal furnace temperature curve" in this problem should consider both symmetry and the smallest area. The skewness calculation formula for sample X has been given in the analysis of the model to optimize the furnace temperature curve to minimize the over-temperature region:

$$Sk(X) = E\left[\left(\frac{X-\mu}{\sigma X}\right)^3\right] \tag{26}$$

where μ and X are the mean and standard deviation of sample X, respectively, and E is the mathematical expectation symbol. The skewness of the sample can measure the symmetry of the whole curve, the value range of *Sk(X)* is (-1,+1), and the positive and negative of *Sk(X)* means that the symmetry of the whole curve is positive and negative, and the closer *Sk(X)* is to 0, the more symmetrical the curve. We normalize the skewness and map the skewness from (-1,+1) to (0,1) with the x-function, and we find that the arctangent function has this property. The symmetry of the curve is measured by $1-\frac{2}{\pi}\arctan\left(2\left|Sk(X)\right|\right)$, the range of $1-\frac{2}{\pi}\arctan\left(2\left|Sk(X)\right|\right)$ is between 0 to 1, the closer $1-\frac{2}{\pi}\arctan\left(2\left|Sk(X)\right|\right)$ is to 1, the better the symmetry of the curve, and the closer $1-\frac{2}{\pi}\arctan\left(2\left|Sk(X)\right|\right)$ is to 0, the poorer the symmetry of the curve. The biggest advantage of using the arctan function is that arctan(x) changes very quickly when it is close to 0, and arctan(x) does not change significantly when x is relatively large, which is very consistent with the characteristics of skewness.

Equation (22) defines the fitness degree f_i of the vector $_i$, f_i is a physical quantity located between 0 to 1, the closer f_i is to 1, the smaller the area, that is, the closer to the ideal curve, the closer f_i is to 0, the larger the area, that is, the farther away from the ideal curve. For the $1-\frac{2}{\pi}\arctan\left(2\left|Sk(X)\right|\right)$ and f variables, consider using the TOPSIS method:

$$C = \left(1-\frac{2}{\pi}\arctan\left(2\left|Sk(X)\right|\right), f\right) \tag{27}$$

$C^+ = (1,1)$ is the ideal positive solution and $C = (0,0)$ is the ideal negative solution. Define $S^+ = \|C - C^+\|$ is the distance from an alternative to the ideal positive solution, and $S^- = \|C - C\|$ is the distance from an alternative to the ideal negative solution, and the objective function is defined as:

$$y = \frac{S^-}{S^+ + S^-} \tag{28}$$

In this problem, the larger the value of y, the better, and the differential evolution algorithm is used to find the optimal furnace temperature curve.

(1) Establish a population of 6 individuals, denoted as $\vec{x}_1$, $\vec{x}_2$, $\vec{x}_3$, $\vec{x}_4$, $\vec{x}_5$, $\vec{x}_6$, where each component of $\vec{x}_i$ should be in the given range, let n be the quantity of record population algebra so that $n = 0$.

(2) For the 6 individuals in the population in the first step, firstly calculate the ambient temperature Ts in the reflow furnace under the corresponding situation by using **Equation (6)**, and then combine the different parameters given in **Equations (1)–(15)** and the reflow oven welding heat transfer model to obtain the data (t_i, T_i) of several groups of welding center temperature and time and record these data (the implementation method is the same as the implementation method in the reflow oven welding heat transfer model).

(3) For a plurality of groups of data (t_i, T_i) obtained in step 2, substitute **Equations (18)–(21)** to check whether the process limit is satisfied. If satisfied, enter step 4, and return to step 1 if not satisfied.

(4) Utilize the data in step 2, according to **Equation (28)** and the parameter calculation method in the TOPSIS method, find the value y of the objective function of 6 individuals (6 vectors), take the maximum value of the objective function y_m, let $y_0 = y_b$. Save the vector i at this time, so that $\vec{x}_0 = \vec{x}_i$.

(5) Take any 3 individuals from the population, according to the (t_i, T_i) of each individual recorded in step 2, find the area A_i according to **Equation (19)**, sort the area from small to large A_w, A_m, A_b, and record the corresponding vectors as $\vec{x}_b$, $\vec{x}_m$, $\vec{x}_w$.

(6) In the three vectors given in step 5, f_b, f_m, and f_w are obtained according to **Equation (23)**, and the fitness of the six vectors $f_1, f_2, \ldots, f_6$, and their average $\bar{f}$, maximum f_m, minimum f_w.

(7) For $\vec{x}_1$, check whether each component of $\vec{H}_1$ satisfies the value range given at the beginning of the model in "optimizing furnace temperature curve to minimize over-temperature areas". If it satisfies, record $\vec{H}_1$ and enter step 8, and return to step 5 if not.

(8) Repeat steps 5–7 five more times to ensure that all 6 individuals in the population have corresponding $\vec{H}_i$, $\vec{F}_i$.

(9) For each set of vectors $\vec{x}_i$, $\vec{H}_i$, calculate and record the cr_i of the six vectors according to the definition of **Equation (24)**.

(10) For each group of vectors $\vec{x}_i$, $\vec{H}_i$, reset $\vec{T}_i$ according to the reset algorithm of **Equation (25)**.

(11) According to the test method in step 2 to step 3, check the corresponding 6 groups of vectors in step 10. Whether the furnace temperature curve in the case of Ti meets the process limit. If satisfied, $\vec{T}_i$ is left unaltered. If not, then let $\vec{T}_i = \vec{x}_i$.

(12) Let $\vec{T}_i$ be $\vec{x}_i$, which gives you a new generation of 6 initial entities. For the new generation of individuals, repeat the operation in step 4 to find the maximum value of the objective function y'_0 in the new generation of individuals and compare it with y_0, and record the vector $\vec{T}_0$ at this time.

(13) If $y'_0 > y_0$, then let $y_0 = y'_0$ and $\vec{x}_0 = \vec{T}_0$, if $y'_0 \le y_0$ leave the value of y_0 unchanged.

(14) Let $n = n + 1$, if $n > 1000$, then terminate the operation, with y_0 and $\vec{x}_0$ as the final result. If $n < 1000$, go back to step 1.

After repeating the whole process of the differential evolution algorithm many times, we get the following results: the set temperature T_1 = 174.88 °C in the small temperature zones (1–5), the set temperature T_2 = 193.67 °C in the small temperature zone (6), the set temperature T_3 = 229.15 °C in the small temperature zone

(7), the set temperature T_4 = 262.00 °C in the small temperature zones (8–9), the set temperature in the small temperature zones (10–11) is 25 °C, the conveyor belt passing speed v = 85.90 cm/min, and the minimum area A_0 = 401.85 cm^2, the skewness is 0.17.

According to the furnace temperature curve in **Figure 8**, the part of the furnace temperature curve with a temperature higher than 217 °C is not completely symmetrical, the skewness is 0.17, and the area is 401.84 cm^2. The skewness of the furnace temperature curve in "optimizing furnace temperature curve to minimize over-temperature areas" is 0.19, and the area between 217 °C and the peak temperature is 366.02 cm^2. In comparison, the skewness of the furnace temperature curve of the result of "pursue symmetry of the furnace temperature curve and minimize the over-temperature area" has decreased by 10.53%, and the area higher than 217 °C increased by 9.56%. It is in line with the evaluation results of the symmetry and area of the furnace temperature curve above 217 °C. The symmetry of the furnace temperature curve and the furnace temperature curve of the model that minimizes the over-temperature region are affected by the temperature difference between the reflow zone and the cooling zone in the reflow furnace, and the drop in this problem is more than 200, which is difficult to achieve complete symmetry.

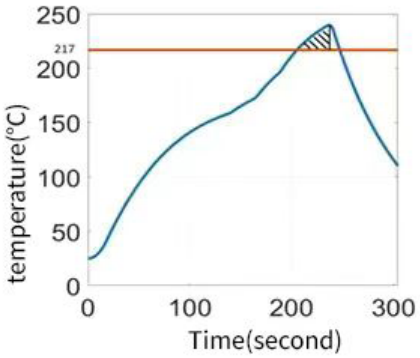


Figure 8. Optimal furnace temperature curve

In the process of optimizing the furnace temperature curve, the differential evolution algorithm is used in this model, which is an effective global optimization method. By simulating the process of natural selection and genetic variation, the algorithm can quickly search for the optimal solution in the parameter space. Compared with the traditional optimization algorithm, the implementation of the differential evolution algorithm in this model has a shorter running time and higher optimization efficiency, which not only accelerates the optimization process but also improves the practicability of solving the problem, so that the model can quickly respond to changes in production and provide timely process parameter adjustment for actual production.

The TOPSIS method, which is a multi-criteria decision-making method based on ideal points, is adopted. In this model, the TOPSIS method is used to comprehensively evaluate the performance of different furnace temperature curves, and the advantages and disadvantages of the furnace temperature curves are effectively quantified by calculating the distance between each alternative and the ideal positive and ideal negative solutions. When dealing with complex problems with multiple evaluation indicators, this method can objectively deal with the weight of decision-making variables, avoid the bias that may be brought about by subjective judgment, and improve the accuracy and reliability of evaluation results. Through the TOPSIS method, the model can provide scientific decision support for the selection of process parameters, and further optimize the control strategy of the welding process.

4. Summary

In this paper, an optimization model of the furnace temperature curve based on a differential evolution algorithm is proposed, which aims to improve the consistency and reliability of welding quality in the electronics assembly industry. The article first introduces the importance of reflow furnace in electronic assembly and points out the necessity of optimizing the furnace temperature curve to improve product quality, and reduce energy consumption and cost. By establishing the heat transfer model, considering the thermal radiation, thermal convection effect, and the thermal properties of the welding material, the furnace temperature curve was optimized with precise control.

In this study, the authors use the Differential Evolution (DE) algorithm for parameter optimization, which shows great potential in solving complex system optimization problems due to its simplicity, robustness, and high efficiency. Through this algorithm, the model not only optimizes the temperature and conveyor speed of each temperature zone but also further considers the symmetry of the furnace temperature curve through the TOPSIS method to achieve better welding results.

The model is described in detail, including a model of the temperature distribution in the reflow furnace and a model of the printed circuit board being heated in the furnace. By solving the model, the optimal furnace temperature curves under different conditions, as well as the corresponding set temperature of each temperature zone and the conveyor belt passing speed are obtained. In addition, it discussed how to determine the maximum conveyor belt speed of the furnace and maximize the production efficiency without sacrificing the quality of the weld.

The model in this study has several advantages, which provide a scientific method for optimizing furnace temperature curves based on the basic laws of heat transfer based on the actual production conditions. The efficiency of the differential evolution algorithm ensures that the model can quickly respond to changes in production, and the application of the TOPSIS method provides objective decision support for the selection of process parameters. These advantages make this model not only innovative in theory but also has high practical value in application, which helps to promote the development of electronic manufacturing technology.

Disclosure statement

The author declares no conflict of interest.

References

[1] Yang SM, Tao WQ, 2006, Heat Transfer. Higher Education Press Publication, Beijing.

[2] Yao H, 2018, Modeling and Simulation of Plate Level Reflow Soldering Based on Ansys Icepak, thesis, Beihua Institute of Aerospace Technology.

[3] Hou Y, 2014, Numerical Simulation and Experimental Research on Creep Shaping Process of 2A14 Aluminum Alloy, thesis, Harbin Institute of Technology.

[4] Hong J, Xu Z, 2018, Simulation Study of Reflow Soldering Process Based on Finite Element Theory. 2018 China High-end SMT Academic Conference, 2018: 181–186.

[5] He C, Feng X, 2001, Principles of Chemical Engineering. Science Press, Beijing.

Publisher's note

Bio-Byword Scientific Publishing remains neutral with regard to jurisdictional claims in published maps and institutional affiliations.

Journal of Electronic Research and Application, 2024, Volume 8, Issue 4
http://ojs.bbwpublisher.com/index.php/JERA
ISSN Online: 2208-3510
ISSN Print: 2208-3502

Penetration Study of Key Technologies for Cybersecurity Risk Assessment

Lin Ma*

Zhejiang Testing & Inspection Institute for Mechanical and Electrical Products Quality, Hangzhou 310051, China

***Corresponding author:** Lin Ma, malin4050@163.com

Copyright: © 2024 Author(s). This is an open-access article distributed under the terms of the Creative Commons Attribution License (CC BY 4.0), permitting distribution and reproduction in any medium, provided the original work is cited.

Abstract: In recent years, with the frequent occurrence of cyber security incidents, people have paid more attention to it. Information security risk assessment is a very important research topic. This paper gives a brief overview of the theory of cybersecurity risk assessment, focuses on the description of the current mainstream cybersecurity risk assessment methods, classifies and compares the existing methods according to the nature of the methods, and analyses the advantages, disadvantages, and application scope of each method. Finally, the main factors affecting the evaluation results are summarized and refined, and future research hotspots in this field are proposed. Through the empirical analysis of the three factors, the influence of the correlation of the three factors, the uncertainty of the evaluation indexes, and the timeliness of the evaluation on the evaluation results are concluded, which provides a reference for future research on evaluation methods.

Keywords: Risk assessment; Correlation; Real-time analysis; Uncertainty analysis; Quantitative analysis

Online publication: August 13, 2024

1. Introduction

In recent years, with the continuous promotion of the national information technology development strategy, the information technology and Internet industry have also developed rapidly [1]. With the progress of information technology and the rapid development of the Internet industry, network security has become a focus of attention, and it is also a key issue that urgently needs to be solved in the new era [2].

2. Basic concepts of cybersecurity risk assessment

A security incident is a situation on a system, a service, or a network that can be identified as a situation that causes a failure of a system's security policy, a loss of a system's privileges, or a system's inability to function properly [3].

The main components of cybersecurity risk evaluation are assets, vulnerabilities, threats, risks, events, and security measures. A so-called security event is the process by which a vulnerability is exploited, thereby increasing the risk of network security and developing into a security event, that is, a network system, that develops from a potential, normal system state into an obvious, abnormal system state after being induced by a

cyber-attack [4]. By analyzing the interrelationships between the factors, we find that the presence of more flaws within an asset implies more potential threats, conversely, if more effective protective measures can be taken, the danger of the system can be reduced. This can be summarized in **Figure 1**.

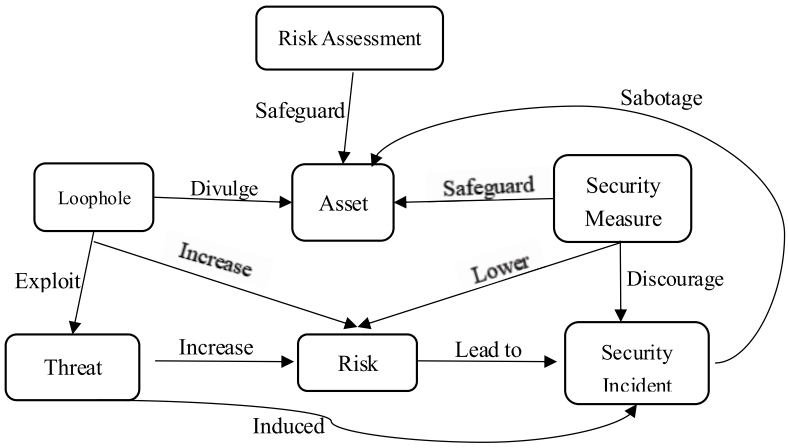


Figure 1. Relationship model between elements of cybersecurity risk assessment

In cybersecurity risk evaluation, the causal relationship between factors is summarized as follows:

(1) Attackers can take advantage of these weaknesses to trigger some security events, thus increasing the risk of the network.

(2) The security measures taken can prevent security incidents, thus reducing the risk of the network.

(3) Vulnerabilities may increase the risk of a system, but do not directly trigger a security incident in the system, but are exploited in the system by other parts of the system, thus triggering an attack on the system.

(4) There are flaws in the system that leak assets to malicious users.

(5) When a vulnerability in a system is used to carry out a single attack that exposes the assets of that system to an attacker, it creates a single threat or increases the danger one at a time.

(6) Security measures are mainly aimed at mitigating or preventing the occurrence of security events to reduce cyber risks.

From the current research, the primary goal of network security risk evaluation is to identify the possible risks in the network and then propose the best protection strategy to control these risks [5-8]. **Figure 2** shows the specific relationships in the principles of cybersecurity risk evaluation, described as follows:

(1) Asset identification: Quantifying the value of assets such as software and hardware in the network system and their degree of impact on the security of the network system.

(2) Vulnerability identification: Detecting the vulnerabilities existing in the network system and analyzing the possibility of their exploitation.

(3) Threat identification: Identifying the harmfulness of potential threats caused by vulnerabilities and the types of attack events they trigger.

(4) Security risk confirmation: Confirming the risk status caused by vulnerabilities and threats.

(5) Security event analysis: Analysis and calculation of the possibility of security events caused by system vulnerabilities and threats and the damage that will be caused to the network system after the security event.

(6) Security strategy program formulation: Combining the five aspects above, developing a reasonable security protection program for the network system's risk situation.

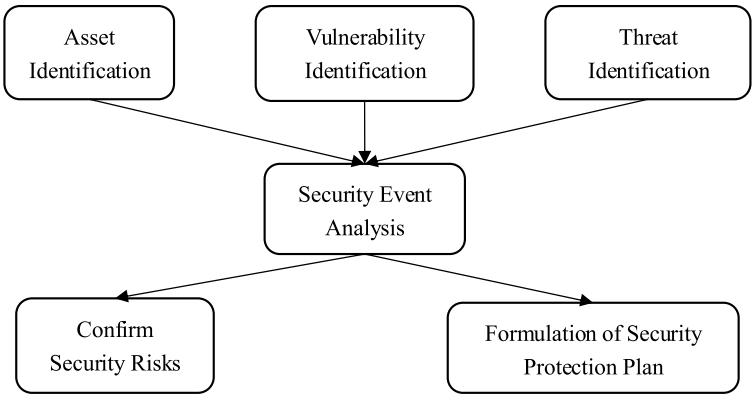


Figure 2. Principle of network security risk assessment

3. Network security risk assessment implementation process

This paper combines the attack graph risk analysis module and the intelligent optimization algorithm protection strategy selection module to propose a network security risk assessment implementation process oriented to risk analysis and risk management, the specific content is shown in **Figure 3**.

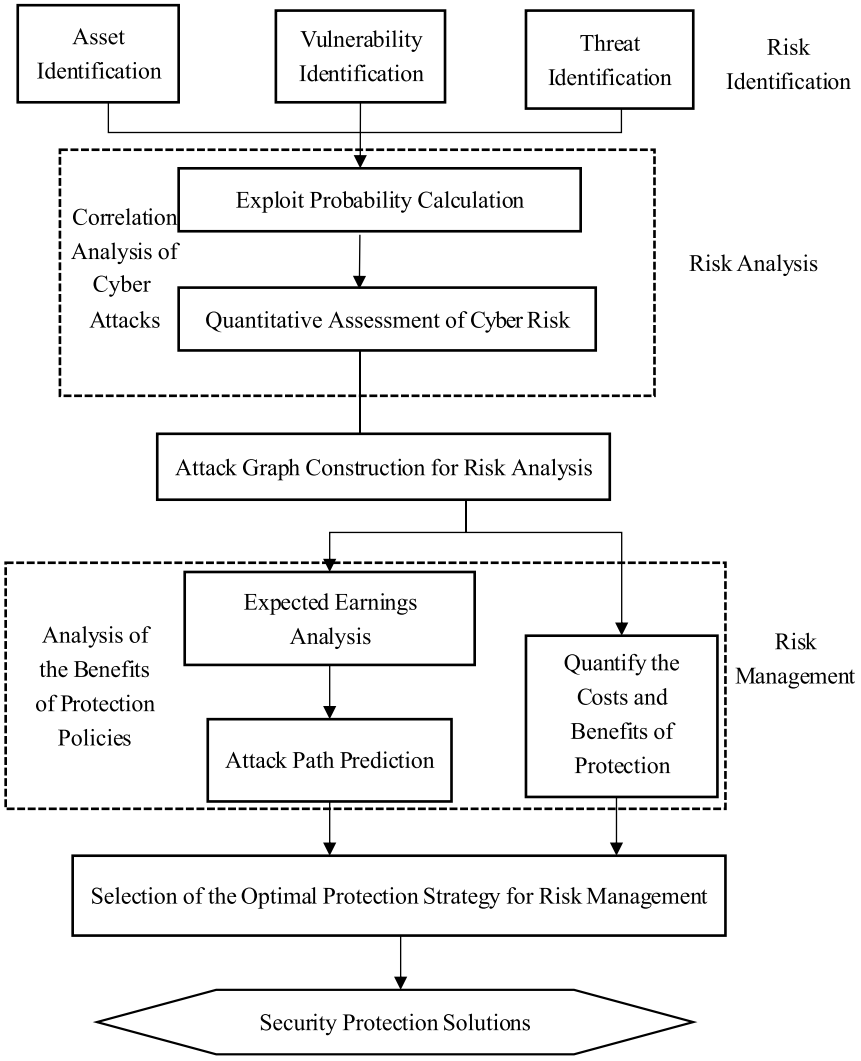


Figure 3. Implementation process of network security risk assessment

(1) Asset identification: The resources in the network system mainly include data, software, and hardware, and a cyber-attack will lead to the loss of resources, that is, the integrity, availability, and security of the network system is damaged.

(2) Vulnerability identification: Vulnerability identification mainly includes two parts, identifying the type of vulnerability, and assessing the possibility of vulnerability exploitation and the degree of harm.

(3) Threat identification: By identifying the potential threats generated by the vulnerabilities and identifying them through the threat database, the threats generated by them are evaluated.

(4) Network attack correlation analysis: By analyzing and calculating the probability of security events caused by weaknesses or threats existing in the network, and analyzing the losses caused by these security events.

(5) Quantitative assessment of network risk: Analyzing the degree of harm of security events triggered by vulnerabilities and threats, and taking corresponding security precautions for different levels of risk.

(6) Attack path prediction: Based on the expected return and cumulative probability, the attacker's intention to attack is surmised and the attack path is predicted to formulate corresponding defense strategies.

(7) Protection strategy benefit analysis: On this basis, using the intelligent optimal algorithm and the cost-benefit model, to achieve the balance of the cost and benefit of the defense strategy.

(8) Security strategy program formulation: On this basis, the vulnerability, threat, risk, and harm of the attack on the information system are clarified through the establishment of a unified security risk evaluation system.

4. Research on key technologies for cybersecurity risk assessment

4.1. Qualitative assessment method

Qualitative assessment methods are based on elements such as threats, vulnerabilities, and security measures faced by the system, and based on the knowledge and experience of the assessor, the network security level is assessed and judged [9]. The expert evaluation method, Delphi method, and fault tree method are the main means of qualitative evaluation [10].

(1) Expert evaluation method: Experts from various parties evaluated the potential risks in the network system based on their knowledge and experience, combined with relevant evaluation guidelines, and assigned corresponding risk weights.

(2) Fault tree analysis method: This method focuses on the results of the faults and follows the corresponding steps to find the causes of the faults. When using the fault tree analysis method, because each element in the tree structure is closely related, this makes the process of risk analysis also from the whole to the local.

(3) Delphi method: The Delphi method is a method of qualitatively analyzing the level of risk. It adopts the form of anonymity to ask for opinions from several experts who do not know each other, and several experts work independently, and then synthesize according to their respective opinions, and finally arrive at a more objective and precise evaluation.

4.2. Quantitative risk assessment methods

Different from the qualitative risk assessment method, the quantitative risk assessment method takes the numerical value as the standard to assess the network security risk, quantifies the network security risk assessment, and then uses the computer to measure the security risk in the network and the degree of impact; the results of the measurement are to visualize the data embodied in the assessment results, so it has the

advantages of being more objective, scientific, and rigorous [11-14]. In the quantitative risk evaluation, there are some representative evaluation methods as follows [15]:

(1) Decision tree method: Decision tree analysis is a top-down tree structure constructed based on probability theory, and each decision may cause several different events.

(2) Cluster analysis: Cluster analysis is a method of classifying data objects according to their similarity.

(3) Factor analysis method: The goal of factor analysis is to portray the connection between multiple indicators with a few factors, that is, to group multiple indicators with high correlation into one category, and to reflect the main information of the original indicators with a few factors, which reduces the complexity and ambiguity of the evaluation indicator system.

4.3. Integrated risk assessment method

The integrated risk assessment method is a method that organically combines both qualitative and quantitative methods [16]. There are two main methods: the assessment method based on the index system and the assessment method based on the modeling method.

4.3.1. Risk assessment based on the index system

This form of risk assessment is mainly based on the index system to assess the network risk [17]. Specifically, the network risk assessment is quantified to reflect the security factors affecting the network risk, and then, combined with the characteristics of the reflected factors, it is divided into several groups, thus forming a risk indicator system, and finally, the constructed indicator system is used as the basis to assess the risk in the network.

4.3.2. Risk assessment based on the modeling method

This method can combine each risk factor with the state of the system and can scientifically model each risk factor to obtain the safety level of the system. On this basis, a new risk evaluation method is proposed.

(1) Evaluation method based on graph model: Combining the correlation between security events and network security, a visual attack behavior and network security evaluation model is established. Zhang *et al.* combined complex networks with attack graph theory and proposed a risk evaluation method for railway train information security based on attack graph theory [18]. Semertzis *et al.* proposed a quantitative evaluation method for system attack behavior based on an attack graph, whose main research contents include [19]: (I) Establishing a probability model for information threat scenarios based on the attack graph. (II) Based on the probabilistic model for attack scenarios. (III) Based on this model construct the probability model of the information threat scenario.

(2) Evaluation method based on the theoretical model of artificial intelligence: Due to the topology of complex networks having the characteristics of vagueness and uncertainty, and artificial intelligence is suitable for modeling them, the risk evaluation method based on artificial intelligence is studied on this basis. Currently, Bayesian networks and Hidden Markov Models are widely used in the field of risk evaluation.

5. Summary

This paper launched a systematic comprehensive analysis of the literature on cybersecurity risk assessment and came up with four categories of factors, such as relevance, real-time, uncertainty, and quantification, which have an impact on the assessment results. The analysis results showed that the technology of cyber

risk assessment is not mature enough, and it is necessary to further study the related technology of cyber risk assessment, optimize the assessment algorithm, and look for more reasonable and accurate assessment methods and assessment standards. On this basis, this paper also put forward the issues that need to be further studied in the next step: (1) To further reduce the subjectivity and uncertainty of evaluation. (2) Based on the evaluation results, to automatically generate security recommendations for managers to make decisions to make the evaluation process more automated. (3) Due to the differences in the types of networks, the main controlling factors affecting the evaluation results vary. (4) To explore an environment that can simulate actual network attacks to enhance the efficiency of risk evaluation of the system.

Disclosure statement

The author declares no conflict of interest.

References

[1] Liu F, Yang Y, You Y, 2021, Research on the risk evaluation of ship network security information based on artificial intelligence technology. Ship Science and Technology, 43(12): 151–153.

[2] Liu J, Ling X, Zhang L, et al., 2022, A Framework for Cybersecurity Risk Assessment Based on Tactical Correlation. Computer Science, 49(09): 306–311.

[3] Zhang J, Wang Q, Zhao S, 2022, Research on the application of HAZOP-LOPA coal mine safety risk evaluation method based on Bayesian network. Mining Safety and Environmental Protection, 49(01): 114–120.

[4] Deng Y, Meng M, Zhang Y, et al., 2021, Knowledge mapping and visualization analysis of metro safety research based on CiteSpace. Journal of Civil Engineering and Management, 38(05): 57–63.

[5] Mu L, Li W, Chen H, et al., 2021, Current Status and Insights of Global Cyber Biosecurity Research. Science and Technology Management Research, 41(06): 28–32.

[6] Wang P, 2021, Design of Network Security Protection for Intelligent Devices in Nuclear Power Plants. Automation Instrumentation, 42(S1): 314–318.

[7] Lin L, 2021, Research on Safety Risk Assessment of Petrochemical Plants Based on Fuzzy Comprehensive Evaluation Method. Energy and Environmental Protection, 43(07): 100–104 + 113.

[8] Luo Y, 2021, Research on Safety Risk Assessment of Network System Based on Combinatorial Optimization Theory. Microcomputer Applications, 37(07): 144–146 + 162.

[9] Yan W, 2022, Security risk assessment and control of wireless network based on convolutional neural network. Journal of Shenyang University of Technology, 44(05): 565–569.

[10] Wang S, Liu C, Liu S, et al., 2021, An attack tree-based security risk assessment method for 4G networks. Computer Engineering, 47(03): 139–146 + 154.

[11] Lu Y, Chen L, 2021, Research on network security situational awareness risk assessment technology based on FAHP. Computer and Digital Engineering, 49(05): 957–960 + 976.

[12] Qiang R, 2022, Random forest algorithm-based security risk assessment method for communication networks. Automation and Instrumentation, 2022(11): 189–193.

[13] Kang W, 2022, Security risk assessment method for power monitoring network based on improved AHP algorithm. Automation and Instrumentation, 2022(10): 171–174.

[14] Xu IL, Chen T, 2021, Optical communication data security risk assessment model based on blockchain. Automation and Instrumentation, 2021(11): 40–44.

[15] Ding Y, Wang R, Li L, et al., 2022, BN-MNA model and application for safety risk assessment and control of

assembled building construction. Journal of Civil Engineering and Management, 39(04): 153–161 + 184.

[16] Zhao D, Chen C, Yi L, 2021, A temporal risk assessment model for disaster evolution network. Chinese Journal of Safety Science, 31(03): 171–177.

[17] Cai J, Ma Q, Tan S, 2022, Research on the construction of scientific and technological security risk assessment and monitoring and early warning system. Science and Technology Progress and Countermeasures, 39(24): 100–108.

[18] Zhang F, Chen Y, 2019, Current status and improvement measures of pantograph crack fault detection. Shandong Industrial Technology, 2019(17): 116.

[19] Semertzis I, Goyel H, Rajkumar VS, et al., 2024, Towards Real-Time Distinction of Power System Faults and Cyber Attacks on Digital Substations Using Cyber-Physical Event Correlation. 12th Workshop on Modeling and Simulation of Cyber-Physical Energy Systems (MSCPES), 2024: 1–6.

Publisher's note

Bio-Byword Scientific Publishing remains neutral with regard to jurisdictional claims in published maps and institutional affiliations.

Journal of Electronic Research and Application, 2024, Volume 8, Issue 4
http://ojs.bbwpublisher.com/index.php/JERA
ISSN Online: 2208-3510
ISSN Print: 2208-3502

Application of Bayesian Analysis Based on Neural Network and Deep Learning in Data Visualization

Jiying Yang*, Qi Long, Xiaoyun Zhu, Yuan Yang

Yunnan Open University, Kunming 650224, Yunnan Province, China

Corresponding author: Jiying Yang, 19446964@qq.com

Copyright: © 2024 Author(s). This is an open-access article distributed under the terms of the Creative Commons Attribution License (CC BY 4.0), permitting distribution and reproduction in any medium, provided the original work is cited.

Abstract: This study aims to explore the application of Bayesian analysis based on neural networks and deep learning in data visualization. The research background is that with the increasing amount and complexity of data, traditional data analysis methods have been unable to meet the needs. Research methods include building neural networks and deep learning models, optimizing and improving them through Bayesian analysis, and applying them to the visualization of large-scale data sets. The results show that the neural network combined with Bayesian analysis and deep learning method can effectively improve the accuracy and efficiency of data visualization, and enhance the intuitiveness and depth of data interpretation. The significance of the research is that it provides a new solution for data visualization in the big data environment and helps to further promote the development and application of data science.

Keywords: Neural network; Deep learning; Bayesian analysis; Data visualization; Big data environment

Online publication: August 12, 2024

1. Introduction

In the data-driven era, the volume and complexity of data have exploded, challenging traditional data analysis and visualization methods. Traditional approaches struggle with large, high-dimensional, and unstructured data. Therefore, we explore new approaches that combine neural networks, deep learning, and Bayesian analysis. Neural networks and deep learning are good at processing large amounts of data and recognizing patterns, while Bayesian analysis can accurately quantify the uncertainty of data. By constructing and optimizing this method, we successfully realized the efficient visualization of large-scale data sets, demonstrating the great potential of this method in the field of data visualization. The results show that this method improves the efficiency and accuracy of data visualization. This not only promotes the development of data science but also provides technical support for research and application in related fields. To sum up, our study not only discusses the combination of these three methods in theory but also validates its effect in practice, which is of great significance.

2. Theoretical background and technical basis

2.1. Development of data visualization

As an important means of information presentation and data analysis, data visualization has experienced a long development process [1]. Early data visualizations relied on simple charts and hand drawings, and examples of this period include the 18th-century statistician John Snow's cholera map of London, and a 19th-century French engineer, Charles Joseph Minard, drawing the march of Napoleon's army. Simple as these early visualizations were, they demonstrated the power of data and graphics to convey information [2].

After entering the 20th century, with the rise and development of computer technology, data visualization began to change to the digital direction. In the 1960s, computer scientist John Tukey proposed the concept of Exploratory Data Analysis (EDA), which emphasizes the use of data visualization to discover patterns and anomalies in data [3]. During this period, basic statistical charts such as histograms and box plots were gradually popularized, providing intuitive tools for data analysis.

In the 1980s, data visualization entered a period of rapid development, and the progress of computer graphics technology promoted the emergence of interactive data visualization tools. In 1987, John Chambers, a scientist at Bell Labs, developed the famous statistical software S to graphically present the results of data analysis. During this period, more interactive visualization software such as Tableau and D3.js came out one after another, making data visualization not limited to static charts, and users could explore data through interactive operations.

In the 21st century, with the advent of the era of big data, the rapid growth of data volume and data dimension has put forward new challenges and requirements for data visualization [4]. Traditional 2D charts have been unable to cope with the demand for the presentation of complex data sets. High-dimensional data visualization and multivariate data visualization technologies have emerged. The development of machine learning and artificial intelligence has brought new opportunities for data visualization, and the accuracy and intelligence level of data visualization has been significantly improved through neural networks and deep learning models.

In recent years, visualization technology based on deep learning has gradually become a research hotspot [5]. Deep learning models can automatically extract features from massive amounts of data to produce more complex and precise visualizations. The neural network model combined with Bayesian analysis further improves the credibility and interpretation of the visualization results and provides a new idea and method for the research and application of data science.

The development of data visualization, from simple manual charts to complex interactive tools to intelligent visualization based on deep learning, fully reflects the profound impact of technological advances on data analysis and presentation. As technology continues to evolve, data visualization will continue to play an important role in the field of big data and artificial intelligence.

1.2. Overview of neural networks and deep learning

Neural networks and deep learning are two key technologies in the field of artificial intelligence in recent years [6]. Neural network simulates the structure of the human brain and realize the approximation of complex nonlinear functions by transmitting information layer by layer. A typical neural network consists of an input layer, a hidden layer, and an output layer. Each layer is connected by weighting, and the activation function is used to introduce nonlinear characteristics. Deep learning, a subfield of neural networks, enables the capture of more complex patterns and features by increasing the depth of the network, i.e. the number of hidden layers. With the improvement of computing power and the accumulation of massive data, deep learning models have demonstrated excellent performance in areas such as image recognition, speech processing, and natural

language processing. Deep learning methods mainly include convolutional neural network (CNN), recurrent neural network (RNN), and generative adversarial network (GAN) [7]. CNN is usually used to process two-dimensional data such as images and extract multi-level image features through convolution and pooling operations. RNNs are suitable for processing sequence data, such as time series and text, in which a long short-term memory network (LSTM) solves the gradient disappearance problem of traditional RNNs. GAN generates realistic data samples through the antagonistic training of the generator and discriminator.

2.3. Basis of Bayesian analysis

Bayesian analysis is a statistical method that deduces the distribution of unknown parameters by calculating the posterior probability of data. The underlying theory is derived from Bayes' theorem, which describes the process of updating a probability distribution with prior knowledge and new data. Bayesian analysis excels in dealing with uncertainty and incorporating prior knowledge, making it particularly suitable for complex data environments. Bayesian networks and Bayesian inference are its main tools, the former for modeling dependencies between variables and the latter for parameter estimation. Combined with neural networks and deep learning, Bayesian analysis can further optimize model performance and improve the accuracy and intuitiveness of data visualization [8].

3. Bayesian analysis method based on neural network and deep learning

3.1. Combination of deep learning and Bayesian analysis

Deep learning and Bayesian analysis respectively show significant advantages in data processing and uncertainty quantification. Their combination not only enables in-depth mining of features in the data but also provides uncertainty assessment for the model, thus improving the robustness and interpretability of the model. Deep learning usually realizes efficient information processing and feature extraction through large amounts of data and complex models [9]. Bayesian analysis, on the other hand, describes the probabilistic nature of the model through statistical theory, enabling the model to have the functions of interpretability and uncertainty assessment. The combination of the two realizes the effective integration of data-driven and uncertainty-driven, providing comprehensive and reliable support for the visualization of complex data sets.

The superior performance of deep learning models in large amounts of data and complex tasks is widely recognized. Through multi-layer nonlinear transformation, deep learning models can automatically learn effective features from data, which greatly improves the efficiency of data processing and the accuracy of results [10]. Because of its powerful presentation capabilities, deep learning is increasingly becoming an important tool in data science. Deep learning models are often regarded as "black boxes", which are difficult to explain the model output and its decision-making process [11]. Bayesian analysis can effectively solve this problem by providing a probabilistic framework that can provide a clear explanation for the model output and its uncertainty.

By integrating the Bayesian statistical framework into the training process of neural networks, the deep learning model can not only process the data efficiently but also quantify the uncertainty. A common method is to model the weights in the neural network through the Bayesian model, to obtain the posterior distribution of the weights [12]. This method can not only capture the uncertainty of the model but also effectively avoid overfitting. In the concrete implementation process, variational inference or Markov Chain Monte Carlo (MCMC) method is usually used to approximate the posterior distribution, to realize the efficient training of the Bayesian deep learning model [13,14].

The quantification of model uncertainty through Bayesian analysis is helpful to improve the accuracy and

efficiency of data visualization. In data visualization, it is not only necessary to show the basic characteristics of the data but also to clarify the uncertainty of the data and the model prediction results. Bayesian deep learning model can provide the confidence interval or probability distribution of the predicted results so that the data visualization chart can not only show the predicted results but also reflect its reliability, providing more comprehensive information support for data analysis and decision-making.

On the application side, Bayesian deep learning has made great strides in fields as diverse as medical image analysis, finance, and environmental science. In medical image analysis, the deep learning model combined with Bayesian analysis can provide disease detection results and uncertainty assessment, which significantly improves the reliability and accuracy of diagnosis and treatment. At the same time, in the financial field, the method is widely used in market risk analysis and prediction, which provides a probabilistic basis for investment decisions. In addition, in the field of environmental science, Bayesian deep learning models have also been applied to the prediction of climate change to better reflect the reliability and uncertainty of the prediction results [20].

3.2. Strategies for data visualization

In the process of data visualization based on the Bayesian analysis method based on neural networks and deep learning, the key is to transform the complex data processing process into intuitive and easy-to-understand visual information. To achieve this goal, we need to design the strategy from three levels data input, processing, and output.

The pre-processing stage of data is crucial [15,16]. It is important to ensure that the input data is sufficiently cleaned and normalized so that the model can be trained most efficiently. Data preprocessing not only includes traditional processing methods such as missing value filling, outlier processing, and feature scaling but also requires special processing of time series data and high-dimensional data to adapt to the needs of neural networks and deep learning models [17,18].

In the data processing stage, by constructing a suitable data flow graph, the neural network and deep learning model are used for multi-layer feature extraction and analysis. Specific strategies include choosing appropriate network architectures, such as convolutional neural networks (CNN) for image data analysis and recurrent neural networks (RNN) for time series data analysis. Bayesian analysis can provide uncertainty quantification for parameter estimation of deep learning models, which can improve the robustness and generalization ability of the models [19].

In the data output stage, the analysis results are presented in the form of graphs and charts through visualization techniques. Use graphical tools such as Matplotlib, Seaborn, or D3.js to generate rich visualizations, including but not limited to scatter, line, heat maps, and 3D maps [20]. Interactive visualization platforms, such as Plotly and Tableau, provide a deeper user interaction experience where users can dynamically adjust visual parameters to explore deeper layers of data.

4. Closing remarks

By constructing a neural network and deep learning model, combined with Bayesian analysis, this study has conducted in-depth discussion and application verification of data visualization. The study found that this approach can significantly improve the accuracy and efficiency of data visualization when processing large-scale data, making the data easier to understand and analyze. This method provides a new solution for data visualization in big data environments and shows a wide range of application prospects. However, there are some problems with the research. Firstly, the process of building and optimizing the model requires a lot of

computational resources and may be difficult to apply in resource-limited environments. Secondly, the data set used in the study has its particularity, and the effect of the model on other data sets needs to be further verified. Finally, the complexity of Bayesian analysis increases the difficulty of model interpretation and requires further simplification and optimization. Future research can be deepened in the following aspects: The first is more extensive testing of different types of data sets to evaluate the versatility of the method. The second is to study more efficient computing methods to reduce the consumption of computing resources. The third is to explore the application of Bayesian analysis to other data science problems and expand its scope. The fourth is to optimize the interpretability of the model and develop more intuitive tools to help users better understand and utilize the data. In conclusion, this study provides a useful exploration and lays a foundation for the application of Bayesian analysis in data visualization. It is hoped that future research will overcome existing limitations, promote the development of data science, and provide more effective tools and methods.

Disclosure statement

The authors declare no conflict of interest.

References

[1] Zhang W, Migiti A, Zheng F, et al., 2021, Uyghur Speech Keyword Retrieval Based on Deep Neural Network. Computer Age, 2021(11): 21–24.

[2] Tang JY, Zhou M, 2019, Case Analysis of Network Data Visualization Based on Big Data. Integrated Circuit Applications, 38(11): 80–81.

[3] Shi Y, Pu X, Shen L, et al., 2021, Object Detection System Based on Convolutional Neural Networks and Keywords. Computer Knowledge and Technology: Academic Edition, 17(08): 162–164.

[4] Ruan L, Wen SS, Niu YM, et al., 2021, Deep Neural Network Visualization Based on Explainable Basis Disassembly and Knowledge Graph. Chinese Journal of Computers, 44(09): 1786–1805.

[5] Lou YS, Guo W, 2022, Prediction of Nuclear Mass by Bayesian Deep Neural Networks. Acta Physica Sinica, 71(10): 32–41.

[6] Zhang W, 2021, Visual Research on Keywords of Master's Thesis in Fine Arts. The Classic of Shanhaijing, 2021(13): 0337–0337.

[7] Liu S, Chang J, 2019, The Concept and Application of Big Data Visualization. Information Recording Materials, 22(09): 42–44.

[8] Cao R, Huang R, Huang X, et al., 2019, A Review of Deep Learning Research in China: Visual Analysis Based on CNKI Literature Keywords. Electronic Education in Primary and Secondary Schools, 2019(Z2): 91–94.

[9] Cao Q, 2020, Research on Keyword Distribution Visualization Based on Long Tail Theory. Science and Technology Achievements Management and Research, 2020(06): 32–37.

[10] Peng T, Qian H, Zhou J, 2022, Keywords and Visualizing the "Twin Engines" of Major Report Communication. Urban Party Newspaper Research, 2022(04): 61–64.

[11] Wang K, Yu H, 2021, Patent Keyword Analysis Method Based on Bayesian Network and Factor Analysis. China Science and Technology Information, 2021(18): 23–26.

[12] Zhang Y, 2019, Visual Analysis of Literature in Environmental Journals. Environmental Protection and Circular Economy, 41(05): 97–101.

[13] Langenberg B, Helm LJ, Mayer A,2024, Bayesian Analysis of Multi-Factorial Experimental Designs Using SEM. Multivariate Behavioral Research, 2024: 21–22.

[14] Huang Z, Zhou Y, Shu X, et al., 2019, Speech Enhancement Method by Combining Bayesian Estimation and Deep Neural Network. Minicomputer Systems, 40(01): 40–44.

[15] Liu Z, Liu D, 2024, Dynamic Modulus Analysis of Resonance Fracture Layer of Old Cement Concrete Slab Based on BP Neural Network and Deep Learning Model. Highway, 2024(06): 44–51.

[16] Zhang L, Liu X, 2024, Research on Two-Dimensional Rectangular Layout Optimization Method Based on Graph Neural Network and Deep Reinforcement Learning. Forging Equipment and Manufacturing Technology, 59(02): 117–122.

[17] Zhao J, Zhang Y, Shi Q, et al., 2024, Automatic Pedicle Screw Planning Based on Deep Learning Neural Network Technology. China Digital Medicine, 19(04): 84–91.

[18] Han XY, Xie MX, Yu K, et al., 2024, A Computational Power Network Resource Allocation Method Combining Graph Neural Networks and Deep Reinforcement Learning. Frontiers of Information Technology and Electronic Engineering, 25(05): 701–713.

[19] Chen Y, Huang X, 2024, Solution of Time Disturbance Wave Equation Based on Physical Information Neural Network. Oil and Gas Geophysics Committee of the Chinese Geophysical Society, Proceedings of the 6th Annual Petroleum Geophysical Conference, 2024: 4.

[20] Zhang W, Lin A, Yang X, et al., 2024, Fusion deep learning Bayesian filtering review. Acta Automatica Sinica, 50: 1–16.

Publisher's note

Bio-Byword Scientific Publishing remains neutral with regard to jurisdictional claims in published maps and institutional affiliations.

Journal of Electronic Research and Application, 2024, Volume 8, Issue 4
http://ojs.bbwpublisher.com/index.php/JERA
ISSN Online: 2208-3510
ISSN Print: 2208-3502

Research on Integrated Communication Perception Technology Based on RIS Assistance

Hao Yang*, Chuanjiang Wang, Xiaoyi Li, Qi Xiang, Taoyong He

Wuhan Ruisi Communication Technology Co., Ltd., Wuhan 430000, Hubei Province, China

Corresponding author: Hao Yang, dspyang@163.com

Copyright: © 2024 Author(s). This is an open-access article distributed under the terms of the Creative Commons Attribution License (CC BY 4.0), permitting distribution and reproduction in any medium, provided the original work is cited.

Abstract: Reconfigurable Intelligent Surface (RIS) assisted communication perception integration technology is an emerging communication technology that introduces reconfigurable intelligent surfaces in the communication environment to achieve real-time perception and control of signals, thereby improving the performance and efficiency of communication systems. This article studies the integrated communication perception technology assisted by RIS, including system principles, key technologies, and performance analysis. Through literature review and analysis of relevant research, the potential application prospects of this technology in future communication systems have been revealed.

Keywords: RIS-assisted communication; Perception integration; Reconfigurable intelligent surfaces; Performance analysis; Application prospects

Online publication: August 12, 2024

1. Introduction

The integrated communication perception technology assisted by RIS is an innovative method that introduces Reconfigurable Intelligent Surface (RIS) based on traditional wireless communication systems to improve communication performance. This technology achieves intelligent control of signal perception, reflection, and transmission by deploying a large number of RIS components in the communication environment and utilizing their controllable phase or amplitude characteristics, thereby optimizing signal quality, enhancing system capacity, and suppressing interference. RIS, as an intelligent surface with a reflection function, can change the propagation path and interference situation of the signal by adjusting the phase and amplitude of the reflected signal, thereby offsetting signal fading, reducing multipath interference, and improving signal reception quality and reliability. This intelligent regulation capability makes RIS an ideal choice for dealing with complex channel environments. By intelligently regulating the reflected signals on RIS, optimization strategies such as signal beamforming, elimination of multi-user interference, and spatial frequency multiplexing can be achieved, greatly improving the system's capacity and spectral efficiency. This flexible resource allocation method makes it possible for multiple users to transmit simultaneously, greatly enhancing the system's throughput and coverage. RIS can suppress and isolate interference by sensing surrounding interference signals and

intelligently regulating their reflected signals. The ability to manage interference can significantly improve the anti-interference performance of the system, enabling wireless communication systems to maintain good communication quality even in high-density users and complex interference environments.

2. Overview of traditional communication perception technology

2.1. Definition and basic principles of communication perception

Communication perception is a technology that obtains information about channel status, interference conditions, user location, and movement by perceiving and analyzing various parameters and features in the wireless communication environment [1]. It is an important technological means that can provide real-time information about the communication environment to support the optimization and decision-making of wireless communication systems.

The basic principle of communication perception is to receive and process signals from wireless channels and use the characteristics and parameters of the signals to obtain information about the communication environment. This information can include channel fading, signal-to-noise ratio, channel capacity, spectrum usage, interference sources and types, user location and movement speed, etc. Communication perception can be achieved through various technical means, including channel estimation, spectrum sensing, position sensing, and so on [2].

In terms of channel perception, communication systems can use the received signal to estimate the characteristics of the channel, such as fading, multipath propagation, etc. By perceiving the channel state, the system can adopt corresponding modulation methods, power control strategies, and beamforming techniques to improve communication quality and system performance.

In terms of spectrum sensing, communication systems can obtain information on available spectrum resources by monitoring and analyzing spectrum usage [3]. This is crucial for technologies such as dynamic spectrum access, spectrum sharing, and cognitive radio to improve spectrum utilization efficiency and address spectrum resource shortages.

In terms of interference perception, communication systems can obtain information on interference sources and types by monitoring and analyzing interference signals in wireless communication systems. This helps to implement strategies such as interference suppression, interference localization, and interference management to improve the performance and reliability of communication systems.

In terms of location perception, communication systems can use information such as the time, angle, and power of the received signal to obtain the user's location and movement situation. This is crucial for applications such as wireless positioning, location services, and mobile management, as it can provide precise location information support [4].

2.2. Classification and characteristics of traditional communication perception technologies

Traditional communication perception technology can be classified based on its application field and target, mainly including channel perception, spectrum perception, interference perception, and position perception. These technologies play an important role in wireless communication systems, providing critical information support for system optimization and performance improvement [5].

Channel perception refers to obtaining information about channel status by receiving and analyzing signals. It can be used in applications such as adaptive modulation, power control, beamforming, etc. to improve communication quality and system capacity. The characteristic of channel perception is the need to accurately estimate channel characteristics, which requires high requirements for signal sampling and processing.

Spectrum perception refers to obtaining information on available spectrum resources through monitoring and analyzing spectrum usage. It can be used in technologies such as dynamic spectrum access, spectrum sharing, and cognitive radio to improve spectrum utilization efficiency and solve the problem of spectrum resource shortage. The characteristic of spectrum perception is the need to monitor and analyze spectrum usage in real-time, and accurately identify available spectrum resources.

Interference perception refers to obtaining information on interference sources and types by monitoring and analyzing interference signals in wireless communication systems [6]. It can be used in applications such as interference suppression, interference localization, and interference management to improve the performance and reliability of communication systems. The characteristic of interference perception is the need to accurately identify and analyze interference signals, and adopt corresponding interference processing strategies.

Location perception refers to obtaining the user's position and movement situation by utilizing information such as time, angle, and power of the received signal. It can be used in applications such as wireless positioning, location services, and mobile management to provide users with precise location information support. The characteristic of location awareness is the need to accurately determine the user's location and be able to track their movement in real-time. The characteristic of traditional communication perception technology is to obtain information related to the communication environment through the reception and processing of wireless signals.

This information can be used to optimize system parameters, improve communication quality, enhance spectrum utilization efficiency, and solve interference problems [7]. However, traditional communication perception techniques are often limited by the accuracy of sensors, limitations in computing resources, and the impact of complex channel environments. To overcome these limitations, new perception technologies and algorithms continue to emerge, such as machine learning-based perception technology and distributed perception technology, to improve the accuracy and efficiency of perception [8].

2.3. Analysis of the advantages and disadvantages of traditional communication perception technology

Traditional communication perception technology plays an important role in wireless communication systems, helping to optimize resource allocation, power control, and interference management, thereby improving system capacity and coverage. By perceiving changes in the wireless communication environment, traditional communication perception techniques can achieve adaptive adjustment of the system to adapt to different channel conditions and interference situations. One of the advantages of traditional communication perception technology is that it can provide detailed information about the communication environment, providing a basis for system decision-making and optimization [9]. For example, spectrum sensing can help to understand the distribution of available spectrum resources, thereby achieving dynamic spectrum access and spectrum sharing. Interference perception can identify interference sources and adopt corresponding interference management strategies to improve the system's anti-interference performance. Wireless positioning and positioning services can be achieved through location awareness to meet the requirements of location-related applications.

However, traditional communication perception technologies also have some drawbacks. Firstly, traditional communication perception technologies typically require a large amount of computation and signal processing, which places high demands on the system's computation and energy consumption [10]. This may lead to application limitations in resource-limited devices or networks. Secondly, the performance of traditional communication perception technologies is limited by the performance of hardware devices and sensors, such as the sensitivity and spectral resolution of receivers. This may limit the accuracy and reliability of perception. Finally, traditional communication perception technologies require processing and analysis of a large amount of

perception data, posing challenges to data processing and privacy protection. In the process of data collection, transmission, and storage, it is necessary to consider the security and privacy protection of data. Further research and innovation are needed to overcome its shortcomings and challenges, improve perception accuracy, reduce energy consumption, improve data processing and privacy protection performance, and meet the growing demands of communication and application scenarios.

3. Overview of RIS technology

3.1. The basic and working principle of RIS

RIS is a surface composed of a large number of passive components that can precisely manipulate electromagnetic waves by adjusting the reflection and transmission characteristics of the components. The basic principle of RIS is to use the adjustable reflection coefficient on the component to change the propagation characteristics of electromagnetic waves. RIS consists of many small units, each of which can control the amplitude and phase of reflected waves by adjusting their phase and amplitude, thereby achieving precise control of propagating waves. The working principle of RIS can be simply described as the following steps:

(1) Receiving stage: RIS receives signals from transmitters, usually transmitted through antennas or base stations.

(2) Reflection regulation: Each unit in RIS adjusts its reflection coefficient and changes the amplitude and phase of the propagating wave based on a predetermined algorithm and regulation strategy.

(3) Propagation stage: The regulated wave is reflected by RIS and propagates along a specific path to the target receiver, forming a channel that affects signal transmission.

3.2. Potential application of RIS in communication systems

RIS technology has broad application potential in communication systems, which can significantly improve the performance and resource utilization efficiency of communication systems. The following are some of the main applications of RIS in communication systems:

(1) Channel gain enhancement: RIS can focus or merge signals during propagation by adjusting the amplitude and phase of reflected waves, enhancing the energy of signals at specific positions, thereby improving channel gain and coverage range.

(2) Beamforming: RIS can adjust the phase and amplitude of reflected waves based on the position and communication requirements of the receiver, achieving precise beamforming. This improves signal directionality and reception quality.

(3) Multi-user interference management: RIS can effectively suppress and manage interference between multiple users by adjusting the phase and amplitude of reflected waves, improving system capacity and performance.

(4) Spectrum resource optimization: RIS can dynamically adjust the frequency response of reflected waves to achieve dynamic allocation and sharing of spectrum resources, improving spectrum utilization efficiency and system capacity.

(5) Security and privacy enhancement: RIS can achieve information protection and privacy enhancement by adjusting the characteristics of reflected waves, and resisting eavesdropping and attack behavior.

3.3. Comparative analysis of RIS technology and traditional communication perception technology

Compared with traditional communication sensing technology, RIS technology has the following advantages

and characteristics:

(1) Accuracy and flexibility: RIS can accurately control the amplitude and phase of propagating waves, providing more precise and flexible transmission control, while traditional communication sensing technology is usually limited by hardware and environmental conditions.

(2) Resource efficiency: RIS can perform signal processing and control at the receiver end, while traditional communication sensing technologies typically require processing at the base station or central controller, saving communication resources and energy consumption.

(3) Real-time performance: RIS can adjust the characteristics of reflected waves in real time to adapt to dynamic communication environment changes, while traditional communication perception technologies usually require periodic sampling and processing, which cannot respond to environmental changes in real-time.

(4) Cost-effectiveness: RIS consists of a large number of passive components, which have lower costs and energy consumption compared to the active devices and sensors required in traditional communication perception technologies.

However, RIS technology also has some challenges and limitations:

(1) Complexity: The design and implementation of RIS involve a large number of components and algorithms, which require addressing technical issues such as phase modulation, power consumption, and computational complexity.

(2) Communication system integration: The introduction of RIS requires close integration and optimization with existing communication systems to achieve optimal performance and interoperability.

(3) Feasibility and scalability: The feasibility and scalability of RIS technology in practical applications still need further research and verification, especially in large-scale deployment and real-time control.

4. Performance analysis of RIS-assisted communication perception integration technology

4.1. System performance evaluation indicators and methods

For the performance evaluation of RIS-assisted communication perception integration technology, the following indicators and methods are usually used for evaluation:

(1) Signal quality: The performance of the communication system largely depends on the quality of the received signal. Common indicators include signal-to-noise ratio (SNR), bit error rate (BER), and channel capacity. These indicators can evaluate whether the signal quality has been improved after RIS regulation.

(2) Energy efficiency: Energy efficiency measures the ratio of the energy consumed by a communication system during data transmission to the effective information transmitted. By comparing the energy efficiency of RIS-assisted communication perception integration technology with traditional communication systems, the improvement effect of RIS on energy utilization can be evaluated.

(3) System capacity: System capacity refers to the maximum number of users or data throughput that a communication system can carry. By utilizing the ability of RIS to regulate reflected waves, the transmission characteristics of the channel can be improved, thereby increasing system capacity.

(4) Interference management: RIS technology can manage and suppress interference between multiple users by adjusting the phase and amplitude of reflected waves. By evaluating the performance of RIS-assisted communication perception integration technology in interference management, the improvement effect on system performance can be determined.

4.2. Performance analysis model of RIS-assisted communication perception integration technology

To conduct performance analysis, researchers usually establish a performance analysis model based on RIS-assisted communication perception integration technology. These models are typically based on methods such as probability theory, information theory, and communication theory, combined with the characteristics of RIS and system parameters for modeling [11]. The following are some common performance analysis models:

(1) Signal transmission model: This model describes the signal transmission process from the transmitter to the receiver, considering the reflection and transmission characteristics of RIS. Modeling can be done using geometric optics, vector transmission theory, and other methods.

(2) Channel capacity model: This model is used to evaluate the improvement effect of RIS-assisted communication perception integration technology on channel capacity. The capacity formula in information theory can be used to model RIS considering factors such as reflection gain and transmission loss.

(3) Interference management model: This model is used to evaluate the performance of RIS technology in interference management. We can consider the interference relationship between multiple users and model it using methods such as interference matrix and interference elimination.

4.3. Discussion on simulation experiments and performance analysis results

To verify the performance of RIS-assisted communication perception integration technology, researchers usually conduct simulation experiments and conduct performance analysis based on the above performance evaluation indicators and models. Through simulation experiments, the performance results of RIS technology can be obtained in different scenarios and parameters, and compared with traditional communication systems. In the discussion of performance analysis results, quantitative analysis and comparison can be conducted on different performance indicators. For example, by plotting the curves of SNR and BER, the improvement effect of RIS technology on signal quality can be evaluated. By comparing the curve of system capacity with the number of users, the effect of RIS on increasing system capacity can be evaluated. Additionally, the performance of RIS can be discussed under different operating frequency bands, number and position of reflective elements, and their impact on system performance can be analyzed. The discussion of performance analysis results can also be further explored for different application scenarios and system requirements. For example, in mobile communication, the improvement effect of RIS technology on the coverage range and mobile performance of mobile users can be discussed. In indoor communication, the suppression effect of RIS technology on signal fading and multipath effects, as well as the improvement effect on indoor coverage and capacity, can be evaluated [12].

5. Conclusion

Communication perception, as a key technology, provides real-time environmental information for wireless communication systems by perceiving and analyzing various parameters and features in the wireless communication environment, thereby supporting system optimization and decision-making. Traditional communication sensing technologies include channel sensing, spectrum sensing, interference sensing, and position sensing, which play important roles in adaptive modulation, power control, beamforming, dynamic spectrum access, spectrum sharing, interference suppression, interference localization, wireless localization, and more. Nonetheless, traditional perception technologies face challenges such as accuracy limitations,

computational resource limitations, and complex channel environments. With the continuous development of technology, new perception technologies and algorithms continue to emerge, such as machine learning-based perception technology and distributed perception technology, to improve the accuracy and efficiency of perception. These new technologies have brought new opportunities and challenges to the development of communication perception. Through further research and innovation, communication perception technology will provide stronger and more reliable support for performance optimization, spectrum resource utilization, and interference management of wireless communication systems.

Disclosure statement

The authors declare no conflict of interest.

References

[1] Zhang J, Li H, Zhang H, 2017, Spectrum Sensing Techniques in Cognitive Radio Networks: A Survey. Wireless Personal Communications, 97(1): 1–26.

[2] Zhao C, Jiang H, 2018, Joint Sensing and Access in Cognitive Radio Networks: A Survey. IEEE Communications Surveys and Tutorials, 20(2): 1067–1091.

[3] Chen X, Hossain E, Leung VC, 2019, Interference Sensing and Management in 5G and Beyond: Recent Advances and Future Trends. IEEE Communications Magazine, 57(7): 52–59.

[4] Wang C, Li Y, Zhang W, 2020, Machine Learning-Based Spectrum Sensing in Cognitive Radio Networks: A Survey. IEEE Access, 8: 192861–192875.

[5] Li Y, Liang YC, Shen X, 2021, From Cognitive Radio to Intelligent Radio: A Comprehensive Survey. IEEE Communications Surveys and Tutorials, 23(1): 3–35.

[6] Tang J, Gao X, Li GY, 2021, Distributed Spectrum Sensing for Cognitive Radio Networks: A Survey. IEEE Communications Surveys and Tutorials, 23(1): 36–54.

[7] Zeng T, Cai Y, Zhang J, et al., 2024, Research on Key Technologies and System Architecture for 6G Communication Perception Integration. Wireless Communication Technology, 2024(03): 59–66.

[8] Yang J, Li M, Zhang S, 2024, Research on Integrated Communication Perception Technology Based on RIS Assistance. Wireless Communication Technology, 50(02): 334–341.

[9] Wang Q, Xing Y, Fan W, et al., 2023, Research on Key Technologies of 6G Core Network Supporting Communication Perception Integration. Electronic Technology Applications, 49(12): 50–55.

[10] Yang X, 2023, Key Technology Design and Implementation of Perception Integration System for 6G Communication. Electronic Manufacturing, 31(16): 81–83 + 96.

[11] Wang J, 2023, Key Technology Research on Wireless Communication Perception Integrated Waveform, thesis, Zhejiang University of Business and Technology.

[12] Wang Y, Jin J, Lou M, et al., 2022, Key Technologies and Applications of Communication Perception Integration. Communication World, 2022(21): 27–30.

Publisher's note

Bio-Byword Scientific Publishing remains neutral with regard to jurisdictional claims in published maps and institutional affiliations.

Journal of Electronic Research and Application, 2024, Volume 8, Issue 4
http://ojs.bbwpublisher.com/index.php/JERA
ISSN Online: 2208-3510
ISSN Print: 2208-3502

Application of Power Electronics Converters in Renewable Energy

Tao Cheng*

Xi'an Kedagaoxin University, Xi'an 710100, China

***Corresponding author:** Tao Cheng, ct1364215794@sina.com

Copyright: © 2024 Author(s). This is an open-access article distributed under the terms of the Creative Commons Attribution License (CC BY 4.0), permitting distribution and reproduction in any medium, provided the original work is cited.

Abstract: Against the backdrop of global energy shortages and increasingly severe environmental pollution, renewable energy is gradually becoming a significant direction for future energy development. Power electronics converters, as the core technology for energy conversion and control, play a crucial role in enhancing the efficiency and stability of renewable energy systems. This paper explores the basic principles and functions of power electronics converters and their specific applications in photovoltaic power generation, wind power generation, and energy storage systems. Additionally, it analyzes the current innovations in high-efficiency energy conversion, multilevel conversion technology, and the application of new materials and devices. By studying these technologies, the aim is to promote the widespread application of power electronics converters in renewable energy systems and provide theoretical and technical support for achieving sustainable energy development.

Keywords: Power electronics converters; Renewable energy; Photovoltaic power generation; Wind power generation; Energy storage systems; High-efficiency energy conversion; Multilevel conversion; New materials; New devices

Online publication: August 13, 2024

1. Introduction

In addressing global climate change and the energy crisis, the development of renewable energy has become a consensus among governments and research institutions worldwide. Renewable energy sources such as Photovoltaics (PV) and wind energy have become important alternatives to traditional fossil fuels due to their clean, efficient, and sustainable characteristics. However, the output characteristics of these energy sources are volatile and unstable, posing challenges to the stable operation of the power grid. Power electronics converters, as crucial bridges connecting renewable energy and the power grid, directly affect the efficiency and stability of the entire energy system. Therefore, studying the application of power electronics converters in renewable energy is of significant theoretical and practical importance.

Power electronics converters can achieve efficient energy conversion and, through advanced control technologies, optimize and regulate energy output, thereby enhancing the overall performance of renewable energy systems. With technological advancements, new power electronics converters have made significant

progress in high-efficiency energy conversion, multilevel conversion, and the application of new materials and devices, providing new solutions for optimizing renewable energy systems.

2. The importance of power electronics converters in renewable energy

2.1. Basic principles and functions of power electronics converters

Power electronics converters are key devices that convert electrical energy from one form to another and are widely used in renewable energy systems. Their basic principle involves the switching actions of power electronic devices, achieving voltage and current regulation and conversion through high-frequency switching technology with Direct Current (DC) and Alternating Current (AC). Power electronics converters mainly include DC-DC converters, AC-DC converters, DC-AC converters, and AC-AC converters. Each type of converter has specific functions and application scenarios. For instance, DC-DC converters are commonly used for Maximum Power Point Tracking (MPPT) in PV systems, while DC-AC converters convert DC power from PV or wind energy systems into AC power for grid integration.

The core functions of power electronics converters include voltage conversion, energy regulation, harmonic suppression, and power factor correction. By precisely controlling the switching states of power semiconductor devices, converters can achieve efficient energy conversion and transmission, meeting the demands of various loads. Additionally, modern power electronics converters integrate intelligent control algorithms and digital signal processing technologies to achieve real-time monitoring and regulation of complex power quality issues [1].

2.2. The importance of improving energy conversion efficiency

Improving energy conversion efficiency is crucial in renewable energy systems. High-efficiency energy conversion maximizes the utilization of natural resources, significantly reduces energy losses, and enhances the overall performance and economic efficiency of the system. As the core component of energy conversion, the efficiency of power electronics converters directly affects the efficiency of the entire system.

High-efficiency power electronics converters can maintain low energy losses under various operating conditions, ensuring efficient energy transmission and utilization. For example, the application of advanced technologies such as soft-switching, Zero-Voltage Switching (ZVS), and Zero-Current Switching (ZCS) can reduce switching losses and improve converter efficiency. Moreover, multilevel converter technology, through stepped voltage processing, further reduces switching losses and electromagnetic interference, enhancing the overall system efficiency.

Improving energy conversion efficiency also reduces the system's cooling requirements and equipment size, lowering operational costs and maintenance difficulties. Efficient power electronics converters enhance the economic and reliability aspects of renewable energy systems, providing essential support for achieving green energy and sustainable development goals.

2.3. Adapting to variable energy inputs

A significant characteristic of renewable energy is its variable and uncertain input. Natural resources such as solar and wind energy are influenced by climate and environmental conditions, resulting in significant randomness and volatility in their output power. Power electronics converters must possess high adaptability to cope with variable energy inputs and ensure stable system operation.

To adapt to variable energy inputs, power electronics converters employ advanced control strategies and algorithms. For instance, in PV systems, MPPT algorithms can adjust the operating point of the PV array in real-time, ensuring maximum power output under varying sunlight conditions. In wind power generation

systems, variable speed constant frequency control technology adjusts the generator's speed to ensure stable power output under different wind speeds [2].

Furthermore, power electronics converters enhance system reliability and disturbance resistance through multilevel topologies and redundancy designs, maintaining efficient and stable operation in complex and variable environments. The introduction of intelligent and digital technologies endows converters with stronger adaptive capabilities and fault diagnosis abilities, providing a solid foundation for the safe and reliable operation of renewable energy systems.

3. Application of power electronics converters in renewable energy systems

3.1. Application in photovoltaic power generation systems

In PV power generation systems, power electronics converters are primarily used to efficiently convert the DC power generated by PV arrays into AC power and to optimize energy output through MPPT technology. PV inverters are key components in this system, responsible for converting DC power into high-quality AC power synchronized with the grid and ensuring the stability and reliability of the output power.

PV inverters can be categorized into three types based on their topology: centralized inverters, string inverters, and micro-inverters. Centralized inverters are suitable for large-scale PV power plants, offering high efficiency and low cost by processing the power conversion of multiple PV strings through a single inverter. However, the downside of this configuration is the high risk of single-point failures; if the inverter fails, it can lead to significant power loss.

String inverters are suitable for medium and small-scale PV systems. They provide independent control for each string, enhancing system flexibility and energy output efficiency. This approach effectively reduces the risk of single-point failures and better adapts to complex lighting conditions, allowing each string to operate at its optimal point [3].

Micro-inverters are applied to individual PV modules, enabling fine-grained energy optimization and monitoring, making them ideal for distributed PV systems. The advantage of micro-inverters is that each PV module can work and optimize independently, significantly improving overall system efficiency and reducing performance mismatch issues among PV modules. The modular design of micro-inverters also enhances system scalability and maintenance convenience.

3.2. Application in wind power generation systems

In wind power generation systems, the application of power electronics converters mainly focuses on the implementation of Variable Speed Constant Frequency (VSF) technology and the optimization of power quality. Wind power generation systems convert unstable mechanical energy into stable electrical energy through variable-speed wind turbines. Power electronics converters play a crucial role in ensuring that the system efficiently and stably converts wind energy into electrical energy.

In VSF wind power generation systems, Doubly-Fed Induction Generators (DFIG) and Full Power Converters (FPC) are two main technical routes. In DFIG systems, power electronics converters are connected to the rotor side of the generator, achieving variable-speed constant frequency operation by regulating rotor current. This method offers cost and efficiency advantages by using partial power converters (typically 30% of rated power) to adjust rotor-side power for variable-speed operation and constant frequency output. However, DFIG systems are sensitive to grid power quality and may have weak disturbance resistance during grid faults or voltage fluctuations, potentially affecting system stability.

In contrast, FPC systems use full power converters connecting the generator and the grid, enabling a

wider range of speed regulation and higher power quality. In FPC systems, all the generated power passes through the converter, converting variable-frequency and variable-voltage AC power from the generator into constant-frequency and constant-voltage AC power for the grid. Since the entire power path goes through the power electronics converter, FPC systems can better control the quality of the output power, providing stronger adaptability and stability, especially under complex conditions and grid scenarios [4].

Power electronics converters in wind power generation systems not only handle energy conversion but also achieve functions such as power balancing, reactive power compensation, and harmonic suppression through advanced control algorithms. Power balancing involves adjusting generator output power during wind speed changes to maintain stable system operation. Reactive power compensation improves the power factor of the grid by regulating reactive power, enhancing power quality. Harmonic suppression reduces harmonic components in the converter's output current, minimizing electromagnetic interference with the grid and ensuring power purity.

3.3. Application in energy storage systems

Energy storage systems play a key role in balancing energy supply and demand, improving grid stability and reliability in renewable energy systems. Power electronics converters in energy storage systems enable bidirectional energy flow and conversion between storage devices (such as batteries and capacitors) and the grid or load, providing crucial technical support for efficient energy utilization and stable system operation.

In battery storage systems, bidirectional DC-DC converters and DC-AC converters are the main power electronics devices. Bidirectional DC-DC converters control battery charging and discharging, ensuring optimal battery operation through efficient voltage and current regulation. These converters precisely control voltage and current during charging and discharging to maximize battery life and improve system efficiency. Advanced control algorithms, such as Battery Management Systems (BMS), monitor battery status in real-time to prevent overcharging, over-discharging, and overheating, ensuring battery safety and reliability [5].

DC-AC converters convert stored DC power from batteries into AC power for grid or load use. These converters achieve efficient energy conversion while ensuring power quality by reducing harmonics and fluctuations. DC-AC converters must have seamless switching capabilities to ensure that energy storage systems can quickly switch to off-grid mode during grid faults, continuing to supply critical loads and ensuring continuous and stable power supply.

Supercapacitor storage systems utilize their fast charging and discharging capabilities and high-power density as transient response devices for the grid. Supercapacitors offer higher power density and faster charging and discharging speeds than traditional batteries, making them suitable for short-term energy storage and rapid response buffering. Power electronics converters in supercapacitor systems achieve fast energy conversion and power regulation. Using high-frequency switching technology and intelligent control algorithms, converters can respond to grid frequency fluctuations and voltage drops within milliseconds, enhancing grid dynamic stability and disturbance resistance.

Moreover, hybrid energy storage systems combine the advantages of batteries and supercapacitors, leveraging their complementary characteristics. Power electronics converters in hybrid storage systems play a crucial role in coordinated control and energy management. Advanced control strategies and optimization algorithms enable efficient energy utilization and optimized system operation in hybrid storage systems. For example, the system can primarily rely on battery storage during low daily loads and use supercapacitors for rapid response during sudden load increases or grid fluctuations, maintaining system stability.

4. Innovative applications of power electronics converters in renewable energy systems

4.1. High-efficiency energy conversion technologies

High-efficiency energy conversion is one of the core goals of applying power electronics converters in renewable energy systems. With increasing demands for energy efficiency, various high-efficiency energy conversion technologies have emerged [6].

Soft-switching technology is one of the crucial means to improve energy conversion efficiency. Compared to traditional hard-switching technology, soft-switching achieves zero-voltage or zero-current switching during the on-and-off states of switching devices, significantly reducing switching losses and Electromagnetic Interference (EMI). Common soft-switching technologies include ZVS and ZCS. By optimizing circuit topologies and control strategies, these technologies further enhance the efficiency and reliability of converters.

High-frequency converter design is also key to achieving high-efficiency energy conversion. By increasing the switching frequency, converters can achieve smaller size and higher power density, while reducing the size and weight of filters and transformers. However, high-frequency converter design faces challenges such as switching losses and thermal management, which require advanced materials and cooling technologies to address.

Additionally, energy management technologies based on digital control and intelligent control play an important role in improving converter efficiency. Through real-time monitoring and dynamic adjustment, intelligent control technologies can optimize the operating state of converters, achieving efficient energy utilization and minimizing losses.

4.2. Advances in multilevel conversion technology

Multilevel conversion technology has gained widespread attention in the field of power electronics converters. By increasing the number of output voltage levels, it can significantly reduce harmonic content and switching losses, improving converter efficiency and power quality.

Neutral-Point Clamped (NPC) multilevel converters are a classic topology in multilevel conversion, achieving voltage clamping through diodes, resulting in multiple output voltage levels. This technology features a simple structure and convenient control, but in high-level applications, the number of diodes and losses increase significantly.

Flying Capacitor (FC) multilevel converters achieve voltage clamping through capacitors, reducing the use of diodes while improving voltage utilization and system efficiency. This technology has significant advantages in high-power applications, although capacitors tend to be larger and more expensive.

Cascaded H-Bridge (CHB) multilevel converters achieve high-level output by cascading multiple low-voltage units, featuring modular design and strong fault tolerance. This technology has broad application prospects in large-scale renewable energy grid-connected systems but requires complex control and coordination strategies.

In recent years, multilevel conversion technology has made significant progress in topology structures, control strategies, and application fields. For example, hybrid multilevel converters combine the advantages of various topologies and achieve higher efficiency and better power quality through intelligent control algorithms.

4.3. Application of new materials and devices

The application of new materials and devices is a key driving force in the development of power electronics converter technology. Wide bandgap semiconductor materials, such as silicon carbide (SiC) and gallium nitride (GaN), significantly enhance converter performance.

SiC devices have characteristics of high voltage resistance, high frequency, and high-temperature stability. Compared to traditional silicon-based devices, they exhibit lower switching losses and smaller on-resistance. SiC devices show great potential in high-frequency high-efficiency energy conversion applications, such as PV inverters and electric vehicle charging systems, improving system efficiency and power density.

GaN devices, with higher electron mobility and smaller device sizes, perform excellently in high-frequency and high-power applications. GaN devices have been widely used in communication power supplies, data center power supplies, and portable device chargers, significantly enhancing system energy efficiency and performance.

Moreover, the development of nanomaterials and advanced packaging technologies provides new avenues for enhancing the performance of power electronics converters. The high thermal conductivity and strength of nanomaterials help improve device heat dissipation efficiency and mechanical strength. Advanced packaging technologies further reduce device size, increase power density, and enhance reliability.

By continuously exploring the application of new materials and devices, power electronics converters will achieve higher efficiency, smaller size, and longer lifespan in renewable energy systems, providing strong support for the widespread application and technological advancement of renewable energy.

5. Conclusion

This paper systematically analyzed the application of power electronics converters in PV power generation, wind power generation, and energy storage systems. It discussed their basic principles and functions in detail and introduced current innovations in high-efficiency energy conversion, multilevel conversion technology, and the application of new materials and devices. The research indicates that power electronics converters play an irreplaceable role in enhancing the efficiency and stability of renewable energy systems.

In the future, with continuous technological advancements, power electronics converters will develop towards higher efficiency, higher power density, and increased intelligence. The application of new materials and devices will further enhance converter performance, providing more possibilities for the widespread application and optimization of renewable energy systems. Additionally, power electronics converters have broad application prospects in smart grids and microgrids, warranting further in-depth research and exploration. Through continuous technological innovation and practical applications, power electronics converters will play an increasingly important role in achieving sustainable energy development goals.

Disclosure statement

The author declares no conflict of interest.

References

[1] Xing X, Yang W, Mi S, et al., 2020, Application of Power Electronics Technology in Renewable Energy Hydrogen Production Systems. Power Electronics, 54(12): 1–4.

[2] Mu S, Yang W, Guo Z, et al., 2020, A Power Electronics Converter Applied to SOC Hydrogen Storage Systems. Power Electronics, 54(12): 17–19 + 46.

[3] Sun Z, Guo X, Wang S, et al., 2023, Research on Real-Time Simulation Modeling Method of High-Frequency Power Electronics Converter Based on Switching State Prediction Correction. Proceedings of the CSEE, 2023(2): 1–12. https://doi.org/10.13334/j.0258-8013.pcsee.230781

[4] Rong J, Tong Y, Chen S, et al., 2023, Application of Simulation Technology in Teaching "Power Electronics Technology". Journal of Electrical and Electronic Education, 45(05): 24–27.

[5] Wang Z, 2023, Fault Diagnosis of Power Converters Based on DSP, thesis, Northeast Electric Power University.

[6] Liang Y, Chen Y, Jiang J, et al., 2023, Design and Development of a Three-Phase Balanced Power Electronics Converter for AC Arc Furnace Power Supply. Electrotechnical Application, 42(05): 97–106 + 9.

Publisher's note

Bio-Byword Scientific Publishing remains neutral with regard to jurisdictional claims in published maps and institutional affiliations.

Journal of Electronic Research and Application, 2024, Volume 8, Issue 4
http://ojs.bbwpublisher.com/index.php/JERA
ISSN Online: 2208-3510
ISSN Print: 2208-3502

Research on Machine Tool Fault Diagnosis and Maintenance Optimization in Intelligent Manufacturing Environments

Feiyang Cao*

Zhengzhou Business University, Zhengzhou 451200, China

***Corresponding author:** Feiyang Cao, caofeiyang1018@126.com

Copyright: © 2024 Author(s). This is an open-access article distributed under the terms of the Creative Commons Attribution License (CC BY 4.0), permitting distribution and reproduction in any medium, provided the original work is cited.

Abstract: In the context of intelligent manufacturing, machine tools, as core equipment, directly influence production efficiency and product quality through their operational reliability. Traditional maintenance methods for machine tools, often characterized by low efficiency and high costs, fail to meet the demands of modern manufacturing industries. Therefore, leveraging intelligent manufacturing technologies, this paper proposes a solution optimized for the diagnosis and maintenance of machine tool faults. Initially, the paper introduces sensor-based data acquisition technologies combined with big data analytics and machine learning algorithms to achieve intelligent fault diagnosis of machine tools. Subsequently, it discusses predictive maintenance strategies by establishing an optimized model for maintenance strategy and resource allocation, thereby enhancing maintenance efficiency and reducing costs. Lastly, the paper explores the architectural design, integration, and testing evaluation methods of intelligent manufacturing systems. The study indicates that optimization of machine tool fault diagnosis and maintenance in an intelligent manufacturing environment not only enhances equipment reliability but also significantly reduces maintenance costs, offering broad application prospects.

Keywords: Intelligent manufacturing; Machine tool fault diagnosis; Predictive maintenance; Big data; Machine learning; System integration

Online publication: August 13, 2024

1. Introduction

With continuous advancements in manufacturing technology, modern industries demand higher reliability and stability from equipment. Machine tools, essential in the manufacturing process, are critical as their failures can cause production halts and affect product quality. Therefore, researching the optimization of fault diagnosis and maintenance for machine tools under intelligent manufacturing environments not only helps enhance the reliability and production efficiency of the equipment but also contributes to reducing maintenance costs and extending the lifespan of the equipment, which holds significant theoretical and practical value.

2. Fault diagnosis technologies for machine tools in intelligent manufacturing environments

2.1. Sensor-based data collection

In intelligent manufacturing environments, the fault diagnosis of machine tools relies heavily on sensor-based data collection technologies. Sensors placed at various parts of the machine tools can collect real-time data on multiple parameters such as temperature, pressure, vibration, current, and voltage. This data reflects the operational state and performance of the machine tools during operation, which is crucial for fault diagnosis.

Sensor-based data collection technologies enable real-time monitoring and tracking of the operational status of machine tools. The sensors transmit collected data to the data processing system, which performs real-time analysis and processing. This setup allows for continuous monitoring of the machine's operational state and timely detection of any anomalies. For instance, if a sensor detects an unusual temperature rise in a part of the machine, it could indicate a potential fault, necessitating timely maintenance.

Moreover, data collected from sensors not only helps in diagnosing faults in machine tools but also supports their maintenance. By analyzing sensor data, it is possible to determine the machine's workload, operating conditions, and other relevant information, which aids in devising a reasonable maintenance plan. For example, sensor data analysis can help predict the working cycles of the machine and estimate the lifespan of critical components, thus facilitating preventative maintenance and avoiding production interruptions due to faults.

Overall, sensor-based data collection technology is a crucial means for implementing fault diagnosis and maintenance optimization in intelligent manufacturing environments. By fully utilizing data collected from sensors, comprehensive monitoring and diagnosis of the operational status of machine tools can be achieved, enhancing their reliability and lifespan while reducing maintenance costs and providing technological support for the development of intelligent manufacturing.

2.2. Big data and fault diagnosis

The importance of big data technology in machine tool fault diagnosis within intelligent manufacturing environments is increasingly pronounced. Its key roles are manifested in several aspects:

(1) Data collection and processing: Big data platforms can collect, store, and manage real-time and historical operational data from machine tool sensors. This data forms the foundation for fault diagnosis, offering comprehensive information to analyze the operational status of the machine tools.

(2) Data analysis and mining: Utilizing technologies such as machine learning, and deep analysis of big data can reveal patterns and anomalies. By training on historical data, diagnostic models for various fault types can be constructed, enabling predictions and diagnoses for future data.

(3) Fault prediction and prevention: Big data analysis allows for more accurate assessments of the operational status of machine tools, timely identification of potential faults, and prediction of possible fault types and timing. This aids in preventing faults and enhancing the reliability and stability of machine tools.

(4) Maintenance optimization: Big data technology supports determining the optimal timing and methods for machine maintenance, avoiding unnecessary or delayed maintenance that could pose fault risks. By optimizing maintenance plans and resource allocation, maintenance efficiency and cost-effectiveness are improved.

(5) Intelligent decision support: Big data analysis provides more extensive data support for decision-making, making maintenance decisions more scientific and accurate. Using big data technology, an intelligent manufacturing system can be established to automate the diagnosis and maintenance of

machine tools, enhancing the stability and reliability of the production line.

2.3. Application of machine learning and artificial intelligence in fault diagnosis

The application of machine learning and artificial intelligence technologies in machine tool fault diagnosis in intelligent manufacturing environments is broad and profound. These technologies, by learning and analyzing a vast amount of operational data from machine tools, enable intelligent recognition and prediction of machine operational statuses, offering new approaches and methods for machine tool fault diagnosis and maintenance.

Firstly, machine learning algorithms can be applied to build fault diagnosis models for machine tools. By training on historical data, diagnostic models for various types of machine tool faults can be developed, allowing for predictions and diagnoses of future data. This machine-learning-based fault diagnosis approach significantly enhances the accuracy and efficiency of fault diagnosis, helping enterprises to timely detect and resolve issues with machine tools.

Moreover, the application of artificial intelligence technology can automate the diagnosis and maintenance of machine tools. By integrating techniques such as deep learning, real-time monitoring and diagnosis of machine tool operation can be performed, automatically triggering maintenance processes. This automated approach to fault diagnosis and maintenance not only enhances diagnostic efficiency and accuracy but also reduces the costs and risks associated with manual intervention, improving the stability and reliability of the production line.

Additionally, machine learning and artificial intelligence technologies can be combined with other technologies, such as the Internet of Things (IoT) and cloud computing, to enable remote monitoring and management of machine tools. By establishing a big data platform in the cloud, centralized monitoring and diagnosis of multiple machine tools can be achieved, providing comprehensive production data support for enterprises and helping them optimize and automate their production processes.

3. Machine tool maintenance optimization strategies

3.1. Predictive maintenance

The application of predictive maintenance in intelligent manufacturing environments not only enhances the reliability and lifespan of machine tools but also offers the following features and advantages:

(1) Real-time monitoring and data analysis: Predictive maintenance involves continuous monitoring of various operational parameters of machine tools and processing this data with advanced analytical techniques to timely detect abnormal operating conditions and preempt potential failures.

(2) Reduced maintenance costs: Compared to traditional periodic maintenance, predictive maintenance reduces unnecessary maintenance and replacements, thereby lowering costs. By strategically planning maintenance activities, it also avoids costs and losses associated with sudden failures and production interruptions.

(3) Increased production efficiency: Predictive maintenance helps prevent production halts caused by machine tool failures, ensuring continuous operation of production lines, and enhancing productivity and capacity utilization. Moreover, maintaining equipment proactively prevents the escalation of faults, further stabilizing and enhancing the reliability of the production line [1].

(4) Optimized maintenance strategies: Predictive maintenance allows for the optimization of maintenance strategies based on the actual operating conditions and maintenance needs of the machine tools, enabling efficient allocation of maintenance resources and improving maintenance responsiveness. Priority can be given to critical components to ensure their stable operation and reduce the risk of

failures.

(5) Intelligent decision support: Leveraging technologies such as artificial intelligence and machine learning, predictive maintenance can perform intelligent analysis and diagnostics of machine tool operational data. Developing diagnostic models enables the prediction and diagnostics of future data, providing a scientific basis and intelligent support for maintenance decisions.

3.2. Maintenance strategy optimization model

The maintenance strategy optimization model plays a crucial role in intelligent manufacturing settings, enhancing machine tool reliability and production efficiency while reducing maintenance costs and risks. It is manifested in several ways:

(1) Optimization of maintenance plans: Using the maintenance strategy optimization model, maintenance plans can be optimized based on real-time operational data and historical maintenance records of machine tools. The model analyzes the operational status, predicts potential fault types and timing, and devises optimal maintenance schedules, thereby minimizing unplanned maintenance and reducing the frequency of maintenance to decrease production downtime and enhance efficiency.

(2) Effective allocation of maintenance resources: The optimization model considers factors like maintenance costs and uses mathematical modeling and optimization algorithms to derive the best maintenance strategies. It takes into account costs, machine downtime, and parts replacement cycles, solving for the most cost-effective and efficient maintenance plans to ensure effective resource allocation.

(3) Enhanced scientific and accurate maintenance decisions: The model considers the usage and environmental factors of machine tools to create personalized maintenance strategies. Scientific data analysis and algorithmic solutions enhance the accuracy and scientific basis of maintenance decisions, minimizing human error and providing a solid foundation for these decisions.

(4) Reduced maintenance costs and risks: The optimization model helps businesses reduce maintenance costs and risks. Implementing a rational maintenance plan and resource allocation prevents unnecessary and delayed maintenance, reducing the risk of machine tool failures and the costs and losses associated with repairs and production interruptions [2].

3.3. Optimization of maintenance resources

In intelligent manufacturing environments, the optimal allocation of maintenance resources for machine tools is crucial. By properly allocating human, material, and time resources, maintenance efficiency can be enhanced, maintenance costs reduced, and smooth production ensured. This includes:

(1) Optimization of human resources: Based on the importance and maintenance needs of machine tools, the number and skill level of maintenance personnel are appropriately allocated. Specialized personnel may be assigned to key equipment to ensure stable operation and flexible maintenance approaches, such as outsourcing, may be adopted for general equipment. Furthermore, training and skill enhancement can improve the professional level of maintenance staff.

(2) Optimization of material resources: Proper allocation of maintenance equipment and tools ensures smooth maintenance operations. Spare parts inventory may be increased based on the frequency of use and maintenance needs of the machine tools to handle emergencies. Maintenance equipment should be regularly updated to enhance efficiency. Additionally, the adoption of intelligent maintenance equipment can increase the automation level of maintenance.

(3) Optimization of time resources: Maintenance schedules should be planned to avoid production interruptions due to maintenance activities. Predictive and planned maintenance can be combined to schedule maintenance work in advance, minimizing production downtime. Concurrent maintenance, where maintenance occurs alongside ongoing production, can also be used to reduce downtime.

(4) Optimization of maintenance strategies: Appropriate maintenance strategies should be developed based on the actual conditions and maintenance needs of the machine tools. Combining regular inspections, condition monitoring, and fault prediction can maximize the use of maintenance resources and enhance the efficiency and quality of maintenance. Furthermore, information technologies such as the Internet of Things and big data can be used to monitor and optimize the maintenance process, further enhancing maintenance efficiency [3].

4. Integration and implementation of intelligent manufacturing systems

4.1. Intelligent manufacturing system architecture design

The architectural design of an intelligent manufacturing system must consider the functionality and interrelationships of various internal modules, as well as the system's interaction with the external environment and its capacity to accommodate future development needs. An effective architecture should have the following features:

(1) Modular design: The system should adopt a modular design, dividing it into several independent modules, each responsible for specific functions. This reduces system complexity, facilitates maintenance and upgrades, and allows for the flexible addition of new functional modules as needed.

(2) Distributed architecture: Given the extensive data collection and processing involved, a distributed architecture can disperse these tasks across different nodes, enhancing the system's processing capabilities and overall performance. This architecture also enhances system reliability, as the failure of one node does not compromise the entire system's operation.

(3) Data security and privacy protection: With considerable data exchange and sharing involved, data security and privacy protection are paramount. The system should employ encryption technologies to safeguard data transmission and storage and implement stringent access controls to ensure that only authorized users can access the data [4].

(4) Intelligent decision support: The system should possess capabilities for intelligent decision-making support, analyzing real-time and historical data to provide a scientific basis for production decisions. This requires integrating advanced data analytics and machine learning technologies to enable intelligent monitoring and optimization of the production process.

4.2. System integration and implementation

System integration and implementation are critical phases in the construction of intelligent manufacturing systems. These phases involve integrating and coordinating various subsystem components to transform the design scheme into an operational system. During this stage, several aspects must be considered:

(1) Implementation of system architecture: Based on the designed architecture, organize and integrate the various subsystem components according to specific rules and standards. Ensure that the interfaces and communications between components function correctly to achieve the system's overall functionality.

(2) Implementation of hardware and software compatibility: Install and configure hardware devices and software systems. This includes the setup and debugging of hardware devices and the installation and deployment of software systems, ensuring compatibility and interoperability between hardware and

software.

(3) Implementation of data flows: Establish data processes and transmission channels to enable the flow and exchange of data among the subsystems. Ensure that data is transmitted and processed accurately and promptly to support the normal operation and decision-making processes of the system.

(4) Implementation of functional modules: Gradually implement each functional module according to the system design requirements. This includes developing and testing core modules such as fault diagnosis and predictive maintenance to ensure the completeness and stability of these functions [5].

(5) Ensuring safety and stability: Consider potential safety hazards and stability issues that may arise during system operation and take appropriate measures to ensure the system operates safely and reliably throughout.

By implementing these strategies, the design principles of intelligent manufacturing systems can be realized in practical operating systems, providing technical support for machine tool diagnostics and maintenance while promoting the advancement and application of intelligent manufacturing technologies.

4.3. System testing and evaluation

In system testing and evaluation, it is necessary first to conduct comprehensive tests of the system's functionalities to verify whether the system meets design specifications. Functional testing should cover all functional modules of the system to ensure they operate correctly and interact effectively with each other. Next, performance testing assesses how the system performs under various loads, including response speed and resource utilization, to ensure sufficient performance in actual operation. Additionally, security testing is crucial to ensure that the system can withstand various security threats and attacks, safeguarding both the system and its data.

In terms of system evaluation, aspects such as the system's stability, reliability, and security need to be considered. Stability evaluation assesses whether the system can maintain stable performance and functionality over extended periods. Reliability evaluation examines how the system performs in the face of various faults and anomalies, including its recovery capabilities and fault tolerance. Security evaluation assesses the system's ability to protect against various security threats, including data protection and user access management. Comprehensive system evaluation can identify potential issues and suggest improvements, ensuring that the system operates normally and achieves the desired outcomes [6].

Additionally, system testing and evaluation must involve communication with users and relevant stakeholders to gather their feedback on system usability and their specific requirements. This feedback is crucial for refining the system's design and functionality, enhancing user satisfaction and applicability. Therefore, system testing and evaluation are indispensable components of intelligent manufacturing system construction. Through scientific testing and evaluation methods, the quality and performance of the system can be ensured, providing a solid foundation for the development and application of intelligent manufacturing technologies.

5. Conclusion

This paper has achieved the following main outcomes through the study of machine tool fault diagnosis and maintenance optimization in an intelligent manufacturing environment: Intelligent diagnosis of machine tool faults has been realized through sensor-based data collection technology combined with big data analysis and machine learning algorithms. A predictive maintenance strategy was proposed, and by establishing an optimized maintenance strategy model and optimizing maintenance resource allocation, maintenance efficiency

has been improved and maintenance costs have been reduced. The architecture of the intelligent manufacturing system was designed and implemented, and its feasibility and effectiveness were verified through testing and evaluation.

Future research could delve deeper into the following areas: Further optimization and refinement of machine tool fault diagnosis algorithms to enhance diagnostic accuracy and real-time capabilities. As well as exploration of more application scenarios and maintenance strategies in intelligent manufacturing environments to expand the system's applicability. Additionally, investigation into the deep integration of intelligent manufacturing systems with other advanced manufacturing technologies such as the Internet of Things and cloud computing to create more intelligent and efficient manufacturing systems. Furthermore, comprehensive experiments involving multiple scenarios and devices could be conducted to verify the system's performance and effectiveness in different application settings.

Disclosure statement

The author declares no conflict of interest.

References

[1] Li Q, 2022, Practice of Digital Factory Construction by Qin Chuan Group. Journal of Intelligent Manufacturing, 2022(03): 26–29.

[2] Cao W, 2023, Analysis of Fault Diagnosis and Maintenance of CNC Machine Tools. Papermaking Equipment and Materials, 52(11): 55–57.

[3] Xue P, 2023, Research on Intelligent Fault Diagnosis Technology for CNC Machine Tools. Modern Manufacturing Technology Equipment, 59(09): 66–68.

[4] Han L, 2023, Fault Diagnosis and Maintenance of Mechanical CNC Machine Tool Processing. China Plant Engineering, 2023(11): 177–179.

[5] Wang B, 2022, Preliminary Exploration of Maintenance and Repair Methods for CNC Machine Tools. China Southern Agricultural Machinery, 53(21): 142–144.

[6] Fu Z, 2021, A Brief Analysis of Fault Diagnosis and Maintenance of CNC Machine Tool Feed Systems. China Plant Engineering, 2021(23): 193–195.

Publisher's note

Bio-Byword Scientific Publishing remains neutral with regard to jurisdictional claims in published maps and institutional affiliations.

Journal of Electronic Research and Application, 2024, Volume 8, Issue 4
http://ojs.bbwpublisher.com/index.php/JERA
ISSN Online: 2208-3510
ISSN Print: 2208-3502

Visual Representation and Cognitive Models in Information Visualization

Yingquan Wang[1,2]*, Mustaffa Halabi Azahari[3]

[1]City Graduate School, City University Malaysia, Kuala Lumpur 46100, Malaysia
[2]College of Design and Fine Arts, Qingdao Huanghai University, Qingdao 266427, China
[3]Faculty of Creative Industries, City University Malaysia, Kuala Lumpur 46100, Malaysia

***Corresponding author:** Yingquan Wang, wangyq@qdhhc.edu.cn

Copyright: © 2024 Author(s). This is an open-access article distributed under the terms of the Creative Commons Attribution License (CC BY 4.0), permitting distribution and reproduction in any medium, provided the original work is cited.

Abstract: As a branch of computer science, information visualization aims to help users understand and analyze complex data through graphical interfaces and interactive technologies. Information visualization primarily includes various visual structures such as time-series structures, spatial relationship structures, statistical distribution structures, and geographic map structures, each with unique functions and application scenarios. To better explain the cognitive process of visualization, researchers have proposed various cognitive models based on interaction mechanisms, visual perception steps, and novice use of visualization. These models help understand user cognition in information visualization, enhancing the effectiveness of data analysis and decision-making.

Keywords: Information visualization; Visual structures; Cognitive models; Interaction design

Online publication: August 12, 2024

1. Introduction

Information visualization, initially a branch of computer science, is an essential part of visualization research. It was first systematically articulated by Stuart K. Card, George G. Robertson, and Jock D. Mackinlay in 1990. They introduced a system called the "information visualizer," designed to help users process and understand large amounts of complex data through graphical interfaces and interactive technologies [1]. The paper detailed how computer graphics and user interface technologies could transform abstract data into easily understandable visual forms, enhancing users' cognitive and analytical abilities. Ben Shneiderman and Ben Bederson defined information visualization as using computers to interactively display abstract data, enhancing people's cognition of abstract information. Both Shneiderman and Bederson made significant contributions to the field of information visualization. They proposed a visualization taxonomy based on data types and tasks, designing a high-level graphical user interface framework: "Overview first, zoom and filter, then detail-on-demand" [2]. This approach helps users better understand and interact with large and complex data sets. Many scholars also believe that the information objects in information visualization include text, images, and sounds, realized through different model methods. Information visualization maps abstract data into images on computer

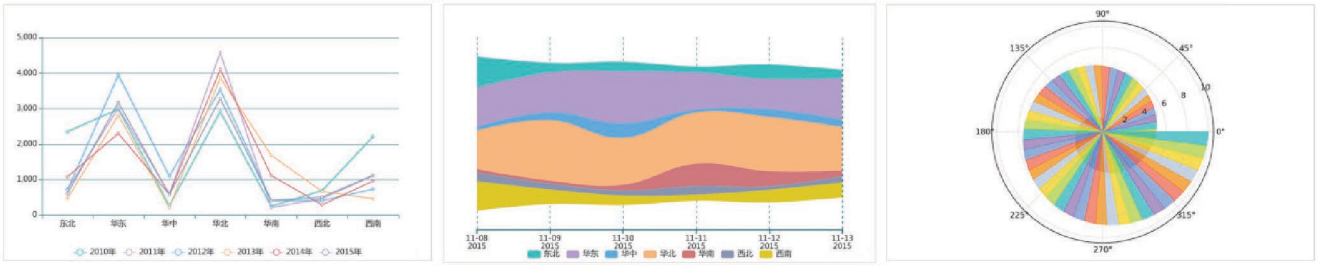
screens, helping users quickly extract useful information from large datasets.

2. Visual structures of information visualization

Information visualization maps abstract data to visual forms for understanding through visual cognitive tasks. Designers must first consider how to present these visualizations, which generally follow a basic framework with three levels. The highest level is the visualization interface, the medium for human-computer interaction, possibly containing multiple sub-interfaces. The middle level is the visual structure, organizing data with methods like bar charts, scatter plots, and tree diagrams. The lowest level consists of visual units, the smallest components like points, lines, and text, encoded by variables such as color, shape, and size.

2.1. Time-series structures

Data sets that change over time are one of the most common forms of recorded data. Time-series data involving state changes are core to many fields, such as finance (stock prices, exchange rates), science (temperature, pollution levels, potential), and public policy (crime rates). People can often extract patterns of data changes over time from temporal phenomena, but it is difficult to quickly obtain effective information through visual observation alone. Therefore, various charts representing time-series data have emerged and have achieved outstanding results in data presentation. Common visualization visual structures based on time-series include line charts, streamgraphs, and spiral plots, as shown in Figure 1.



(a) Line chart (b) Streamgraph (c) Spiral plot

Figure 1. Time-series structures

The concept of line charts was first proposed by Scottish economist William Playfair. He used this type of chart to represent changes in economic data, such as annual changes in export and import data. William Playfair is considered the founder of graphical statistics, and his work profoundly influenced later data visualization methods. The X-axis of line charts usually represents time, while the Y-axis represents variables of other attributes, making it intuitive to see the patterns of data points changing over time.

Streamgraphs, first proposed by Lee Byron and Martin Wattenberg in 2008, were designed to better represent changes in time-series data, especially those with hierarchical structures. Streamgraphs display the flow and trends of data over time using color and shape variations, making them very suitable for showing changes in complex data sets [3]. In addition to representing information by time, streamgraphs also allow users to discover the dynamic trends of thematic events through information changes, providing an effective way to reveal internal relationships between events over time within documents.

The concept of spiral plots was first proposed by Dutch mathematician and graphic designer Gerard ’t Hooft in the 1980s. Spiral plots arrange time-series data along a spiral path, commonly used to display cyclical data, such as seasonal changes or periodic events. This chart form makes periodic patterns more apparent and intuitive by arranging data points along a spiral line [3].

2.2. Spatial relationship structures

In daily life, information is often organized by logical relationships, such as books in a library classified by themes for easy access. Similarly, in information visualization, the interface design must organize information organically, summarizing relationships and reflecting spatial structure. Most data can form natural hierarchical structures. Visualization techniques for these structures enable rapid multi-scale reasoning, allowing both micro-level observation of individual elements and macro-level observation of groups [5]. Common visual structures for spatial relationships include tree diagrams, rack diagrams, and node-link diagrams, as shown in **Figure 2**.



(a) Tree diagram (b) Rack diagram (c) Node-Link diagram

Figure 2. Spatial relationship structures

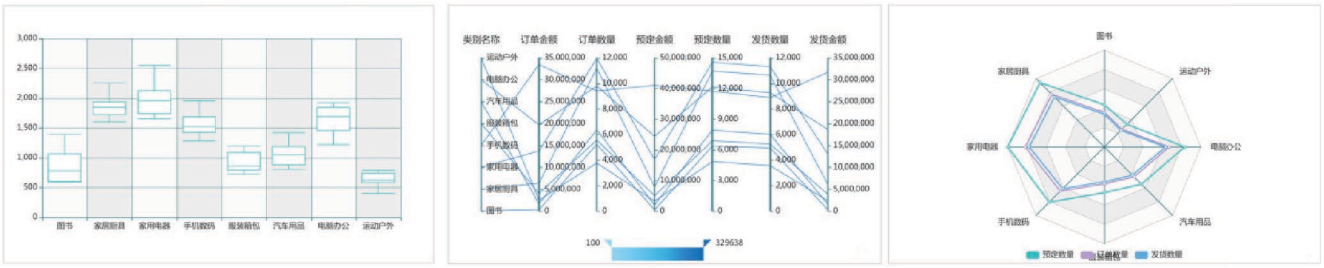
Tree diagrams were first proposed by Johann Vogel in 1661. A tree diagram is a graphical tool used to represent hierarchical structures, widely used in mathematics, computer science, organizational structure diagrams, and other fields. Tree diagrams show hierarchical relationships between pieces of information, where connected information has parent-child relationships. One child information can only correspond to one parent information, but one parent information can contain multiple child information.

Rack diagrams were first proposed by Ben Shneiderman in 1991. By editing information areas into rectangles and using different colors and size codes, rack diagrams can significantly distinguish hierarchical and associative attributes of information, with good readability and size estimation capabilities. Rack diagrams are a variant of traditional tree diagrams, where each information area is edited into a rectangle. The size of any node is quickly displayed.

The concept of node-link diagrams can be traced back to the study of graph theory. Graph theory was introduced by Swiss mathematician Leonhard Euler in 1736 when he was studying the Seven Bridges of Königsberg problem. The concepts of Eulerian graph and Eulerian circuit laid the foundation for graph theory, from which the representation method of node-link diagrams was derived. Since then, graph theory has been widely used in computer science, network science, social network analysis, and other fields. Node-link diagrams, as an intuitive graphical representation method, gradually began to be used to describe various complex relationships and network structures.

2.3. Statistical distribution structures

Visualization design aims to reveal the distribution of data, helping data analysts better understand the statistical characteristics of data. Data analysts often want to match their data with statistical models, especially in hypothesis testing or predicting the value of the next point. However, wrong model choices may lead to incorrect predictions. Therefore, one important use of visualization is exploratory data analysis, understanding how data is distributed to inform data transformation and modeling decisions. Common statistical distribution structures include box plots, parallel coordinates plots, and radar charts as shown in **Figure 3**.



(a) Box plot (b) Parallel coordinates plot (c) Radar chart

Figure 3. Statistical distribution structures

Box plots were first proposed by American statistician John Tukey in the 1970s. Box plots are statistical charts used to describe the distribution of data sets, displaying five main summaries of the data set: minimum value, first quartile, median, third quartile, and maximum value. They can also display outliers, providing an intuitive representation of data distribution and variation. Box plots are often used for numerical statistics, drawn horizontally or vertically.

Parallel coordinates plots were first proposed by French mathematician Maurice d'Ocagne in 1885. In his work, he introduced this chart as a tool for visualizing multidimensional data. Parallel coordinates plots represent each data dimension as a parallel axis and connect data points on each axis, realizing the visualization of multidimensional data. This chart has been widely used in later data analysis and visualization fields.

Radar charts were first proposed by American engineer and industrial designer Charles Joseph Minard in the 19th century. Radar charts display multivariate data in a two-dimensional chart form with three or more quantitative variables starting from the same point. They can represent multidimensional data, but the relative positions of points and the angles between coordinate axes carry no information.

3. Cognitive patterns in information visualization

3.1. Cognitive models of information visualization interaction mechanisms

Card *et al.*, as cited by Xu, proposed the information visualization reference model, which details the basic processes and interaction mechanisms of information visualization. This model explains how raw data is transformed into effective visual displays to enhance users' understanding and analytical abilities [4]. From this cognitive model, we can clearly understand the task goals that information visualization aims to solve and the steps to achieve these goals: starting from raw data, through mapping, exchange, and interaction control, and finally achieving effective visualization. In this process, there are two intermediate results between raw data and the final view: data tables and visualization structures. Through data transformation, visualization mapping, and view transformation, raw data is ultimately converted into visualization views. Users can interact with information visualization during these three transformations, adjusting data tables, visualization structures, and views, as shown in **Figure 4**.

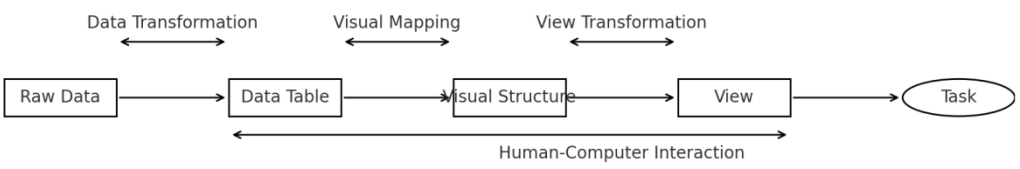


Figure 4. Cognitive models of information visualization

This model involves three stages: structuring raw data, mapping it to visual structures, and presenting it as visual charts. Proposed in 1999, it emphasizes user interaction with data to enhance understanding and analysis. The data transformation stage cleans, organizes, and filters raw data into structured tables. In the visualization mapping stage, structured data is converted into visual elements like points and lines. The view transformation stage adjusts and optimizes visual charts for better data presentation. User interaction is crucial, allowing adjustments to data tables, visualization structures, and views to explore different perspectives. This model by Card *et al.* offers a systematic framework for applying information visualization technology, improving data analysis efficiency and effectiveness.

3.2. Visual perception steps model of information visualization

Rodrigues *et al.*, as cited by Shi, Cheng, and Hof, proposed a model for the visualization expression process, detailing the steps data visualization undergoes in the visual cognitive process. The model includes four main parts: pre-attentive stimuli, analytical perception, abstract patterns, and decision support [5].

Firstly, the pre-attentive stimuli stage involves the initial neural response to light, quickly scanning visual information to identify key features and reduce cognitive load. Secondly, the analytical perception stage focuses attention on a single element for detailed analysis, using pattern matching to identify and classify visual elements. For example, in data visualization, this stage helps identify data points and trends. Thirdly, the abstract patterns stage transforms specific visual information into abstract concepts, simplifying complex data for easy understanding and memory storage. Finally, the decision support stage combines abstract patterns with long-term memory knowledge to aid decision-making, forming a dynamic cognitive process [6].

The bidirectional arrows indicate simultaneous bottom-up and top-down interactions during tasks. Low-level perceptual inputs influence high-level cognitive processing, and vice versa. For example, seeing a new data visualization chart involves initial perception shaped by existing knowledge, while new information updates our cognitive framework [7]. This process may generate new information needs, prompting redefinition of visualization through new interaction parameters. Users may seek more details or different perspectives, driving further optimization of visualization. This model describes the cognitive process from perception to complex cognition, offering a framework for designing effective and user-friendly data visualization tools.

4. Conclusion

Information visualization, a crucial branch of computer science, has evolved into a powerful tool for processing and understanding complex data. It integrates computer graphics, user interface technology, and human-computer interaction, enhancing cognitive abilities and advancing information and cognitive science. From Stuart Card and colleagues' "information visualizer" to Shneiderman and Bederson's visualization taxonomy, research has continually progressed. The core of information visualization is transforming abstract data into visual forms for intuitive understanding. Widely applied in scientific research, business, and public policy, its importance grows with increasing data complexity. Future research must explore new technologies and methods to meet these expanding needs.

Disclosure statement

The authors declare no conflict of interest.

References

[1] Zhang L, 2021, Analysis of User Interface Animation Design in Digital Media Art. Art and Design, 08: 45–48. https://doi.org/10.16824/j.cnki.issn10082832.2021.08.021

[2] Wang N, Qiu X, 2021, Simulation of UI Interface Data Visualization Transmission Based on Perceptual Feedback. Computer Simulation, 38(10): 34–36.

[3] Jason F, 2012, The Mobile Interface Theory: Embodied Space and Locative Media. Routledge, London, 2012: 56–60.

[4] Xu H, 2017, Study on the Styling Style Characteristics in Dynamic Graphic Design. Packaging World, 05: 120–121. https://doi.org/10.13337/j.cnki.packaging.world.2017.05.040

[5] Shi S, Cheng X, Hof PMJVD, 2020, Excitation Allocation for Generic Identifiability of a Single Module in Dynamic Networks: A Graphic Approach. IFAC-PapersOnLine, 53(2): 40–45.

[6] Liu Y, Zhang Y, 2022, Research on Dynamic Graphics Features in Digital Media Interface. Digital Communication World, 5: 121–123.

[7] Spiliotopoulos D, Tzoannos E, Stavropoulou P, et al., 2012, Designing User Interfaces for Social Media Driven Digital Preservation and Information Retrieval. Springer-Verlag Berlin Heidelberg, 7382: 581–584.

Publisher's note

Bio-Byword Scientific Publishing remains neutral with regard to jurisdictional claims in published maps and institutional affiliations.

Journal of Electronic Research and Application, 2024, Volume 8, Issue 4
http://ojs.bbwpublisher.com/index.php/JERA
ISSN Online: 2208-3510
ISSN Print: 2208-3502

A Cell Screening Algorithm Integrating Genetic and Numerical Differentiation

Zhen Wu*, Feijing Fu, Yirga Eyasu Tenawerk, Weize Quan, Wanwen Wu

College of Information Engineering, Nanchang Hangkong University, Fenghenan Road, No. 696, Nanchang 330063, Jiangxi Province, China

Corresponding author: Zhen Wu, 1067977498@qq.com

Copyright: © 2024 Author(s). This is an open-access article distributed under the terms of the Creative Commons Attribution License (CC BY 4.0), permitting distribution and reproduction in any medium, provided the original work is cited.

Abstract: The consistency of the cell has a significant impact on battery capacity, endurance, overall performance, safety, and service life extension. However, it is challenging to identify cells with high consistency and no loss of battery energy. This paper presents a cell screening algorithm that integrates genetic and numerical differentiation techniques. Initially, a mathematical model for battery consistency is established, and a multi-step charging strategy is proposed to satisfy the demands of fast charging technology. Subsequently, the genetic algorithm simulates biological evolution to efficiently search for superior cell combinations within a short time while evaluating capacity, voltage consistency, and charge/discharge efficiency. Finally, through experimental validation and comparative analysis with similar algorithms, our proposed method demonstrates notable advantages in terms of both search efficiency and performance.

Keywords: Genetic differentiation method; Battery consistency; Voltage fluctuation; Fast charging technology; Battery cell screening

Online publication: August 13, 2024

1. Introduction

In the context of increasing attention to climate change and environmental degradation, Battery Electric Vehicles or Pure Electric Vehicles (BEV or EV) have become an alternative to traditional Internal Combustion Engine (ICE) vehicles, and lithium batteries open a new era [1]. They are a promising energy storage device for electric vehicles and renewable energy systems. Compared with traditional lead acid, nickel-iron, and nickel metal hydride batteries, advanced Lithium-Ion Batteries (LIBs) are considered the most promising electrochemical energy storage devices [2,3]. However, current chargers typically require over eight hours to add 200 miles of range to electric vehicles, making them unsuitable for highway journeys and extended trips. Therefore, there is an urgent need to improve the charging speed of on-board battery chargers, so that they can rapidly improve the charging capacity of batteries [4].

In practical applications, to meet the requirements of power and energy, the battery is usually connected in series to form a high-voltage battery pack, and the inconsistency between the cells is the key factor affecting the overall performance of the battery pack [5]. The cell is the cornerstone of the whole battery system, but

due to some uncontrollable reasons, the actual voltage and State of Charge (SOC) of the battery in the same battery pack may vary, and this inconsistency of the battery will damage the durability and safety of the battery pack [6]. Related studies show that the temperature of the power battery pack and its consistent state are important indicators of thermal runaway risk. When the battery consistency is poor, there is likely to be a thermal failure or high cell temperature in the battery pack, which can easily lead to thermal runaway [7,8]. The battery inconsistency usually comes from the battery manufacturing process, and this inconsistency may be further expanded during the operation of the battery system [9]. Although this difference is small from a macro perspective, it causes significant changes during battery operation. Therefore, in the process of battery manufacturing, the selection of cells is a crucial link. The selection of cells will affect the performance and safety of electronic products, and the selection of high-consistency and small voltage fluctuation cells is crucial to ensure the best performance, service life, and safety of these electronic products.

In the existing literature, there has been a variety of cell screening algorithms that have been widely discussed. Among them, the machine learning algorithm gradually emerged, providing a new perspective for cell selection, commonly used machine learning-based battery cell selection methods generally include the K-means algorithm, fuzzy C-means algorithm, and Kohonen network method [10–16]. Recently, the Particle Swarm Optimization (PSO) algorithm has also shown its potential in cell selection [17]. In addition, Genetic Algorithm (GA) is also applied in the preferred process of lithium-ion batteries for electric vehicles. By integrating multiple parameters such as capacity, internal resistance, and cost, they explore the optimal battery combination with the GA algorithm. Compared with the conventional method, the dual optimization of cost reduction and performance improvement is achieved [18]. Moreover, the numerical differential method can also be used for the screening of battery cells. Its principle is to use some discrete points of the original function to construct a specific function to approximate the original function, and then take the derivative of the constructor as the approximate derivative of the original function [19]. This paper presents a novel integration of the Differential Genetic (DG) algorithm and numerical algorithm, based on the widely used cell screening method. Simultaneously constructing an optimized cell screening model for the DG algorithm, this approach efficiently and accurately screens high-consistency and low-voltage fluctuation cell combinations to address the challenges related to charging efficiency and stability in new energy automotive batteries.

2. Problem analysis

In order to ensure the high efficiency and accuracy of the cell screening process, appropriate screening strategies must be adopted. However, the task of directly screening the cell is particularly complicated. From the classical mathematical perspective, the calculation screens 24 suitable cells from 76 cells, and its calculation amount is undoubtedly huge. Specifically, the combined formula in combinatorial mathematics is used to perform the calculation. The combination number $C(n,k)$ is defined as the total number of methods for screening k elements from n elements, and the formula is:

$$C(n,k)=\frac{n!}{k!(n-k)} \tag{1}$$

Where $n!$ is the factorial n, i.e. $n\times(n-1)\times...\times1$, in this problem, we propose, n = 76, k = 24. C(76,24) can therefore be expressed as follows:

$$C(76,24)=\frac{76!}{24!(76-24)!}=\frac{76!}{24!52!}=\frac{76\times75\times74\times...\times53}{24\times23\times22\times...\times1}=75287520 \tag{2}$$

After the above calculation, up to 75,287,520 different combinations were screened from 76 samples, a number that intuitively reveals the great challenges and complexity of the cell screening task. Therefore, the traditional mathematical method is inadequate when dealing with such a large cell scale, which is time-consuming and inefficient. The accuracy and efficiency are difficult to reach the standard in the face of the urgent social demand for high-performance batteries.

3. Model construction

3.1. Optimized cell screening model

To evaluate the impact of cell inconsistency on the overall performance of the battery pack, it is necessary to construct an effective battery pack consistency model, which can describe both the statistical characteristics of the battery consistency parameters and the correlation between the parameters [20]. Therefore, based on the above battery consistency problem, this experiment builds an optimized cell screening model. The model aims to serve for physical experiments. Through the DG algorithm proposed in this paper, the best-performing 24 cells were selected from 76 ternary lithium-ion cells to form a cell combination, improving the stability of the battery.

3.2. Multi-step charging strategy

This experiment designs a multi-step constant current charging strategy suitable for the optimized cell screening model to test the ternary lithium-ion cells. In most experiments, the constant current charging method is the preferred charging strategy because it provides accurate and practical information on battery performance, in line with the experimental objectives and requirements [21]. To satisfy the demand for fast charging, this experiment improved the constant current charging process by adopting a multi-step constant current charging strategy.

The specific steps are as follows: Before cell charging, all the cell samples are set to an initial voltage of 3.6 V for charging. Then, enter three stages of the rapid charging process, a constant current of 57 A for 200 s, then a current of 44 A for 95 s for charging and monitoring the temperature to prevent overheating. At 295 s, the qualified cells are screened by checking the voltage difference. After that, the current is further reduced to 33 A until the cell voltage reaches the cut-off voltage of 4.35 V, which avoids voltage overshooting. Finally, after the cell reaches 4.35 V, the system automatically switches to the slow charging mode of low current until the cell is filled, effectively preventing the damage caused by overcharging the cell.

3.3. Voltage difference

The optimized cell screening model requires ensuring that the battery pack shows the highest consistency possible during the rapid charging process while ensuring that the overall voltage fluctuation is as small as possible. In the experimental process of fast charging, the voltage detection compared to capacity is real-time, fast, and easy to implement and is well suited for assessment research [22]. Therefore, this experiment needs to calculate the voltage of the cell at each time point and screen the cell with high consistency by comparing the voltage difference of each cell at a certain time point. After calculating the voltage difference of each cell at the same specific time, the consistency level of the whole battery pack can be quantified.

The calculation method of voltage differential, V_d pressure of the cell is first to calculate a voltage measurement sequence, $V = [V_1, V_2, ..., V_n]$, according to the test data, n is the total test time of the cell. The model is mainly based on the optimization of the cell screening model using a multi-step constant current charging strategy of three obvious voltage drops at the end of the stage (200 s, 295 s, and cell reaches the off

voltage) violent voltage fluctuations to calculate the voltage difference, in the three moments cell will appear a voltage maximum recorded as V_t^{max}. At the same time, a minimum voltage value is recorded as V_t^{min}, so the voltage difference of the cell V_d is calculated as follows:

$$V_d = V_t^{\max} - V_t^{\min} \tag{3}$$

The V_t^{max} represents the maximum voltage value of the cell at the time t, and the V_t^{min} represents the minimum voltage value of the cell at the time t, calculate the voltage difference V_d of the moment between the maximum and minimum voltage values, at the end of the seconds fast charging period, the optimized cell selection model will control the voltage difference of the cell within a preset threshold range, and screen the battery combination meeting the conditions.

3.4. Voltage fluctuation

The calculation of voltage fluctuation is the core part of the optimized cell screening model. Choosing a cell with small voltage fluctuation can reduce the negative voltage effect and improve the performance of operating efficiency [23]. Specifically, the numerical differential method is used to calculate the voltage fluctuations. The first task is to calculate the voltage change rate per second of each cell, the calculation formula is:

$$V_f = \left| V_{i+1} - V_i \right| \tag{4}$$

The V_f represents the voltage rate of change per second of the cell, the V_i represents the voltage value at the time i, and the V_{i+1} represents the voltage value at the time $i+1$. All voltage change rates are then added up to obtain the total value of the voltage change rates $\sum_{i=1}^{n-1} V_d$ in this voltage curve can be expressed as:

$$\sum_{i=1}^{n-1} V_d = \sum_{i=1}^{n-1} \left| V_{i+1} - V_i \right| \tag{5}$$

Next, the total charging time T needs to be calculated. In the actual experiment, because the cell test time has been obtained, the start and end time of each cell charging has been determined, so that T can be accurately expressed as:

$$T = t_n - t_1 \tag{6}$$

Where, t_n is the n seconds which is the end of the fast-charging stage, and t_1 seconds is the time when the charging begins. Divide the cumulative voltage difference value $\sum_{i=1}^{n-1} V_d$ by the total time T to get the average voltage and fluctuation value. Therefore, the mathematical formula for calculating the voltage fluctuation value ΔU of the whole curve can be summarized as follows:

$$\Delta U = \frac{\sum_{i=1}^{n-1} V_d}{T} \tag{7}$$

The calculation formula of the ΔU can be further expressed as follows:

$$\Delta U = \frac{\sum_{i=1}^{n-1} \left| V_{i+1} - V_i \right|}{t_n - t_1} \tag{8}$$

This formula briefly describes how to calculate a series of voltage measurements to obtain the average voltage fluctuation amplitude per second at the same interval of data sampling, and finally get the overall voltage fluctuation value of each cell.

4. Algorithm description

4.1. DG algorithm

To meet the challenges of efficient cell screening in the rapid charging technology of new energy vehicle batteries, a DG cell optimization algorithm is proposed in this study, which combines the global search advantage of the genetic algorithm with the accurate evaluation ability of the numerical difference method [24–27]. Specifically, the DG algorithm aims to screen out cell combinations with high consistency and low voltage fluctuations, and the DG algorithm can exploit the advantages of genetic algorithms, including its parallel processing power and a broad global search range. It can quickly traverse the space and explore potential high-quality solutions. At the same time, the gradient information of the function is accurately calculated by the numerical differentiation method to provide detailed performance feedback for each step of the search. This not only significantly accelerates the convergence speed of the optimization process, but also improves the quality of the obtained cell combination scheme, and greatly reduces the time required to screen a required cell combination to improve the overall consistency and stability of the battery.

4.2. Algorithmic pseudo-code

According to the above description of the DG algorithm, to understand the core execution logic of the DG algorithm more deeply, this paper summarizes the DG algorithm pseudo-code as shown below.

DG algorithm

Import:

Cell sample set: cells_total, the selected number of cells: cells_sel, cell voltage difference threshold: v_threshold, critical test moment of voltage difference: timing, Last second of the fast-charging phase: endtime.

Output:

The file name list: unique_best_individual.

1. foreach cells_total, numbered for each cell and recorded at cells_number.
2. foreach cells_number
   while time < endtime
      time = timing
         If the cell has data at the time
            The voltage difference voltage_difference of the cell is calculated using the formula $V_d = V_t^{\max} - V_t^{\min}$.
            if voltage_difference > v_threshold in timing
               Excluding the cell, and break
            else add the cell number to the preferred cell list cells_better, calculates the voltage fluctuation value voltage_diffs of the cell using the numerical differential formula $\Delta U = \frac{\sum_{i=1}^{n-1} \left| V_{i+1} - V_i \right|}{t_n - t_1}$ and returns the value, and break.
   Else time = time + 1
3. foreach cells_better performed the genetic algorithm

   Initialize a population of 24-cell individuals and perform iterative genetic operations based on voltage fluctuation values (voltage_diffs) over multiple generations. These operations, including selection, crossover, and variation, refine the population's fitness values at each generation's end. After completing the iterations, record the individual with the highest fitness level as the optimal combination of cells in the 'unique_best_individual' list.

4. Return unique_best_individual.

5. Experiment

5.1. Data analysis

This experiment is based on the optimized cell screening model design of a multi-step constant current charging strategy, for the 76 ternary lithium-ion battery samples through the physical experiment equipment charge test and obtain the data of the cell. To better screen the cell, firstly, need to analyze the cell voltage data. **Figure 1** shows the 76-cell charging voltage curve.

The voltage curve data in **Figure 1** only goes up to 700 seconds as this experiment focuses on the cell's performance during fast charging. Each cell is represented by a different color, revealing its charging characteristics. The red, green, and yellow dotted lines in **Figure 1** mark the three stages of the charging strategy at 200 s, 295 s, and 400 s respectively. From **Figure 1**, it can be observed that the cell's voltage rises rapidly initially due to the higher current used by the test device to speed up charging and restore battery capacity quickly. When the voltage reaches around 4.35 V (the cut-off voltage set by the multi-step charging strategy), usually after about 400 s, there is a brief drop in voltage forming a platform which indicates the end of the rapid charging phase. Subsequently, the system automatically switches to a slow charging phase with significantly reduced and stable current while maintaining relatively stable voltage levels to prevent overcharging and overheating while ensuring full charge. The discharge voltage curves of 76 ternary lithium-ion cells are shown in **Figure 2**.

According to **Figure 2**, the discharge voltage curve turns from falling to rising in the period of 6000 s to 8000 s, marking the end of the discharge process of the cell. Fast charging technology can complete the charging of the cell in a short time. To prolong the battery life, it usually reduces the discharge rate of the cell, so the discharge time is longer than the charging time. Next, at the critical test moment, 295 s, the cell data, to more intuitively analyze the voltage difference change of the cell at this time, as shown in **Figure 3**.

The X axis in **Figure 3** represents the time point, the Y axis represents the voltage difference, and the Z axis represents the file index of the cell from 1 to 76, where each data point represents the voltage difference of the cell at the end of the second's fast charge phase. If there is no data or large voltage fluctuation at 295 s, the end time of the seconds' fast charging phase is delayed. In this case, the voltage difference at 296 s is screened in this experiment to represent the end of the seconds fast charging phase of the cell. The voltage difference of the cell in **Figure 3** is mainly distributed in the range of 0023 V to 003 V, and there is a difference of 0007 V in the range. Therefore, it can be determined that the threshold value V_d of the voltage difference is 0026 V, that is, the voltage difference is less than 0026 V at the end of the period is good. Finally, 40 cells meeting the voltage difference threshold requirement of 0026 V are screened from the 76 cells. The voltage fluctuation value curves of the 40 candidate cells meeting the voltage difference threshold requirements are shown in **Figure 4**.

In **Figure 4**, each data point on the voltage fluctuation value curve marks the corresponding cell number. **Figure 4** directly reflects the overall condition of the 40-voltage fluctuation, but the voltage fluctuation of some cells has large or small overall voltage fluctuation. Therefore, the genetic algorithm to further screens the 40 cells, with the average voltage fluctuation value of 76 cells as the fitness evaluation criterion, screens the cells with relatively small voltage fluctuation.

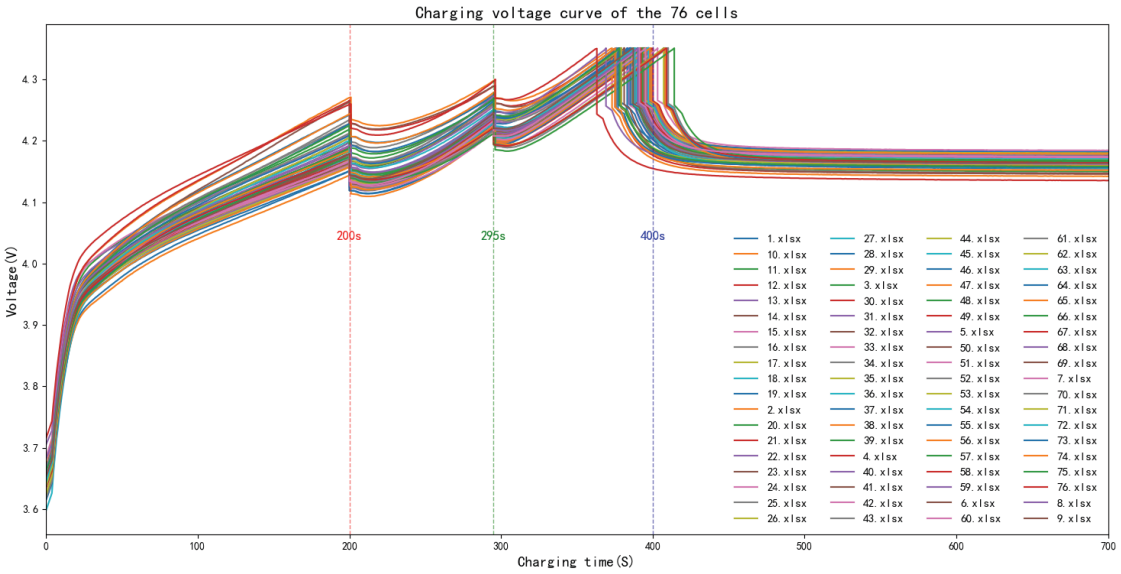


Figure 1. Charging voltage curve diagram of the initial 76 cells

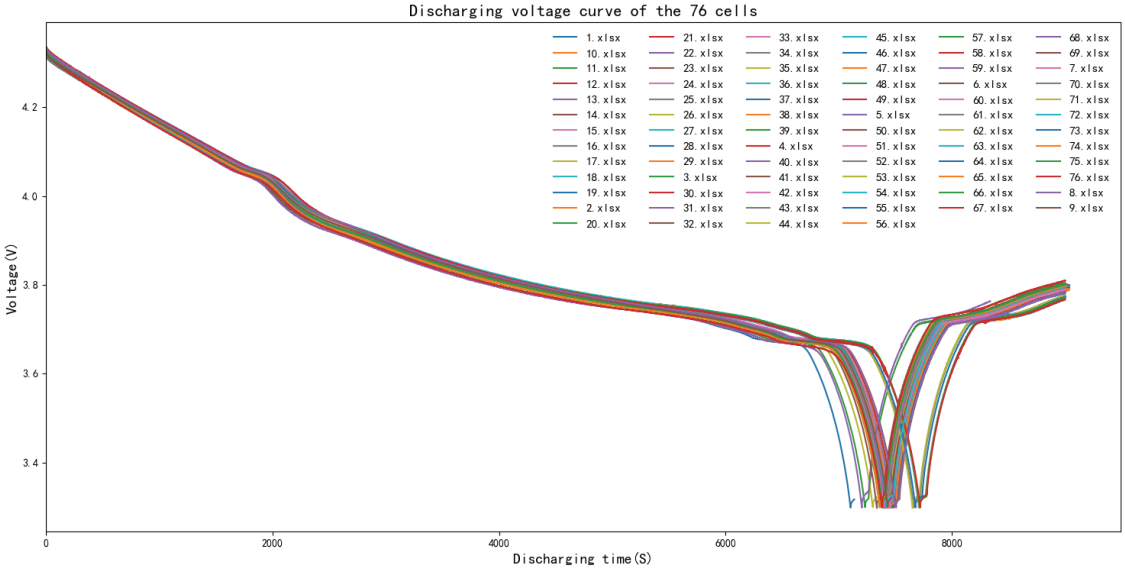


Figure 2. The discharge voltage curve diagram of the initial 76 cells

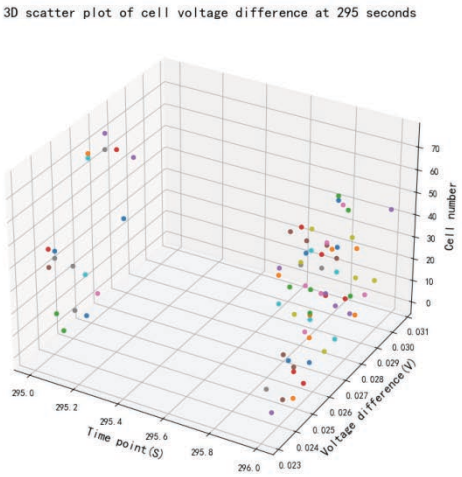


Figure 3. 3D scatter plot of the voltage difference of 76 cells at 295 s

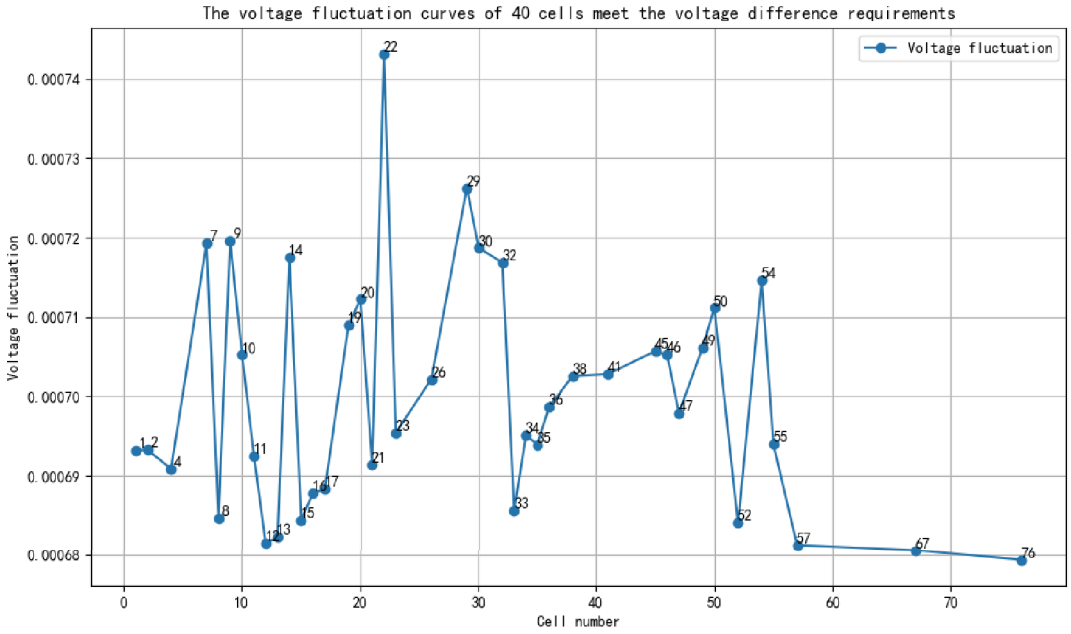


Figure 4. Graph of the voltage fluctuation value of the cell meeting the voltage difference requirements

5.2. Experimental results

The genetic algorithm is used to further screen the cells that meet the voltage difference standard requirements, and the charging voltage curve of the 24 preferred cells is shown in **Figure 5**. Compared with **Figure 1**, it can be observed that the different cells are smaller in the abscissa in **Figure 5** and the voltage curve is more concentrated. Similar differences are presented when comparing the discharge voltage curves of the initial 76 cells in **Figure 6** and **Figure 2**. This indicates that the preferred cells screened by using the DG algorithm can show a more and smaller voltage difference.

The 3D scatter plot of the voltage difference of the preferred cell at 295 s is shown in **Figure 6**. By comparing **Figure 6** and **Figure 3**, there is a finding that the overall voltage difference of the cell combination in **Figure 6** is mainly distributed between 0024 V and 002575 V, with a difference of only 000175 V, which is much less than the 0007 V voltage difference shown in **Figure 3**. This further confirms the superiority of the DG algorithm in screening the cells. The 3D scatter plot of the voltage difference of the preferred cell at 295 s is shown in **Figure 7**.

At the same time, the overall voltage difference of the cell combination in **Figure 7** is mainly distributed between 0024 V and 002575 V, with a difference of only 000175 V, which is much less than the 0007 V voltage difference as shown in **Figure 3**. Then the comparison diagram of the voltage fluctuation values of 40 cells and 24 preferred cells that meet the voltage difference threshold is shown in **Figure 8**.

The yellow line in **Figure 8** represents the 40 cells meeting the voltage difference threshold, and the blue line represents the final screened 24 preferred cells. In **Figure 8**, it can be found that the voltage fluctuation of the preferred cell is in a smaller range, which can prove that the DG algorithm can effectively improve the overall stability of the battery pack.

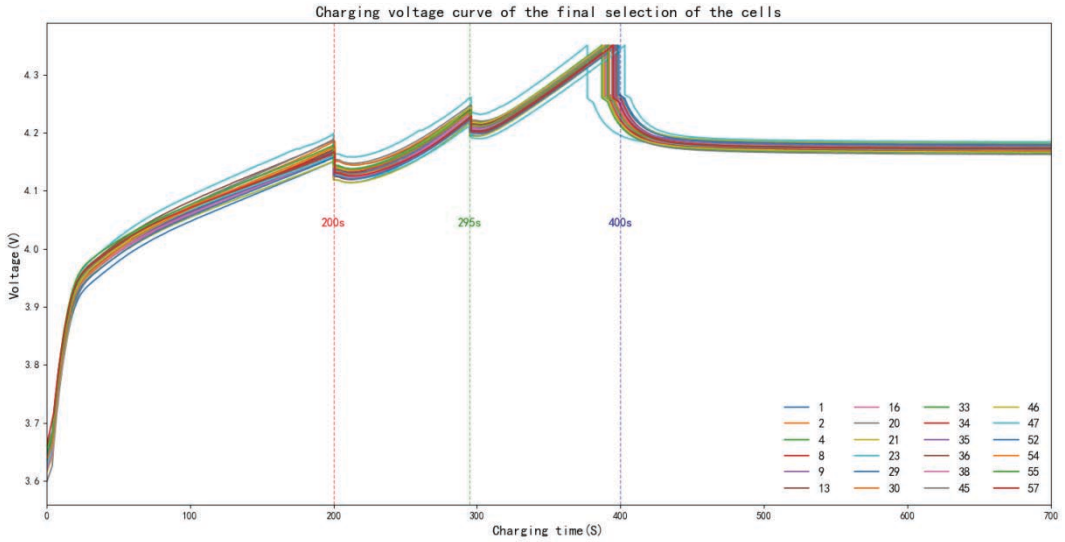


Figure 5. Graph of the final screened cell charging voltage curve

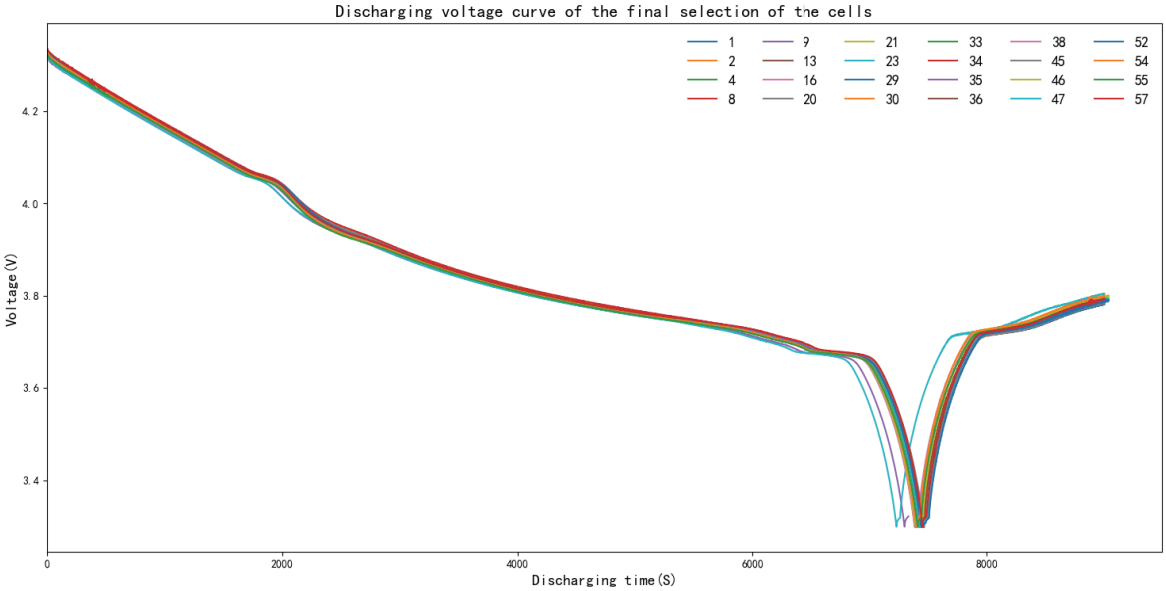


Figure 6. Discharge voltage curve diagram of the final screened cell

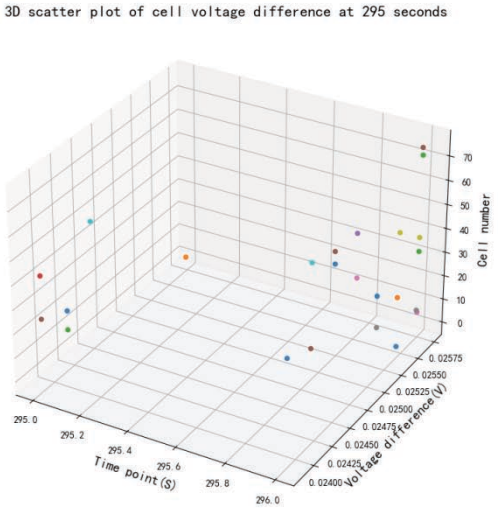


Figure 7. 3D scatter plot of the voltage difference of the final screened cell at 295 s

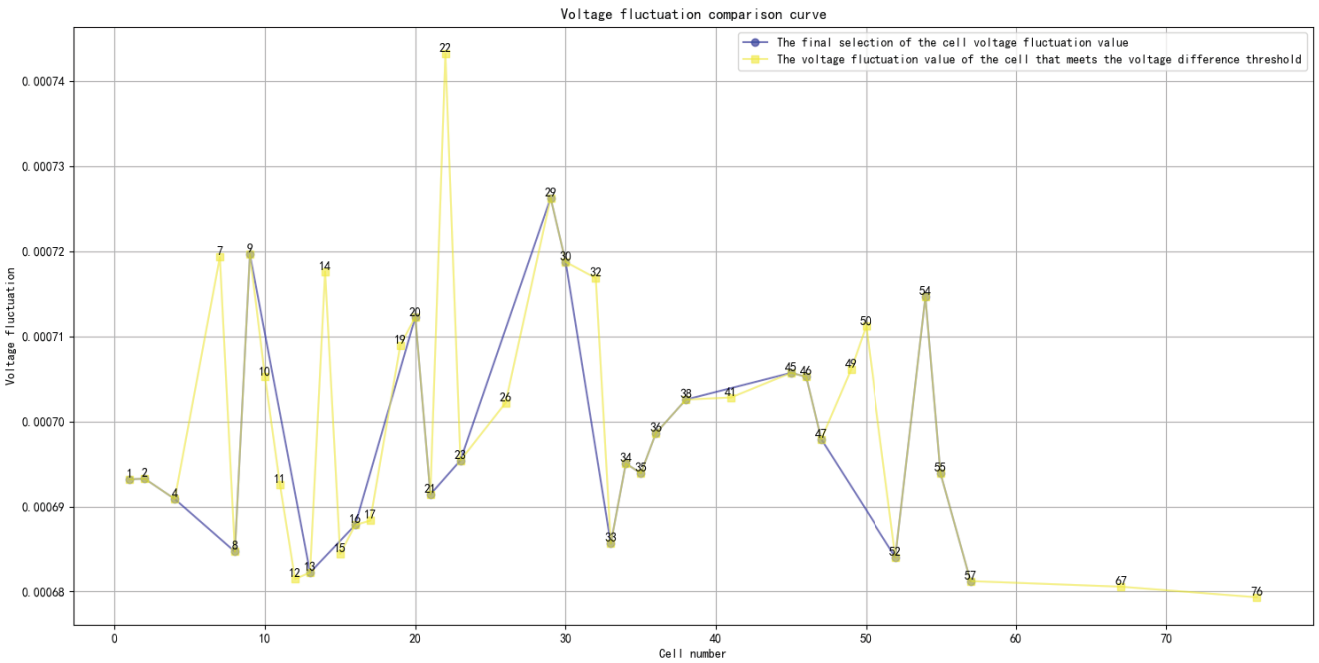


Figure 8. Comparison of the voltage fluctuation values of the two cells

6. Conclusion

In the background of the rapid development of new energy vehicles, how to screen out the cell combination with high consistency and small voltage fluctuation to improve the overall performance of new energy vehicle batteries is facing important challenges. To address this issue, the present study proposes a novel DG algorithm that combines the global search capability of genetic algorithms with the precise evaluation ability of numerical differentiation. Subsequently, an optimized cell screening model is developed to support the DG algorithm. By utilizing this approach, a set of 24 cells exhibiting high performance out of 76 ternary lithium-ion cell samples are screened based on their high consistency and low-voltage volatility, resulting in a combination with superior overall performance. In summary, the DG algorithm not only improves battery performance significantly but also simplifies decision-making, enhances screening efficiency and accuracy, effectively resolves battery consistency issues, and meets consumer demands for faster charging of new energy vehicles. Additionally, the DG algorithm is expected to promote the widespread adoption of new energy technology and sustainable traffic development.

Disclosure statement

The authors declare no conflict of interest.

Author contribution

Writing – abstract: Weize Quan
Writing – body: Zhen Wu
Investigation: Zhen Wu
Analysis – data plot: Wanwen Wu

Figures: Feijing Fu
Literature research: Yirga Eyasu Tenawerk

References

[1] Demir-Cakan R, Palacin MR, Croguennec L, 2019, Rechargeable Aqueous Electrolyte Batteries: From Univalent to Multivalent Cation Chemistry. Journal of Materials Chemistry A, 7(36): 20519–20539.

[2] Wu F, Maier J, Yu Y, 2020, Guidelines and Trends for Next-Generation Rechargeable Lithium and Lithium-Ion Batteries. Chemical Society Reviews, 49(5): 1569–1614.

[3] Dai H, Jiang B, Hu X, et al., 2021, Advanced Battery Management Strategies for a Sustainable Energy Future: Multilayer Design Concepts and Research Trends. Renewable and Sustainable Energy Reviews, 138: 110480.

[4] Ronanki D, Kelkar A, Williamson SS, 2019, Extreme Fast Charging Technology—Prospects to Enhance Sustainable Electric Transportation. Energies, 12(19): 3721.

[5] Zhang C, Jiang Y, Jiang J, et al., 2017, Study on Battery Pack Consistency Evolutions and Equilibrium Diagnosis for Series-Connected Lithium-Ion Batteries. Applied Energy, 207(C): 510–519.

[6] Lyu C, Song Y, Wang L, et al., 2019, A New Method for Lithium-Ion Battery Uniformity Sorting Based on Internal Criteria. Journal of Energy Storage, 25: 100885.

[7] Hong JC, Wang ZP, Liu P, 2017, Big Data-Based Thermal Runaway Prognosis of Battery Systems for Electric Vehicles. Energies, 7: 919.

[8] Wang QS, Mao BB, Stoliarov SI, et al., 2019, A Review of Lithium-Ion Battery Failure Mechanisms and Fire Prevention Strategies. Progress in Energy and Combustion Science, 73: 95–131.

[9] Yang N, Zhang X, Shang BB, et al., 2016, Unbalanced Discharging and Aging due to Temperature Differences Among the Cells in a Lithium-Ion Battery Pack with Parallel Combination. Journal of Power Sources, 306: 733–741.

[10] Yoon T, Kim Y, Cho D, 2019, On Battery Cell Selection using a Decision Tree-Based Algorithm. Energies, 12(5): 863.

[11] Hashemi SE, Gholian-Jouybari F, Hajiaghaei-Keshteli M, 2023, A Fuzzy C-Means Algorithm For Optimizing Data Clustering. Expert Systems with Applications, 227: 120377.

[12] Ikotun AM, Ezugwu AE, Abualigah L, et al., 2023, K-Means Clustering Algorithms: A Comprehensive Review, Variants Analysis, and Advances in the Era of Big Data. Information Sciences, 622: 178210.

[13] Ahmed M, Seraj R, Islam SMS, 2020, The K-Means Algorithm: A Comprehensive Survey and Performance Evaluation. Electronics, 9(8): 1295.

[14] Sinaga KP, Yang MS, 2020, Unsupervised K-Means Clustering Algorithm. IEEE Access, 8: 80716–80727.

[15] Fahim A, 2021, K and Starting Means for K-Means Algorithm. Journal of Computational Science, 55: 101445.

[16] Barletta V, Caivano D, Nannavecchia A, et al., 2020, A Kohonen SOM Architecture for Intrusion Detection on In-Vehicle Communication Networks. Applied Sciences, 10: 5062.

[17] Ren X, Liu S, Yu X, et al., 2021, A Method for State-of-Charge Estimation of Lithium-Ion Batteries based on PSO-LSTM. Energy, 234: 121236.

[18] Hossain LMS, Miah MS, Ansari S, et al., 2022, Smart Battery Management Technology in Electric Vehicle Applications: Analytical and Technical Assessment Toward Emerging Future Directions. Batteries, 8(11): 219.

[19] Khodapanah M, Ghanbari T, Moshksar E, et al., 2023, Partial Shading Detection and Hotspot Prediction in Photovoltaic Systems based on Numerical Differentiation and Integration of the P−V Curves. IET Renewable Power Generation, 17(2): 279–295.

[20] Jiang Y, Jiang J, Zhang C, et al., 2019, A Copula-Based Battery Pack Consistency Modeling Method and its Application on the Energy Utilization Efficiency Estimation. Energy, 189: 116219.

[21] Yu Y, Nduka OS, Nazir FU, et al., 2022, A Three-Stage Stochastic Framework for Smart Electric Vehicle Charging. IEEE Access, 11: 655–666.

[22] Wang SL, Shi JY, Fernandez C, et al., 2019, An Improved Packing Equivalent Circuit Modeling Method with the Cell-to-Cell Consistency State Evaluation of the Internal Connected Lithium-Ion Batteries. Energy Science and Engineering, 7(2): 546–556.

[23] Huang S, Wu Q, Liao W, et al., 2021, Adaptive Droop-Based Hierarchical Optimal Voltage Control Scheme for VSC-HVDC Connected Offshore Wind Farm. IEEE Transactions on Industrial Informatics, 17(12): 8165–8176.

[24] Kim C, Batra R, Chen L, et al., 2021, Polymer Design using Genetic Algorithm and Machine Learning. Computational Materials Science, 186: 110067.

[25] Hamdia KM, Zhuang X, Rabczuk T, 2021, An Efficient Optimization Approach for Designing Machine Learning Models based on Genetic Algorithm. Neural Computing and Applications, 33(6): 1923–1933.

[26] Solodky SG, Stasyuk SA, 2022, Optimization of the Methods of Numerical Differentiation for Bivariate Functions. Ukrainian Mathematical Journal, 74(2): 289–313.

[27] Zhao Z, 2021, A Hermite Extension Method for Numerical Differentiation. Applied Numerical Mathematics, 159: 46–60.

Publisher's note

Bio-Byword Scientific Publishing remains neutral with regard to jurisdictional claims in published maps and institutional affiliations.

Journal of Electronic Research and Application, 2024, Volume 8, Issue 4
http://ojs.bbwpublisher.com/index.php/JERA
ISSN Online: 2208-3510
ISSN Print: 2208-3502

Integrated Experimental and Simulation Investigation of Breakdown Voltage Characteristics Across Electrode Configurations in SF_6 Circuit Breakers

Bo Guan[1], Qi Yu[1], Qingpeng Yuan[2], Shiwen Chen[2], Lailin Chen[1], Su Guo[1], Peilong Zhu[3]*

[1]Xiangshan Research Institute, Ningbo University of Technology, Ningbo 315799, China
[2]Lotus Cars, Ningbo 315336, China
[3]Naisen Electric, Ningbo 315712, China

***Corresponding author:** Peilong Zhu, xszpl@163.com

Copyright: © 2024 Author(s). This is an open-access article distributed under the terms of the Creative Commons Attribution License (CC BY 4.0), permitting distribution and reproduction in any medium, provided the original work is cited.

Abstract: This study investigates the breakdown voltage characteristics in sulfur hexafluoride (SF_6) circuit breakers, employing a novel approach that integrates both experimental investigations and finite element simulations. Utilizing a sphere-sphere electrode configuration, we meticulously measured the relationship between breakdown voltage and electrode gap distances ranging from 1 cm to 4.5 cm. Subsequent simulations, conducted using COMSOL Multiphysics, mirrored the experimental setup to validate the model's accuracy through a comparison of the breakdown voltage-electrode gap distance curves. The simulation results not only aligned closely with the experimental data but also allowed the extraction of detailed electric field strength, electric potential contours, and electric current flow curves at the breakdown voltage for gap distances extending from 1 to 4.5 cm. Extending the analysis, the study explored the electric field and potential distribution at a constant voltage of 72.5 kV for gap distances between 1 to 10 cm, identifying the maximum electric field strength. A comprehensive comparison of five different electrode configurations (sphere-sphere, sphere-rod, sphere-plane, rod-plane, rod-rod) at 72.5 kV and a gap distance of 1.84 cm underscored the significant influence of electrode geometry on the breakdown process. Moreover, the research contrasts the breakdown voltage in SF_6 with that in air, emphasizing SF_6's superior insulating properties. This investigation not only elucidates the intricate dynamics of electrical breakdown in SF_6 circuit breakers but also contributes valuable insights into the optimal electrode configurations and the potential for alternative insulating gases, steering future advancements in high-voltage circuit breaker technology.

Keywords: SF_6 circuit breaker; Breakdown voltage; Electrode configurations; COMSOL simulation; Electrical insulation

***O*nline publication:** August 13, 2024

1. Introduction

Sulfur hexafluoride (SF_6) is widely used in high-voltage circuit breakers due to its superior insulating and arc-quenching properties. This literature review focuses on the breakdown voltage characteristics of SF_6

circuit breakers, integrating experimental and simulation studies to explore the impact of different electrode configurations and gap distances.

Extensive experimental studies have been conducted to understand the dielectric breakdown of SF_6 under various conditions. Lin *et al.* demonstrated the dynamic dielectric strength of mixed gases, showing SF_6's robustness under different electrical stresses [1,2]. Experimental setups often vary electrode gap distances and configurations to measure breakdown voltages accurately, providing critical insights into SF_6's behavior under high voltage conditions. Jiang *et al.* analyzed dielectric breakdown properties for different electrode configurations and gap distances, revealing the crucial role of electrode shape and spacing in determining breakdown voltage [3]. Additionally, studies have examined the performance of SF_6 mixtures, such as sulfur hexafluoride and nitrogen (SF_6-N_2) and sulfur hexafluoride and carbon dioxide (SF_6-CO_2), under various voltage conditions, further illustrating SF_6's effectiveness as an insulating gas. The effectiveness of SF_6 in maintaining high breakdown voltages compared to air and other gases has also been highlighted in studies by Guo *et al.* and Xiao *et al.* [4,5].

Simulations using software like COMSOL Multiphysics have become indispensable for predicting the breakdown voltage characteristics of SF_6 circuit breakers. Ou *et al.* utilized numerical simulations to explore the development of streamer discharge in SF_6, providing detailed electric field distributions and potential contours that closely align with experimental results [2]. Such simulations validate experimental findings, ensuring data reliability and accuracy.

The configuration of electrodes significantly influences the breakdown voltage in SF_6 circuit breakers. Different geometries, such as sphere-sphere, sphere-rod, and rod-rod, exhibit distinct breakdown characteristics. Studies by Okubo *et al.* and Xiao *et al.* have shown that electrode shape and spacing critically impact the breakdown voltage, with sphere-sphere configurations often providing the highest breakdown voltages due to uniform electric field distribution [6,7]. Further investigations by Geng *et al.* and Liu *et al.* have explored the effects of various electrode configurations on the electric field distribution and breakdown voltage, contributing to the optimization of circuit breaker designs [8,9].

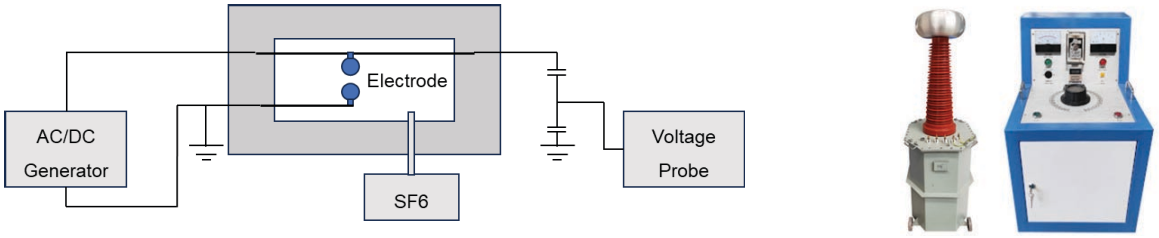
In addition to SF_6, researchers have investigated the breakdown voltage characteristics of alternative insulating gases. For example, the arc interruption performance of CO_2 and the use of SF_6-N_2 mixtures have been explored as potential substitutes for SF_6. Guo *et al.* highlighted CO_2's potential as a viable alternative, while other studies by Krämer *et al.* and Ito *et al.* emphasized the environmental benefits of mixed gases without compromising performance [4,10,11]. Environmental considerations have driven research into eco-friendly alternatives like green gas for grid (g^3), which offers equivalent dielectric strength to SF_6 while significantly reducing environmental impact. Studies by Zhou *et al.* have supported the viability of these alternatives in high-voltage applications [12]. SF_6 is a potent greenhouse gas, and its environmental impact has led to research into more sustainable alternatives. Studies by Kapetanovic and Jia *et al.* have examined the use of SF_6-N_2 and SF_6-CO_2 mixtures, which offer reduced environmental impact while maintaining high-insulating properties [13,14]. The push for greener alternatives is driving innovations in gas insulation technology, balancing performance with environmental sustainability.

This paper advances prior research to deepen understanding of SF_6 gas dielectric breakdown in high-voltage applications, particularly under non-homogeneous fields and varying gaps. Through experiments and simulations using COMSOL Multiphysics, this study explores SF_6's breakdown characteristics, focusing on electrode geometry and gap distances, and demonstrates its superior insulation properties compared to air. The research, utilizing sphere-sphere electrode configurations and varying gap distances, highlights the impact of electrode geometry on breakdown and the superior insulation of SF_6.

2. Methodology

2.1. Experiment

In the experimental setup illustrated in **Figure 1**, a sphere-sphere electrode configuration was placed within a sealed chamber filled with SF_6 gas, sourced from an SF_6 gas pump. This configuration was then connected to an alternating current/direct current (AC/DC) generator to facilitate the application of electrical potential across the electrodes. The differential in electric potential between the two electrodes was meticulously recorded using a voltage probe. The testing apparatus, depicted in **Figure 1(b)**, was acquired from Hezhong Electric Equipment, capable of generating voltages up to 150 kV at power frequency. For this experiment, the SF_6 gas was maintained at a pressure of 0.15 MPa. Both sphere electrodes, utilized in the setup, boasted a diameter of 4 cm, ensuring uniformity in the experimental conditions.

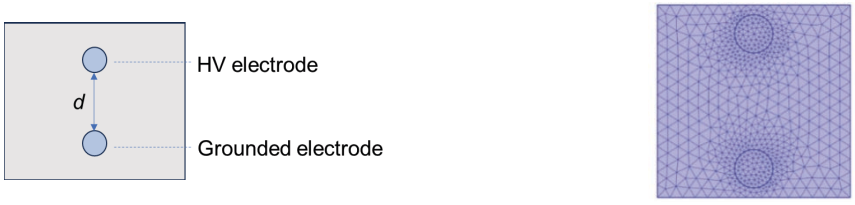


(a) (b)

Figure 1. (a) A schematic drawing of the schematic experiment setup (b) Test machine

2.2. Simulation

To complement the experimental investigation, a detailed finite element simulation was conducted using COMSOL Multiphysics software. The simulation began with the creation of a two-dimensional model representing the sphere-sphere electrode configuration within a chamber filled with SF_6 gas, as shown in **Figure 2**. The geometrical dimensions, including the 4 cm diameter of the sphere electrodes and the variable gap distances ranging from 1 cm to 4.5 cm, were precisely replicated as per the experimental design. The geometry domain was discretized using a triangular mesh to ensure detailed and accurate representation of the geometry for the finite element analysis.



(a) (b)

Figure 2. (a) The two-dimensional geometry model created in COMSOL Multiphysics (b) The finite element model

To thoroughly investigate the impact of electrode configurations on electric breakdown, the simulation extended to include various electrode setups: sphere-sphere, rod-rod, sphere-rod, rod-plane, and sphere-plane as shown in **Figure 3**.

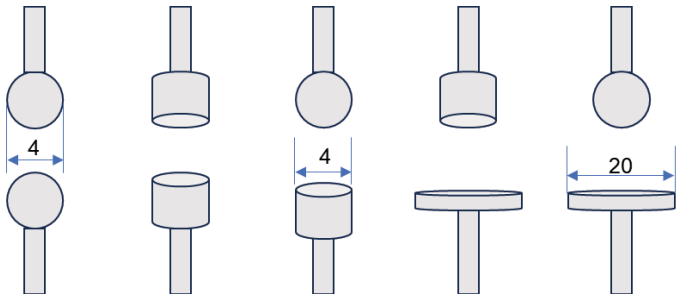


Figure 3. A schematic drawing of different electrode configurations: sphere-sphere, rod-rod, sphere-rod, rod-plane, and sphere-plane

The electrical properties of the materials were crucial for accurate simulation. Specifically, the relative permittivity (dielectric constant) of SF_6 was set to 1.002, and for air, it was set at 1, with the breakdown electric field strength in SF_6 considered to be 89 kV/cm, and in air, 30 kV/cm. The AC/DC module of COMSOL Multiphysics was utilized to simulate the electric field distribution, potential difference, and current flow within the setup for the range of electrode gap distances and configurations. Incremental application of potential difference across the electrodes was performed until electric breakdown was observed in the model. The simulation's scope included analyzing electric field strength, potential contours, and current flow paths at critical points leading to breakdown, especially at a constant voltage of 72.5 kV and varying electrode gap distances up to 10 cm.

3. Results

The primary objective of our research was to compare the breakdown voltage in an SF_6 circuit breaker as a function of the electrode gap distance, using both experimental methods and finite element simulation. The experimentally measured and simulated breakdown voltages across electrode gap distances ranging from 1 cm to 4.5 cm are presented in **Figure 4**.

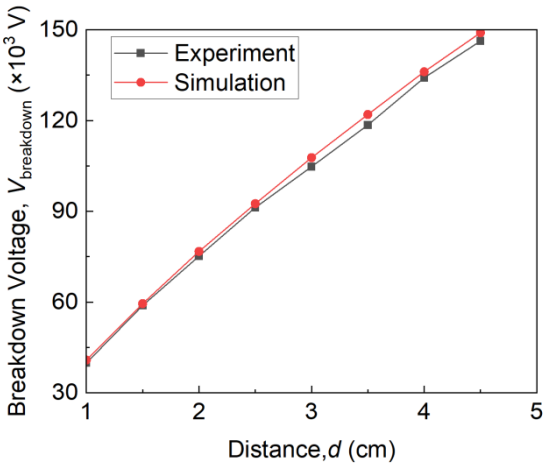


Figure 4. The breakdown voltage of sphere-sphere configuration in SF_6 circuit breaker from experiment and simulation

The experimental data showed a clear linear correlation between the breakdown voltage and the electrode gap distance, confirming classical Paschen's Law. The breakdown voltage increased from 39.8 kV at a 1 cm gap to 146 kV at 4.5 cm. Similarly, COMSOL Multiphysics simulations closely matched the experimental data,

with breakdown voltages ranging from 40.8 kV at 1 cm to 149 kV at 4.5 cm. The strong agreement between the experimental and simulated data validates the simulation model as a reliable predictive tool for electrical breakdown in SF_6 circuit breakers. **Figure 5** illustrates these simulations, showing changes in electric field strength, potential, and current flow at gap distances from 1 to 4.5 cm.

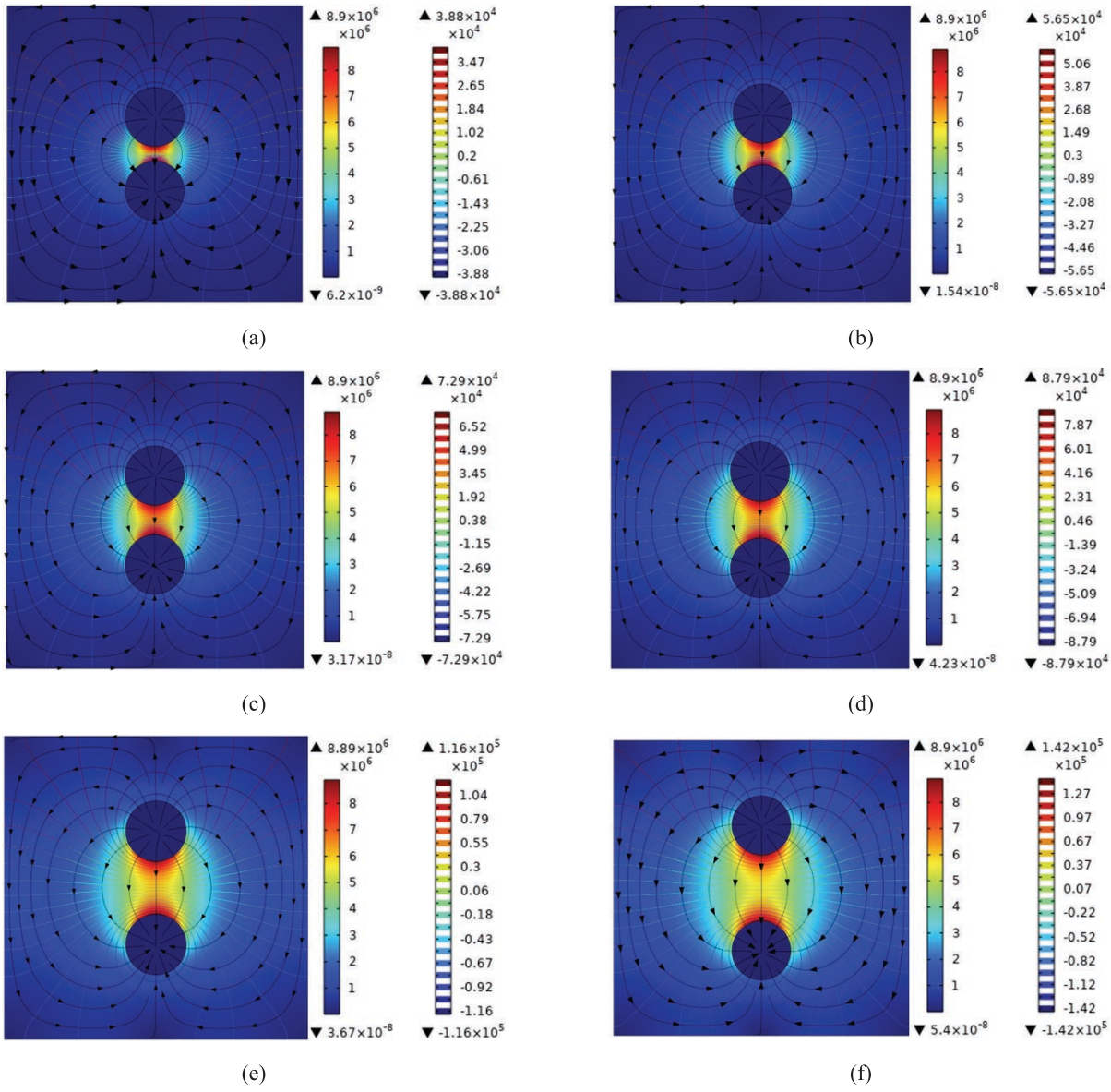


Figure 5. The electric field strength, potential distribution, and current flow within a sphere-sphere electrode setup in an SF_6 circuit breaker environment at varying gap distances of (a) 1 cm (b) 1.5 cm (c) 2 cm (d) 2.5 cm (e) 3.5 cm (f) 4.5 cm

At a 1 cm gap distance, the electric field strength is highly concentrated between the electrodes, with a rapid decrease outward, and the potential distribution is relatively uniform, directing most current flow directly between the electrodes. As the gap increases to 1.5 cm and 2 cm, the electric field spreads wider, the potential gradient becomes more pronounced, and current dispersion slightly increases. At 2.5 cm, the electric field spreads further and less intensely between the electrodes, with a steeper potential gradient and more dispersed current flow. At 3.5 cm and 4.5 cm, the electric field distribution broadens and intensifies less between electrodes, with a significant gradient in potential and widespread current flow, showing a transition from a concentrated to a more evenly distributed electric field as the gap widens.

4. Discussion

4.1. Electric field strength with gap distance

Figure 6 illustrates the electric field intensity, potential distribution, and current flow patterns at a fixed voltage of 72.5 kV for various electrode gap distances in an SF_6 circuit breaker model.

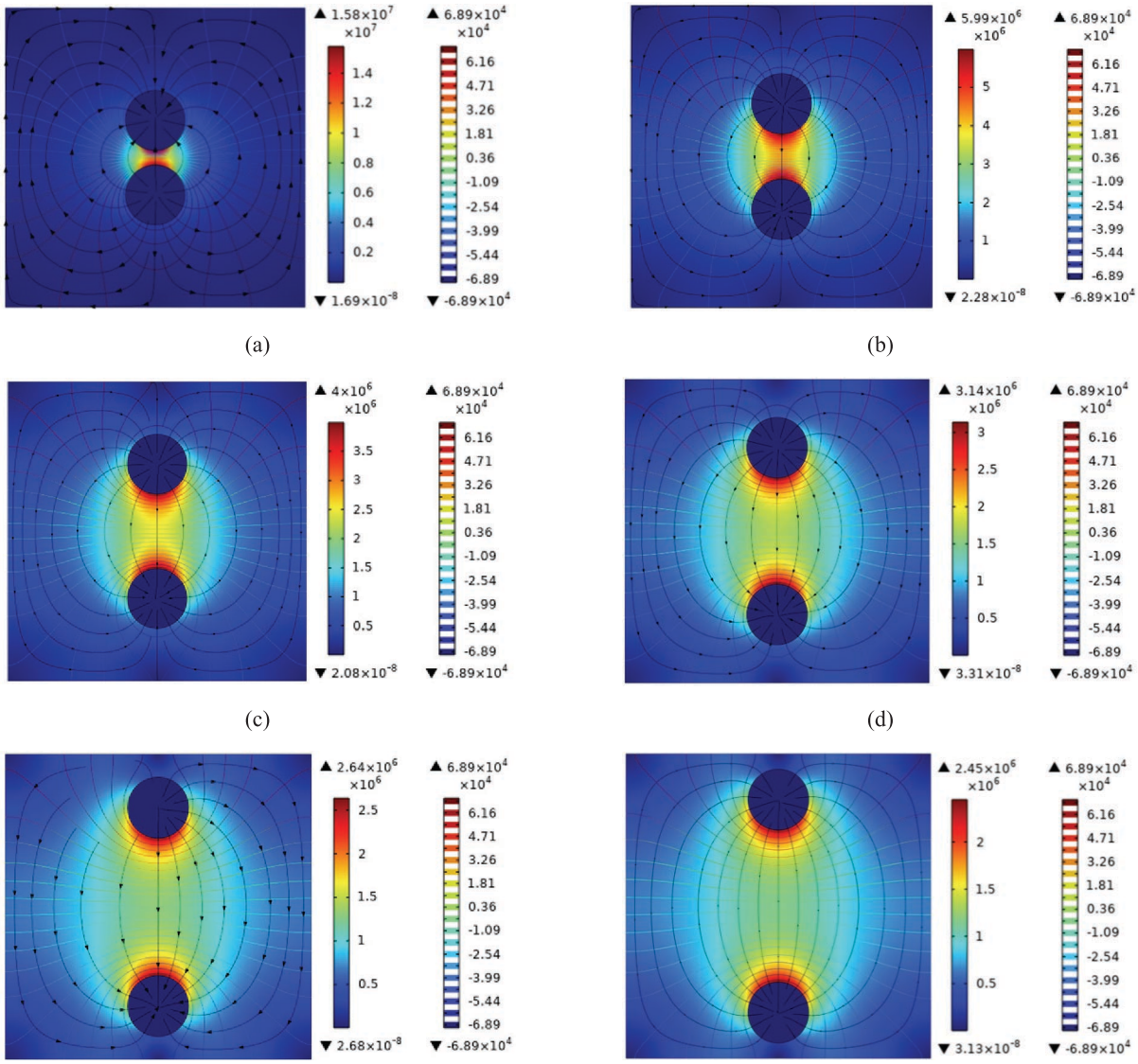


Figure 6. The electric field strength, potential distribution, and current flow within a sphere-sphere electrode setup at a fixed voltage of 72.5 kV for different electrode gap distances in an SF_6 circuit breaker model at (a) 1 cm (b) 3 cm (c) 5 cm (d) 7 cm (e) 9 cm (f) 10 cm

Figure 6 shows the electric field at a 1 cm gap displaying peak concentration between the electrodes, with a steep potential gradient and densely packed current flow lines, indicating a strong localized field conducive to breakdown. As gaps increase to 3 cm and 5 cm, the electric field spreads more evenly, with a less steep potential and broader current distribution. At gaps of 7 cm and 9 cm, the field's intensity and the potential gradient decrease, with current flow covering a wider area, reducing localized breakdown likelihood. At a 10 cm gap, shows the most distributed electric field, the flattest potential gradient, and the most dispersed current flow, indicating the lowest electric stress and breakdown propensity. The trend shows that as gap distance increases,

electric field distribution becomes more even, potential gradients flatten, and current flow extends across a broader area.

Figure 7 illustrates the variation in maximum electric field strength as the electrode gap distance is increased from 1 to 10 cm.

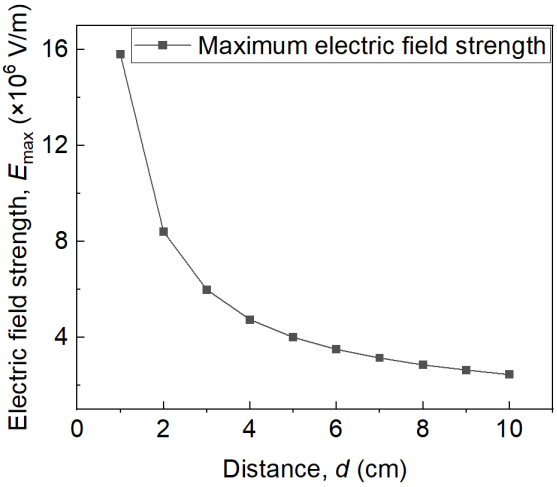


Figure 7. The variation in maximum electric field strength as the electrode gap distance increased from 1 to 10 cm

Figure 7 illustrates the variation in maximum electric field strength (E_{max}) as a function of the electrode gap distance (d) in SF_6 circuit breakers. The relationship is an inverse correlation, where the maximum electric field strength decreases as the electrode gap distance increases from 1 cm to 10 cm. This trend indicates the classical behavior described by Paschen's Law, which states that the breakdown voltage is a function of the product of pressure and gap distance.

At smaller gap distances (1–2 cm), the electric field strength is significantly high, reaching up to 16 × 10^6 V/m at a 1 cm gap. This high electric field strength is due to the concentrated potential difference over a small distance, resulting in a stronger field. As the gap distance increases, the electric field strength diminishes, decreasing sharply initially and then more gradually. By 10 cm, the electric field strength reduces to approximately 2 × 10^6 V/m. This reduction is due to the dispersion of the electric field over a larger distance, leading to a less intense field between the electrodes.

4.2. Electric field strength with different configurations

Figure 8 depicts the simulation results for the electric field intensity, potential distribution, and current flow patterns at a critical voltage of 72.5 kV and a gap distance of 1.84 cm, which has been identified as the critical distance for electric breakdown in a sphere-sphere electrode configuration within an SF_6 environment.

Figure 8 illustrates various electrode configurations and their impact on electric field strength. In the sphere-sphere setup, the maximum field strength is 89 kV/cm, with a symmetrical, high-intensity distribution between the electrodes. The sphere-rod configuration shows a higher field strength of 97.3 kV/cm, intensified at the rod's tip, indicating a greater breakdown risk there. The sphere-plane disperses the field more, with a strength of 88.7 kV/cm, and a wider current spread reducing electrical stress. The rod-plane reaches the highest field strength at 105 kV/cm due to intense concentration at the rod's tip. Lastly, the rod-rod records a strength of 100 kV/cm, with a symmetric but intense field between the rods, underscoring the effect of electrode shape on field dynamics.

The result shows that electric field strength varies greatly with electrode shape, particularly at a critical

1.84 cm gap under 72.5 kV in an SF_6 environment. The rod-plane configuration, with the highest field strength of 105 kV/cm, is most susceptible to breakdown due to intense field concentration at the rod's tip. Conversely, the sphere-plane and sphere-sphere configurations show lower strengths around 88.7 kV/cm, indicating greater resistance to breakdown compared to other configurations.

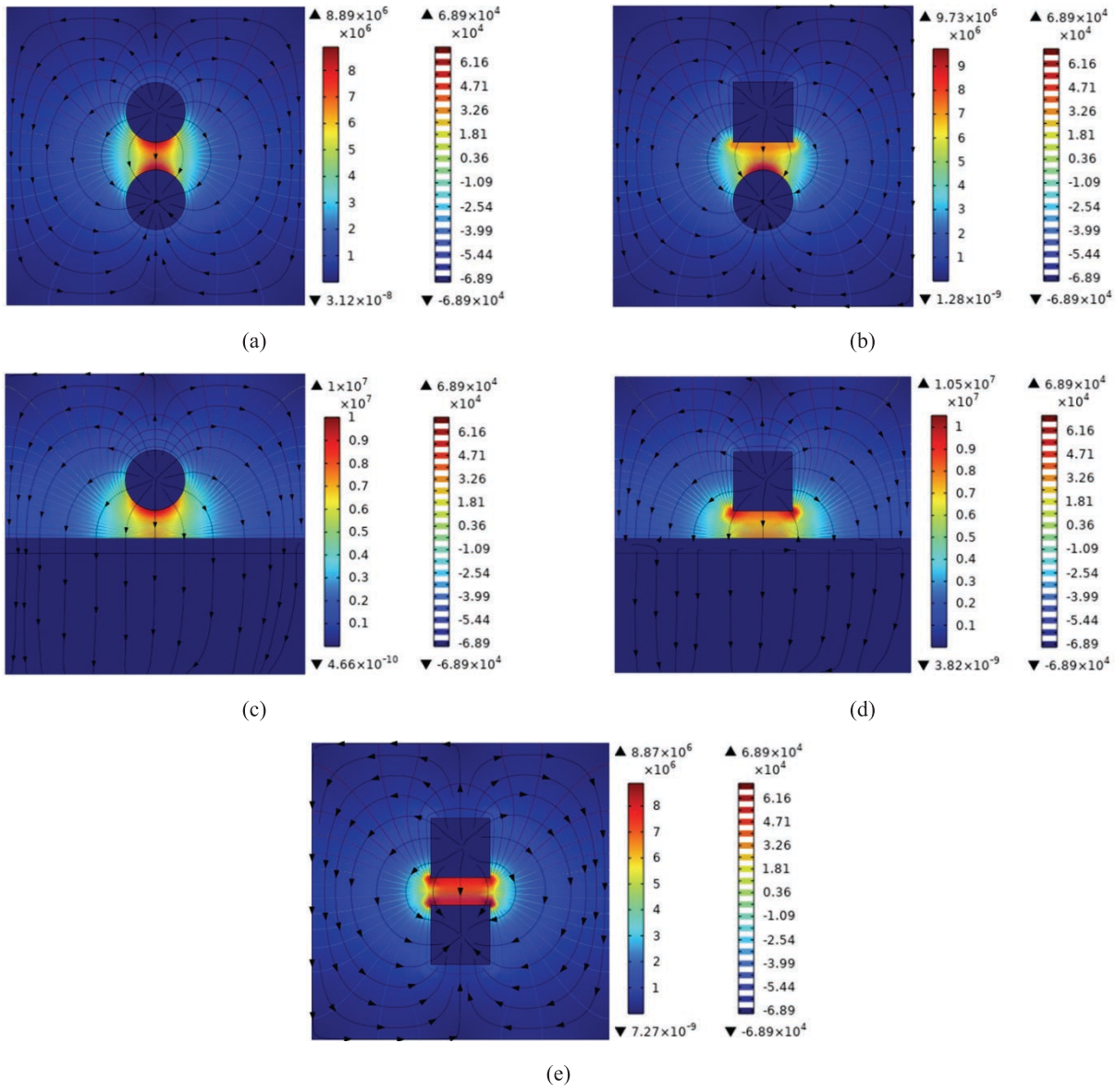


Figure 8. Simulation results for the electric field intensity, potential distribution, and current flow patterns at a critical voltage of 72.5 kV and a gap distance of 1.84 cm

4.3. Breakdown voltage with insulating gas

Figure 9 presents a comparative analysis of the breakdown voltage as a function of the electrode gap distance in two different gaseous environments: sulfur hexafluoride (SF_6) and air.

For SF_6, the breakdown voltage linearly increases from approximately 40.8 kV at a 1 cm gap to 149 kV at a 4.5 cm gap, highlighting its robust insulating properties and high dielectric strength. In contrast, air shows a much lower and flatter breakdown voltage curve, starting from 13.8 kV at a 1 cm gap and only reaching about 50.2 kV at 4.5 cm, indicating its lesser insulating effectiveness. The significant disparity between SF_6 and air in these tests underscores SF_6's superiority as an insulator in high-voltage applications, essential for maintaining

electrical integrity over various gap distances.

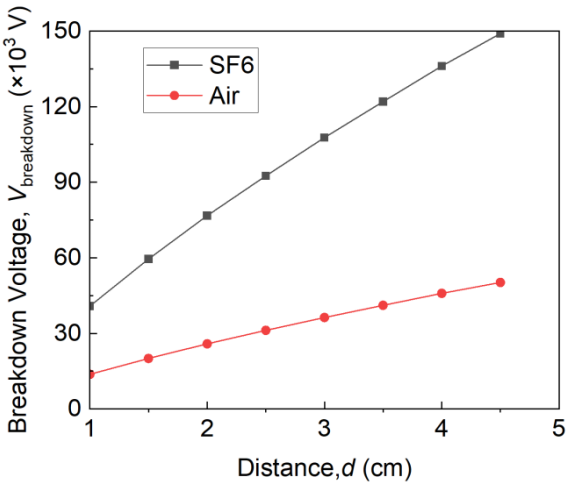


Figure 9. The breakdown voltage changes with the electrode gap distance in sulfur SF_6 and air environment

5. Conclusion

This comprehensive study, through experimental analysis and finite element simulation, has confirmed the linear relationship between breakdown voltage and electrode gap distance in SF_6 circuit breakers, aligning with Paschen's Law. The close match between experimental and simulated data validates our finite element model for predicting electrical breakdown. We found that electrode configuration significantly affects electric field distribution; the rod-plane setup was most prone to breakdown, while the sphere-plane showed the greatest resistance. The study highlights SF_6's superiority over air as an insulating medium, emphasizing the critical role of electrode geometry in the design and performance of high-voltage circuit breakers. This research enhances our understanding of electric breakdown in SF_6 systems and underscores the importance of electrode design in optimizing high-voltage electrical infrastructure.

Funding

Ningbo Science and Technology Plan Project (Grant No. 2023Z043)

Disclosure statement

The authors declare no conflict of interest.

Author contributions

Conceptualization: Peilong Zhu
Investigation – experiments: Qi Yu, Su Guo, Lailin Chen
Investigation – simulation: Qingpeng Yuan, Shiwen Chen
Formal analysis: Bo Guan
Writing: Bo Guan

References

[1] Lin X, Zhang J, Xu J, et al., 2022, Dynamic dielectric strength of C3F7CN/CO2 and C3F7CN/N2 mixtures in high voltage circuit breakers. IEEE Transactions on Power Delivery, 37(5): 4032–4041.

[2] Ou X, Wang L, Liu J, et al., 2020, Numerical simulation of streamer discharge development processes with multi-component SF6 mixed gas. Physics of Plasmas, 27: 073504.

[3] Jiang X, Li X, Zhao H, et al., 2013, Analysis of the Dielectric Breakdown Characteristics for a 252-kV Gas Circuit Breaker. IEEE Transactions on Power Delivery, 28(3): 1592–1599.

[4] Guo Z, Liu S, Pu Y, et al., 2019, Study of the Arc Interruption Performance of CO2 Gas in High-Voltage Circuit Breaker. IEEE Transactions on Plasma Science, 47(5): 2742–2751.

[5] Xiao D, 2016, Insulation Characteristics of Sulfur Hexafluoride (SF6). in: Gas Discharge and Gas Insulation. Springer Berlin, Heidelberg, 195–229.

[6] Okubo H, Yamada T, Hatta K, et al., 2002, Partial Discharge and Breakdown Mechanisms in Ultra-Dilute SF6 and PFC Gases Mixed with N2 Gas. Journal of Physics D: Applied Physics, 35: 2760–2765.

[7] Xiao D, 1999, Research on Discharge Characteristics of the Avalanche in SF6 Gas Mixtures, thesis, Xi'an Jiao Tong University.

[8] Geng J, Yang J, Shu T, et al., 2023. Stability of Breakdown Phenomenon in N2, SF6, and their Mixture under Impulse Voltages. AIP Advances, 13: 035033.

[9] Liu W, Yang A, 2011, Unsupervised Learning Algorithm for Finite Mixture Model Based on BIC Criterion and Gibbs Sampling. Acta Electronica Sinica, 39: 134–139.

[10] Krämer W, 1998, Fractional integration and the augmented Dickey-Fuller Test. Economics Letters, 61: 269–273.

[11] Ito T, Bulger M, Pazin MJ, et al., 1997, ACF, an ISWI-Containing and ATP-Utilizing Chromatin Assembly and Remodeling Factor. Cell, 90(1): 145.

[12] Zhou Z, Han D, Zhao M, et al., 2020, Review on Decomposition Characteristics of SF6 Alternative Gases. Transactions of China Electrotechnical Society, 35(23): 4998–5014.

[13] Kapetanovic M, 2011, High Voltage Circuit Breakers. Sarajevo.

[14] Jia SL, Zhao H, Li XW, et al., 2011, Survey of recent researches on the arc quenching characteristics of SF6 substitute gases. High Voltage Apparatus, 47(11): 87–91 + 97.

Publisher's note

Bio-Byword Scientific Publishing remains neutral with regard to jurisdictional claims in published maps and institutional affiliations.

Journal of Electronic Research and Application, 2024, Volume 8, Issue 4
http://ojs.bbwpublisher.com/index.php/JERA
ISSN Online: 2208-3510
ISSN Print: 2208-3502

Crawler Vehicle Rescue Robot Based on Arduino NANO

Haiwei Wang*, Juntong Chen, Tianyu Jin

College of Civil Engineering and Transportation, Northeast Forestry University, Harbin 150040, China

Corresponding author: Haiwei Wang, wangdiesel2001@163.com

Copyright: © 2024 Author(s). This is an open-access article distributed under the terms of the Creative Commons Attribution License (CC BY 4.0), permitting distribution and reproduction in any medium, provided the original work is cited.

Abstract: This paper introduces the Arduino NANO-based crawler vehicle rescue robot, including the traveling device. The traveling device includes an electrical screw jack, a power mechanism, a power supply, a camera, a curved snow shovel, a lighting device, and a control circuit. The control circuit is connected to the power supply, camera, lighting device, power unit, and electrical screw jack. The beneficial effect is that the control circuit can accurately control the height of the jack to ensure an effective rescue, power the rescue device and electronics, and effectively improve the efficiency of rescue.

Keywords: Image recognition; Traffic safety; Travel security

Online publication: August 12, 2024

1. Project overview

1.1. Study significance

The vehicle rescue robot can carry out tasks under harsh conditions, such as at disaster sites, battlefields, etc. Through independent operation, it can quickly carry out effective rescue operations, and improve the rescue efficiency and speed.

Traditional vehicle rescue often requires personnel to go to the scene to carry out tasks, facing a variety of dangers and risks, such as traffic accidents, bad weather, poisonous gas, and so on. The crawler vehicle rescue robot can replace personnel to perform tasks, reducing the risk of injury and life safety. It can deal with a variety of complex environments and terrain, such as mountains, deserts, etc. It has strong adaptability and flexibility traits and can perform rescue missions in different scenarios [1]. The crawler vehicle rescue robot is usually equipped with high-precision sensors, robotic arms, cameras, and other types of equipment. These help to obtain real-time field information to conduct analysis and judgment. It has strong execution ability, can effectively perform rescue tasks, and improves the ability and effect of rescue missions. In natural disasters or man-made accidents, there are often vehicles falling into dangerous situations, such as landslides, floods, earthquakes, and so on. The research and application of crawler vehicle rescue robots can help to meet these challenges, rescue trapped people in time, and reduce the losses caused by disasters.

1.2. Project background

With the development of robotics technology and the improvement of intelligent algorithms, researchers have begun to apply robots to rescue fields. The vehicle rescue robot project is based on this technological progress, aiming to use the autonomy, flexibility, and efficiency of the robot to improve rescue missions. In the process of vehicle rescue, rescue workers often face various risks, such as traffic accidents, bad weather, poisonous gas, and so on [2]. Therefore, the development of a crawler vehicle rescue robot can reduce the risk of people directly involved and ensure the safety of rescue workers. Different car trap situations may occur in urban roads, suburban villages, mountain woodland, and other diversified scenes with complex terrains and harsh environments. The purpose of the project is to develop adaptable, multi-functional robot systems that can perform rescue missions in various scenarios.

1.3. Analysis of current domestic and foreign research

Zhao from Qingdao Peak Jin Shengda Mould Co. LTD. patented an innovative jack [1]. He optimized the mechanical structure of the design of a traditional jack. Using the top plate hinge design technology to overcome the limitations of a traditional jack prevents the fixed angle of the top disc from causing changes to the car's chassis angle when lifted. It also reduces damage to the chassis by increasing the contact area of the top plate.

1.4. Study objectives

Given the vehicle rescue challenges, this study focuses on efficient rescue implementation. Arduino develops a robot system that can accurately identify vehicle rescue, perform rescue operations, adapt to different environments, have communication and cooperation ability, and ensure safety and reliability. This ensures improvement in the efficiency and success rate of vehicle rescue.

2. System composition

2.1. Video image transmission identification subsystem

The video image transmission identification subsystem is an important part of the crawler vehicle rescue robot. It is responsible for the identification and analysis of the real-time image data obtained by the video image sensor to help the robot understand the surrounding environment, identify the trap situation, and perform rescue tasks [3]. The on-site image data in real-time can be accessed or captured through the camera or other video image sensors. These sensors can monitor the surrounding environment of the vehicle, providing a comprehensive full range of view. Based on the identified target and environment characteristics, the environment understanding and map construction of the vehicle site are built, including the vehicle location, surrounding road conditions, obstacle distribution, and other information. The recognition results are displayed on the human-computer interaction interface in images, text, or other forms for the operators to monitor and operate the actions of the robot in real-time. Real-time image data can be transmitted to terminals such as mobile phones through the network or other communication means. The robot can also perform fault diagnosis of the video image transmission equipment, promptly identify and report any equipment issues, and attempt self-repair or switch to standby equipment to ensure stable system operation.

2.2. Drive control subsystem

The drive control subsystem is one of the key components of the crawler vehicle rescue robot, which is responsible for controlling its movement and enabling various tasks at the rescue site [4]. The electric drive

system includes the motor control of wheels, tracks, joints, and other components. By adjusting the speed and direction of the motor, the robot adapts to the movement with steering and attitude adjustment. Based on the sensor data and the target position, motion planning and path tracking are conducted to ensure that the robot can safely reach the target position according to the predetermined path while avoiding collision and danger. According to the environmental conditions and task requirements, the speed and acceleration of the robot are adjusted to achieve flexible dynamic control and adapt to different terrain and working scenarios. The sensor data is used to monitor the environment around the robot in real-time, detecting obstacles and potential collision risks. It then takes corresponding measures to avoid obstacles or stop moving to ensure the safety of the robot and the surrounding environment. The energy system is managed and optimized, including battery status monitoring, charging control, etc., to ensure long-term operation of the robot and smooth completion of rescue tasks. It can monitor and diagnose the faults of the drive control system in time and take repair measures to ensure the stability and reliability of the system.

3. Specific implementation methods

3.1. Overview of the robot

The following will provide a clear description and technical scheme of the crawler vehicle rescue robot along with the attached drawings. The embodiment described is only part of the crawler vehicle rescue robot, not all of them [5].

Figure 1 and **Figure 2** show the technical scheme of the crawler vehicle rescue robot based on Arduino NANO from the side and top view. The components include the chassis (1), electrical screw jack (2), stepper motor (3), multiple tracks (4), camera (5), lighting device (6), power supply (7), control circuit (8), cradle (9), and curved snow shovel (10). The power supply is removable and can be used with a rechargeable lithium battery. Power is given to the control unit which connects to the other components through wires. The control circuit contains a trigger, transmission, and receiving circuit which receives instructions from devices like a mobile phone that can be connected through Bluetooth or a 2.4 GHz wireless LAN connection.

The electrical screw jack is positioned on the chassis. The robot's movement is facilitated from the multiple tracks, driven by the stepper motor connected to the control unit. The cradle, equipped with a camera and lighting device can perform coaxial rotation following instructions from the control unit. The curved snow shovel is positioned in front of the robot with bolts. The overall movement of the robotic vehicle is based on directions provided to the control circuit.

To use the robot during a mission where a vehicle is trapped, the personnel start by identifying the trapped vehicle and removing the integral unit. Subsequently, the personnel activate the control circuit by establishing Bluetooth or 2.4 GHz wireless LAN connection to a mobile phone. The camera feed can be viewed directly from the mobile phone. From here, the personnel can send instructions from the mobile phone to the control circuit. This includes sending control signals to drive the motor under the trapped vehicle. Once the control circuit receives the signal for instructions, it follows accordingly. The personnel can adjust the camera perspective as instructed. For clear vision, the lighting device can also be activated. With further instructions, the robot will then move and position the electrical screw jack correctly to lift the trapped vehicle. Hence, necessary repairs and rescue operations on the trapped vehicle can be carried out.

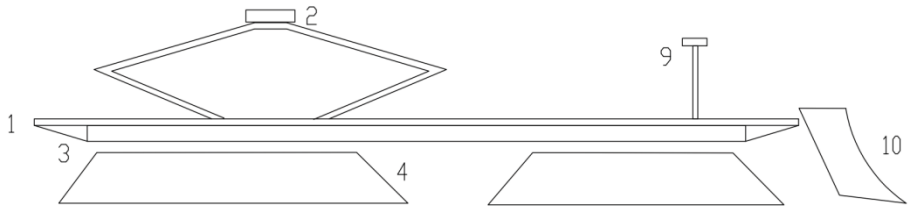


Figure 1. Overall side view of the robot

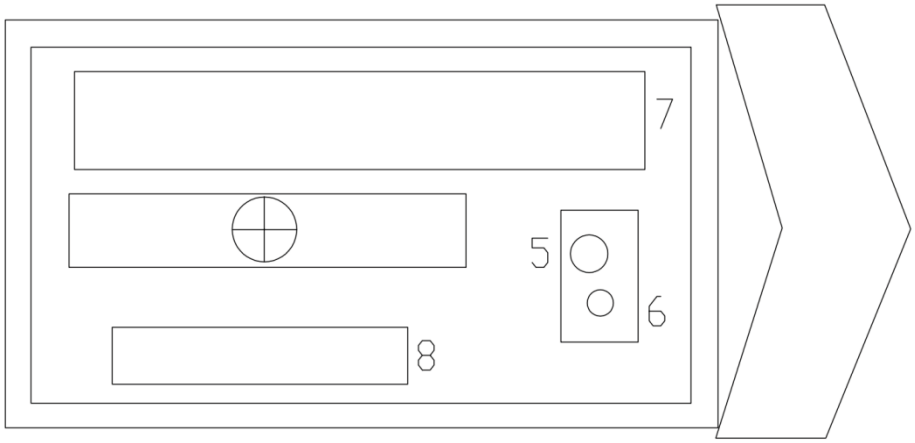


Figure 2. Overall top view of the robot

3.2. Innovation

By using a variety of sensors, the crawler vehicle rescue robot achieves comprehensive awareness, utilizing advanced technologies like deep learning for intelligent recognition. This includes identifying situations where vehicles are trapped and assessing environmental conditions, enhancing the precision and effectiveness of rescue operations. The crawler vehicle rescue robot is designed to adapt to various terrains and environments, from urban roads to mountainous forests. With diverse robotic equipment, it can effectively carry out rescue missions in complex scenarios.

4. Conclusion

The success of this project is the result of various scientific and technological progress. From mechanical design to artificial intelligence, from sensing technology to emergency management, the results of multi-party cooperation enable crawler vehicle rescue robots to play a role in a variety of scenarios. This result is just a small step in this aspect. With the continuous development of technology, the crawler vehicle rescue robot will become more intelligent, flexible, and reliable. We look forward to seeing these technologies play a greater role in the future of disaster relief, bringing more safety and hope to people.

Disclosure statement

The authors declare no conflict of interest.

References

[1] He X, 2023, Status and solution of emergency rescue technology for Highway Vehicles. China High-Tech, 2023(16): 65–66 + 72.

[2] Li R, 2023, Research on the Trajectory Planning and Tracking Control Method of Tracked Rescue Robot, thesis, Central South University. https://doi.org/10.27661/d.cnki.gzhnu.2023.000665

[3] Li H, 2015, Dynamics Analysis and Optimization of a Wheel-Track Composite Rescue Robot Chassis, thesis, Tianjin University of Technology.

[4] Wu X, 2014, Structural design of the transmission system of a wheel-track composite rescue robot, thesis, Tianjin University of Technology.

[5] Li Z, Qian Y, Gu Y, 2023, Research on the road rescue mode of intelligent robot based on the concept of service design. Machinery, 50(07): 51–57.

Publisher's note

Bio-Byword Scientific Publishing remains neutral with regard to jurisdictional claims in published maps and institutional affiliations.

Journal of Electronic Research and Application, 2024, Volume 8, Issue 4
http://ojs.bbwpublisher.com/index.php/JERA
ISSN Online: 2208-3510
ISSN Print: 2208-3502

Exploration of Construction Organization for Maintenance of Steam Turbine Equipment in Thermal Power Plants

Zhu Yang*

Guodian Construction Investment Inner Mongolia Energy Co. Ltd. Bulian Power Plant, Ordos 017004, China

***Corresponding author:** Zhu Yang, Colin.wang@soarcore.com

Copyright: © 2024 Author(s). This is an open-access article distributed under the terms of the Creative Commons Attribution License (CC BY 4.0), permitting distribution and reproduction in any medium, provided the original work is cited.

Abstract: The continuous development of the power industry has had a positive impact on thermal power plants, helping them maintain a good production form. In the use of steam turbine equipment in thermal power plants, to prolong its lifespan and avoid safety hazards, it is necessary to pay attention to strengthening maintenance and construction organization, better implementing effective organizational work, and effectively applying steam turbine equipment to ensure the sustainable development of thermal power plants. This article discusses the concept of equipment maintenance from the perspective of steam turbine equipment in thermal power plants, analyzes the current situation of equipment maintenance, and proposes a specific construction organization to provide a reference for steam turbine equipment maintenance.

Keywords: Thermal power plant; Steam turbine equipment; Construction organization

Online publication: August 12, 2024

1. Introduction

Steam turbine equipment can provide guarantees for the normal operation of thermal power plants. Due to the high cost of steam turbine equipment, it is necessary to pay attention to the maintenance and upkeep of equipment in daily work. However, maintenance costs for steam turbine equipment in thermal power plants are very high. Simultaneously, due to the lack of professionalism, traditional equipment maintenance activities take a long time. Although routine maintenance can timely detect faults in steam turbine equipment and perform dynamic management, actual maintenance will consume a lot of manpower and material resources. Therefore, the actual maintenance cost is relatively high, which is contrary to the operation of steam turbine equipment in thermal power plants in the new era [1]. In this regard, thermal power plants need to pay attention to the updating of maintenance methods, adopt the formation of construction organization, better play the significance of maintenance activities, and provide guarantees for the normal operation of thermal power plants.

2. Concept of maintenance of steam turbine equipment in thermal power plants

To better carry out the maintenance of steam turbine equipment and play the role of maintenance activities, the most crucial point for thermal power plants is to deepen the understanding of relevant content in this area. The specific concepts include the following: Firstly, thermal power plants adopt activities such as improving maintenance mechanisms and adjusting work methods, implementing comprehensive considerations, and achieving more significant results in steam turbine equipment maintenance, minimizing the occurrence of faults, and better meeting the smooth implementation of production activities in thermal power plants. Secondly, the maintenance of steam turbine equipment focuses on the construction organization of maintenance. By clarifying the key points of organization, the performance of steam turbine equipment can be better optimized, assuring its high-quality operation [2]. In short, turbine equipment maintenance refers to the use of maintenance and repair activities to keep relevant equipment in a normal state at all times, thereby bringing higher economic benefits to thermal power plants.

3. The significance of steam turbine equipment maintenance in thermal power plants

Steam turbine equipment plays an important role in thermal power plants. Conducting maintenance activities can provide guarantees for the normal operation of steam turbine equipment, minimize the occurrence of risk problems, and promote the improvement of business efficiency. From the perspective of cost control in enterprise production, the maintenance of steam turbine equipment often requires a lot of time and energy and does not directly affect operational efficiency. In actual operation, if the maintenance work receives insufficient attention, it is easy to have unreasonable maintenance methods, procedures, and other aspects, leading to an increase in maintenance costs and hindering the achievement of production benefits.

In addition, the maintenance of steam turbine equipment in thermal power plants has systematic characteristics. Therefore, it is necessary to carry out scientific planning, change the previous maintenance methods, significantly shorten the practice of maintenance consumption, and achieve good efficiency in the use of steam turbine equipment [3]. Thermal power plants need to pay attention to the maintenance of steam turbine equipment, design reasonable maintenance time and content, and achieve good maintenance quality while improving maintenance efficiency. From the perspective of steam turbine equipment, it is easy to encounter minor mechanical problems during use. Although these minor problems may not affect the operation of the machinery in the short term, the lack of maintenance and repair can not only have adverse effects on production but also lead to safety accidents. Therefore, it is necessary to strengthen the attention to equipment maintenance activities, adopt dynamic and information-based methods to carry out maintenance activities, timely discover problems, and provide guarantees for the operation of thermal power plants.

4. Current status of steam turbine equipment maintenance in thermal power plants

Currently, there are many problems in the maintenance of steam turbine equipment carried out by thermal power plants, resulting in poor maintenance efficiency and quality. The following summarizes the current status of steam turbine maintenance. Firstly, equipment maintenance is too formal. During the process of repairing steam turbine equipment, staff are influenced by traditional methods and only carry out maintenance based on time and content, rather than starting from the operation of the steam turbine equipment. The actual maintenance content is rigid, and in most cases, the maintenance work is just a formality, making it difficult

to fully realize the value of maintenance. Secondly, the comprehensive management of maintenance data is insufficient [4]. The maintenance of steam turbine equipment belongs to the process of system maintenance. Only by focusing on the management of maintenance content can the quality of maintenance be guaranteed. However, due to insufficient information management, there is less data in the maintenance process, which increases the maintenance cost. Thirdly, there is a lack of risk prediction management. In the maintenance of steam turbine equipment, although a maintenance plan has been formulated, other operational problems may arise, which not only affect operational efficiency but also lead to safety issues.

5. Practical strategies for organizing maintenance and construction of steam turbine equipment in thermal power plants

5.1. Adjust the construction organization structure and improve the working mechanism

Thermal power plants should focus on the maintenance of steam turbine equipment and adhere to construction requirements. By optimizing the construction organization structure and leveraging application advantages, they can enhance the professionalism of their construction activities and demonstrate a positive development trend [5]. Through improving regulations and optimizing personnel allocation, professional support can be provided for construction organizations to better play their role in turbine equipment maintenance. This ensures the formulation of relevant plans and demonstrates stronger professional implementation to avoid affecting the production efficiency and performance of thermal power plants. In establishing the construction organization structure, it is important to consider the rationality of the construction plan for steam turbine operations. By actively conducting effective maintenance and construction activities and thoroughly analyzing the operation and performance of the steam turbine equipment, valuable reference information can be gathered. This promotes the improvement of production efficiency in thermal power plants and achieves better operational efficiency of the steam turbine equipment.

Furthermore, thermal power plants should take into account the operation of steam turbine equipment, construction organization, and other aspects. To promote the improvement of related work levels, they can take a better approach from an institutional perspective. Firstly, in the process of forming the working mechanism of the construction organization, attention can be paid to the integration of practical experience, work philosophy, and other elements. This aids in improving the system, providing a reference basis for it, making maintenance activities more professional, and promoting the improvement of work level. Secondly, in improving the working mechanism of construction organizations, it is necessary to pay attention to its implementation and better promote the maintenance of steam turbine equipment [6]. Thirdly, from the perspectives of quality, safety, and progress, a good construction organization mechanism can be established to significantly reduce the frequency of construction problems and meet the development needs of thermal power plants.

5.2. Deploying skilled personnel to improve equipment maintenance efficiency

The maintenance of steam turbines in thermal power plants requires advanced skills, and not everyone can complete it. Therefore, power plants need to equip skilled personnel to carry out better maintenance activities and avoid various problems caused by maintenance. Specifically, professional maintenance personnel can be recruited to form an effective team for steam turbine equipment maintenance, control maintenance costs, and improve maintenance quality. Additionally, the training of steam turbine equipment personnel should be strengthened [7]. Steam turbine equipment exhibits high system complexity, necessitating technical personnel to possess proficient skills for conducting effective maintenance activities. Finally, thermal power plants need to clarify the maintenance objectives of steam turbines and clarify the primary and secondary relationships.

Maintenance work is integral to the operational system, where professionals can identify key points and perform effective maintenance activities to prevent increased maintenance costs resulting from decreased efficiency.

5.3. Enhancing design and construction organization: optimizing work methods

The design of construction organization refers to the adoption of a comprehensive technical and economic document that can carry out activities such as construction preparation, control, and resource allocation. It can start from the construction process and carry out scientific management activities. Construction organizations can analyze the characteristics of the project, equipment conditions, etc., to formulate specific work policies and ensure the smooth implementation of equipment maintenance. Firstly, considering feasibility and depth of meaning, the design maintenance and construction organization for steam turbine equipment can be defined. From a refined perspective, innovative concepts can be integrated to make this plan more applicable, improving construction organization work efficiency, and providing support for the good development of thermal power plants [8]. Secondly, after determining the design scheme, the construction organization can provide professional guidance based on specific work plans, effectively conduct turbine equipment maintenance, ensure the smooth implementation of related work, lay the foundation for performance, optimization, and efficiency of thermal power plants, and make them have strong development vitality.

Furthermore, when dealing with the maintenance and construction of mechanical energy for steam turbine equipment, it is necessary to pay attention to the improvement of technical content in the work process. From the working mode of the construction organization, attention should be paid to work optimization. This includes attention to the application of information technology, better sorting out the various information resources generated in the maintenance of steam turbine equipment, and implementing good induction and application. These aspects provide technical guarantees for the optimization of construction organization work and improve its application effect [9]. Simultaneously, we attach great importance to the development of refinement work, refining the workflow of steam turbine equipment, forming a work form that meets the needs of power plants, promoting the improvement of work level, and ensuring the correct operation of steam turbine equipment [10].

5.4. Strengthen spare parts application and reduce maintenance costs

The use of steam turbine equipment in thermal power plants is influenced by traditional maintenance methods, resulting in high maintenance costs [11]. From an economic perspective, it is necessary to improve the efficiency of spare parts utilization and strengthen its application according to the following steps: Firstly, staff need to clarify the focus of work, and carry out reasonable numbering activities based on the use of steam turbine equipment. Frequently used parts can be classified as class A, infrequently used parts can be classified as class B, and almost unused parts can be classified as class C [12]. Secondly, thermal power plants should prepare spare parts based on their actual categories, with a focus on purchasing Class A spare parts, to better cope with frequent mechanical problems of steam turbine equipment. Through the application of spare parts, it is possible to significantly reduce the time spent on procurement due to damage to equipment components and reduce maintenance costs.

5.5. Attention to daily maintenance to ensure operational effectiveness

The maintenance of traditional steam turbine equipment often consumes a large amount of manpower and material resources, leading to an increase in maintenance costs. Therefore, to avoid multiple maintenance activities, thermal power plants need to pay attention to the daily maintenance of equipment, promptly identify problems, and eliminate them. Firstly, it is necessary to monitor the steam turbine equipment [13]. Starting from the operation of the steam turbine equipment, it can be found that problems arise during the

operation process, effectively reducing the frequency of maintenance. In this process, thermal power plants can strengthen the application of computers, carry out better detection activities, timely discover problems, and carry out good maintenance and upkeep. Secondly, pay attention to the improvement of the equipment operation status detection system. The operation of steam turbine equipment is influenced by many factors and is prone to various problems, such as clearance between the stator and the rotor. Hence, it is essential to ensure comprehensive testing to promptly identify issues and conduct daily maintenance tasks [14]. Therefore, it is important to pay attention to daily maintenance, such as the application of lubricating oil, equipment cleaning, etc., promptly identify problems, and carry out handling activities to avoid the accumulation of small problems that hinder the normal operation of the equipment.

6. Conclusion

In conclusion, thermal power plants can enhance maintenance results and extend the service life of steam turbine equipment through construction organization, thereby providing guarantees for the development of production plans [15]. Therefore, it is necessary to pay more attention to construction organization, implement organizational work, avoid affecting its safety performance, and significantly reduce the maintenance costs brought by power plant equipment to ensure the normal operation of steam turbine equipment.

Disclosure statement

The author declares no conflict of interest.

References

[1] Gao G, 2022, Exploration of Economic Maintenance Management of Steam Turbine Equipment in Thermal Power Plants. Shanghai Xiaoyu Culture Communication Co., Ltd., Intelligent Learning and Innovation Research Committee of China Smart Engineering Research Association Proceedings of 2022 Shanghai Forum on Engineering Technology and New Materials (ETM2022), 1: 2.

[2] Gao J, 2022, Analysis of Maintenance and Repair of Mechanical Equipment in Thermal Power Plants. Paper Equipment and Materials, 51(07): 56–58.

[3] Wang Y, 2022, Analysis of Mechanical Equipment Maintenance and Repair in Thermal Power Plants. Science and Technology Innovation and Application, 12(14): 94–97.

[4] Yang J, 2019, Practical application research on the economic maintenance mode of steam turbine professional equipment in thermal power plants. Low Carbon World, 9(08): 126–127.

[5] Guo Q, Zhao Y, Yang S, 2023, Maintenance and Repair of Electrical Equipment in Thermal Power Plants. Automation Application, 64(22): 113–115.

[6] Feng L, 2023, Analysis of Problems and Countermeasures in Electrical Equipment Maintenance Management of Thermal Power Plants. Electrical Technology and Economics, 2023(06): 175–177.

[7] Fan S, 2023, Management and Maintenance Analysis of Coal Handling System Equipment in Power Plants. Integrated Circuit Application, 40(06): 283–285.

[8] Hou X, 2023, Exploration of Electrical Maintenance Methods for Thermal Power Plants. Modern Industrial Economy and Information Technology, 13(04): 317–318.

[9] Zhang H, Ma Y, 2022, Maintenance and Repair of Fuel Transportation Equipment in Thermal Power Plants. Modern Industrial Economy and Information Technology, 12(10): 218–220.

[10] Liu F, Liu X, Zuo Q, et al., 2022, Research on Boiler Equipment Management and Renovation in Thermal Power Plants. Metallurgical Management, 2022(19): 86–88.

[11] Cheng C, 2022, Analysis of Causes and Countermeasures for Electrical Operation Faults in Thermal Power Plants. Light Source and Lighting, 2022(08): 180–182.

[12] Liang G, 2022, Analysis of Maintenance and Renovation Issues of Boiler Equipment in Thermal Power Plants. Science and Technology Information, 20(17): 49–51.

[13] Deng X, 2022, Fault Detection and Maintenance of Primary Electrical Equipment in Thermal Power Plants. Equipment Management and Maintenance, 2022(06): 83–85.

[14] Zhao R, 2022, Maintenance Technology of Thermal Power Equipment. Technological Innovation and Application, 12(02): 162–164.

[15] Yan Q, 2021, New Methods and Maintenance Strategies for Boiler Maintenance in Thermal Power Plants. China Electric Power Technology Market Association, Excellent Papers on Technical Supervision in the Power Industry in 2021, Huadian Hubei Power Generation Co., Ltd. Power Engineering Branch, 2021: 4.

Publisher's note

Bio-Byword Scientific Publishing remains neutral with regard to jurisdictional claims in published maps and institutional affiliations.

Journal of Electronic Research and Application, 2024, Volume 8, Issue 4
http://ojs.bbwpublisher.com/index.php/JERA
ISSN Online: 2208-3510
ISSN Print: 2208-3502

Street Lamp Status Warning System Based on Internet of Things Technology

Hanli Wang[1]*, Yuanzhi Liu[2], Yilin Wu[3]

[1]College of Computer and Control Engineering, Northeast Forestry University, Harbin 150040, China
[2]College of Civil Engineering and Transportation, Northeast Forestry University, Harbin 150040, China
[3]College of Wildlife and Nature Reserves, Northeast Forestry University, Harbin 150040, China

Corresponding author: Hanli Wang, w18737226902@163.com

Copyright: © 2024 Author(s). This is an open-access article distributed under the terms of the Creative Commons Attribution License (CC BY 4.0), permitting distribution and reproduction in any medium, provided the original work is cited.

Abstract: This paper proposes a street light warning system based on Internet of Things (IoT) technology, which uses cameras to detect moving targets such as vehicles and pedestrians around the system and adjust the brightness of street lights according to road conditions to reduce unnecessary power waste. The system has a mature self-fault detection mechanism and is equipped with a wireless communication device for data exchange and timely communication with the host computer terminal. The intelligent street lamp system in this paper can be used to reduce the occurrence of pedestrian and vehicle accidents at intersections, and at the same time reduce the consumption of manpower and material resources for street lamp troubleshooting, to achieve energy conservation and emission reduction.

Keywords: Internet of Things; Early warning system; Intelligent transportation

Online publication: August 13, 2024

1. Introduction

China is a big traffic country, with the construction of smart cities and the continuous development of roads, street lighting facilities are also being used on a large scale, so street lights are of great significance for urban lighting and traffic safety. On the one hand, with the change of seasons, the length of the day will also change, and only relying on the time point to control the brightness and darkness of the lamp lacks accurate time series trend prediction, which will cause a waste of energy. On the other hand, although the smart street lamp system in some cities is also equipped with relevant fault detection, the diagnostic function is limited to the preliminary fault phenomenon, and there is no supporting related system. The staff needs to investigate the problem one by one, which is very time-consuming and laborious. Therefore, effective fault diagnosis and intelligent early warning play a vital role in ensuring the safe and stable operation of urban lighting systems. Based on the above phenomenon, we designed a street light warning system based on Internet of Things technology. The system will control the operation of street lights and detect faults through two sets of subsystems.

The system framework design consists of a main control system and an auxiliary control system. The main control system is used to monitor the running status of the street lamp, and at the same time upload the relevant

light, current, and other parameters to achieve real-time control of the street lamp, and upload the data to the control terminal. Smart street lights detect vehicles and pedestrians through cameras and adjust their brightness in time according to road conditions to ensure sufficient visibility for pedestrians and vehicles.

The auxiliary control system, also known as the detection system, will monitor the operating status of the circuit and compare it with the set standard value, predict the future circuit operation trend through the circuit's current habits of deep learning, and report to the control terminal in time if a component of the circuit system is found or predicted to fail. The interface of the control terminal will display the location of the faulty street lamp and the faulty parts, and the maintenance personnel will achieve accurate repair through the content displayed by the terminal.

The two systems are loaded on the main control unit (MCU) at the same time, and the communication between the two systems and the host computer will be connected through the Internet of Things module. The IoT module adopts the ESP8266-01S Wi-Fi communication unit, which can withstand large data exchange and reduce communication delay. The Wi-Fi module communicates by sending heartbeat packets to the terminal server at regular intervals at the application layer to keep the connection alive and ensure the reliability of the communication [1].

Figure 1 is the overall structure of the intersection intelligent lighting system, which comprises: a light emitting diode (LED) lamp as the lighting unit, light dependent resistors (LDR) light sensor, and a passive infrared sensor (PIR) motion sensor as perception unit, Arduino microcontroller as system control unit, Wi-Fi module as wireless communication unit and signal transmission unit, power supply unit that provides energy for other units of the system. The overall structure of the system is as follows: LED lamp, Wi-Fi module, LDR light sensor, and PIR motion sensor are connected to the Arduino microcontroller while the power supply unit is connected to the LED lamp, LDR light sensor, PIR motion sensor, and Arduino microcontroller respectively. The single-chip microcomputer and the control terminal uses the Wi-Fi module as a bridge to ensure the smooth flow of information.

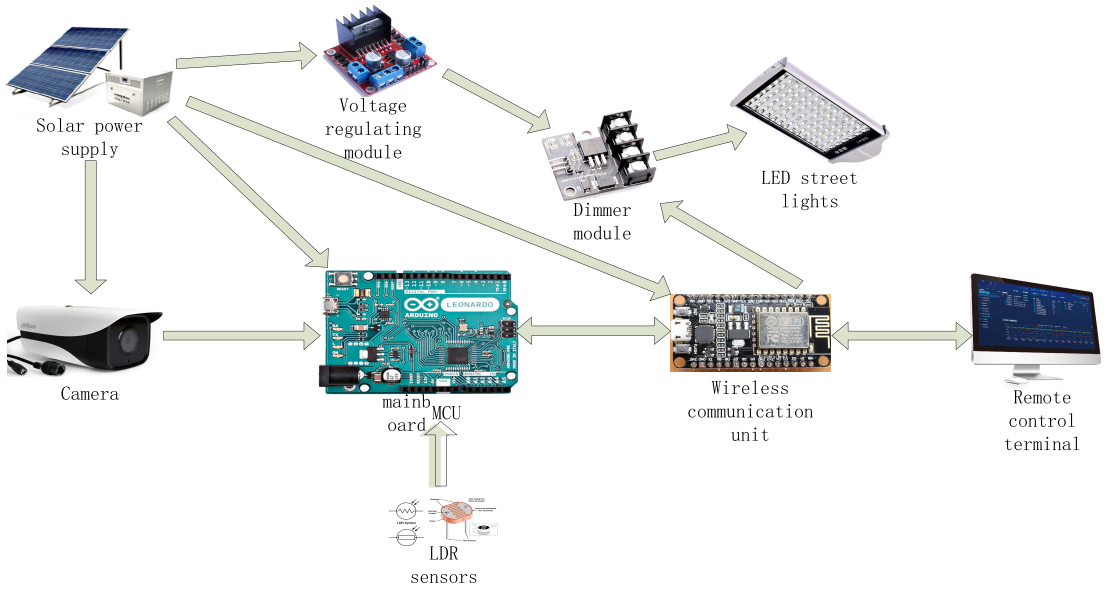


Figure 1. Structure of intelligent lighting system at an intersection

2. Method

2.1. Control unit to adjust the brightness of the lighting unit

When the light intensity is greater than the set threshold, the system obtains the light intensity information

through the LDR sensor, and the control program will turn off the street lights to save energy. With the gradual weakening of the light intensity, the photosensitive resistance will gradually decrease, the current inside the sensor will gradually increase, and then the current signal will be converted into a digital signal through the filter. When the light intensity signal obtained by the system is less than the threshold, the street lighting will be started, and the lighting power will be adjusted through the following scheme:

(1) In the case that pedestrians or vehicles do not appear at the same time, the street lights run at low power and only have basic lighting functions to save energy.

(2) When pedestrians and vehicles appear at the same time, through the prediction of the road trajectory of the vehicle, the system will judge whether the vehicle and the pedestrian will collide, and adjust the intensity of the street light in time to remind the pedestrian and the vehicle to reduce the occurrence of traffic accidents.

2.2. Road user trajectory prediction based on deep learning

Combined with the state-of-the-art you only look once (YOLOv8) object detection algorithm and DeepSORT object tracking algorithm, the movement trajectory of a variety of common road users is predicted to quantify the degree of night risk at intersections. Video data is collected with a variety of road users (vehicles, pedestrians, and bicycles) and the target location and category in each frame of the image are labeled. Next, the pre-trained YOLOv8 model was used for object detection, and the video frames were input into the model and the detection results such as the position, category, and confidence level of the targets in each frame were obtained. Then, the target detected by YOLOv8 was used as the input of the DeepSORT target tracking algorithm, and the target was tracked by the combination of Kalman filter and depth feature representation, and a unique ID was assigned to each target, to obtain the trajectory information of the target, and the nonlinear regression model was used to predict the trajectory. Finally, object detection, object tracking, and motion trajectory prediction are continuously carried out in the video stream, and updated in real-time based on the latest data, to achieve real-time road user motion trajectory prediction and provide continuously updated prediction results.

2.3. Communication establishment based on TCP/IP protocol

The communication module of the system adopts transmission control protocol/internet protocol (TCP/IP), which is a connection-oriented communication protocol that ensures the reliability and orderliness of data transmission. Firstly, establish a network server to connect the communication module with the host computer terminal and the client, the client is the street lamp end, and the main control system and the auxiliary system will establish a database respectively by the detected results, send the data to be transmitted to the communication module in the form of data stream, and the communication module will package these data and send them to the host computer terminal for analysis, and intuitively visually present to the staff. The communication module, the host computer terminal, and the client ensure a smooth data transmission link by continuously sending data packets.

2.4. Fault detection and protection system

For the auxiliary self-test system, we convert the current of the street lamp from the current transformer into a small current signal, then convert it into a voltage signal again and process it by the Kalman filter algorithm, and then convert the electrical signal into a digital signal for the microprocessor to read. Considering the fluctuations of its working circuit, when the circuit current is set to be greater than 2 times the working current, it is considered that a short circuit occurs. When a short circuit occurs, the MCU of the motherboard sends a signal to the relay through the driving circuit and turns off the street light circuit for short-circuit protection.

When the street lamp is damaged, the single-chip microcomputer cannot detect the current signal or the value is too small, and it is judged to be broken. Regardless of whether there is a short circuit or an open circuit, the device will use the wireless communication unit to send relevant activity logs to the remote terminal to realize self-inspection of street lamp faults.

3. System hardware design

The intelligent early warning system uses the Arduino board as the main control MCU, and the Arduino supports a wealth of expansion modules, such as sensors, actuators, etc., with good compatibility and powerful data processing capabilities. The main control board will be directly connected to the LDR sensor and night vision camera through the serial port. The LDR sensor will provide light-sensing information to the motherboard in real time, and the night vision camera will provide the detected vehicle and pedestrian conditions. The MCU will automatically control the LEDs based on the implanted system program combined with the information obtained.

The communication module uses the ESP8266 microcontroller for real-time contact with the control terminal. The main control MCU will adopt a more accurate serial communication mode with the communication module, and the data transmission between the communication module and the terminal will be based on TCP/IP wireless communication. Data transmission is divided into reliable transmission and unreliable transmission. Generally, TCP/IP-based transmission is connection-oriented, reliable, and byte-stream transmission, while user datagram protocol (UDP) transmission is a non-connection-oriented, broadcast-oriented, and unreliable transmission mode. TCP/IP data transmission requires that the link is always connected. In terms of efficiency, UDP is more efficient than TCP/IP. In terms of security, TCP/IP is more secure. In recent years, most of the lighting control systems designed are TCP/IP communication where the control terminal communicates with the Wi-Fi module, and the application layer sends heartbeat packets at regular intervals to keep the connection alive and ensure the reliability of the communication.

4. System software design

The control terminal adopts a graphical operation interface to provide more intuitive data information and convenient control. According to the design requirements of the software and the characteristics and advantages of the current mainstream system development platform, LabVIEW programming software was finally selected to develop the lighting control software. The Lighting Control Software for Smart Lighting Systems developed based on LabVIEW is a multi-modular application designed to provide comprehensive lighting control functions and a user-friendly interface. Since personnel generally detect the operation status of each street lamp in real-time through the terminal system, it will be extremely important for the design of the control terminal system. Its main design is as follows:

4.1. Status interface

The status of each street lamp will be displayed in the status interface.

(1) Display the status information of all street lights in the form of a list or grid on the interface, which can include the street lamp number, location, etc., use icons or colors to indicate the status of street lights, with green indicating that it is on and red indicating that it is off, and at the same time providing a real-time refresh function to ensure the timeliness of the displayed status information.

(2) For each street lamp, a graph percentage will be used to represent the current brightness level to visually

show the change in brightness level.

4.2. Operation interface

In the operation interface, manual and automatic mode control will be displayed.

For the auto-adjustment function, the interface will display the current auto-adjustment mode, and automatically adjust according to the set ambient light intensity and road conditions. Each street light will be provided with an on/off button, allowing staff to manually control the street light on or off. After clicking the button, the system will immediately respond to the command and change the set brightness value to change the status of the street light, and update the status information on the interface in real-time.

4.3. Data analysis interface

(1) Display the statistics of street lamp usage: Display the average brightness of street lamps every day on the interface, in the form of a line chart, and users can choose to view the data on different days. The failure rate of each street lamp is presented in the form of a graph so that users can clearly understand which street lights have problems.

(2) Energy saving analysis: Showing the energy consumption of each street lamp and comparing the energy consumption of different street lamps can help staff find potential opportunities for energy saving. Based on the energy consumption statistics, the system can provide energy-saving recommendations, such as adjusting the brightness level, changing the opening time, etc., to reduce energy consumption. At the same time, the staff can see the effect of implementing the energy-saving recommendations, such as the reduction of energy use and cost savings.

4.4. Alarm function

In the design of the host computer template of the street lamp status warning system based on the Internet of Things technology, the alarm function is very important. It can help the staff to find and deal with the fault or abnormal situation of the street lamp in time. When the system detects a fault or abnormal condition of a street lamp, it can automatically trigger an alarm. Situations include street lights not turning on properly, abnormal brightness, communication interruptions, etc. The system will send an alarm message in a pop-up window, and the main contents are as follows:

(1) Alarm information content: Display the number and location of the street lamp that is faulty or abnormal, which can enable the staff to quickly locate the specific street lamp. Indicate the type of fault or anomaly, such as brightness anomaly, communication failure, etc. Record the time when the alarm occurred, so that the staff can understand the time when the fault occurred.

(2) Alarm processing: After receiving the alarm information, the staff can view the detailed information through the system interface and take corresponding measures, such as sending maintenance personnel to the scene to deal with it. The system supports real-time push of alarm information to relevant personnel, which can be notified by SMS, email, or applications.

(3) Alarm record: The system will record the details of each alarm, including the alarm time, the location of the street lamp, the type of fault, etc. Relevant personnel can view the historical alarm records in the system to understand the fault situation and treatment of the street lamp.

In this early warning system, the system can read the user's work data through various circuits and sensors, enable the corresponding program to control the lighting of the solar street lamp according to the data judgment, and upload the activity log to the remote terminal for recording through the communication program. For the communication module, the socket communication mechanism, MySQL database, and TCP/IP communication

protocol are used. The specific process is that the street lamp sends a Synchronize (SYN) packet to the communication module, the server returns the corresponding Synchronize-Acknowledge (SYN-ACK) response and a new SYN package, and then the client returns the corresponding Acknowledge (ACK).

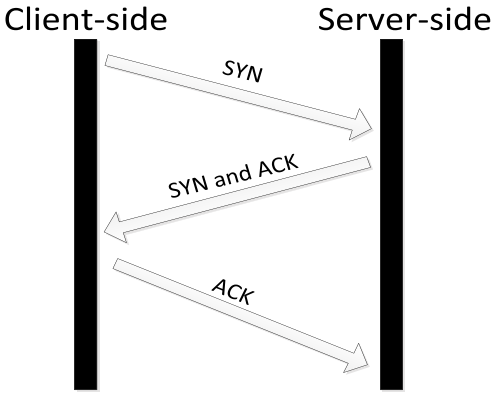


Figure 2. Connection established

SYN is the synchronization sequence number, which is the handshake information used by TCP/IP to establish a connection. ACK is an acknowledgment character, which is a transmission control character sent by the receiving station to the sending station in data communication. Indicates that the data sent has been acknowledged to have been received. In TCP/IP, if the receiver receives the data successfully, it will reply with an ACK message. Signals via ACK have their own fixed format, and length, and are replied to by the receiver to the sender [2].

When the first handshake and the connection are established, the client sends a SYN packet to the server and enters the SYN_SENT state, waiting for the server to acknowledge, where SYN is the synchronization sequence number. In the second handshake, the server receives the SYN packet and must confirm the customer's SYN, and at the same time sends a SYN packet, that is, the SYN-ACK packet, and the server enters the SYN_RECV state. In the third handshake, the client receives the SYN-ACK packet from the server and sends an acknowledgment packet ACK to the server.

The self-inspection program can timely and effectively determine whether the solar battery and street lamp head are faulty and can start corresponding measures to maintain and report the fault point for the fault, which is also convenient for maintenance personnel to carry out maintenance treatment [4].

5. Conclusion

In this paper, a street lamp status warning system based on Internet of Things technology is proposed, which connects the upper terminal and the main control MCU by using the communication module as a bridge and uses the TCP/IP protocol to ensure a smooth communication channel. The host computer will remotely monitor the operation status of the street lamp, obtain the fault situation and precise location of the street lamp in time, reduce the use of human and material resources for later maintenance, promote the development of the urban street lamp system to intelligence and energy saving, and help the dual carbon strategy. To sum up, compared with traditional street lights, the street lamp status warning system based on the Internet of Things technology designed in this paper has great advantages and good application prospects in many aspects.

Disclosure statement

The authors declare no conflict of interest.

References

[1] Cheng T, Hu W, Cui J, 2018, Design and implementation of remote monitoring platform for smart street lamp. Computer Application and Software, 35(03): 93–97 + 101.

[2] Pan H, 2018, Design and implementation of message push module reconstruction of road side rescue system, thesis, Shanghai Jiao Tong University. https://doi.org/10.27307/d.cnki.gsjtu.2018.003799

[3] Wang Y, 2014, Comparison of the performance of three typical versions of TCP on satellite link. Wireless Internet Technology, 2014(03): 131 + 157.

[4] Bai J, Zhang Y, 2014, A Solar Street Lamp Control System with Fault Self-Test Display. Management and Technology of Small and Medium-sized Enterprises (Mid-Term), 2014(11): 185.

Publisher's note

Bio-Byword Scientific Publishing remains neutral with regard to jurisdictional claims in published maps and institutional affiliations.

Journal of Electronic Research and Application, 2024, Volume 8, Issue 4
http://ojs.bbwpublisher.com/index.php/JERA
ISSN Online: 2208-3510
ISSN Print: 2208-3502

Chip Surface Character Recognition Based on OpenCV

Lihang Yin*

Henan Open University, Zhengzhou 450008, China

***Corresponding author:** Lihang Yin, yinlihang2018@163.com

Copyright: © 2024 Author(s). This is an open-access article distributed under the terms of the Creative Commons Attribution License (CC BY 4.0), permitting distribution and reproduction in any medium, provided the original work is cited.

Abstract: Chip surface character recognition is an important part of quality inspection in the field of microelectronics manufacturing. By recognizing the character information on the chip, automated production, quality control, and data collection and analysis can be achieved. This article studies a chip surface character recognition method based on the OpenCV vision library. Firstly, the obtained chip images are preprocessed. Secondly, the template matching method is used to locate the chip position. In addition, the surface characters on the chip are individually segmented, and each character image is extracted separately. Finally, a Support Vector Machine (SVM) is used to classify and recognize characters. The results show that this method can accurately recognize the surface characters of chips and meet the requirements of chip quality inspection.

Keywords: Template matching; Character recognition; SVM; OpenCV

Online publication: August 20, 2024

1. Introduction

The quality inspection of chip surface characters plays an important role in reducing manufacturing defects and improving the quality and reliability of chip products. In chip surface character recognition, commonly used methods include template matching, feature extraction, deep learning, and statistical model-based methods. The template matching method determines the best matching character by matching it with predefined character templates [1,2]. This method is suitable for situations where the character shape is regular and the background interference is small. It performs character recognition by comparing the similarity with the template. The method based on feature extraction usually extracts the shape, texture, edge, and other features of characters, establishes feature vectors, and uses classifiers for character classification and recognition [3-6]. The method based on deep learning utilizes deep learning models such as Convolutional Neural Networks (CNN) or Recurrent Neural Networks (RNN) to learn and extract features from a large amount of data, thereby achieving recognition of chip characters [7-11]. Statistical model-based methods typically use Hidden Markov Models, Conditional Random Fields, and other models to model and recognize character sequences [12,13]. This article uses C++ programming language and the computer vision library OpenCV to achieve recognition of surface

characters on chips [14].

2. Chip vision system

Chip machine vision systems typically consist of computers, motion control modules, camera modules, etc. The images of the chips come from the production line, and the industrial camera model is MV-CU120-10GC, with a color resolution of 4,024 × 3,036. Chip surface character recognition includes image acquisition, chip image preprocessing, chip positioning, character region acquisition, character segmentation, and character recognition, as shown in **Figure 1**.

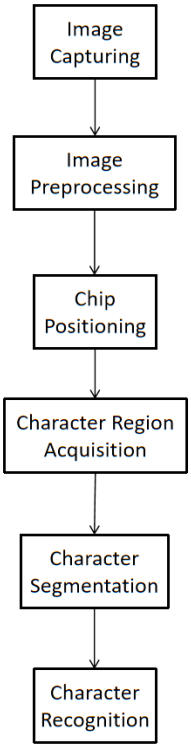


Figure 1. Chip surface character recognition process

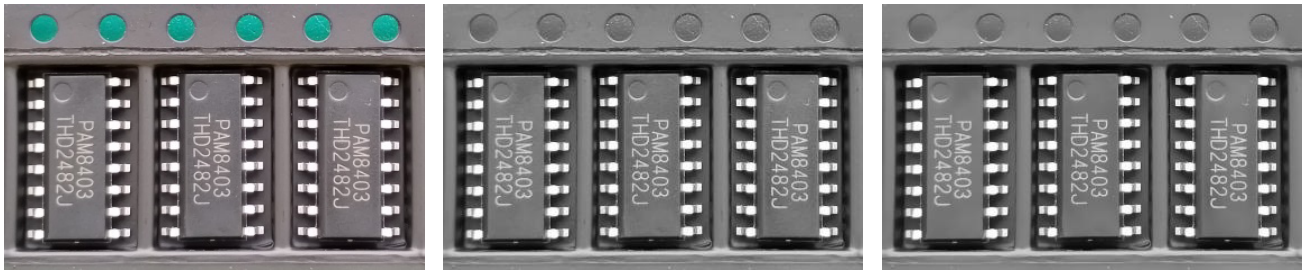
3. Chip image preprocessing

The purpose of chip image preprocessing is to reduce noise in the image, highlight character features, and thereby improve recognition accuracy and robustness. Chip image preprocessing includes image grayscale and image filtering. Image grayscale is the process of converting color images into grayscale images. In character recognition, only the brightness information of characters is usually considered. Grayscale can convert the red, green and blue (RGB) channel values of each pixel in a color image into a single grayscale value. This can not only reduce the dimensionality of the data and simplify the complexity of subsequent processing, but also better highlight the brightness differences of characters. For the chip image, the average weighting method is used to convert the image into a grayscale image, and the weighted values of the RGB three channels are 0.299, 0.587, and 0.114, respectively.

Due to the rich details of the chip image, bilateral filtering is used to enhance the chip image. Bilateral filtering is a non-linear filtering method, and its filter kernel consists of two functions: spatial domain

kernel and value domain kernel. It can not only remove noise but also protect image details. OpenCV provides the bilateral filter function to implement bilateral filtering operations. The specific method is: void cv::bilateralFilter(InputArray src,OutputArray dst,int d,double sigmaColor,double sigmaSpace,int borderType = BORDER_DEFAULT).

Figure 2 shows a comparison between converting the original image of the chip to grayscale and using bilateral filtering.



(a) Original image (b) Color to grayscale image (c) Bilateral filtered image

Figure 2. Chip image preprocessing

4. Chip positioning

Before performing character segmentation, it is necessary to locate the position of the chip in order to determine the position of the chip characters and improve detection speed. A method based on normalized cross-correlation is used to locate the chip. The normalized cross-correlation matching function in OpenCV is: void matchTemplate (InputArray image, InputArray template, OutputArray result, int method, InputArray mask=noArray()), where method=cv:: TM_CCOEFF_NORMED.**Figure 3** shows the effect of using this method for chip positioning.

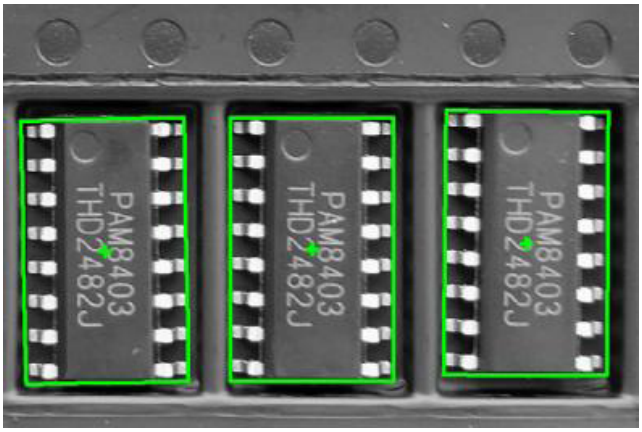


Figure 3. Chip positioning results

5. Chip surface character segmentation

5.1. Binarization of chip images

In character recognition, we usually only focus on the shape and edge information of characters. Here, we use

binarization technology to process chip images. Binarization is the process of converting a grayscale image into a black and white binary image. Through binarization, the pixel values in the grayscale image can be segmented according to a threshold. Pixels with brightness higher than the threshold are set to white (255), and pixels with brightness lower than the threshold are set to black (0). This can better highlight the edges and contours of characters, making it easier for subsequent character segmentation and recognition.

5.2. Morphological filtering

Morphological filtering is a series of shape-based image processing operations commonly used in Digital Image Processing [15]. Since there will be slight fractures on the characters on the chip surface, we can use the closing operation to deal with it. The calculation process of closed operations is to first expand and then corrode. It can connect adjacent pixels, fill small holes in the target, and smooth the boundaries without significantly changing the area of the region. The function of morphological filtering in OpenCV is: void morphologyEx (InputArray src, OutputArray dst, int op, InputArray kernel, Point anchor=Point (-1, -1), int iterations=1, int borderType=BORDER_CONSTENT, const Scalar&borderValue=morphologyDefault BorderValue). When using a closed operation, the parameter op is MORPH_CLOSE.

5.3. Character segmentation

In chip surface character recognition, characters are usually arranged consecutively together with small intervals between them. To accurately recognize each character, it is necessary to segment the character from the image and use it as a separate image block for training and feature acquisition. This system adopts a contour based character segmentation method, using the functions provided by the OpenCV image processing library, findContours and boundingRect. These two functions can find the character contours in the image and determine the bounding boxes of each character. Their definitions are as follows:

findContours(binaryImage,contours,RETR_EXTERNAL,CHAIN_APPROX_SIMPLE);

boundingRect (InputArray array);

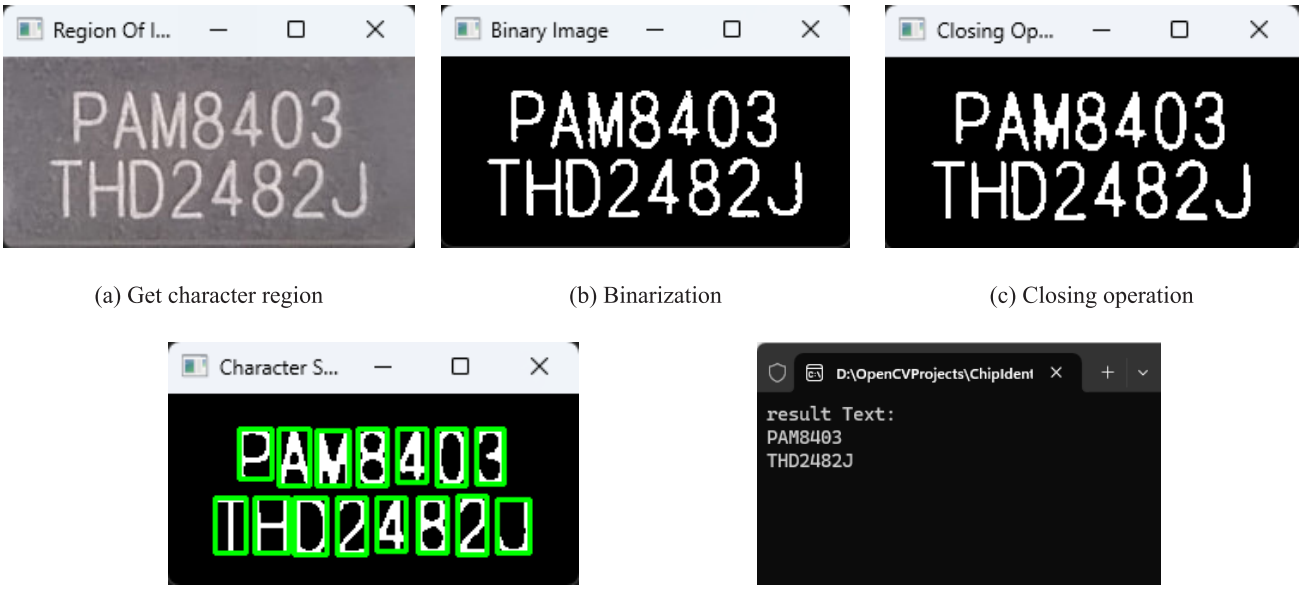
The findContours function takes a binary image as input and returns a vector containing all contours. A contour is a closed curve composed of a series of points that surround the edges of a character. By traversing the contour vector, the contour information of each character can be obtained. The boundingRect function takes the contour as input and returns a rectangular box that completely surrounds the contour. By calculating the bounding boxes of each contour, the position and size of each character can be obtained. However, not all contours represent characters, so when performing character segmentation, it is necessary to add some filtering conditions to remove inappropriate bounding boxes. Filtering is performed by setting the minimum width, minimum height, and aspect ratio to select the character bounding boxes that meet the conditions, and ultimately obtain the character segmentation result.The core code for character segmentation is as follows:

```
vector<vector<Point>> contours; vector<cv::Rect> charRects; Mat colorImage;
findContours(closing, contours, RETR_EXTERNAL, CHAIN_APPROX_SIMPLE);
int minWidth = 10; int minHeight = 10; float aspectRatioMin = 0.2; float aspectRatioMax =2;
cvtColor(closing, colorImage, COLOR_GRAY2BGR);
for (const auto& contour : contours)
 {
   Rect rect = cv::boundingRect(contour);
   if (rect.width >= minWidth && rect.height >= minHeight)
   {
```

```
            float aspectRatio = static_cast<float>(rect.width) / rect.height;
            if (aspectRatio >= aspectRatioMin && aspectRatio <= aspectRatioMax)
            {
                charRects.push_back(rect);
                rectangle(image, rect, cv::Scalar(0, 255, 0), 2);
                rectangle(colorImage, rect, cv::Scalar(0, 255, 0), 2);
            }
        }
    }
```

6. Surface character recognition

Through the previous processing, images containing individual characters have been obtained, and then these character images can be classified and recognized. A Support Vector Machine (SVM) is used to classify the surface characters of the chip. Support Vector Machine (SVM) is a supervised learning algorithm widely used in the fields of pattern recognition, machine learning, and data mining. The core idea of a support vector machine is an optimal decision hyperplane that maximizes the interval between classification boundaries and sample points, effectively separating sample points of different categories. SVM can effectively handle nonlinear problems, is suitable for high-dimensional spatial data classification, and the model is relatively simple and easy to implement. In addition, the choice of SVM kernel function is also very important. The kernels of SVM include linear kernel function (linear), polynomial kernel function (poly), radial basis kernel function (RBF), and sigmoid kernel function. Through testing, when the kernel function is selected as "RBF", the recognition rate is highest, so the radial basis function is chosen here. This experiment was conducted under the conditions of Inter (R) Core (TM) i5-7500 CPU @ 3.40 GHz, 16 GB memory, and SSD256G. **Figure 4** shows the recognition results of the chip's surface characters.



(a) Get character region (b) Binarization (c) Closing operation

(d) Character segmentation (e) Recognition results

Figure 4. Chip character recognition

7. Conclusion

This article focuses on the recognition of printed characters on the surface of chips and implements an efficient and accurate recognition method using C++ language combined with the OpenCV library. After testing, it can meet the needs of detection and provide reliable assurance for quality control in the field of microelectronics manufacturing. However, due to the rich font styles and inconsistent character sizes on the chip surface, there is no unified standard. To further improve the robustness of character recognition, the next step will be to train a large number of custom character models to adapt to more character sets and application scenarios.

Funding

Henan Province Science and Technology Research Project "Key Technologies for Intelligent Recognition of Chip Surface Defects Based on Machine Vision" (Project No. 242102210161).

Disclosure statement

The author declares no conflict of interest.

References

[1] Zhao J, Chen W, Li G, et al., 2022, Research on Template Matching Character Wheel Recognition Method Based on Canny Operator. Instrumentation Technology, 2022(01): 48–52.

[2] Wang S, Liu G, Li J, et al., 2024, Research on License Plate Character Recognition Algorithm Based on Template Matching. Journal of Wuhan Institute of Shipbuilding Technology, 23(01): 97–102.

[3] Hu L, Sun H, Fan A, 2013, Research on Feature Extraction in Handwritten Character Recognition. Automation & Instrumentation, 2013(02): 15–17.

[4] Huang F, Li X, Wang K, et al., 2023, Diode Character Recognition Based on Grayscale Co-Occurrence Matrix Texture Features and MLP. Journal of Jiangsu University of Technology, 29(02): 64–71.

[5] Yang M, Chen L, Zheng B, 2012, Character Recognition Feature Extraction Based on Lifting Wavelet. Journal of Jilin Institute of Chemical Technology, 29(11): 97–99.

[6] Zhu S, 2014, Research on License Plate Recognition Algorithm Based on Character Multi-Feature Extraction, thesis, Central South University.

[7] Yu Z, 2023, Research on Circuit Board Character Detection Method Based on Deep Learning, thesis, Jiangnan University.

[8] Weng L, Liu L, 2023, Application of Machine Vision Based on Deep Learning in Industrial Instrument Inspection. Intelligent Manufacturing, 2023(05): 40–44.

[9] Zhang C, 2016, Character Recognition Based on Deep Learning, thesis, University of Electronic Science and Technology of China.

[10] Li J, 2023, Research on Inkjet Character Recognition and Verification Based on Deep Learning, thesis, Fujian University of Technology.

[11] Wang R, Ma W, 2021, Character Recognition Algorithm Based on BP Network. Modern Computer, 27(24): 47–50.

[12] Wang X, 2013, Offline Handwritten Chinese Character Recognition Based on BP Neural Network and HMM Hybrid Model, thesis, Tianjin Normal University.

[13] Yang Y, 2013, Research on Image Classification Method Based on Conditional Random Fields, thesis, East China

Normal University.

[14] Mao X, Leng X, Deng, 2015, Introduction to OpenCV3 Programming. Electronic Industry Press, Beijing.

[15] Gonzalez RC, Woods RE, 2020, Digital Image Processing (Fourth Edition). Pearson, London.

Publisher's note

Bio-Byword Scientific Publishing remains neutral with regard to jurisdictional claims in published maps and institutional affiliations.

Journal of Electronic Research and Application, 2024, Volume 8, Issue 4
http://ojs.bbwpublisher.com/index.php/JERA
ISSN Online: 2208-3510
ISSN Print: 2208-3502

Research on the Practice of Cross-Border E-Commerce Strategies: Taking Alibaba International Station as an Example

Jiong'en Xiao[1], Xiaosha He[2]*, Yiyang Lu[1]

[1]International Business School of Guangdong University of Finance and Economics, Guangzhou 510320, Guangdong Province, China

[2]School of Accounting, Guangzhou University of Business, Guangzhou 511363, Guangdong Province, China

Corresponding author: Xiaosha He, 20230125@gcc.edu.cn

Copyright: © 2024 Author(s). This is an open-access article distributed under the terms of the Creative Commons Attribution License (CC BY 4.0), permitting distribution and reproduction in any medium, provided the original work is cited.

Abstract: Currently, Alibaba International Station, as an emerging e-commerce platform in recent years, plays a crucial role in cross-border e-commerce trade. This article describes an overview of Alibaba International Station, as well as the methods of attracting traffic and some current problems encountered. Simultaneously, relevant suggestions are provided based on the problems.

Keywords: Alibaba International Station; Drainage; User

Online publication: August 12, 2024

1. Introduction to Alibaba International Station

Alibaba International Station, as a new emerging force in the field of e-commerce in recent years, is playing an increasingly important role in cross-border e-commerce trade [1]. The Alibaba International Station is mainly composed of platform rules, cross-border e-commerce platforms, dual-tier market operations, and cross-border risk control systems, ensuring the shopping experience of consumers and sellers in the cross-border e-commerce process.

Platform rules are the foundation of Alibaba International Station's operation, including general rules, content and information publishing rules, transaction rules, supply chain regulations, and other regulations. These rules provide clear guidance and constraints for the behavior of sellers and buyers on the platform, ensuring fairness, impartiality, and transparency of the platform. As a cross-border e-commerce platform under the Alibaba Group, it operates under the "merchant + overseas warehouse" model, providing one-stop cross-border e-commerce services for domestic and foreign merchants [2]. Merchants can display products on the platform to achieve direct transactions of goods between domestic and foreign customers, while overseas warehouses provide trade services to support customers' cross-border trade. Through a dual market operation model, it provides a massive commodity procurement business in one market to meet the diverse procurement

needs of buyers. Providing convenient service sales business in another market to help sellers promote and sell products more efficiently, aiming to provide customers with a convenient, fast, safe, and reliable procurement experience.

2. How to attract traffic to Alibaba International Station

Traffic is the foundation for the survival and development of cross-border e-commerce websites [3]. In the fiercely competitive e-commerce market, no traffic means no users, and websites lose their meaning of existence. Acquiring traffic is the primary task of website operation. Only with sufficient traffic can a website have more opportunities to showcase products, attract potential customers, and achieve sales and profitability. Simultaneously, by obtaining a large amount of traffic, the website can expand its exposure range and improve brand awareness.

Alibaba International Station utilizes traffic for precise marketing and personalized recommendations. By analyzing data such as traffic sources, user behavior, and interest preferences, websites can more accurately understand user needs, develop more precise marketing strategies, and provide personalized recommendation services [4]. This can not only improve user satisfaction and conversion rates but also enhance the engagement between users and websites, promoting long-term cooperation and repeat purchases. Additionally, Alibaba International Station is a necessary condition for achieving business growth and expansion through traffic acquisition. With the increase in traffic, the user base of the website will continue to expand, bringing more sales opportunities and growth potential.

2.1. Search traffic optimization

This is the main source of store traffic. By optimizing search rankings, we can increase the exposure of our store and products, thereby attracting more potential customers. This includes keyword optimization, image optimization, product description optimization, etc., to improve the website's ranking on search engines and increase organic traffic [5].

2.2. Shopping guide venue and channel activities

Pay attention to the activities of the international platform, such as the annual March and September procurement festivals. Actively participate in these events and meet their requirements to gain more exposure opportunities. Additionally, stay informed about official activities and consistently accumulate product data to achieve a higher ranking in these events.

2.3. Customer inquiry utilization with RFQ

Request for Quotation (RFQ) is one of the customer acquisition channels, especially for niche industries, where its value is more prominent. Sellers can regularly review and respond to RFQs to attract potential customers. In addition, if the RFQ recommended by the system is inaccurate or insufficient, subscription categories can be set in the business opportunity subscription, and subscription key questions can be added to obtain more accurate RFQs [6].

2.4. Visitor marketing

Through the visitor details function, sellers can view, filter countries and regions, and actively market potential customers. Moreover, for customers who have initiated inquiries or consultations, this feature can also be used for further communication and marketing [7].

2.5. Online and offline marketing promotion

Utilize online channels such as marketing in social media, email, and search engines for advertising and promotional activities. Furthermore, offline participation in relevant industry exhibitions and holding offline promotion activities can increase brand awareness and exposure.

2.6. Cross-border e-commerce cooperation

Collaborate with other cross-border e-commerce platforms to achieve traffic exchange. This can attract more users to visit Alibaba International Station through collaborative promotion and mutual benefit [8].

3. The current problems faced by Alibaba International Station

3.1. Low user activity

As an e-commerce platform targeting the global market, although Alibaba International Station has a large number of registered users, low user activity has always been a major challenge [9]. This is mainly manifested in two aspects: Firstly, the growth of traffic is limited, and as the market gradually saturates, obtaining new traffic becomes increasingly difficult. Secondly, a shortage of high-quality buyers. Although there are many new and small buyers, their purchasing power and frequency are relatively low, and their contribution to the platform is also negligible. These situations has made it extremely difficult for Alibaba International to attract and retain high-quality buyers, not only affecting the overall transaction activity of the platform but also limiting its further potential in development.

3.2. Increasing cost of promotion

With the increase in market competition, the cost of promoting Alibaba International Station is constantly rising [10]. In the current period of traffic stock, advertising has become the main means for businesses to obtain exposure and traffic, but it also brings high promotion costs. Merchants need to achieve efficient promotion within a limited budget to attract more potential customers, which undoubtedly increases their business pressure. In addition, with the intensification of advertising competition, advertising effectiveness may also be affected to a certain extent, making merchants face greater challenges in promotion.

3.3. User source is affected

With the development of the global Internet, the diversification trend of overseas customer development channels is becoming more and more obvious [11]. In addition to traditional e-commerce platforms, various customer-end platforms such as short videos, live streaming, and independent websites are also rapidly rising, becoming new channels for customers to find sources of goods. This requires Alibaba International to face more diversified competition, not only competing with similar e-commerce platforms but also with various emerging customer-end platforms. Meanwhile, with changes in the way customers search for sources of goods, the existing customer resources of Alibaba International may also be diluted, further affecting its user activity and transaction volume. Therefore, how to adapt to this change and expand new user sources has become an urgent problem that Alibaba International Station needs to solve.

4. Solutions to overcome problems at Alibaba International Station

4.1. Improve user experience and activity

(1) Optimize user interface and interaction design

Ensure that the interface of the platform is concise, intuitive, and easy to use [12]. Additionally, iterate and update based on user feedback to improve user satisfaction. This can be done by benchmarking against mainstream e-commerce platforms, optimizing the interface to better suit the preferences of young and existing consumers, and improving the shopping experience for users.

(2) Rich platform content

Provide high-quality product and industry information to attract users to browse and share. For example, industry columns and expert interpretation columns can be established to increase user engagement. Optimize the introduction and usage functions of the seller filter product information through measures; Provide real-time industry and product information for the platform [13].

(3) Strengthen social functions

Introducing social elements such as community forums, customer testimonials, and interactive reviews to encourage communication and interaction among users [14]. This helps to increase user engagement, and further enhance communication between users by strengthening the website's social functions, guiding them to bring traffic to the platform.

(4) Precision marketing and personalized recommendations

Analyze user behavior and preferences to increase their purchasing intention and satisfaction. Based on the analysis of user profiles for different users, provide personalized recommendation services, targeting the content that users are interested in, thereby achieving personalized websites, building the user's content portfolio, and improving the user experience.

4.2. Reduce promotion costs and improve promotion efficiency

(1) Optimize search engine optimization (SEO)

In order to improve the ranking of Alibaba International in search engines, we need to take a series of SEO optimization measures [15]. Firstly, conduct keyword research to identify keywords that are highly relevant to the platform's business and have a high search volume, and layout them reasonably at key positions such as the website's title, description, and content. Secondly, continuously publish high-quality and valuable content to not only meet the needs of users but also enhance visibility for search engine spiders to crawl and index, thereby improving the website's weight and ranking. Moreover, we focus on optimizing website structure and internal links to ensure that users can easily find the information they need and improve the user experience. Finally, actively build external links by establishing links with other high-quality websites, and improve the website's visibility and influence.

(2) Precise advertising placement

By utilizing the advertising system of Alibaba International, we can accurately target users and improve the click-through and conversion rates of advertisements. Firstly, through data analysis and market research, identify the characteristics and needs of target users, and develop targeted advertising strategies. Secondly, choose appropriate advertising spaces and forms, such as search, display, and video advertisements, etc., to maximize the attention of target users. In addition, continuously optimizing advertising creativity and copywriting to ensure that the content accurately conveys the value of products or services, and increases user purchasing intention. Finally, by real-time monitoring of advertising effectiveness, adjusting advertising strategies, reducing advertising costs, and improving advertising effectiveness.

(3) Collaboration and alliance marketing

Collaborating with other relevant platforms or institutions to jointly promote products and services is an effective way to expand brand influence and user coverage. Looking for influential partners related to Alibaba's

international website business, such as industry media, well-known bloggers, opinion leaders, etc., to establish cooperative relationships. By jointly organizing events, sharing resources, and other means, we can jointly promote products and services, and enhance brand awareness and user engagement. At the same time, alliances can be established with other e-commerce platforms or institutions to share user data and traffic resources, achieving mutual benefit and win-win outcomes.

(4) Utilize emerging channels such as short videos and live-streaming

With the rise of new media such as short videos and live streaming, these channels have become important platforms for attracting user attention and interaction. Alibaba International Station can actively utilize these emerging channels to attract traffic. Firstly, publish product-related short video content on short video platforms, such as product introductions, user tutorials, industry trends, etc., to attract user attention and likes. Secondly, by using live streaming to showcase and promote products, through the host's explanation and demonstration, users can have a more intuitive understanding of the characteristics and advantages of the product. Furthermore, industry experts or celebrities can be invited for live-streaming sessions to enhance the product attraction. Finally, guide short videos and live content to Alibaba International Station platform for purchase or consultation, achieving traffic conversion.

5. Conclusion

Alibaba International Station actively responds to market competition through a series of innovative strategies. Optimizing user experience, enriching platform content, strengthening social functions, and precision marketing have effectively increased user engagement and satisfaction. Concurrently, through search engine optimization, precise advertising placement, cooperation and alliance marketing, and the use of emerging channels, the promotion cost has been reduced and the promotion efficiency has been improved. In addition, international social media marketing and cross-border e-commerce platform cooperation have also expanded new user sources for the platform and enhanced brand influence. These measures have jointly promoted the sustainable development of Alibaba International Station and gain more competitive advantages in the fierce international e-commerce market.

Funding

Humanities and Social Sciences Fund of the Ministry of Education, "Research and Implementation Suggestions on Collaborative Case Handling of Political and Legal Cross-departmental Data Sharing under the Background of Rapid Development of Artificial Intelligence" (Project No. 22YJC630167)

Disclosure statement

The authors declare no conflict of interest.

References

[1] Huang W, 2022, Web Content Construction of B2B Cross-Border E-Commerce Enterprises from a Multimodal Perspective, thesis, Southwest University of Finance and Economics.

[2] Hu C, Zheng C, Luo Y, et al., 2023, Research on the Problems and Countermeasures of Domestic Enterprises Developing Cross-Border E-Commerce–Taking Alibaba International Station as an Example. Modern Commerce and

Industry, 44(23): 20–22.

[3] Li X, 2023, Analysis of Alibaba International Station Marketing Discourse from the Perspective of Linguistic Economics. Chinese and Foreign Corporate Culture, 2023(08): 109–111.

[4] Huang S, 2024, Research on Cross-Border E-commerce Live Streaming Marketing Based on International Station Platforms–Taking Alibaba International Station Live Streaming Luggage Stores as an Example. Brand Marketing of Time honored Brands, 2024(03): 36–38.

[5] Xu Z, 2022, Analysis of the Marketing Model of Independent Export Cross-Border E-Commerce Stations, thesis, Jilin University.

[6] Shi H, 2024, The Impact of User Generated Content on Consumer Behavior Intention on Cross-Border E-Commerce Platforms. Journal of Xi'an University of Electronic Science and Technology (Social Science Edition), 34(01): 72–81.

[7] Wang F, Zhang Y, 2024, Analysis of Diversion Strategies for Independent Cross-border E-commerce Stations. Foreign Economic and Trade Practice, 42(01): 63–67 + 73.

[8] Wu J, Liu C, 2023, Research on the Strategy of Introducing Independent Websites for Cross-Border E-Commerce Enterprises Considering Brand Promotion. Journal of Dali University, 8(12): 79–87.

[9] Lai Y, Wu M, Cai Q, et al., 2023, Practice and Research on the Transformation of Traditional Cross-Border E-Commerce Platform Models to Independent Sites Under the New Development Pattern of Dual Circulation. China Business Review, 2023(23): 14–17. https://doi.org/10.19699/j.cnki.issn2096-0298.2023.23.014

[10] Xu J, Cha Y, 2023, Research on the Development Strategy of Agricultural Product Live Streaming Business on Cross-border E-commerce Platforms–Taking S Platform as an Example. Modern Commerce and Industry, 44(21): 61–63. https://doi.org/10.19311/j.cnki.1672-3198.2023.21.020

[11] Ke T, 2023, Research on Marketing Strategy of SD Company's Amazon US Site Store, thesis, University of Electronic Science and Technology of China. https://doi.org/10.27005/d.cnki.gdzku.2023.005906

[12] Li Q, Zhao H, 2023, Marketing Research on Amazon Cross-Border E-commerce Platform–Taking a Certain Company as an Example. Industrial Innovation Research, 2023(13): 73–75.

[13] Shen Y, 2023, Exploration of operational issues and improvement strategies for small and medium-sized cross-border e-commerce enterprises in the new era. Chinese and Foreign Corporate Culture, 2023(06): 126–128.

[14] Li M, 2023, Research on Marketing Strategy of Cross-border E-commerce KL Company, thesis, Qingdao University of Science and Technology.

[15] Dong X, 2023, Research on Optimization Strategies for Cross-border E-commerce Live Streaming Marketing of Company A, thesis, Guangxi University, 2023.

Publisher's note

Bio-Byword Scientific Publishing remains neutral with regard to jurisdictional claims in published maps and institutional affiliations.

Journal of Electronic Research and Application, 2024, Volume 8, Issue 4
http://ojs.bbwpublisher.com/index.php/JERA
ISSN Online: 2208-3510
ISSN Print: 2208-3502

Research on Electrical Automation Control Design Based on PLC Technology

He Yu*

Guangxi Electrical Polytechnic Institute, Nanning 530007, Guangxi Zhuang Autonomous Region, China

***Corresponding author:** He Yu, thinf@sina.com

Copyright: © 2024 Author(s). This is an open-access article distributed under the terms of the Creative Commons Attribution License (CC BY 4.0), permitting distribution and reproduction in any medium, provided the original work is cited.

Abstract: As science and technology continue to progress forward, electrical automation engineering is also developing, of which programmable logic controller (PLC) technology is widely being used. Through the integration of PLC technology and traditional electrical automation technology, good development of modern science and technology is promoted while traditional automation is preserved. The development of electrical engineering can greatly improve the strength of science, technology, and economy in our country. Based on PLC technology, this paper analyzes the design of electrical automation control.

Keywords: PLC technology; Electrical automation control; Design

Online publication: August 12, 2024

1. Introduction

Programmable logic controller (PLC) refers to a programmable memory that is applied to the internal storage program, the real timing, logic operations, and counting activities. In the field of electrical automation control, leveraging PLC technology can effectively showcase the advanced scientific and technological capabilities in overseas furniture. In the recent developing era, the application of electrical engineering automation technology is becoming more and more extensive. Among them, PLC technology has become the mainstream technology in electrical automation control.

2. PLC technology concept

PLC technology begins from engineering requirements, develops the corresponding control strategy, and better achieves sequence control and logic operations. This technology combines computers with traditional control technology, which is different from other control technologies such as single-chip microcomputers. It can effectively carry out logical control with the help of software, and it is relatively simple in the process of configuration and parameter change, which can meet the development needs of electrical engineering. PLC technology originated in the United States. After years of development, it is used worldwide. It has a very

significant impact on electrical automation control technology as it progresses further. The application of PLC technology helps to carry out electrical automation control, thus greatly reducing the input of manpower and material resources, and lowering the cost of construction. PLC control technology includes two types: module and box type. The module type consists of the power module, input/output (I/O) module, and memory. The box type includes the power supply, display board, and memory. The selection of an appropriate central processing unit (CPU) is based on the system performance requirements to meet the demands of electrical engineering. The two system structures each have distinct advantages, but both utilize the open bus structure. The primary feature of the modular structure is its ability to facilitate system expansion based on practical engineering needs [1].

In the application process of modern engineering, PLC technology has many advantages. Firstly, PLC technology has strong anti-interference ability, which can cope with the system control needs in different situations and meet all kinds of working conditions. Secondly, PLC technology has a very wide range of applications. It has been widely used in the medical, electrical, and aviation fields. Thirdly, PLC technology is compact in size. It can effectively save space, thus promoting the miniaturization development of automation control systems. Finally, PLC technology offers significant advantages in maintenance. It excels in data processing, logic control, and other functions to effectively meet the automation control needs of electrical engineering [2,3].

3. Design principles of electrical automation control

3.1. Design principle

In the design process of an electrical automation control system, the following principles need to be observed to ensure the reliability and effectiveness of the system. Firstly, follow the principle of integration. Individual components such as sensors, controllers, etc., can be seamlessly integrated to form a coordinated system. Secondly, follow the principle of modularity. The system needs to have good scalability and flexibility, to facilitate subsequent upgrades and maintenance. Thirdly, follow the principle of user-friendliness. In the design activities, it is necessary to pay attention to the optimization of the system interface, so that it is more intuitive, understandable, and convenient for the operator to carry out management and control. Finally, implement the principle of maximization of economy and benefit. This principle pays attention to cost control and resource optimization to provide a guarantee for the achievement of economic benefits. By following the above principles, you can design a more efficient, stable, and easy-to-maintain automated control system. These principles guide the system design framework, ensuring it can adapt to evolving technological and market needs [4-6].

3.2. The importance of system characteristics

Reliability, safety, and efficiency are the important characteristics of the electrical automation control system.

In the electrical automation control system, reliability is the first factor to be considered. Through a reliable system, stable operation can be guaranteed, the time consumed by failure and downtime can be greatly reduced, and the continuity of the production process and product quality can be guaranteed so that it has consistency. Therefore, the system needs to have self-diagnosis and fault tolerance, to better cope with possible software and hardware problems [7,8].

Safety is an important aspect in need of high attention. The system must ensure the safety of operators and devices to prevent accidents. These include safety features such as emergency stop mechanisms and electrical isolation [9].

Efficiency directly impacts the system's performance and resource utilization. The construction of an efficient electrical automation control system can significantly enhance production efficiency and effectively

reduce energy and material waste. This promotes improved economic efficiency of enterprises while also supporting environmental conservation efforts.

4. Electrical automation control design based on PLC technology

4.1. Design sequence control for electrical engineering

In electrical engineering, sequence control is crucial, facilitated by the application of PLC technology, enabling effective control activities essential for modern societal development. PLC technology can be utilized specifically as a sequence controller. For example, in thermal energy power plants, PLC technology enables technicians to clean residue and dust from power generator furnaces. By replacing traditional sequence controllers, PLC technology significantly improves work and production efficiency during residue cleaning in thermal power generators. Enhanced efficiency plays a crucial role in power plant operations, where PLC technology ensures increased power generation efficiency. In the final stages of applying PLC technology, staff can focus on residue cleaning with enhanced management center and field data management capabilities. Adopting PLC technology in power plants substantially reduces production costs and labor demands. Technicians can monitor and control operations efficiently using control procedures, thereby boosting overall production efficiency. The sequence control flow of electrical engineering is shown in **Figure 1** [10].

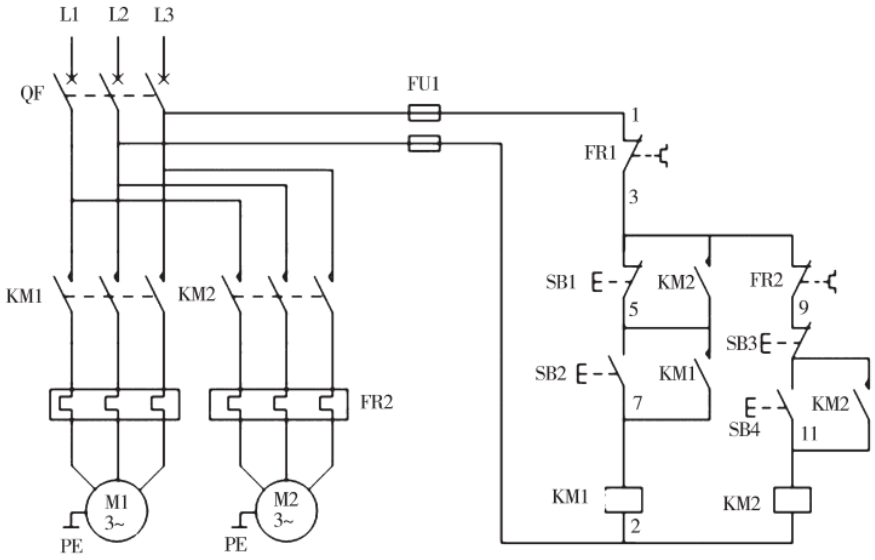


Figure 1. Sequence control flow of electrical engineering

4.2. Design switching quantities for electrical engineering

In the application of PLC technology, switching control plays a pivotal role. PLC technology demonstrates significant advantages in achieving effective switching control. Its primary objective is to leverage programmable memory for enhanced relay application, thereby effectively replacing traditional mechanical relays. When using virtual relays, improving reaction speed is crucial. The negligible reaction time of virtual relays allows for more precise control over switching quantities. PLC technology effectively addresses the issue of slow response times in traditional relay-based electrical control operations. It facilitates automatic switching, ensuring reliable relay connections, safeguards electrical systems, and migrates risks such as short circuits. In short, PLC technology resolves issues inherent in traditional control methods within electrical automation. By effectively addressing these challenges, it ensures improvements in the level of electrical automation control [11-13].

4.3. Program control design

In program control design, attention must be given to the configuration of various modules, including the organization and control modules. The organization module acts as the interface between the operating system and the user program, facilitating system calls, and managing loops and driver modules. Cyclic program processing is a key aspect of PLC technology, involving the execution of the main program and its organization block. The user program within the organization block achieves cyclic execution, meeting the programming requirements through function modules. This dynamic display subroutines ensures effective implementation.

Additionally, during loop execution, the display bit increments with each cycle. When the display bit exceeds 8, it resets to 0, facilitating dynamic visualization of the loop call and showcasing data dynamics.

5. PLC technology under the electrical automation control project case

5.1. Case overview

This case study focuses on a state-owned manufacturing enterprise that initiated a workshop renovation project to promote production efficiency and quality. The core of the project is the integration of PLC technology in the automation control system to improve workshop management and ensure smooth production processes [14].

5.2. System implementation

In the electrical automation control system, PLC and automation technology are primarily used to enable the automatic transportation of raw materials and precise machine control to ensure the automatic sorting of finished products. By connecting sensors and monitoring equipment in the workshop, production data can be collected in real-time, allowing for continuous supervision and control during the production process. As shown in **Table 1**, the application of PLC technology in this case study has increased production efficiency by 50%, mainly due to the reduction of time, automatic processes, and prevention of errors from manual operation. Additionally, the failure rate has been reduced to 2%, attributed to the great precision and optimized failure management capabilities of PLC technology. Therefore, the reduction in energy consumption highlights the importance of automated control systems in improving production efficiency. Following implementation, employee satisfaction improved due to reduced work intensity, creating a safer and more comfortable working environment. These achievements highlight the significant impact of PLC technology.

Table 1. Production changes of intelligent manufacturing workshop

Index	Before modification	After transformation	Improvement ratio
Production efficiency	100 units/hour	150 units/hour	+ 50%
Failure rate	5%	2%	- 60%
Energy consumption	100 units/production unit	80 units/production units	- 20%
Employee satisfaction	70%	85%	+ 15%

6. The advantages of PLC technology in electrical automation control

6.1. Improve anti-interference capability

With continuous economic development, PLC technology has been widely adopted in the electrical engineering industry to enhance its anti-interference capabilities. Technical personnel, responding to the needs of the modern era, have set higher standards for PLC technology. The integration of isolation transformers and radio

wave signal filtering equipment in electrical automation control systems optimizes the use of PLC technology. Consequently, the level and efficiency of electrical automation control will affect social development and internal competitiveness. The anti-interference ability of PLC technology is crucial for improving an enterprise's competitiveness [15].

6.2. Development of network digitization

In the current era, although economic technological improvements have faced challenges, PLC technology has advanced significantly, driving electrical automation control toward greater intelligence. As the knowledge economy accelerates, PLC technology is increasingly applied in electrical automation, fostering network digitization. Technical staff can focus on societal needs by adjusting network digital systems and digital programming, thereby showcasing the advantages of PLC technology, and promoting the development of electrical automation management.

6.3. Enable advanced perception and decision-making

The introduction of visual neural network extends PLC capabilities beyond the traditional logic control. With visual neural networks, PLCs can perform real-time recognition and analysis of visual images. For example, on a production line, PLCs integrated with visual neural networks can accurately detect the quality, shape, or position of a product, enabling automated quality control and positioning. They can also handle complex visual tasks such as pattern recognition and object classification. This enhances the PLC's ability to adapt to different production needs and environments, thus improving production efficiency and product quality.

7. Closing remarks

In summary, PLC technology demonstrates its universality and efficiency in the field of electrical automation control, promoting industrial automation and intelligent manufacturing. With continuous technological and market development ongoing research and innovation are essential. PLC technology must continue to evolve, aligning with industry trends to optimize processes, enhance competitiveness, and support the healthy development of the industry.

Funding

2021 Guangxi Electrical Polytechnic Institute Scientific Research Capability Enhancement Project: Research and development based on Siemens 1200 Visual Material Sorting device (Project No. 2021KY03)

Disclosure statement

The author declares no conflict of interest.

References

[1] Guo D, 2023, Research on Electrical Control Application Based on PLC Automation Technology. Journal of Information Recording Materials, 24(7): 65–67.

[2] Shan Z, Fu J, Electrical Engineering Automation Control Design Based on PLC. Office Automation, 28(14): 7–9.

[3] Liu X, Wang B, Hou D, 2023, Application Research of Electrical Automation Control Based on PLC Technology.

Electrical Technology & Economics, 2023(6): 126–128.

[4] Gong B, 2023, The Application of PLC Technology in the Electric Instrument Automation Control. Building Development, 7(2): 10–12. https://doi.org/10.12238/bd.V7i2.4035

[5] Zhu S, 2023, Research on the Application of PLC Technology in Mechanical Electrical Control Device. Mechanical and Electronic Control Engineering, 5(3): 182–184. https://doi.org/10.37155/2717-5197-0503-61

[6] Lu S, 2023, Research on Electrical Automatic Control of Mechanical Equipment Based on PLC. Paper Making Equipment and Materials, 52(1): 32–34.

[7] Zhong J, 2023, Application Analysis of Electrical Equipment Automation Control Based on PLC Technology. China Equipment Engineering, 2023(20): 233–235.

[8] Wu J, 2023, Application Analysis of PLC Technology in Electrical Engineering Automation Control. Science and Technology in China, 2023(23): 109–111.

[9] Yin J, 2024, Analysis of Automatic Electrical Control Technology Based on PLC. Electronic Technology, 2024(001): 053.

[10] Bai Q, 2024, Application of PLC Technology in Electrical Engineering Automation Control. Electric Power Equipment Management, 000(002): 176–178.

[11] Tao Y, 2023, Application of PLC in Engineering Automation Control Design. Integrated Circuit Applications, 40(1): 56–57.

[12] Zhu F, 2023, Exploring the Application of PLC Technology in Electrical Automation Control. Times Automobile, 2023(8): 7–9.

[13] Ren H, Xu TP, Ju XC, 2023, Application research of Plc Technology in Electrical Automation Control, 000(006): 0161–0164.

[14] Fan W, Chen Z, Cao Z, 2023, Application of PLC Technology in Electrical Automation Control. Paper Making Equipment and Materials, 52(6): 125–127.

[15] Jiao L, 2023, Application of PLC Technology in Automatic Control of Electrical Equipment. Automation Today, 2023(6): 1–3.

Publisher's note

Bio-Byword Scientific Publishing remains neutral with regard to jurisdictional claims in published maps and institutional affiliations.

Journal of Electronic Research and Application, 2024, Volume 8, Issue 4
http://ojs.bbwpublisher.com/index.php/JERA
ISSN Online: 2208-3510
ISSN Print: 2208-3502

The Application of Intelligent Lighting in Thermal Power Plants

Xiaozhong Kang*, Shuangqiang Liu, Guoqing Hu, Haibin Huang

Guoneng (Quanzhou) Thermal Power Co., Ltd., Quanzhou 362804, China

Corresponding author: Xiaozhong Kang, 12021947@chnenergy.com.cn

Copyright: © 2024 Author(s). This is an open-access article distributed under the terms of the Creative Commons Attribution License (CC BY 4.0), permitting distribution and reproduction in any medium, provided the original work is cited.

Abstract: With the rapid development of electronic information technology, the Internet of Things (IoT), Internet technology, and modern communication technology, people are demanding higher standards for the building environment. Especially in modern large-scale buildings with high levels of industrialization, lighting systems should also be optimized accordingly. This article explores the application path of intelligent lighting in thermal power plants for reference.

Keywords: Intelligent lighting; Thermal power plants; Application path

Online publication: August 12,2024

1. Introduction

The intelligent lighting system mainly combines lighting control with various technologies which are computer networks, network communication, power electronics, sensors, and automation. This also includes control of lighting fixtures such as switching, dimming, and timing through network signal transmission. Its main function is to automatically adjust the brightness of the lighting fixtures or turn them off according to necessity. It can also automatically adjust and control the lighting fixtures according to different seasons and weather conditions to conserve energy, reduce emissions, and lower maintenance costs. It also has network communication and information management functions.

2. Control requirements for intelligent lighting systems

Firstly, the intelligent lighting control system can achieve real-time control of on-site lighting, including illumination, lighting time, brightness adjustment, etc., which can be automatically adjusted as needed. Secondly, the system allows lighting to be adjusted according to on-site conditions, times, and locations, achieving energy-saving and environmental protection. Thirdly, remote monitoring and management of lighting can be achieved through network communication technology, facilitating office automation. Finally, the system uses the international standard transmission control protocol/internet protocol (TCP/IP) for easy integration into the automation control system, aiding in system configuration and maintenance.

3. The advantages of intelligent lighting systems

3.1. Intelligent control is simple and convenient

Traditional lighting systems require manual intervention, leading to issues such as labor waste, complex control circuits, and low lighting quality. With the continuous progress and development of science and technology, intelligent technology has impacted people's lives. Intelligent lighting systems offer a certain degree of flexibility and convenience in design and installation. Generally, intelligent lighting systems are divided into three parts: information collection, information transmission, and information processing. These systems can achieve intelligent control and energy conservation by monitoring and adjusting different environments. Additionally, the intelligent lighting system can also independently control the lighting. For example, it can centralize the control of the lighting in a room or area, achieving both separate and centralized control. This is a function that traditional lighting systems cannot achieve.

3.2. Protection of lighting fixtures, extended lifespan, and cost reduction

Intelligent lighting systems can protect lighting fixtures at different stages of use, extend their lifespan, and reduce maintenance costs. During normal operation, the system can automatically turn on the lighting fixtures according to the set program. In abnormal situations, the system can automatically cut off the power supply to avoid overheating and damage. When an abnormality is detected, the system can automatically turn off or on the lighting fixture based on certain logic. Additionally, the intelligent lighting system has a remote diagnosis function, allowing for remote diagnosis and maintenance. For example, in a factory where the lighting system frequently malfunctions, leading to reduced production efficiency or safety accidents, this diagnostic function can quickly and effectively solve problems, improving both production efficiency and product quality.

3.3. Energy-saving and environmentally friendly

Energy conservation is an important indicator of lighting control systems. To achieve energy efficiency, multiple methods must be used, such as using dimmable and non-dimmable lighting fixtures. Dimmable lighting allows for controlling the brightness by making adjustments, while non-dimmable lighting changes the brightness by altering the on/off time of the light source or fixture. For example, a dimmable system can automatically adjust the brightness of lights based on environmental factors to save energy, whereas a non-dimmable system can only change the brightness by adjusting the switch time. Multiple lighting functions can be achieved by using different types of dimmers. Both dimmable and non-dimmable systems can be automatically adjusted according to environmental factors. The lighting control system can also use digital logic and analog signals for control to improve lighting quality and save electricity.

4. The main modes of intelligent lighting systems

4.1. Working mode

The working mode refers to the operation when the system is started. The system will first switch all the lights it controls in the order of the scene. When the system switches to the working scene, it will adjust all the lights involved in that scene accordingly. Similarly, when the system switches to accident lighting, it will adjust all the lights involved in that scene in the same order. When the system is in work mode and outdoor lighting is good (similar to indoor lighting), the intelligent lighting system will automatically adjust the brightness of the lights to meet the needs of the workers.

4.2. Adjust the illuminance according to different times and locations

Work mode refers to the operation of the intelligent lighting system during the day. The system will be fully turned on to maintain maximum illumination brightness in the lighting area. When the system detects someone entering or moving, it automatically adjusts the brightness of the lights to meet the requirements of the scene. In this mode, the entire illuminated area is at maximum brightness.

To ensure uniform illumination, it is generally necessary to divide the lamps into several groups. The illumination of each group can be controlled separately through a panel. Additionally, the illuminance of each group can be merged into one group and controlled with a single switch.

In daytime mode, indoor lighting will be adjusted from low light to a darker state. For frequently used areas such as stairwells, corridors, etc., high-brightness lighting is recommended to improve work efficiency. For larger indoor spaces such as offices and meeting rooms, medium or low-brightness lighting is recommended. Attention should be paid to the human body sensing system to ensure personnel safety. When all indoor lighting fixtures are turned off in night mode, significant energy savings can be achieved. Considering the short rest time of night workers, a small period (such as 7:00 pm–8:00 pm) should be set as a working period in night mode to ensure that the lighting area provides workers with a comfortable working environment to the maximum extent at night.

4.3. Accident lighting mode

The function of accident lighting is to provide timely warnings during emergencies such as fires, ensuring swift measures are taken. In environments like thermal power plants where electrical failures leading to power outages are common, restoring power promptly is essential to minimize disruptions to work and ensure safety. Therefore, it is necessary to immediately activate accident lighting when an accident occurs.

The accident lighting control system mainly consists of an automatic fire alarm system, fire detectors, emergency lighting controllers, etc. Upon detecting a fire, the fire detector activates audible and visual alarm signals and relays this information to the fire control room. Simultaneously, the automatic fire alarm system signals the emergency lighting controller to activate on-site emergency lighting fixtures. The controller manages the operation of these fixtures based on real-time conditions.

Emergency lighting activation relies on synchronized alarm and control signals. When a fire is detected, the fire detector triggers audible and visual alarms and communicates with the fire control room. It also sends signals to the emergency lighting controller, prompting it to illuminate emergency lighting fixtures on site. Control of the emergency lighting controller can be managed from the fire control room via keyboard or mouse, facilitating swift response to on-site issues and restoration of the power supply.

5. The main functions of intelligent lighting systems

5.1. Controlling lighting areas

Tailor electricity usage to regional specifics to achieve energy-saving goals and accomplish the following functions:

(1) Automatically adjust the lighting based on electricity usage to avoid unnecessary energy waste.

(2) Adjust lighting brightness according to the different requirements of each area at any time, ensuring the working environment and improving the lighting quality.

(3) Controlling the lights in specific areas to turn off at any time during emergencies, ensuring safety and energy conservation.

5.2. Illumination adjustments across different times and locations

The intelligent lighting system can regulate the lighting fixtures through computer control devices, and adjust its illumination according to different times and locations. Illumination adjustment mainly includes two aspects:

(1) During the day and night, the illumination can be adjusted according to different times and locations.

(2) At night, the illumination can be automatically adjusted based on the human body sensing.

5.3. Network communication and information management functions

The intelligent lighting control system adopts TCP/IP network protocol and can communicate and exchange information with an on-site programmable logic controller (PLC) and other automation systems. This network communication method can meet the information communication needs between different control units and higher-level monitoring computers. The network communication interface and management platform facilitate centralized control and remote monitoring of lighting areas.

5.4. Remote monitoring function

The intelligent lighting control system features remote monitoring and can manage lighting fixtures via computers. In addition, the system can be monitored for operational status and fault diagnosis through intelligent lighting controllers and various sensors. This provides real-time monitoring of the entire system. For example, you can switch to manual operation mode as needed at any time during emergencies.

5.5. Multiple modes and timed switch functions

According to the requirements of different regions and times, different intelligent lighting control methods can be set. For example, during the day, the lights in various areas can be turned off whereas at night, the lights are turned on based on the human body sensing. Under normal conditions, the lights in each area can be turned off as needed at any time. Additionally, the timed switch function can also be used to adjust the lighting switch time in various areas.

5.6. Strong anti-interference ability

When installing intelligent lighting controllers or sensors of different types, brands, quality levels, and price ranges in different areas, their anti-interference ability will vary significantly. For example, ballast isolation technology is suitable for dense installation positions of lighting fixtures while photoelectric isolation technology is more suitable for sparse installations. High voltage discharge technology applies to dense installations whereas surge absorption technology is effective for sparse installations. This enhances the anti-interference ability of intelligent lighting systems against various signals, including surges, electromagnetic interference, and signals from other sources.

6. Application of intelligent lighting systems in thermal power plants

6.1. Central control room

The central control room is the core area for the production and operation of thermal power plants and requires continuous on-duty management. It consists of three areas: the duty room, distribution room, and duty area. The duty room is located at the top of the central control room. The lighting supports the daily office tasks for duty personnel, as well as their safety readiness for emergencies. The distribution room is located below the duty room. The lighting in this area ensures equipment operates smoothly. The duty area is located below the distribution room. The lighting caters to the daily life of the duty personnel. Due to the large space in the control

room, the lighting system must be designed to meet specific needs. Intelligent lighting controllers installed in areas such as entrances and exits, stairwells, passages, and corridors ensure unified control over all light sources and fixtures throughout the control room, facilitating centralized management of the entire lighting system.

6.2. Using high-efficiency and long-life electric light sources

To meet the current requirements of energy conservation and emission reduction, the power industry continues to promote efficient and energy-saving electric light sources. Due to its characteristics, it is necessary to consider meeting the lifespan requirements of electric light sources during the design and construction stages. Generally, electric light sources with a lifespan exceeding 10,000 hours are required. From an energy conservation perspective, high-efficiency options like incandescent lamps, halogen tungsten lamps, etc. are the preferred choice. However, advancements in materials, technologies, and processes are driving the adoption of high-efficiency, long-life electro-optical sources, gradually replacing traditional lighting sources. Commonly used electric light sources in large industrial plants include high-pressure sodium lamps, metal halide lamps (mercury-containing or mercury-free), and gas discharge light sources (e.g., high-pressure mercury lamps, metal halide lamps). When selecting these sources, performance and applicability should be comprehensively considered to ensure lighting quality while minimizing electrical energy consumption. Furthermore, optimizing lighting fixture design, such as using multi-cavity absorptive light emitting diode (LED) fixtures can enhance light efficiency, reduce electricity consumption, and achieve superior lighting effects.

6.3. Optimal wiring practices

In electrical design, reasonable wiring is the key to ensuring the stable and reliable operation of intelligent lighting systems. Reasonable wiring should consider the following points:

(1) Circuit configuration: According to control requirements, determine the number of circuits and length of each line. Utilize centralized or decentralized power supply in the same lighting control circuit. In different lighting control circuits, centralized and decentralized power supply should be used separately.

(2) Distribution level: Determine the distribution level of the lighting circuit based on the type and capacity of the electrical equipment used. For single-phase, three-phase, and low-voltage distribution lines, the wiring should be carried out according to the “three-phase five-wire system” principle, and a dedicated distribution box or neutral grounding device should be installed inside the cabinet.

(3) Fixture selection: In low-voltage distribution systems, suitable lighting fixtures should be selected. Currently, there are various lighting fixtures available for selection in the market, such as energy-saving lamps, LED lamps, metal halide lamps, etc. Improper selection will lead to significant waste and increase electricity costs. Therefore, select lighting fixtures based on site-specific conditions. Consider replacing traditional lighting fixtures with new products such as energy-saving lamps, LED lamps, and metal halide lamps to improve lighting efficiency.

6.4. Adopting effective lighting control methods

There are mainly two types of intelligent lighting control methods: manual and automatic. Currently, most lighting systems in thermal power plants in China still use manual control methods with gradual automation enhancements being implemented. Specifically, light or motion sensors are strategically installed in each circuit to meet site-specific needs. When someone or a vehicle enters, the relevant lighting circuits will be automatically activated. Conversely, when no movement is detected, the lighting circuit will be automatically turned off. This approach can effectively manage energy consumption and reduce labor during maintenance and repair periods, especially at night. However, this approach has its limitations. It may prove inadequate

in scenarios requiring frequent circuit activation for personnel inspections or maintenance. Additionally, adjustments are necessary when on-site illumination falls short of requirements.

7. Epilogue

The intelligent lighting control system has a good control effect, which not only makes good use of traditional lighting but also saves energy. It is a new energy-saving product for thermal power plants, and the system can automatically adjust the light source according to the on-site conditions. The application of an intelligent lighting control system in thermal power plants can also effectively reduce operating costs. The system has good flexibility and scalability, capable of ongoing refinement and enhancement in tandem with the development of thermal power plants. This aligns with the future trend of our intelligent lighting control system.

Disclosure statement

The authors declare no conflict of interest.

References

[1] Lan S, Zhang K, 2023, Analysis of the Use of Intelligent Lighting Control System in the Lighting of Central Control Room of Thermal Power Plants. Guangdong Science and Technology, 2023(22): 126–126, 107.

[2] Lv M, Su Z, 2019, Discussion on the Use of Intelligent Lighting Control Systems in the Lighting of Centralized Control Rooms in Thermal Power Plants. Inner Mongolia Petrochemical, 2019, 35(3): 36–37.

[3] Zhang Y, Zheng J, Chen B, 2022, Application of Intelligent Lighting System Based on Network Control in Thermal Power Plants. Building Engineering Technology and Design, 2022(23): 1642–1642.

[4] Su G, 2021, Research on the Application of Intelligent Lighting Control System in the Control Room of Thermal Power Plants. Urban Construction Theory Research (Electronic Edition), 2021(29): 3560–3560.

[5] Zhou Y, 2022, Research on Intelligent Lighting Design Scheme for Thermal Power Plants. Building Engineering Technology and Design, 2022(35): 1354–1355.

Publisher's note

Bio-Byword Scientific Publishing remains neutral with regard to jurisdictional claims in published maps and institutional affiliations.

Integrated Services Platform of International Scientific Cooperation

Innoscience Research (Malaysia), which is global market oriented, was founded in 2016.Innoscience Research focuses on services based on scientific research. By cooperating with universities and scientific institutes all over the world, it performs medical researches to benefit human beings and promotes the interdisciplinary and international exchanges among researchers.

Innoscience Research covers biology, chemistry, physics and many other disciplines. It mainly focuses on the improvement of human health. It aims to promote the cooperation, exploration and exchange among researchers from different countries. By establishing platforms, Innoscience integrates the demands from different fields to realize the combination of clinical research and basic research and to accelerate and deepen the international scientific cooperation.

Cooperation Mode



Clinical Workers



In-service Doctors





Foreign Researchers

China Collaborators



Oversea Collaborators



Hospital



University



Scientific institutions

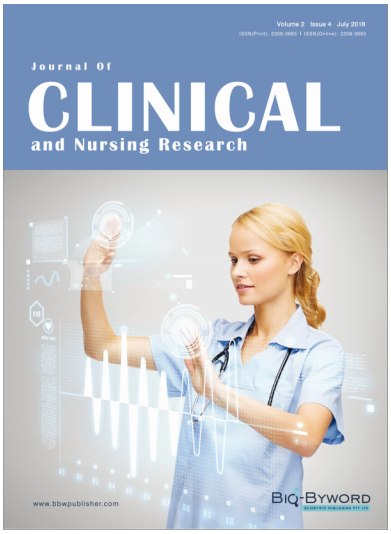
Our Journals



The *Journal of Architectural Research and Development* is an international peer-reviewed and open access journal which is devoted to establish a bridge between theory and practice in the fields of architectural and design research, urban planning and built environment research.

Topics covered but not limited to:

- Architectural design
- Architectural technology, including new technologies and energy saving technologies
- Architectural practice
- Urban planning
- Impacts of architecture on environment



Journal of Clinical and Nursing Research (JCNR) is an international, peer reviewed and open access journal that seeks to promote the development and exchange of knowledge which is directly relevant to all clinical and nursing research and practice. Articles which explore the meaning, prevention, treatment, outcome and impact of a high standard clinical and nursing practice and discipline are encouraged to be submitted as original article, review, case report, short communication and letters.

Topics covered by not limited to:

- Development of clinical and nursing research, evaluation, evidence-based practice and scientific enquiry
- Patients and family experiences of health care
- Clinical and nursing research to enhance patient safety and reduce harm to patients
- Ethics
- Clinical and Nursing history
- Medicine



Journal of Electronic Research and Application is an international, peer-reviewed and open access journal which publishes original articles, reviews, short communications, case studies and letters in the field of electronic research and application.

Topics covered but not limited to:

- Automation
- Circuit Analysis and Application
- Electric and Electronic Measurement Systems
- Electrical Engineering
- Electronic Materials
- Electronics and Communications Engineering
- Power Systems and Power Electronics
- Signal Processing
- Telecommunications Engineering
- Wireless and Mobile Communication